“Engineering Preeclampsia” Through Overexpression of the Epidermal Growth Factor Receptor in Uterine Artery Endothelial Cells

By

Luca Clemente

A dissertation submitted in partial fulfillment of
the requirements for the degree of

Doctor of Philosophy

(Endocrinology and Reproductive Physiology)

at the

UNIVERSITY OF WISCONSIN-MADISON

2018

Date of final oral examination: 02/26/2018

The dissertation is approved by the following members of the Final Oral Committee:

Ian M Bird, Professor, Obstetrics and Gynecology
Anjon Audhya, Associate Professor, Biomolecular Chemistry
Deane Mosher, Professor, Medicine and Biomolecular Chemistry
Linda Schuler, Professor, Comparative Biosciences
Milo Wiltbank, Professor, Dairy Science

Acknowledgments

Firstly, I would like to express my deepest gratitude to Valerie Gallegos, the former Director of the Ronald McNair Scholars Program at Colorado State University, with whom I worked as a student and as an employee. Without Valerie's fierce advocacy, my enrollment in graduate school simply would not have been possible. Her support at every step not only facilitated my academic success, but also freed my family from a life of poverty and stagnation, giving us the possibility of a better future.

Thanks to my friend Bruce Wallbaum for providing me with the large desktop computer with which I wrote this dissertation. The loud water pump cooling system was particularly helpful, providing a buffer of white noise that helped remove all outside distractions.

I would like to thank Craig Atwood for his support during my early days at UW as a visiting undergraduate. His decision to include my summer research in a published paper no doubt contributed to my acceptance into the UW graduate school.

I am also grateful to the late Paul Bertics for accepting me into his laboratory. Shortly before the date of my defense, I realized that I will be the very last graduate student of Paul's to obtain a PhD. Paul was a first class researcher and teacher, loved by all who knew him. Whatever career path I follow in the future, I will strive to honor Paul's memory.

Thanks to Ian Bird for inviting me to join his laboratory when I had nowhere else to go. He takes his work very seriously and sets high standards. His guidance has been invaluable. While it is common for highly driven researchers to be unavailable for their students, this is not true for Ian. Having worked under several professors from three universities, I can honestly say that Ian is the most student-oriented professor I have ever known. He once said to me that he did not measure his success by the number of publications he accumulates, but rather by the quality of work done by his students. When I was going through a series of particularly difficult family emergencies and considered dropping out of the program, Ian allowed me the flexibility I needed to keep going. I will always be indebted to him.

I also appreciate my colleagues from the Bird and Boeldt Laboratories—Amanda A., Amanda M., Aishu, Derek, Jason, Mary, Fuxian, and Roxanne (with honorable mention to Beth and Kenna). Their support and camaraderie always made being in the laboratory more fun than it would have been otherwise.

Special thanks to my sons—Jason, Gabriel, and Sasha—for the time that we spent together during my time in graduate school, and for their understanding when my work kept me apart from them. Their journey was far more profound than mine. When I first enrolled at UW, they were merely boys. Before I finished, they had all become men. Each one of them faced profound struggles during this time and each one of them persevered. I am proud of them.

Finally, I would like to thank my beautiful wife Trina, whose contribution to the completion of my degree is immeasurable. Obtaining a PhD would have been impossible for me if Trina had not been working tirelessly behind the scenes taking care of the vital mundane infrastructure and the many spontaneous crises that intruded into our lives. While I was observing the calcium responses of endothelial cells, Trina was fighting the lion's share of difficult emotional, financial, and legal battles with little fanfare or recognition. For this, I am forever grateful. Any rewards to come are hers as much as mine. I look forward to sharing many adventures together with Trina—my love and best friend—in the days, months, and years ahead of us.

Abstract

During pregnancy, the cardiovascular system undergoes sweeping changes to accommodate the needs of mother and fetus. We have previously shown that optimum vasodilation is achieved by improvements in endothelial cell function, controlled specifically by increased activity of connexin 43 (Cx43). Enhanced Cx43 gap junctional communication (GJC) improves agonist-stimulated capacitative calcium entry (CCE), which is required to sustain the maximum rate of nitric oxide (NO) production by endothelial nitric oxide synthase (eNOS). We have also shown that cytokines such as tumor necrosis factor alpha (TNFα) and growth factors such as vascular endothelial growth factor (VEGF) downregulate these enhancements by inducing ERK- and Src-mediated inhibitory phosphorylations of Cx43 at Y265 and S279/282. Preeclampsia is a hypertensive disorder of pregnancy associated with endothelial dysfunction, characterized by locally increased levels of VEGF as well as circulating inflammatory cytokines, including TNFα, IL-1β, IL-6, and IL-8. Due to the many practical and ethical concerns associated with obtaining tissues from pregnant women, the mechanism of action is still largely unknown. We have developed a uterine artery endothelial cell model derived from pregnant sheep (P-UAEC) that retains pregnancy-specific differences in signaling at passage 4, including enhanced function of Cx43 gap junctions that underlies the enhancement of pro-vasodilatory Ca2+ bursting, and enhanced growth factor-mediated kinase activation that inhibits Cx43 function. Treatment of P-UAEC with either epidermal growth factor (EGF) or VEGF induces Src and ERK1/2 activation, but only VEGF achieves ERK-mediated inhibitory phosphorylations of Cx43. Prior evidence suggests this action of VEGF is mediated exclusively by VEGFR-2, but the role of VEGFR-1 remains an open question. We hypothesized that Cx43-associated pools of ERK1/2 may be limited and confined to subregions within P-UAEC, and the low level endogenous EGF receptor expression in P-UAEC may not allow direct access to these ERK pools. By augmenting EGFR expression in P-UAEC via adenoviral transduction, we predicted that the receptor would achieve higher levels of kinase activation and likely gain access to Cx43-associated ERK pools, thus potentially enabling EGF to duplicate the inhibitory effect of VEGF on Cx43 GJC and CCE, as measured by reductions in ATP-stimulated Ca2+ bursting. We further predicted that overexpression of exogenous EGFR in P-UAEC at a level that conferred constitutive autophosphorylation would increase basal phosphorylations of Cx43 thereby inducing a permanent downregulation of pregnancy-adapted Ca2+ signaling. Contrary to our hypothesis, P-UAEC that expressed constitutively active EGFR (P-UAEC-

adEGFR) did not permanently downregulate GJC. However, as predicted, EGF treatment of P-UAEC-adEGFR did reproduce the downregulatory effects previously demonstrated by VEGF, suggesting that the higher expression level of EGFR did indeed facilitate access to the relevant ERK pools. Furthermore, we have previously shown in P-UAEC that pharmacological inhibition of ERK or Src protected against VEGF downregulation of GJC. Here we present new data in P-UAEC-adEGFR showing that only U0126-mediated inhibition of MEK/ERK protected against EGF downregulatory effects, suggesting that MEK/ERK activation alone is sufficient to downregulate GJC in P-UAEC. These results also suggest that VEGFR-2 mediates the inhibitory action of VEGF on GJC since we have previously shown that VEGFR-2, but not VEGFR-1, can phosphorylate ERK1/2 in P-UAEC. Further experiments showed that VEGF induces downregulation of GJC via a Src-*dependent* activation of ERK, while the effects of EGF are achieved via a Src-*independent* ERK activation. Interestingly, in P-UAEC-adEGFR, VEGF was no longer able to downregulate CCE, firstly suggesting that EGFR at elevated levels may have a greater affinity for effector molecules of the ERK1/2 pathway than VEGFR-2, and secondly suggesting the possibility that maintaining low endogenous EGFR expression in P-UAEC *in vivo* may be necessary to maintain VEGFR-2 control of ERK-mediated regulation of GJC, a necessary step to initiating angiogenesis. We also made the curious observation that VEGF did not activate the phosphatidylinositide 3-kinase (PI3K)/Akt pathway in P-UAEC, but EGF induced robust phosphorylations of Akt S473 in P-UAEC-adEGFR. This finding led us to investigate the importance of PI3K/Akt signaling on regulation of Cx43 GJC and regulation of endothelial monolayer permeability. Our surprising results suggested that basal PI3K activity in P-UAEC is both *necessary* and already maximally *sufficient* for optimal GJC required for Ca2+ bursting and the maintenance of endothelial barrier function. **In summary**, these studies have confirmed the gating function of Cx43 gap junctional plaques is indeed critically regulated by growth factors capable of Src and ERK activation and inhibitory control is mediated via ERK1/2 kinase. The data are consistent with the proposition that EGFR can substitute for VEGFR2 in mediating inhibition, but roles for VEGFR1 are not excluded. The data also reinforce the idea that specific subpools of ERK regulate Cx43 GJC in the plasma membrane. The finding that exogenous EGFR overwhelmed VEGFR control of GJC offers insight as to why P-UAEC naturally express very low levels of EGFR. Lastly, we have shown that *basal* PI3K/Akt signaling is necessary and sufficient for proper regulation of junctional proteins, including but not limited to Cx43, at the plasma membrane of P-UAEC, and thus further increases in Akt activity provide no protection against growth factor mediated inhibition of GJC.

Table of Contents

List of Figures

Abbreviations

[Ca2+]i	intracellular free Ca^{2+}
ATP	adenosine triphosphate
bFGF	basic fibroblast growth factor
cAMP	cyclic adenosine monophosphate
CDK	cyclin-dependent kinase
cGMP	cyclic guanosine monophosphate
CCE	capacitative calcium entry
CK1	casein kinase 1
COS-7	monkey kidney cell line
COX-1	cyclooxygenase 1
cPLA2	calcium-dependent phospholipase A2
Cx	connexin
DAF-2	4,5-diaminofluorescein diacetate, a NO-sensitive fluorescent dye
ECIS	electric cell-substrate impedance sensing (The term “ECIS” is a trademark of Applied BioPhysics, Inc.)
EDHF	endothelium-derived hyperpolarizing factor
EGF	epidermal growth factor
EGFR	epidermal growth factor receptor (also known as ErbB1)
EGFR	the gene transcript for EGFR protein
EGFR-KDD	EGFR kinase domain duplication, originally named EGFR.TDM/18-25
EGFR.TDM	EGFR tandem duplication mutant
EGFRvIII	EGFR variant three, an oncogenic mutant receptor
EN-1	endothelin 1
eNOS	endothelial nitric oxide synthase

ErbB	erythroblastosis oncogene B; family of four receptor tyrosine kinases that incudes EGFR and HER2
ER	endoplasmic reticulum
ERK	extracellular signal-regulated kinase (also known as MAPK)
FACS	fluorescence-activated cell sorting
Fura-2	[Ca2+]i-sensitive fluorescent dye
GAP26, GAP27	peptide mimetic(s) of extracellular loop of connexin
GJC	gap junctional communication
GPCR	G-protein coupled receptor
HER2	human epidermal growth factor receptor two (also known as ErbB2)
HHVE	human hand vein endothelial cells
Hsp90	heat shock protein 90
HUVEC	human umbilical vein endothelial cells
IFNγ	interferon gamma
IL	interleukin
in cis	occurring within the same monomer
IP3	inositol 1,4,5-triphosphate
IP3R	inositol 1,4,5-triphosphate receptor
IUGR	intrauterine growth restriction
JM-B	juxtamembrane domain B or “juxtamembrane latch”
KDD	kinase domain duplication
L834R-EGFR	EGFR in which leucine 834 is replaced with arginine
L834R-EGFR	the gene transcript for L834R-EGFR protein
LY294002	a selective inhibitor of PI3K
MAPK	mitogen-activated protein kinase (also known as ERK)
MEK	mitogen-activated protein kinase kinase
MOI	multiplicity of adenoviral infection; the number of viruses per cell

NF-κB	nuclear factor kappa-light-chain-enhancer of activated **B** cells
NIH 3T3	fibroblast cell line
NO	nitric oxide
NP	nonpregnant
NRP1 / NRP2	neuropilin-1 / neuropilin-2
NSCLC	non-small cell lung cancer
OFPAE	ovine feto-placental artery endothelial cells
P	pregnant
P-UAEC	pregnant uterine artery endothelial cell(s)
P-UAEC-adEGFR	P-UAEC that have been adenovirally transduced at an MOI of 1000 to overexpress wild-type EGFR
P-UAEC-adGJA1-eGFP	P-UAEC that have been adenovirally transduced at an MOI of 100 to express a Cx43-eGFP fusion protein
P-UAEC-adL834R	P-UAEC that have been adenovirally transduced at an MOI of 1000 to overexpress the constitutively active mutant L834R-EGFR
PAEC	porcine aortic endothelial cells
Parental P-UAEC	P-UAEC that have *not* been exposed to adenovirus
PDGF	platelet-derived growth factor
PE	preeclampsia, preeclamptic
PECAM-1	platelet endothelial cell adhesion molecule 1
PGI2	prostacyclin
PI3K	phosphoinositide 3-kinase
PKC	protein kinase C
PlGF	placental growth factor
PLC	phospholipase C
PP2	a selective inhibitor of SFKs
PVDF	polyvinylidene difluoride
RT-PCR	reverse transcription-polymerase chain reaction

SDS-PAGE	sodium dodecyl sulfate polyacrylamide gel electrophoresis
SFlt-1	soluble vascular endothelial growth factor receptor one
SFK	Src family kinase, particularly Src, Fyn, or Yes
STAT	signal transducer and activator of transcription
TGFα	transforming growth factor alpha
TKD-EGFR	tyrosine kinase domain duplication EGFR, originally named EGFR.TDM/18-26
TDM	tandem duplication mutant
TNFα	tumor necrosis factor alpha
TPA	12-O-tetradecanoyl-phorbol acetate, also called PMA (phorbol myristic acid)
TRPC	transient receptor potentiated channel
U0126	a selective inhibitor of MEK
UA Endo	intact uterine artery endothelium
UAEC	uterine artery endothelial cells
VEGF	vascular endothelial growth factor
VEGFR	vascular endothelial growth factor receptor
vWF	von Willebrand Factor
ZO-1	zona occludens-1

Chapter 1:

A Brief Summary of My Original Project in the Laboratory of Paul Bertics

1.0 Introduction

The laboratory of the late Paul Bertics had a dual research focus: immunology and cancer biology. In May 2009, when I joined Paul's lab, I wasn't sure in which of these fields I would be working. Paul's laissez-faire approach to mentoring meant that I would shadow various students in his laboratory until I was able to choose a subject of research independently and design my own project.

In the Summer of 2009, Byram "Sam" Ozer, an MD/PhD candidate, was nearing the completion of his experiments on a rare oncogenic variant of the epidermal growth factor receptor (EGFR) that had been discovered a decade earlier in glioblastoma tissue. Though the discoverers of this variant named it **EGFR.TDM/18-26** (Fenstermaker, *et al.* 1998), Paul and Sam decided to call it **TKD-EGFR** for reasons I will discuss in a subsequent section of this chapter. Sam's project involved identifying TKD-EGFR's unique pattern of ligand-dependent and independent autophosphorylation and basal localization. I ultimately decided that the focus of my project would be to take Sam's work to the next logical step by attempting to identify the mechanism(s) responsible for the observed properties of TKD-EGFR.

To meaningfully discuss the aberrant activity of the TKD-EGFR variant, however, it is first necessary to present some basic facts about wild-type EGFR. In the sections that follow, I first

provide a simple description of wild-type EGFR structure and function, and then summarize all that was known about this odd EGFR mutation at the time my project began.

1.1 Background

1.1.1 The Epidermal Growth Factor Receptor

The epidermal growth factor receptor (EGFR) is a 170 kDa transmembrane protein expressed in a wide variety of cell types. It is one of four members of the ErbB family of receptor tyrosine kinases comprising EGFR (ErbB1), HER2 (ErbB2), the kinase-impaired ErbB3, and ErbB4. In healthy cells, EGFR sits dormant in the plasma membrane as a monomer (Yamashita, *et al.* 2015) or inactive symmetric dimer (Jura, *et al.* 2009) until it is activated by binding with one of eight known ligands, including the eponymous epidermal growth factor (EGF) and transforming growth factor alpha (TGFα) (Wilson, *et al.* 2009). Binding of ligand to the receptor induces a conformational change in its transmembrane domain that releases EGFR from its basal inactive state, allowing the receptor to form active asymmetric dimers (Reviewed in Purba *et al.* 2017). This asymmetric dimerization stimulates EGFR's tyrosine kinase activity, which results in the autophosphorylation of several tyrosines in the receptor's C-terminal tail and, subsequently, receptor internalization. These phosphotyrosine residues serve as docking sites for a diverse array of effector molecules that initiate signaling cascades along major pathways, including PI3K/Akt, MAPK, JAK-STAT, and PLCγ (Reviewed in Wee and Wang, 2017; Jones and Rappoport, 2014). In some cellular environments, EGFR can also phosphorylate tyrosine residues of other receptors, and be transactivated by G-protein coupled receptor (GPCR) agonists (Daub, *et al.* 1996).

Under normal conditions, EGFR signaling plays key roles in cell proliferation, tissue homeostasis, embryogenesis, organismal growth and development, wound healing, and immune function (Reviewed in Wee and Wang, 2017). Precisely because of its critical importance in so many biological processes, however, the consequences of aberrant EGFR signaling can be deadly. Deficient EGFR signaling is associated with skin disorders, inflammatory bowel disease, and improper cartilage formation leading to osteoarthritis (Brooke, *et al.* 2014, Jia, *et al.* 2016). Excessive EGFR signaling due to overexpression or activating mutation of the receptor is associated with many cancers, including aggressive cancers of the breast, ovary, prostate, lung, colon, and brain (Reviewed in Normanno, *et al.* 2006).

1.1.2 Oncogenic EGFR Mutations

Numerous oncogenic EGFR variants have been observed in tumor cells. These can arise from missense, deletion, or duplication mutations. For example, **L834R EGFR**, commonly observed in non-small cell lung cancer (NSCLC), is a constitutively active and ligand hypersensitive mutant EGFR that results from a single *missense* mutation in the activation loop of the kinase domain. Crystallography data suggest the L834R mutation promotes the active asymmetric dimer configuration by preventing key hydrophobic interactions involving leucine-834 that lock the regulatory αC helix of the wild-type receptor in the inactive conformation (Choi, *et al.* 2007). **EGFRvIII** (pronounced "*variant three*" or "*vee three*"), another common EGFR variant observed in several cancers, owes its constitutive activity to the *deletion* of exons 2-7. This deletion mutation results in the loss of a significant portion of the extracellular domain of EGFRvIII, which releases it from the autoinhibited state of wild-type EGFR and confers ligand independency. EGFRvIII also resists down-regulation due to impaired ubiquitinylation and internalization (Grandal, et al. 2007). **TKD-EGFR**, the oncogenic EGFR variant of interest in the Bertics Laboratory, is the product of a *duplication* mutation. Though it was first observed in glioblastoma as mentioned earlier, it has recently also been detected in NSCLC (Baik, et al. 2015). The unusual structure and activity of

this unlikely receptor—and my proposal for determining the mechanism of its activity—will be the major focus of this chapter.

1.1.3 Mechanism of EGFR Activation

The fact that mutation of a single leucine to arginine (L834R) in the kinase activation loop confers constitutive activity and oncogenicity to the receptor reveals that the wild-type EGFR kinase domain is in an autoinhibited state. When leucine-834, normally packed tightly against hydrophobic side-chains in the kinase, is replaced with the positively charged arginine, the loop opens and the kinase becomes active. Therefore, it seemed likely that ligand-induced dimerization of the receptor would result in a similar conformational change in the activation loop, but empirical evidence supporting a dimerization model that could induce such a change eluded researchers for decades. Then, in 2006, the journal **Cell** published a landmark paper from the laboratory of UC Berkeley Professor John Kuriyan that presented evidence for a novel mechanism of EGFR dimerization and activation (Zhang, *et al.* 2006). Using crystallography, his team identified two dimerization motifs for the receptor's kinase domain—one, a *symmetric* dimer of two kinases that is unassociated with receptor activation, and the other, an *asymmetric* dimer in which the C-lobe of the first kinase domain (the "activator") docks with the N-lobe of the second (the "receiver") (Figure 1.1). The electrostatic and steric changes induced by this asymmetric docking configuration result in the first kinase activating the second, much like the activation of cyclin-dependent kinase (CDK), which remains dormant until binding with its regulatory subunit, cyclin (Jeffrey, *et al.* 1995). This model of EGFR activation also is strongly supported by the observation that mutation of hydrophobic amino acid (AA) residues situated at the dimerization interface significantly reduces or eliminates receptor autophosphorylation (Zhang, *et al.* 2006).

Among the insights obtained from this discovery is a possible answer to the mystery of the kinase-impaired ErbB3. Though it was well established that ligand binding to ErbB3 induced the formation

of heterodimers with other ErbB family members (Tzahar, et al. 1996), its role was the subject of mere speculation. It now seems likely that the major role of ErbB3 is to serve as a “universal activator” for the kinase domain of its ErbB heterodimer partner (Shi, *et al.* 2010).

Another recent discovery from the Kuriyan Laboratory is the role played by the last 19 residues of the 38-AA juxtamembrane region, located between the transmembrane domain and the kinase domain of the EGFR (Jura, *et al.* 2009). This 19-AA sequence, called “the juxtamembrane latch” or JM-B, runs alongside the C-lobe of the activating kinase and “latches” it to the receiving kinase via alignment of hydrophobic surface contacts and hydrogen bonds. Kuriyan’s team confirmed the critical importance of the JM-B sequence using mutational analysis. EGFR autophosphorylation was shown to be severely impaired by mutation of hydrophobic JM-B residues that pack against the kinases or by mutation of charged JM-B residues that form ion pairs with oppositely charged residues in the kinases. The significance of this sequence is further highlighted by the fact that key AA residues associated with JM-B binding at the dimerization interface were found to be conserved in all four members of the ErbB receptor family,

1.1.4 Summary

In the preceding subsections, I have given a very brief description of the epidermal growth factor receptor, its role in healthy cells, and its mechanism of activation. I noted that deficient or excessive EGFR signaling results in disease, and gave examples of activating mutations associated with several cancers. Though this overview of the EGFR is far from complete, it is enough to provide context for the remaining sections of this chapter, which deal directly with my original graduate school project in the laboratory of Paul Bertics. Previous research in his lab had characterized the activity of a rare tandem kinase domain duplication mutation of EGFR. It would be my task to discover the mechanism of its activation.

1.2 The Tandem Kinase Domain Duplication Mutation of EGFR

1.2.1 Discovery and Initial Characterization of EGFR.TDM/18-26 (TKD-EGFR)

The tandem duplication mutant EGF receptor (EGFR.TDM) was first detected in 1988 by a team of researchers from the University of Texas MD Anderson Cancer Center. While characterizing the activity of EGFR in the KE human glioma cell line, they discovered an unknown protein that precipitated with an EGFR-selective monoclonal antibody. Like EGFR, this protein—which they tentatively called “p190” due to its 190-kDa size—exhibited tyrosine kinase activity, but unlike EGFR, it did so constitutively in the absence of EGF ligand. Additionally, proteolytic polypeptide analyses of EGFR and p190 suggested that their phosphopeptides were nearly identical. These observations were further supported by Northern blot analysis in which KE cells expressed a novel EGF receptor RNA of 10.5 kb in addition to the previously reported 10-kb RNA of wild-type EGFR. Together, these results suggested that p190 was a structurally and functionally altered EGF receptor variant, but Steck *et al.* (1988) stopped short of making a definite conclusion.

Ten years later, in 1998, researchers at the Roswell Park Cancer Institute detected p190 in A-172 glioma cells. Reverse transcription-polymerase chain reaction (RT-PCR) sequencing revealed a unique transcript in the cells that encoded an in-frame, tandem duplication of the tyrosine kinase and calcium internalization (TK/CAIN) domains—specifically, exons 18 through 26 (Fenstermaker, *et al.* 1998). Shortly afterward, they discovered a 185-kDa EGFR transcript variant in KE and A-1235 glioma cells that possessed an in-frame tandem duplication of exons 18 through 25. The 190-kDa and 185-kDa EGFR mutants were unofficially named **EGFR.TDM/18-26** and **EGFR.TDM/18-25**, respectively. Both TDM were found to be constitutively autophosphorylated and inefficiently downregulated. Both TDM were also shown to be oncogenic mutants, as nude mice injected with TDM-transfected NR6 fibroblasts experienced significant

tumor growth after 40 days compared to mice injected with wild-type EGFR expressing or non-expressing NR6 cells (Ciesielski and Fenstermaker, 2000).

1.2.2 Further Characterization by the Bertics Laboratory

All the current knowledge (as of this writing) about the molecular function and cellular localization of EGFR.TDM/18-26 was discovered by Byram "Sam" Ozer while he was a graduate student in the laboratory of Paul Bertics. The body of Sam's work on the properties of EGFR.TDM/18-26 was summarized in a single paper published in **Nature: Oncogene** (Ozer, *et al.* 2010).

*NOTE: In the **Oncogene** paper, perhaps for convenience, Paul and Sam decided to change the name of the receptor from the admittedly unwieldly **EGFR.TDM/18-26** (EGFR tandem duplication mutation of exons 18-26) to the simpler but somewhat confusing name of **TKD-EGFR** (tandem kinase duplication EGFR). I say 'confusing' because the EGFR research community and molecular biologists in general have a long history of using the acronym TKD as an abbreviation of the term "tyrosine kinase domain." The name "TKD-EGFR" also makes no distinction between the 190-kDa (EGFR.TDM/18-26) and 185-kDa (EGFR.TDM/18-25) variants of the mutant receptor, perhaps because all of Sam's published data refer only to the 190-kDa variant. The nomenclature became even more confusing in 2015, when a team of researchers at the Vanderbilt University Medical Center detected the 185-kDa EGFR.TDM/18-25 variant in lung, brain, and soft-tissue tumors (Gallant,* et al. *2015). Seemingly without any concern for its relation to the nearly identical EGFR.TDM/18-26 (TKD-EGFR), they named it **EGFR-KDD,** the suffix letters presumably standing for "kinase domain duplication." Incidentally, there also exists a mutation currently called EGFR.TDM/2-7, in which the residues encoded by exons 2 through 7 are duplicated. One can only guess what this variant will be renamed.*

Sam Ozer transfected B82L mouse fibroblast cells devoid of endogenous EGFR with wild-type EGFR, TKD-EGFR, or empty vector to provide a clean system for determining the unique

activation and localization patterns of the TKD-EGFR. Using this murine cell line, Sam identified several unique and surprising properties of the mutant receptor. Firstly, the constitutive autophosphorylation of the TKD-EGFR was confirmed at five major phosphotyrosine sites—Y992, 1068, 1086, 1148, & 1173 (Figure 1.2)—and it occurred in the absence of receptor dimerization, which is required for autophosphorylation of wild-type EGFR (Figure 1.3). Secondly, a significant fraction of TKD-EGFR was localized in the cytosol and phosphorylated, unlike wild-type EGFR, most of which remains embedded in the plasma membrane in an unphosphorylated state until binding with ligand occurs (Figure 1.4).

In addition, two kinase-impaired variants of TKD-EGFR were generated—K721M TKD (N-proximal kinase impaired) and K1088M TKD (C-terminal kinase impaired)—to quantify the relative contribution of each kinase domain to the overall phosphorylation response and basal localization. The K721M TKD variant lost all responsiveness to EGF, but retained its constitutive autophosphorylation (Figure 1.5) and basal intracellular localization (Figure 1.6). In stark contrast, the K1088M TKD variant exhibited robust autophosphorylation when treated with EGF, but lost all constitutive autophosphorylation (Figure 1.5) and remained embedded in the plasma membrane in the absence of EGF (Figure 1.6). This is strong evidence that the ligand-dependent activity of the N-proximal kinase is the result of dimerization with a second monomer, since the C-terminal kinase, impaired by the K1088M mutation, cannot be activated. Thus, it appears that TKD-EGFR has two distinct activation mechanisms: a ligand-independent activation that constitutively occurs in monomers, and a ligand-dependent wild-type-like activation that requires two monomers to dimerize (Figure 1.7).

Following Sam Ozer's characterization of the activation and localization of this glioblastoma-derived mutant receptor, two key questions remained: (1) "The wild-type EGFR requires ligand binding for activation, so why is TKD-EGFR constitutively autophosphorylated?" and (2) "The wild-type EGFR must dimerize before activation and internalization can occur, so why are so many

TKD-EGFR monomers autophosphorylated and observed in the cytosol?" Answering these questions was to form the basis of my project.

1.3 My original project: Determination of the mechanism of constitutive activity and cytosolic localization of TKD-EGFR (EGFR.TDM/18-26)

1.3.1 Hypotheses

In 2010, at the time my project was just beginning to take shape, two hypotheses were proposed—one by Paul Bertics and the other by me—to account for the constitutive autophosphorylation and cytosolic localization of TKD-EGFR. Both hypotheses are plausible and are not mutually exclusive.

Paul Bertics proposed what might be called the *Phosphatase Escape Model*, which arose out of Paul's intimate knowledge of enzyme kinetics. Whereas many molecular biologists become accustomed to thinking of a receptor being in a particular state—e.g. phosphorylated or not phosphorylated, bound or not bound to ligand, etc.—Paul always stressed the fact that these states were never static, but were actually dynamic processes in continuous flux. In the case of EGFR, he said that even unbound EGFR had modest basal kinase activity, but in the cellular environment this activity was out-competed by plasma membrane-associated protein tyrosine phosphatases. In this view, overexpression of EGFR in tumor cells is dangerous precisely because these phosphatases are overwhelmed by the mass action of basal EGFR activity. Paul's assertion was supported by research showing dramatic increases in basal EGFR auto-phosphorylation in multiple mammalian cell types when protein tyrosine phosphatases were inhibited (Knebel, *et al.* 1996). In the case of TKD-EGFR, Paul proposed that the C-terminal

kinase was likely to be sufficiently removed from the plasma membrane such that its basal kinase activity was unchecked by membrane-associated phosphatases.

Alternatively, I proposed what might be called the *Intramolecular Dimerization Model*, which arose out of recent groundbreaking research on the unique asymmetrical docking mechanism of EGFR kinase activation. Because of its kinase duplication, the TKD-EGFR might be able to achieve spontaneous intramolecular *in cis* dimerization of the N-proximal and C-terminal tandem kinases, thus accounting for the constitutive autophosphorylation and cytosol localization exhibited by TKD-EGFR monomers. A number of facts support this hypothesis. Firstly, the length of the ~90-AA residue chain between the tandem kinases is likely to provide enough flexibility to permit asymmetric docking. Secondly, only the C-terminal kinase of TKD-EGFR exhibits basal autophosphorylation (Ozer, *et al.* 2010), which is consistent with the N-proximal kinase assuming the role of the donor/activator of an *in cis* dimer while the C-terminal kinase serves as the activated receiver. Thirdly, in addition to the duplication of the kinase domain, 19 residues of the juxtamembrane domain reported to stabilize kinase dimerization—identified as the "juxtamembrane latch" or JM-B (Jura, *et al.* 2009)—are also duplicated in the TKD-EGFR (Figure 1.8), allowing for the possibility of the duplicated "latch" sequence to further stabilize the *in cis* dimerization of the tandem kinases. Finally, in light of recent evidence supporting the necessity of dimerization for EGFR internalization (Wang, *et al.* 2005), spontaneous *intra*molecular dimerization of the tandem kinase domains provides a plausible explanation for the constitutive internalization of TKD monomers observed in B82L cells.

In the next two subsections, I outline my intended strategies for testing the two hypotheses. Though I never got as far as designing precise experimental protocols, I did think extensively about the general approaches I would take.

1.3.2 Proposed Method for Testing the Phosphatase Escape Model

Sam Ozer's data, briefly outlined in subsection 1.2.2, demonstrated that only a functional C-terminal kinase of TKD-EGFR is necessary to confer constitutive autophosphorylation to the receptor. When he observed the activity of the N-proximal kinase-impaired variant, K721M TKD-EGFR, in B82L cells, he discovered that it possessed the constitutive activity of the original TKD, but lacked any responsiveness to ligand. I reasoned that if the Phosphatase Escape Model were true, then the constitutive activity of K721M TKD-EGFR in B82L cells should be relatively unaffected by phosphatase inhibition. However, if phosphatase inhibition does result in a significant increase of constitutive receptor autophosphorylation, then the Phosphatase Escape Model is probably false.

My plan was to run a time course experiment comparing the constitutive autophosphorylation of TKD-EGFR with K721M TKD-EGFR (with wild-type EGFR added as a reference) in B82L cells in the presence of sodium orthovanadate, a potent protein tyrosine kinase inhibitor suitable for use in cell culture and live animal subjects (Feng, *et al.* 2008). Because the rate of constitutive kinase activity is not known, I would initially grow B82L cells transfected with wild-type EGFR and TKD-EGFR in medium containing 1 mM sterile sodium orthovanadate for 7.5, 15, 30, 60 and 120 minutes before lysing the cells. In the absence of membrane-associated phosphatase activity, I expected to see an increase in basal autophosphorylation of both receptors over time. The autophosphorylation at these selected times would then be quantified by Western blot. My time course for repeat experiments would then be adjusted (expanded or contracted) based on the time that maximum autophosphorylation was achieved.

Once my final time course was established, I would compare the basal autophosphorylation of wild-type EGFR and TKD-EGFR in B82L cells to that of the N-proximal kinase-impaired K721M TKD-EGFR. If the K721M TKD variant exhibited little to no increase in basal autophosphorylation

in comparison to wild-type EGFR in medium containing 1 mM sodium orthovanadate, the result would support the Phosphatase Escape Model.

1.3.3 Proposed Methods for Testing the Intramolecular Dimerization Model

Each of the tandem kinase domains in the TKD-EGFR are molecularly identical to the kinase domain of the wild-type EGFR. Therefore, there is no reason to believe the structure of a functional asymmetric dimer formed by the tandem kinases of TKD-EGFR would be significantly different from the active dimer formed from the docking of two wild-type EGFR kinase domains. If the Intramolecular Dimerization Model were correct, then disruption of the *in cis* dimerization interface—i.e. the surface of contact between the C-lobe of the N-proximal (activator) kinase and the N-lobe of the C-terminal (receiver) kinase—should significantly reduce or eliminate constitutive autophosphorylation of TKD-EGFR. Additionally, the Intramolecular Dimerization Model suggests that constitutive autophosphorylation would be inhibited by blocking JM-B from "latching" the two kinases together. However, if disruption of the *in cis* dimer interface or "juxtamembrane latch" binding sites has no effect on constitutive receptor activity, then the model is false.

To test the Intramolecular Dimerization Model of constitutive activity, I planned to employ a strategy similar to that employed by Xuewu Zhang and Natalie Jura in the laboratory of John Kuriyan—namely, mutation of key residues in the receptor that impede dimerization (Zhang, *et al.* 2006; Jura, *et al.* 2009). Just as Zhang and Jura showed the dimerization and activation of wild-type EGFR could be inhibited in four different ways, there are four regions of the TKD-EGFR in which mutations could inhibit the formation of an intramolecular dimer:

1) The C-lobe of the N-proximal (putative "activator") kinase
2) The N-lobe of the C-terminal (putative "receiver") kinase
3) The "juxtamembrane latch" sequence

4) The latch's binding region on the N-proximal kinase

1.3.3.1 Mutation of the C-lobe of the N-proximal (putative "activator") kinase

Zhang *et al.* (2006) used crystallography to examine the structure of an active asymmetric EGFR kinase dimer. By determining which residues in the C-lobe of the activator kinase made contact with residues in the N-lobe of the receiver kinase, the key residues in the largely hydrophobic dimer interface were identified. Zhang generated four EGFR kinase mutants by replacing selected neutral amino acids in the C-lobe (Figure 1.9a) with arginine (positively-charged and bulky)—I917R, M921R, V924R, & M928R—to quantify the effect of disrupting the dimer interface on receptor autophosphorylation. Western blot results showed that each of the four mutations strongly inhibited EGFR autophosphorylation in transfected NIH3T3 cells.

For my initial experiments, I planned to start with one of the methionine-to-arginine mutations, M921R or M928R, because they only involve a replacement of one base (*ATG→AGG*), whereas the isoleucine and valine-to-arginine mutations each require changing two bases (I917R *ATC→AGG*; V924R *GTC→CGC*). I would also have to account for the fact that residues 664 to 1030 are duplicated in TKD-EGFR, such that performing site-directed mutagenesis in the *TKD-EGFR* gene transcript with a primer for an M921R mutation in the N-proximal kinase, for example, would also create an M1288R mutation in the C-terminal kinase. This problem is avoided by performing site-directed mutagenesis in the wild-type EGFR, and then *constructing* the TKD mutant through the use of restriction enzymes to clip the desired sequences and DNA ligase to assemble them together. In this manner, the intended mutation can be placed in one of the tandem kinases of the newly constructed TKD-EGFR, without placing it in the other. Finally, the mutated TKD-EGFR construct would be transfected into B82L cells, which do not express detectable endogenous EGFR.

It should be noted that mutations of asymmetric dimer-associated residues in the C-lobe of the N-proximal kinase should inhibit ligand-dependent autophosphorylation of TKD-EGFR, even if the Intramolecular Dimerization Model is false. Since only the N-proximal kinase of TKD-EGFR is responsive to ligand, and no N-proximal kinase with a mutated C-lobe can activate another kinase, no ligand-dependent autophosphorylation can occur. Therefore, if the Intramolecular Dimerization Model is correct, mutations of asymmetric dimer-associated residues in the C-lobe of the N-proximal kinase should inhibit ***all*** autophosphorylations of TKD-EGFR.

1.3.3.2 Mutation of the N-lobe of the C-terminal (putative "receiver") kinase

Key residues in the N-lobe of the wild-type EGFR kinase positioned in the asymmetric dimer interface include Leu-736, Leu-758, and Val-762 (Figure 1.9b). Therefore, L736R, L758R, and V762R (i.e. receiver impairing) mutations would be expected to interfere with EGFR dimerization and inhibit autophosphorylation. In the TKD-EGFR, the corresponding mutations in the C-terminal kinase would be L1103R, L1125R, and V1129R. I intended to begin with the leucine-to-arginine mutations for the same reason given in subsection 1.3.3.a—they involve a replacement of one base pair (*CTC→CGC*), whereas the valine-to-arginine mutation requires changing two bases (V1129R *GTG→AGG*).

Unlike C-lobe mutations in the N-proximal kinase of TKD-EGFR, N-lobe mutations in the C-terminal kinase would have no effect on the ability of the N-proximal kinases of two TKD-EGFR monomers to form an active asymmetric dimer in response to ligand. If the Intramolecular Dimerization Model were true, N-lobe mutations in the C-terminal kinase that disrupt the dimer interface should inhibit constitutive activity in the C-terminal kinase of TKD-EGFR, but should have no effect on ligand-dependent autophosphorylation.

1.3.3.3 Mutation of the "juxtamembrane latch" sequence

Jura et al. (2009) identified several mutations in the JM-B sequence that inhibit the autophosphorylation of wild-type EGFR—L664R, V665R, E666A, and L668R. The hydrophobic residues—Leu-664, Val-665, and Leu-668—stabilize the active asymmetric dimer by packing tightly against the C-lobe of the "activator" kinase domain. The negatively-charged Glu-666 stabilizes the active asymmetric dimer by forming an ion pair with Arg-949 in the "activator" kinase (Figure 1.9c).

As stated earlier, TKD-EGFR has two JM-B sequences, one attached to the N-lobe of the N-proximal kinase and one attached to the N-lobe of the C-terminal kinase. The Intramolecular Dimerization Model predicts that mutation of the latter should inhibit constitutive autophosphorylation of the C-terminal kinase. The inhibitory mutations in the TKD-EGFR corresponding to those listed above are L1031R, V1032R, E1033A, and L1035R. Again, the leucine-to-arginine mutations require only a single base pair substitution (*CTT→CGT*), whereas the valine-to-arginine and glutamate-to-alanine mutations involve substituting two base pairs (V1032R *GTG→AGG*; E1033A *GAG→AGG*).

1.3.3.4 Mutation of the latch's binding region on the N-proximal kinase

Jura et al. (2009) identified several C-lobe residues of the wild-type EGFR kinase domain that anchor the "juxtamembrane latch," including Arg-949, Asp-950, Arg-953, and Asn-972 (Figure 1.9d). Mutations of these residues—specifically, R949E, D950A, R953A, and N972A—were found to inhibit EGFR autophosphorylation in cell-based assays, and would be expected to inhibit ligand-dependent and (if the Intramolecular Dimerization Model is correct) constitutive autophosphorylation of TKD-EGFR. This is because disruption of the juxtamembrane latch anchor points on the C-lobe of the N-proximal "activator" kinase inhibit the formation of ***any*** active

asymmetric dimer, whether the dimer is intramolecular or results from the association of two TKD-EGFR monomers.

I would first perform site-directed mutagenesis to create the D950A mutant TKD-EGFR (and transfect B82L cells with it), since the aspartate-to-alanine mutation require only a single base pair substitution (D950A *GAC→GCC*), whereas the arginine-to-glutamate, arginine-to-alanine, and asparagine-to-alanine mutations involve substituting two base pairs (R949E *CGA→GAA*; R953A *CGC→GCC*; N972A *AAC→GCC*).

1.4 Discussion

I wasn't the first person in the Bertics Laboratory to suggest that the tandem kinases of TKD-EGFR might form an *in cis* dimer. Paul Bertics and Sam Ozer had both considered the possibility. Paul, however, believed that an *in cis* symmetric dimer linked by a peptide chain at opposite ends would be too unstable to be functional. He was also reluctant to accept John Kuriyan's *asymmetric* dimerization model of EGFR activation as established fact without substantial confirmation from other laboratories. Having spent decades in the field of EGFR research, Paul had witnessed many apparent discoveries that did not survive subsequent independent examination. Therefore, regarding *in cis* dimerization of TKD-EGFR kinases, he considered asymmetric dimerization as merely a tentative claim awaiting further evidence. Sam, in turn, was perhaps more amenable to the plausibility of an intramolecular dimer, but he also expressed doubt as to how it would be held together.

My conception of the Intramolecular Dimerization Model arose not only out of the early evidence that EGFR is activated by asymmetric dimerization, but also on my observation that the duplicated sequence encoded by exons 18 to 26 includes JM-B, the juxtamembrane latch. In fact, the last

19 residues of the 89-AA peptide chain between the tandem kinase domains is the duplicated JM-B region, which connects directly to the N-lobe of the C-terminal kinase. I speculated that an *in cis* dimer would be stable and functional because the linker sequence, not being particularly proline-rich, would be flexible enough to allow for asymmetric docking, and the duplicated juxtamembrane latch would secure the active dimer by binding to the N-proximal kinase.

Of course, I never was able to test my hypothesis. I cannot say whether EGFR.TDM/18-26, now known as TKD-EGFR, forms an intramolecular active asymmetric dimer or not. However, in 2015, the Intramolecular Dimerization Model received a boost when a team of researchers at the Vanderbilt University Medical Center (re)discovered TKD-EGFR's slightly shorter twin—EGFR.TDM/18-25, or **EGFR-KDD** as they named it—in a variety of tumor types (Gallant, *et al.* 2015). To test the likelihood of an *in cis* dimer being the source of EGFR-KDD's constitutive autophosphorylation, they used PyMOL software to generate the 73-AA linker sequence between the tandem kinases and attached each end of the linker to the appropriate residues of the crystal structure of the active asymmetric dimer published by Zhang, *et al.* (2006). By sampling the conformational space of the linker with Rosetta and Modeller loop modeling software, they confirmed that the linker would theoretically allow proper positioning of the tandem kinase domains required for intramolecular dimerization.

Though the conclusion is tentative, the modeling data supporting intramolecular dimerization of EGFR-KDD's tandem kinases suggest a similar probability of TKD-EGFR forming an intramolecular dimer. Indeed, aside from the fact that the TKD-EGFR linker sequence is 16 residues longer (89 AA vs. 73 AA in EGFR-KDD), the two proteins are identical in structure. Both duplication mutants are oncogenic and exhibit constitutive activity, and both have highly flexible linker chains that end with the dimer-stabilizing 19-AA "juxtamembrane latch" sequence. Their similar activity profiles are likely to result from the same mechanism.

1.4.1 Why study TKD-EGFR?

The frequency (and therefore the medical relevance) of these oncogenic EGFR duplication mutations in cancer is still unknown. Since TKD-EGFR and EGFR-KDD were first detected in glioblastoma, in 1998 and 2000, respectively, they have also been detected in NSCLC and other cancers (Baik, *et al.* 2015; Gallant, *et al.* 2015), suggesting they may be much more common than first assumed at the time of their discovery (Fenstermaker, *et al.* 1998). Future research may reveal that duplication mutations of the EGFR are aggressive drivers of many types of cancer. However, irrespective of any importance in cancer biology or general physiological relevance, Paul Bertics believed the study of the TKD-EGFR (and, by extension, EGFR-KDD) was a worthwhile pursuit on the basis of its biochemistry alone. One day in Paul's office, a few months before his death, I casually and perhaps naively remarked to him that we might be spending a lot of time and money researching an exceedingly rare mutation of little medical significance. Paul's expression became serious, and he responded with (very nearly) these words:

> "I wouldn't say that at all. I wouldn't say we are wasting time. I would say TKD is like no other protein I've ever seen. I would say we are looking at a *naturally-occurring*, *self-activating* receptor with ***two*** functional kinases. I would say it's one of the most unique proteins in all of biochemistry. That alone makes it worth studying."

He paused for a few moments and then he added, "*And what if it **is** the key to understanding glioblastoma?*"

I stared at him, saying nothing.

"Exactly," he said loudly, as if inspired by his own words, "so back to work!"

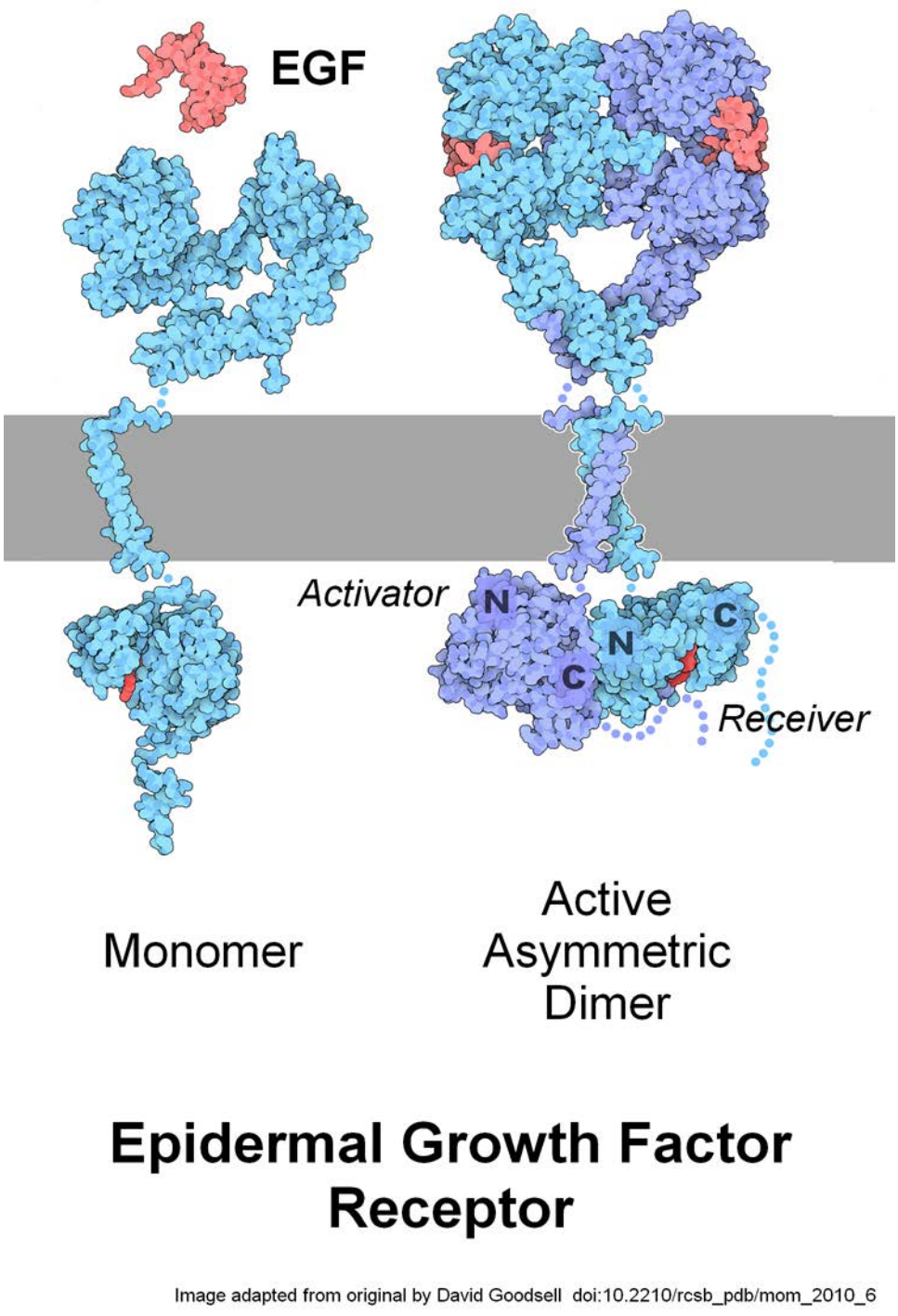

Figure 1.1 Ligand binding initiates an asymmetric dimerization of EGFR. The C-lobe of the first kinase domain (the "activator") docks with the N-lobe of the second (the "receiver") (Figure 1.1). The electrostatic and steric changes induced by this asymmetric docking configuration result in the first kinase activating the second. The juxtamembrane domain (between the transmembrane and kinase domains) and the C-terminal tail are not represented in this illustration.

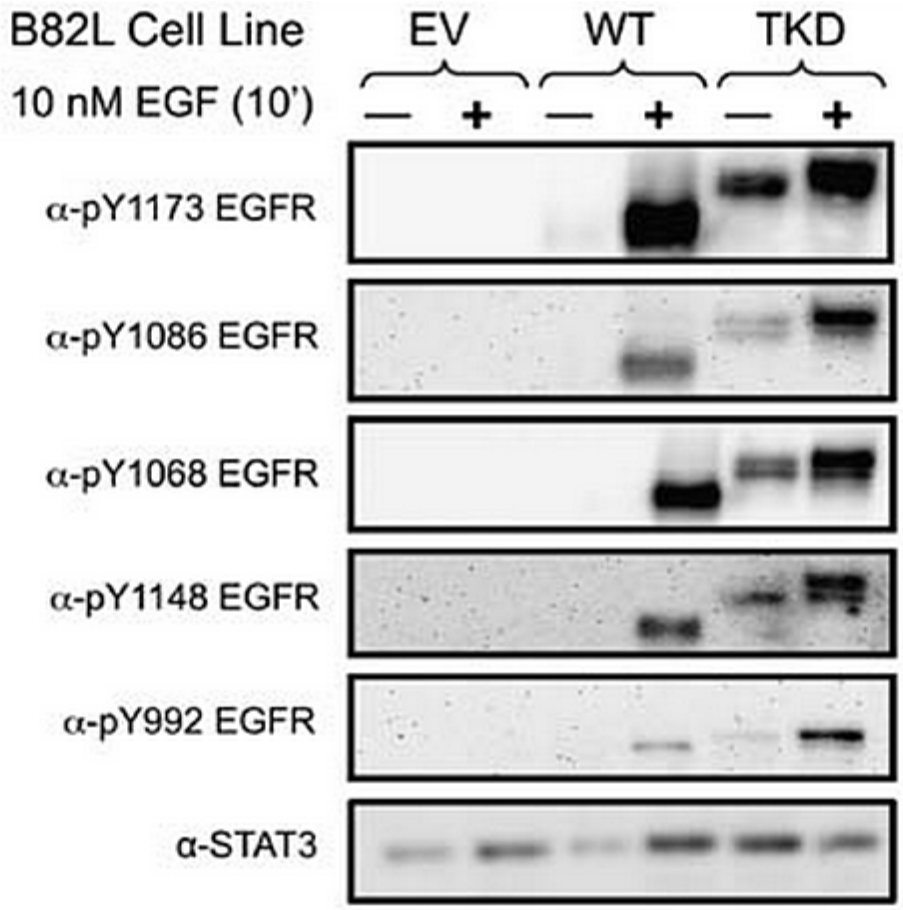

Figure 1.2 TKD-EGFR exhibits basal autophosphorylation at five phosphotyrosine sites. B82L mouse fibroblast cells transfected with empty vector (EV), wild type-EGFR (WT), or TKD-EGFR (TKD) were serum starved for 4 hrs and then treated with 10 nM EGF or 20mM HEPES vehicle for 10 min. Samples (50–60 mg of total protein) were run on 6% SDS–PAGE gels and immunoblotted with phosphor-selective anti-EGFR antibodies (Biosource) for phospho-Y992 (α-pY992), phospho-Y1068 (α-pY1068), phospho-Y1086 (α-pY1086), phospho-Y1148 (α-pY1148) and phospho-Y1173 (α-pY1173) (n = 2–7). (Adapted from Ozer, *et al.* 2010)

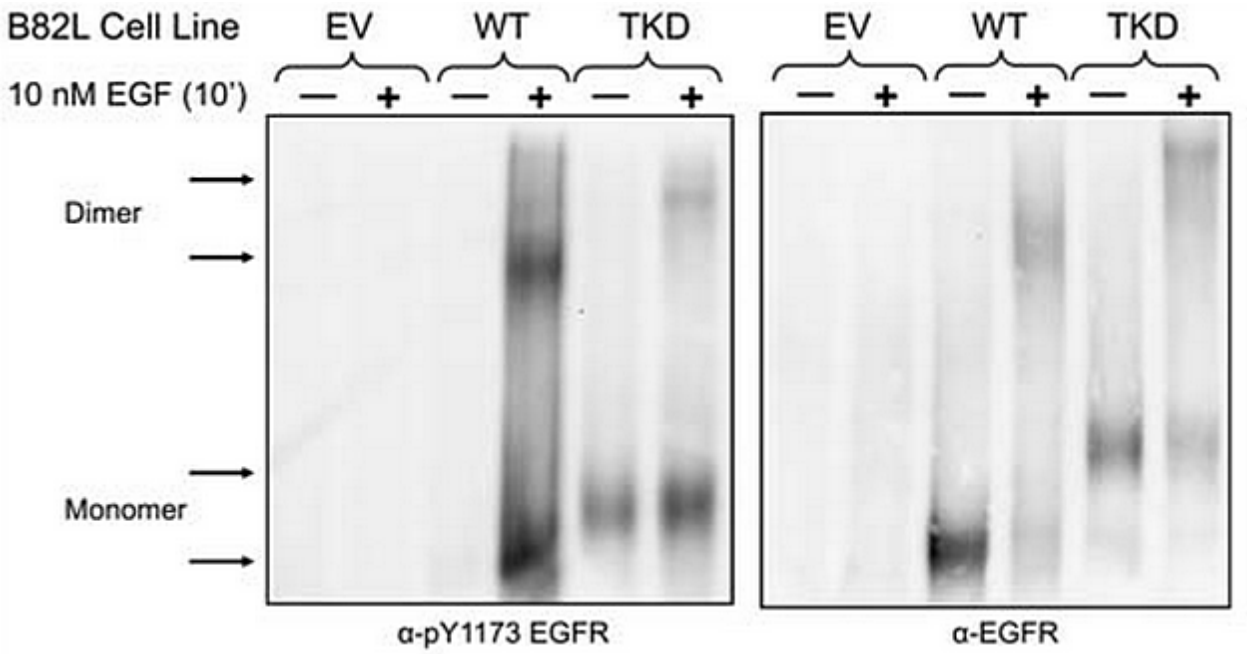

Figure 1.3 TKD-EGFR monomers exhibit basal autophosphorylation. B82L cells transfected with either empty vector (EV) or wild-type EGFR (WT) or TKD-EGFR (TKD) were serum-starved for 4 hrs and then treated with and without 10 nM EGF for 10 min. Cells were subsequently cross-linked using 100mM EDAC for 15 min. Samples (100 mg of total protein) were loaded on 5% SDS–PAGE gels, electrophoresed and immunoblotted with phospho-selective anti-EGFR antibody phospho-Y1173 (a-pY1173) or pan-reactive anti-EGFR (H11) (α-EGFR) antibody (n = 3–4). (Adapted from Ozer, *et al.* 2010)

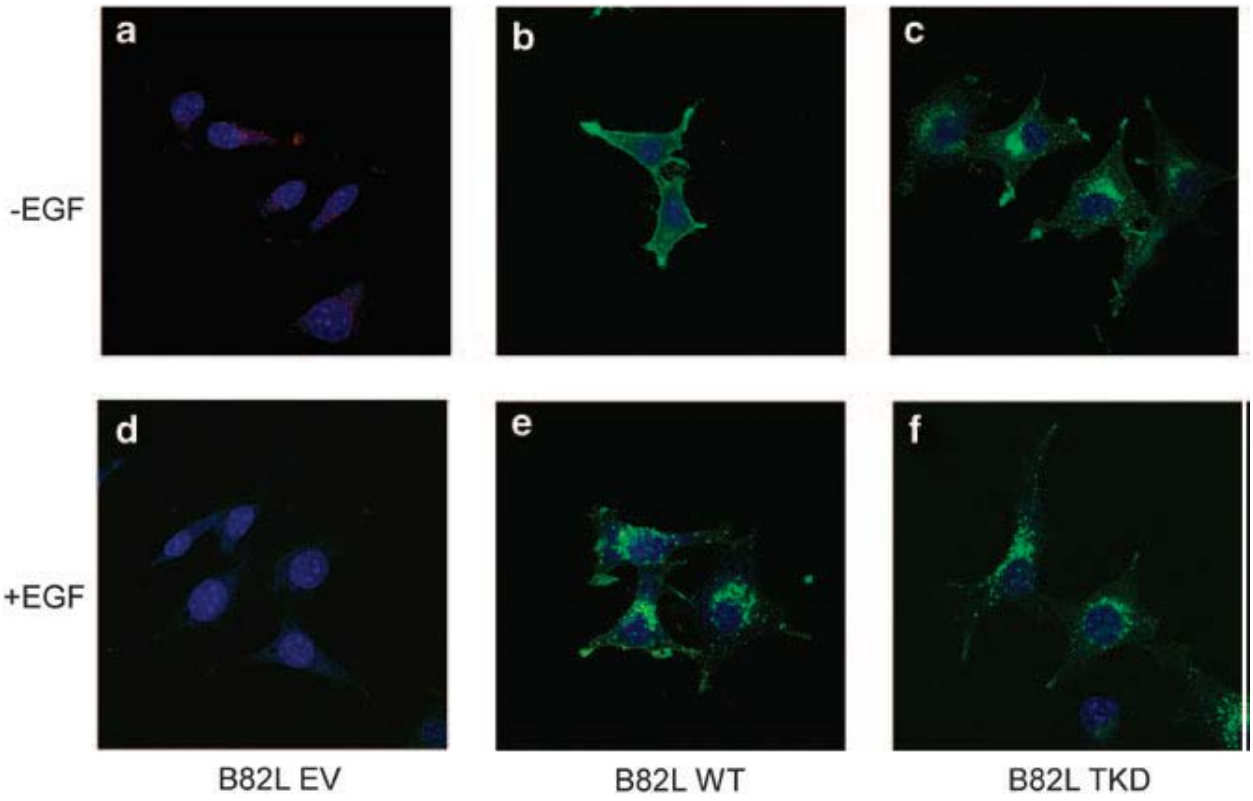

Figure 1.4 TKD-EGFR exhibits basal cytosolic localization. Transfected B82L cells containing empty vector (B82L EV) (a, d), wild-type EGFR (B82L WT) (b, e) and TKD-EGFR (B82L TKD) (c, f) were serum-starved for 4 hrs and then treated for 15 min without (a–c) or with (d–f) 10nM EGF to ensure internalization. Cells were then fixed with 4% paraformaldehyde, permeabilized with 0.1% Triton X-100, blocked and stained for pan-reactive EGFR (Clone H11, Labvision, green), EGFR phosphorylated at Y1086 (pY1086, Upstate, red) and nuclear material (DAPI, Molecular Probes, blue). Colocalization of total receptor (green) and phosphophorylated receptor (red) appears yellow in these merged images. Images were captured at 60X magnification (n = 3). (Adapted from Ozer, *et al.* 2010)

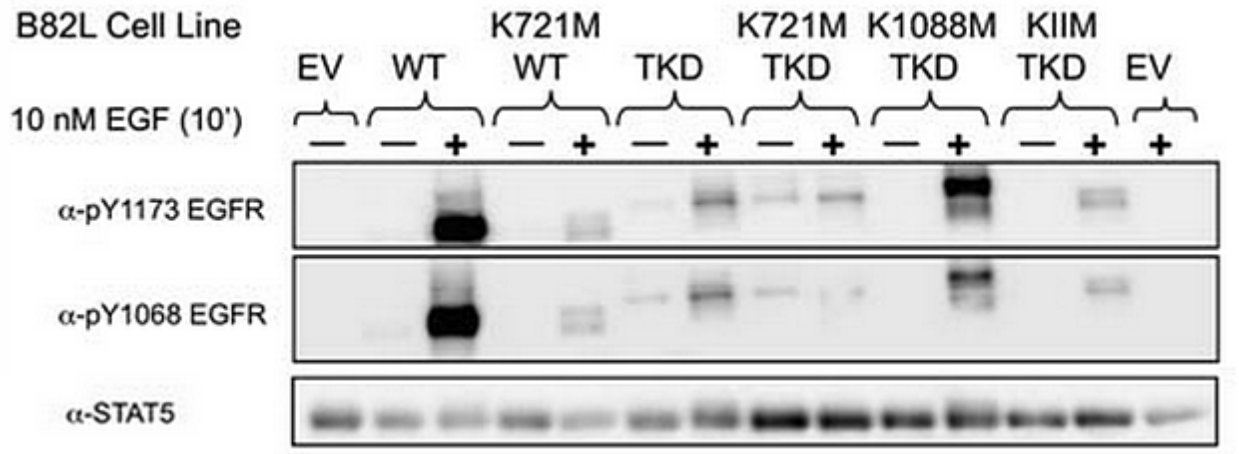

Figure 1.5 Kinase domain knockouts of TKD-EGFR reveal unique activity of N-proximal and C-terminal kinases. B82L cells were stably transfected with empty vector (EV), wild-type EGFR (WT), TKD-EGFR (TKD) and kinase domain knockout EGFR variants—kinase-impaired WT knockout (K721M WT), N-proximal kinase-impaired TKD knockout (K721M TKD), C-terminal kinase-impaired TKD knockout (K1088M TKD), and double kinase TKD knockout (KIIM TKD). The stably transfected B82L cells were serum-starved before a 10-min treatment with 10 nM EGF or vehicle (20mM HEPES). Samples (50–60 mg of total protein) were loaded on 5 or 6% SDS–PAGE gels and immunoblotted with phospho-selective anti-EGFR antibodies for phospho-Y1173 (α-pY1173) and phospho-Y1068 (α-pY1068). Immunoblotting for STAT5 (α-STAT5) was used as a loading control for all blots ($n \leq 15$). (Adapted from Ozer, *et al.* 2010)

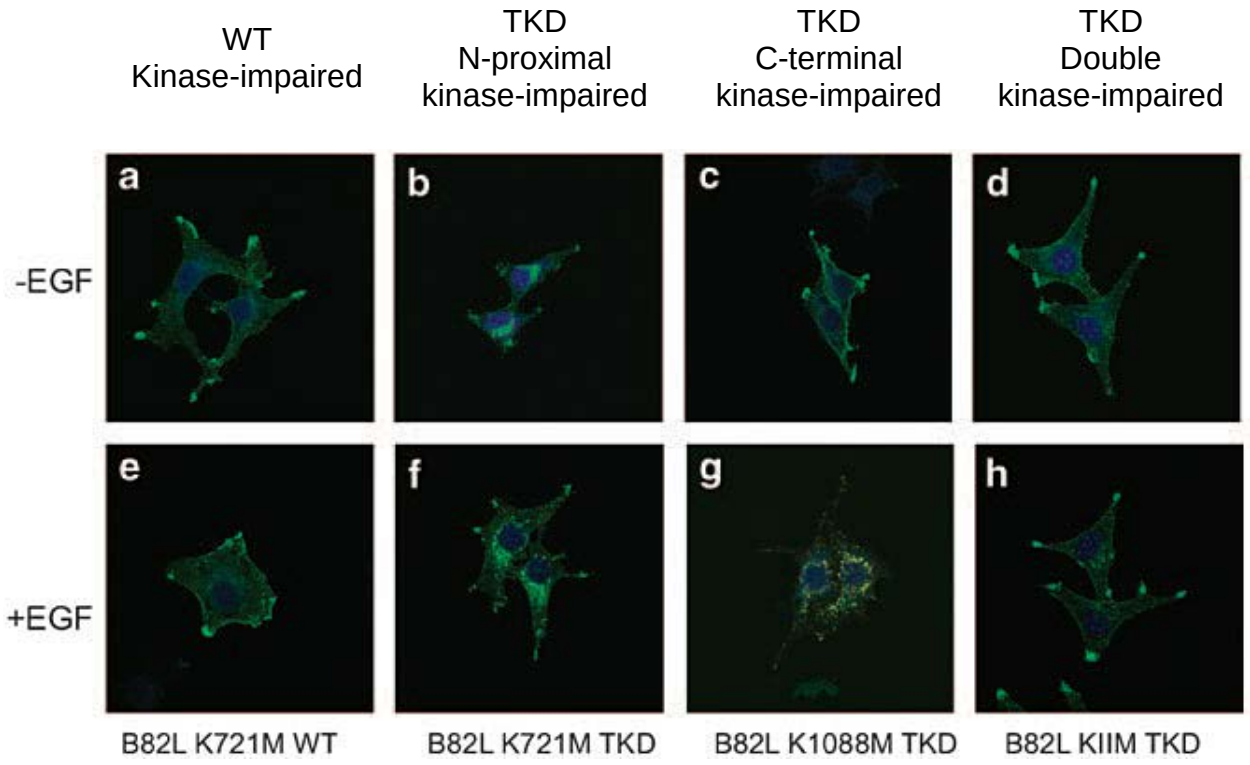

Figure 1.6 The C-terminal kinase of TKD-EGFR confers the receptor's basal cytosolic localization. B82L cells transfected with K721M WT-EGFR (a, e), K721M TKD-EGFR (b, f), K1088M TKD-EGFR (c, g) or KIIM TKD-EGFR (d, h) were treated for 15 min either with vehicle (20mM HEPES) (a–d) or 10nM EGF (e–h) and immunostained for total EGFR expression (green) or phospho-Y1086 activated EGFR (red), as well as for nuclear material using DAPI (blue). Colocalization of total receptor (green) and phosphorylated receptor (red) appears yellow in these merged images. Images were captured at 60X magnification (n = 3). (Adapted from Ozer, *et al.* 2010)

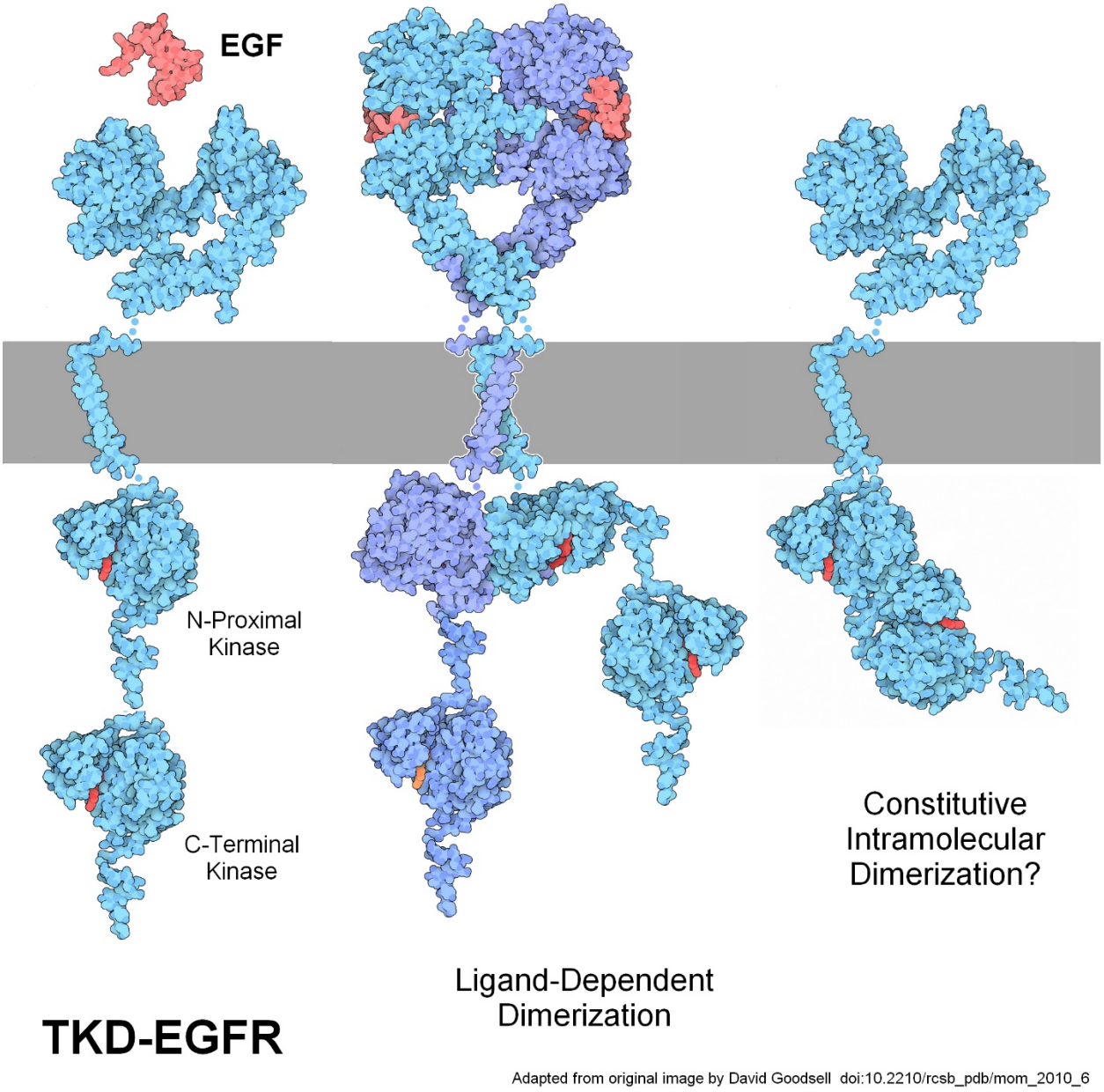

Figure 1.7 TKD-EGFR has distinct ligand dependent and independent activation mechanisms. Ligand binding induces the dimerization of two TKD-EGFR monomers (center), just as it does in the case of wild-type EGFR. The ligand-independent activation of TKD-EGFR may involve the formation of an intramolecular dimer (right), but this possibility has not yet been confirmed. It is also not known whether double dimers, trimers, or other activating configurations are possible. The juxtamembrane domain (between the transmembrane and kinase domains) and the C-terminal tail are not represented in this illustration.

DOMAIN		LENGTH (AAs)	BOUNDARY RESIDUES
Extracellular		621	1-621
Transmembrane		23	622-644
Juxtamembrane	JM-A	19	645-663
	JM-B	19	664-682
N-proximal Kinase		278	683-960
C-Terminus Fragment		70	961-1030
JM Fragment (JM-B only)		19	1031-1049
C-terminal Kinase		278	1050-1327
C-Terminus (full length)		70	1328-1397
		156	1398-1553

Figure 1.8 The Domains of TKD-EGFR. In-frame duplication of exons 18-26 results in a tandem repeat of residues 664-1030. This sequence encodes the JM-B segment of the juxtamembrane ("juxtamembrane latch"), the kinase domain, and 70 residues of the C-terminus are duplicated in tandem. The resulting variant, TKD-EGFR, is a 1553-amino acid 190 kDa protein, significantly larger than the 1186-amino acid 170 kDa wild-type EGFR.

Chapter 2:

General Introduction to Vascular Adaptation in Pregnancy

2.0 Introduction to Pregnancy-Adapted Vascular Function

Soon after implantation, the maternal vasculature begins to exhibit increases in heart rate, stroke volume, plasma and red blood cell volume, and angiogenesis (Reviewed in Page *et al.* 1972). However, the increased cardiac output and blood volume are not associated with hypertension, as they would be in the nonpregnant state, because there is a concomitant fall in vascular resistance associated with pregnancy. There are several reasons for this (Reviewed in Khalil and Granger 2002). Firstly, there is significantly enhanced production of nitric oxide (NO), prostacyclin (PGI2), and endothelium-derived hyperpolarizing factor (EDHF) from the endothelium. Secondly, increased NO output leads to a dramatic elevation of cGMP (Rosenfeld *et al.* 1996; Conrad *et al.* 1999). In late pregnant ewes, this accelerated production of cGMP was significantly downregulated (a 66% reduction) by treatment with L-NAME, an inhibitor of endothelial nitric oxide synthase (eNOS) (Rosenfeld *et al.* 1996). Thirdly, cAMP production in the vascular smooth muscle is elevated 40% due to the increased production of PGI2 (Kopp *et al.* 1977). Additionally, EDHF induces membrane hyperpolarization by opening K+ channels in the smooth muscle. Together, these changes cause vascular smooth muscle to relax (Reviewed in Khalil and Granger 2002). Growth factor-stimulated angiogenesis further helps lower vascular resistance by increasing the cross-sectional area of blood flow and total volume of the circulatory system.

2.0.1 Failure of Vascular Adaptation

Diseases of pregnancy such as intrauterine growth restriction (IUGR) and preeclampsia (PE) are characterized by a failure of these adaptations. For example, expression of eNOS is reduced in placental microvasculature of ovine IUGR pregnancies (Galan *et al.* 2001). Another study found that human umbilical vein endothelial cells (HUVEC) obtained from newborn infants with IUGR displayed a 40% decrease in eNOS activity and a 70% decrease in cGMP compared to HUVEC obtained from healthy pregnancies (Casanello and Sobrevia 2002). Additionally, the harmful effects of smoking on fetal development are due in part to inhibition of NO production. In one study, mothers who smoked exhibited a 40% decrease in eNOS activity compared to nonsmoking mothers (Andersen et al 2004). Like IUGR, PE is also associated with impaired vasodilator production. Long-term inhibition of eNOS in pregnant rats induced PE-like symptoms of hypertension and proteinuria (Molnar et al 1994). Furthermore, HUVEC from newborns of PE patients produced 80% less NO than HUVEC obtained from normotensive pregnancies. (Orpana et al 1996). Similarly, PGI2 production is lower in preeclamptic women (Fitzgerald et al 1987). Preeclampsia is also associated with increased levels of circulating growth factors such as vascular endothelial growth factor (VEGF) (El-Salahy *et al.* 2001). When VEGF or serum from preeclamptic women was administered to myometrial resistance vessels obtained at the time of cesarean section, the vessels exhibited significant downregulation of endothelium-dependent vasodilation (Brockelsby et al 1999). Preeclampsia will be further discussed later in this chapter. More recent studies that identified some of the molecular mechanisms of the effects of VEGF will reviewed in Chapter 3.

Because so many vascular adaptations to pregnancy occur at the level of the endothelium, primary endothelial cells and tissues are the preferred experimental models for research conducted by the Bird Laboratory.

2.1 The Endothelium

The endothelium is the interface between the bloodstream and the vessel, lining the lumen of all veins and arteries. Endothelial cells maintain vascular tone, local blood flow regulation, and blood pressure through the production of vasodilators. The endothelial monolayer also regulates vascular permeability, forming a protective barrier that prevents undesired entry into or exit from the circulation. Crossing the endothelium is achieved by two distinct methods: transcytosis, the vesicular trafficking of molecules through endothelial cells (Minshall *et al.* 2003), and paracytosis, the trafficking of molecules and immune cells through the spaces between endothelial cells. Paracellular trafficking requires the breakdown of the adherens junctions (~80%) and tight junctions (~20%) that form the intercellular barrier (Reviewed in Mehta and Malik 2006). This is a necessary process, for example, when immune cells need to leave the bloodstream to reach their intended target tissue. Loss of endothelial monolayer integrity, however, is associated with numerous pathologies (Reviewed in Vandenbroucke *et al.* 2008).

2.1.1 The Vital Role of Endothelial Cells

Endothelial cells are necessary at the most fundamental level for the angiogenesis required during pregnancy to maintain sufficient blood flow to the uterus. The formation of larger arteries and veins from the spouted capillaries is induced by signals secreted by the endothelium to smooth muscle cells (Beck and D'Amore 1997). Maintenance of vascular tone is dependent on endothelial cell production of vasodilators such as nitric oxide (NO) and prostacyclin (PGI2). The combination of angiogenesis and increased synthesis of vasodilators facilitates a dramatic improvement in blood flow—particularly to the uterus—needed to provide oxygen and nutrients for the developing fetus (reviewed in Bird *et al* 2003). However, endothelial cells have many other cellular functions in addition to angiogenesis and vasodilator production. For example, endothelial cells are the only source of von Willebrand Factor (vWF), a glycoprotein that functions as a binding partner for the

essential blood-clotting protein Factor VIII and as an essential cofactor necessary for platelet adhesion. Endothelial cells release vWF constitutively or in response to histamine or thrombin during blood clotting. Agonist stimulation of endothelial cells induces vWF release via a Ca2+-dependent mechanism. Vesicles containing vWF fuse with the plasma membrane, taking P-selectin with them and depositing it on the cell surface (Reviewed in Pearson 2000). P-selectin (along with E-selectin and L-selectin) capture leukocytes by rapidly and reversibly binding to oligosaccharides on the surface of leukocytes, thereby regulating leukocyte rolling (Toothill *et al*. 1990).

Because the endothelium maintains the barrier between the circulation and the surrounding tissue, endothelial cells are responsible for controlling vascular permeability. The endothelial cell barrier function is maintained by three types of junctions: adherens junctions, which regulate vascular permeability via redistribution of vascular endothelial (VE)-cadherin (reviewed in Bazzoni and Dejana 2004); tight junctions, which seal the endothelial cell monolayer; and gap junctions, which allow transcellular migration of small molecules and ions between cells (Dejana *et al.* 1995, Schnittler *et al.* 1998). I will summarize what is known about the key role of gap junctions in pregnancy-adapted vascular function in Chapter 3.

2.1.2 Some General Observations About Pregnancy-Adapted Programming of the Endothelium

'Pregnancy-adapted programming'—a term coined by Ian Bird—refers to events at the level of cell signaling that enable enhanced function of the maternal vascular endothelium sufficient to accommodate the demands of pregnancy. However, it is a misconception to think of pregnancy-adapted programming as somehow imbuing normal vasculature with a superhuman ability to vasodilate. More accurately, endothelial cells are typically kept in a state of impaired functionality and only allowed to express full vasodilatory potential during pregnancy. Conversely, it is

inaccurate to think of nonpregnant endothelial cells as simply low functioning pregnant cells, because the vascular adaptations in pregnant cells are facilitated by distinct signaling mechanisms not utilized by nonpregnant cells (Alvarez, PhD Dissertation, 2016).

There are two important classes of adaptations that endothelial cells undergo during pregnancy. Firstly, the expression level of vasodilatory pathway proteins (e.g. eNOS, COX-1, cPLA2, etc.) in endothelial cells is initially higher during pregnancy, but in our uterine artery endothelial cell (UAEC) model we observe that this adaptation is lost after four passages (Bird *et al.* 2000). The high levels of these molecules are maintained *in vivo* by the action of chronically elevated hormones at the site of placentation (Meyer *et al.* 2010). When UAEC are removed from the uterine arteries of late pregnant ewes and placed in typical culture conditions, the hormonal signals are lost, thereby returning the elevated expression levels of vasodilation-associated molecules to nonpregnant levels. Secondly, there are pregnancy-specific differences in signaling, persisting at passage 4 and beyond, that relate to the enhancement of pro-vasodilatory Ca2+ bursting. The enhanced function of Cx43 gap junctions and the altered responsiveness of Cx43-associated kinases, for example, is not dependent on local hormone concentrations. These programmed changes may be triggered by placenta-driven hormone secretion, but they persist well after the hormonal signals are absent. Furthermore, these programmed changes are systemic and not confined to the uterine vasculature. In vitro, pregnancy-adapted programming is not only observed in UAEC, but also in human hand vein endothelial cells (HHVE) and HUVEC. The reason the uterus is affected most profoundly is because uterine vessels experience not only both the endocrine/paracrine effects and programmed effects on vascular function, but also increased angiogenesis. Only months after childbirth are these vascular adaptations fully lost *in vivo*, possibly due to the actions of prolactin and other lactation-associated hormones, just as oxytocin mediates the return of the uterus to its nonpregnant state. Perhaps in the future,

epidemiological studies will compare the rates of loss of vascular adaptations to pregnancy of breastfeeding mothers and those that do not breastfeed.

A more specific review of how pregnancy-adapted programming is achieved at the level of cell signaling will be provided in Chapter 3.

2.2 Preeclampsia

Preeclampsia (PE) is a disease of failed vascular adaptation to pregnancy, occurring in 3-8% of pregnancies. and causing ~50,000 deaths per year (Reviewed in Duley 2009). Symptoms include hypertension and proteinuria, with severe cases eventually leading to liver and kidney dysfunction. If untreated, PE can lead to seizures (eclampsia), brain damage, and maternal and/or fetal death (Reviewed in Reslan and Khalil 2010). PE cannot be diagnosed until the 20th week of pregnancy by the onset of hypertension (blood pressure ≥ 140/90 mmHg) accompanied by proteinuria (≥ 300 mg over 24 hours) (Sibai 2003). Aside from damage to the blood vessels, PE negatively affects the heart and lungs, the central nervous system, and the liver and kidneys, and it raises the risk of seizures (Reviewed in Steegers et al. 2010). The only “cure” for PE remains delivery of the infant and expulsion of the placenta, but the induction of a preterm delivery has serious risks as well (Sibai and Barton 2007).

One of the causes of the impaired endothelial dysfunction associated with PE seems to be the release of inflammatory cytokines resulting from placental ischemia (Roberts *et al.* 1989; Roberts *et al.* 1991). The loss of pregnancy-adapted vasodilation only serves to further promote placental ischemia, which triggers a feed forward loop of progressive vascular dysfunction and deterioration.

2.2.1 The Pathology of Preeclampsia

As stated earlier, healthy pregnancy is characterized by enhanced vasodilation and a systemic reduction in vascular resistance, thus allowing the maternal vasculature to accommodate the greater blood volume required to meet the combined demands of the mother and fetus. A preeclamptic pregnancy is characterized by poor vasodilation and a systemic increase in vascular resistance, thus causing hypertension and kidney dysfunction (Dennis *et al.* 2012). Blood flow to the uterus is particularly impaired, but all vessels, even the microvessels of the eyes, are affected (Takata *et al.* 2002). Women with preeclampsia (PE) have elevated serum levels of vasoconstrictors (e.g. endothelin 1 (EN-1), thromboxane) (Aggarwal *et al.* 2012; Wang *et al.* 1991) and display heightened sensitivity to vasopressors (Chesley 1966). Vessels obtained from PE patients exhibited unusually strong responses to vasoconstrictors such as arginine vasopressin (Pascoal *et al.* 1998) and significantly reduced responses to vasodilators (Knock and Poston 1996; McCarthy *et al.* 1993), as well as decreased levels of nitric oxide (NO) (Var *et al.* 2003) and prostacyclin (PGI2) (Chavarria *et al.* 2003). Additionally, endothelium-dependent hyper-polarization (EDH)-induced vasodilation is suppressed in arteries of women with PE. These women express lower levels of placental growth factor (PlGF), which is known to activate EDH (Kenny *et al.* 2002; Luksha *et al.* 2008). Evidence suggests this deficiency in EDH may due to dysfunction in myoendothelial gap junctions (Luksha *et al.* 2010). When resistance vessels from healthy pregnant women are incubated with plasma from preeclamptic women, they exhibit a reduced endothelium-dependent response to bradykinin (Hayman *et al.* 2000). Endothelial dysfunction can even be induced by microparticles extracted from preeclamptic blood plasma in the absence of the plasma itself (VanWijk *et al.* 2002). Plasma-mediated endothelial dysfunction in fresh isolated arteries has been recently shown to be worsened by exposure to oxidized low-density lipoprotein, an effect that can be reversed by inhibition of lectin-like oxidized LDL receptor-1 (LOX-1) (English *et al.* 2013).

Despite the extent to which PE has been characterized, predicting the disease remains difficult, as evidenced by the surprising observation that vessels from healthy pregnant women exhibited suppressed vasodilation when incubated with plasma obtained from pregnant women who had no diagnosis of PE but would *later* go on to develop the disease, suggesting that the failure of vascular adaptation to pregnancy begins long before any symptoms are apparent (Myers *et al.* 2005). In many cases, the manifestation of PE reveals deeper cardiovascular problems that continue to worsen year after year if left untreated (Reviewed in Craisi *et al.* 2008), and there is reason to believe that some of the damage to the maternal vasculature caused by PE is irreversible. Studies have discovered that preeclamptic women exhibit endothelial dysfunction well after delivery, and this is associated with double the risk of death from cardiovascular disease as compared to women that had healthy pregnancies (Agatisa *et al.* 2004; Chambers *et al.* 2001; McDonald *et al.* 2008). This means the importance of finding effective therapies for PE extends beyond the need to reduce the immediate risk to mother and child. Such therapies may be critical for the mother's future health.

2.2.2 Inflammatory Cytokines and Growth Factors in PE

While the etiology of PE is still a subject of much debate, the two most commonly cited processes implicated in causing PE are excessive inflammation and aberrant angiogenesis (reviewed in Myatt and Webster 2009). The cytokine- and growth factor-mediated aggravation of PE can be compared to the cellular response to a wound because these same growth factors and cytokines elevated in PE are also elevated at wound sites. One might even conceptualize PE as the mother's body responding to the progressing pregnancy as if it were a wound. Similarities between PE and the wound response at the level of cell signaling will be discussed further in the next chapter. For now, it is safe to say that the proper regulation of vasodilation and vascular permeability by wound-associated growth factors and cytokines is essential for a healthy pregnancy, and dysregulation of these factors is associated with PE.

Since the clinical profile of PE includes poor uterine blood flow resulting in placental ischemia and hypoxia, one might be tempted to think that an infusion of pro-angiogenic growth factors like VEGF would be beneficial. However, as the data from the Bird Laboratory presented in Chapter 3 will show, VEGF at a maximally mitogenic physiological dose has significant negative effects on vascular function. Further evidence is provided by research outside the Bird Laboratory. When myometrial resistance vessels from pregnant women (obtained at the time of cesarean section) were incubated with VEGF, a significant loss of endothelium-dependent relaxation occurred that was equivalent to the loss induced by plasma from women with PE (Brockelsby *et al.* 1999). Similarly, arteries dissected from subcutaneous fat biopsy specimens of pregnant women displayed impaired bradykinin-mediated dilation, higher basal tone, and intercellular gaps in the endothelial monolayer when incubated with VEGF (Svedas *et al.* 2003). Pregnant mice administered exogenous murine VEGF exhibited hypercoagulation in the placental circulation and a rise in systolic blood pressure (Murakami *et al.* 2005). Other growth factors may also be associated with endothelial dysfunction in PE. EGF and FGF modulate trophoblast invasion in early placental development but could become dysregulated later in pregnancy. Serum concentrations of bFGF were found to be significantly elevated in women with mild PE (Hohlagschwandtner *et al.* 2002) and pregnancy-induced hypertension (Kurz *et al.* 2001) compared to the levels in healthy pregnant women.

Cytokines have long been known to circulate at higher levels during normal pregnancy. However, in 1999, Redman *et al.* proposed that PE might be an *excessive* maternal inflammatory response to pregnancy. Since then, evidence for excessive levels of cytokines in PE patients has accumulated. These include **TNFα** (Kupferminc *et al.* 1994; Vince *et al.* 1995; Conrad *et al.* 1999; Tosun *et al.* 2010; Kronborg *et al.* 2011), **IL-1β** (Rusterholz *et al.* 2007), **IL-6** (Vince *et al.* 1995; Conrad *et al.* 1999; Freeman *et al.* 2004; Casart *et al.* 2007; Lockwood 2008; Tosun *et al.* 2010; Kronborg *et al.* 2011), **IL-8** (Kauma *et al.* 2002; Tosun *et al.* 2010), and **IFNγ** (Banerjee *et al.*

2005; Murphy *et al.* 2009; Tanbe *et al.* 2010; Rytlewski *et al.* 2012). Since PE is a condition of abnormal placentation and hypoxia, it is worth noting that hypoxia alone can raise levels of TNFα, IL-1α and IL-1β even in the normal placenta (Benyo *et al.* 1997). Furthermore, the placenta is not the only source of elevated cytokines. Lockwood *et al.* (2008) suggest the decidua is a greater source of IL-6 in PE. IFNγ levels are elevated in PE patients in plasma, leukocytes, and decidual tissue (Murphy *et al.* 2009). UAEC studies in the Bird Laboratory have already identified expression of several cytokine receptors, including TNFα, IL-1 and IL-6 (Gifford *et al.* 2003). TNFα and IL-1 in particular are known to mediate endothelial cell activation and dysfunction (Reviewed in Pober and Cotran 1990). TNFα impairs endothelial cell function in a number of ways. For example, it suppresses endothelium-dependent relaxation (Bhagat *et al.* 1997) by reducing expression of eNOS (Yoshizumi *et al.* 1993) and inhibiting the activity of argininosuccinate synthase, thus decreasing the availability of arginine needed by eNOS to produce NO (Goodwin *et al.* 2007). Furthermore, TNFα levels are correlated with increased expression of vasoconstrictors, including platelet-derived growth factor (PDGF) (Hajjar *et al.* 1987) and ET-1 (Marsden and Brenner 1992), which are also elevated in the serum of PE patients (Taylor *et al.* 1991; Bussen *et al.* 1999). Amanda Ampey, a former student of Ian Bird and recent graduate of the UW ERP Program, has shown that TNFα is highly destructive to the integrity of the endothelial cell monolayer in culture (Ampey *et al.*, in preparation). Interestingly, preeclamptic women also display increased activity of the immune regulator NF-κB (Luppi *et al.* 2006), but the role of NF-κB in the etiology or maintenance of PE is unclear.

I included this section to illustrate some of the ways that elevated cytokines promote endothelial dysfunction, which is why cytokines are a major focus of research in the Bird Laboratory. My project involved no cytokines, but rather focused on VEGF and its receptors, and how comparisons with the EGF/EGFR system could help us to identify the distinct roles of the MEK/ERK, PI3K/Akt, and Src pathways in regulating the mechanisms of pregnancy-adapted

vasodilation and vascular permeability. Chapter 3 will include a detailed summary of what has been discovered about the effects of VEGF on pregnancy-adapted programming prior to the writing of this dissertation.

2.3 A Novel Method for Investigating Endothelial Dysfunction

The past 20 years of research into the molecular mechanisms of vascular adaptation to pregnancy have revealed that downregulation of these adaptations is mediated by canonical epidermal growth factor receptor (EGFR) cancer signaling pathways. This is not to say that EGFR in particular is necessarily responsible for the dysregulation of these pathways, but rather that the pathways are critical irrespective of which growth factor or cytokine is capable of activating them. “Canonical EGFR cancer signaling pathways” just means pathways that were shown by cancer researchers to be activated by EGFR. Indeed, a recent comparison of 29 PE placentas and 19 healthy placentas found no significant differences in EGF or EGFR expression levels (Kosovic *et al.* 2017). Additionally, there are no documented cases of PE involving activating mutations of EGFR, nor do any known EGFR mutant-expressing pregnant endothelial cell lines exist, so it is not likely that EGFR is a major player in diseases of endothelial dysfunction like PE. Still, a recent transcriptome meta-analysis found that dysregulation of “canonical EGFR cancer signaling pathways” occurs with high frequency in the PE placenta (Moslehi *et al.* 2013).

The fact that EGFR-associated pathways are dysregulated in the PE placenta led us to ask if the simple overexpression of EGFR in pregnancy-adapted uterine artery endothelial cells (P-UAEC), which express very low levels of endogenous receptor, might be sufficient to drive PE-associated endothelial dysfunction. Firstly, we hypothesized that overexpression of EGFR in P-UAEC would enable EGF treatment to inhibit the molecular mechanisms of vascular adaptation to pregnancy

in P-UAEC just as VEGF treatment does. Secondly, we predicted that overexpression of EGFR in P-UAEC at a level sufficient to induce constitutive activity (or expression of a constitutively active EGFR mutant) could result in a permanent basal inhibition of vasodilatory mechanisms, thus “engineering preeclampsia”—i.e. simulating the functionally-impaired state of the vascular endothelium in PE.

Due to decades of relatively well-funded cancer research, the tools associated with the study of EGFR are extensive. A wide variety of pharmacological EGFR inhibitors are commercially available, as are fluorophore-tagged EGFR ligands. Dozens of highly selective antibodies that target specific sites on EGFR have been developed, including reliable antibodies for each of the many distinct phosphotyrosine sites. Site directed mutagenesis of particular EGFR phospho-tyrosine sites can be strategically employed to eliminate the receptor’s ability to activate specific signal transduction pathways. Furthermore, a plethora of naturally occurring and artificially created EGFR mutants have been characterized. There are dozens of identified missense mutations, deletion mutations, and duplication mutations—some that increase ligand sensitivity (L834R), some that decrease it (del746-750), and some that eliminate ligand dependency altogether (EGFRvIII). There are also mutants that exhibit impaired tyrosine kinase activity (K721M).

The focus of this dissertation is how we employed overexpression of EGFR in P-UAEC to gain greater understanding of the molecular mechanisms of pregnancy-adapted programming in endothelial cells. The next two chapters provide a more detailed overview of the relevant signaling events (Chapter 3) and the technical considerations that must be addressed when designing such a project (Chapter 4). The subsequent “Results” chapters provide new insights into the relative contributions of the ERK1/2 and Src pathways in growth factor-induced downregulation of GJC (Chapter 5) and reveal vital roles for the PI3K/Akt pathway in the maintenance of GJC and endothelial cell monolayer integrity (Chapter 6). In the “Final Discussion” chapter, the results will

be summarized, new models will be proposed, and themes that arose along the way will be explored more thoroughly (Chapter 7).

Chapter 3:

Signaling Mechanisms of Pregnancy-Adapted Programming

3.1 Pregnancy-Adapted Programming

A healthy pregnancy requires sweeping adaptations of the maternal vasculature to provide the developing fetus with sufficient oxygen and nutrients for optimal growth. These adaptations comprise not only preferential blood flow to the uterus, but compensatory increases in cardiac output and systemic blood volume (Reviewed in Sanghavi and Rutherford 2014). To accommodate these changes and avoid hypertension, the vascular endothelium must also raise production of vasodilators including nitric oxide (NO) enough to attain the enhanced level of chronic vasodilation that is needed throughout the duration of the pregnancy. Because increased synthesis of NO is achieved by a rise in the activity of endothelial nitric oxide synthase (eNOS), it is important to understand how an endothelial cell regulates eNOS activity. To this end, research in the Bird Laboratory is focused on (1) identifying the specific signaling pathways and effector molecules that facilitate sustained eNOS activation, (2) determining how this mechanism of activation is enhanced during pregnancy to meet the increased needs of mother and fetus, (3) understanding how pregnancy-adapted enhancement of vascular endothelial function is physiologically inhibited in hypertensive diseases of pregnancy such as preeclampsia (PE), and (4) discovering effective therapies for enabling/restoring enhanced endothelial function in PE pregnancies.

Since 1990, it has been known that the concentration of intracellular free calcium (termed [Ca2+]i) was linked to eNOS activity and NO production in vascular endothelium *(*Lopez-Jaramillo *et al.*

1990*)*, but it would take another decade to begin to work out the general mechanism of eNOS activation (Lin *et al*. 2000), which I will discuss later in this chapter. To begin my outline, I would like to present a key finding of a landmark study of vascular adaptation to pregnancy that had a major influence on the subsequent direction of research in the field. Upon observation of human hand vein endothelial cells (HHVE) obtained from nonpregnant (NP-HHVE), pregnant (P-HHVE) (~35 weeks) and preeclamptic (PE-HHVE) women (~36 weeks), Mahdy *et al.*(1998) found that these cells responded differently to treatment with ATP. While cells from all three sources responded to ATP with a transient increase in [Ca2+]i followed by a sustained elevation above basal levels, the responses in the cells from pregnant women were significantly greater than the responses from nonpregnant and preeclamptic women, despite weeks of growth in cell culture outside their natural environment. The authors noted that HHVE obtained from PE patients possessed none of the vascular adaptations exhibited by P-HHVE and instead behaved like NP-HHVE, thereby concluding that "preeclampsia may be a defect in the ability of the endothelium to adapt in pregnancy." Therefore, 'pregnancy-adapted programming'—a term subsequently coined by Ian Bird—refers to events at the level of cell signaling that enable enhanced function of the maternal vascular endothelium sufficient to accommodate the demands of pregnancy.

3.2 The Ovine Uterine Artery Endothelial Cell (UAEC) Model for Studying Vascular Adaptation to Pregnancy

Due to the many practical and ethical concerns associated with obtaining tissues from pregnant women, a suitable animal source of cells and/or tissues is needed. Like HHVE, endothelial cells isolated from the uterine arteries of pregnant ewes are a good choice because they retain their pregnancy-adapted programming and they grow well in cell culture (Bird *et al.* 2000; Gifford *et al.* 2003). While these cells do initially express higher levels of eNOS protein than those taken from

nonpregnant ewes, this difference is lost after four passages. The real value of uterine artery endothelial cells taken from pregnant sheep and cultured to passage 4 (the formal definition of P-UAEC) lies in the fact that they exhibit enhanced eNOS activation and NO production relative to NP-UAEC despite similar levels of eNOS expression (Sullivan *et al.* 2006, Grummer *et al.* 2009). This should not be interpreted to mean that the level of eNOS expression is not important. Clearly, the maximum capacity for NO synthesis in UAEC (or any cell, for that matter) must be a function of the total amount of eNOS available. However, it does mean that pregnancy-adapted programming comprises specific alterations in cell signaling that increase eNOS activation efficiency, independently of eNOS expression level.

While the Bird Laboratory uses a variety of cell and tissue types for its research, all the experimental data I have generated for this dissertation were obtained using P-UAEC. These cells adhere well to commonly used culture dishes and multi-well plates. When plated at low density, they form a confluent monolayer in approximately one week. I have subjected P-UAEC to a wide range of molecular biology techniques, including flow cytometry, Western Blot, adenoviral transduction, calcium imaging, microscopy, and electric cell-substrate impedance sensing (ECIS). They maintain high viability in experiments that require live cells and produce consistent data that enable us to identify the molecular mechanisms of vascular adaptation to pregnancy.

3.3 eNOS Phosphorylation and eNOS Activity

Early studies of eNOS activation were influenced by the assumption that elevated NO production was simply the result of elevated eNOS expression in maternal blood vessels, but the regulation of eNOS activity has continuously proven to be more subtle and complex than previously assumed. When researchers began to examine the phosphorylation status of eNOS, a shear

stress-induced phosphorylation of S1177 was found to be associated with increased eNOS activity (Dimmeler *et al.* 1999), while basal T495 phosphorylation was found to be inhibitory (Fleming *et al.* 2001). Subsequent experiments revealed that phosphomimetic substitution of S615 (Tran *et al*. 2008) or S1177 (Tran *et al.* 2009), which has similar functional effects as phosphorylation of these sites, nearly doubles maximal synthase activity by reducing the [Ca2+]i needed (i.e. lowering the threshold) for eNOS activation. Furthermore, phosphorylation of S615 and S1177 together lowered the activation threshold of eNOS enough to confer enzyme activity at the basal level of [Ca2+]i (50-100 nM) (Tran *et al.* 2009) and maximal activation at [Ca2+]i levels elevated in the physiologic range (~ 300nM).

Despite these seemingly straightforward results, research conducted in the Bird Laboratory prior to Trans study in 2009 had already called the completeness of this phosphorylation control of eNOS paradigm into question with the discovery that the phosphorylation state of eNOS does not necessarily correlate with activity. In P-UAEC, treatment with the calcium-mobilizing agonist ATP induced phosphorylations of eNOS S617, S635, and S1179 (S615, S633, and S1177, respectively, in humans) and promoted eNOS activation, whereas treatment with the phorbol ester TPA (12-O-Tetradecanoylphorbol-13-acetate, also called PMA) increased these same eNOS phosphorylations but *without* activation. Additionally, TPA and ATP cotreatment of P-UAEC reduced ATP-stimulated eNOS activity, despite promoting a strong “activating” phosphorylation of S1179 and having no effect on “inhibitory” T497 phosphorylation (T495 in humans), yet TPA inhibition of ATP-stimulated eNOS activity was associated with an increase in T497 phosphorylation in COS-7 cells transiently transfected to express ovine eNOS. Therefore, phosphorylation status of key residues is connected to eNOS activation, but is not sufficient to predict when or how activation will occur (Cale and Bird 2006).

Phosphorylation of eNOS appears to be analogous to the sound controls on a stereo. The magnitude of eNOS activity can be altered (in a manner partially dependent on cell type) by

phosphorylation, just like the sound produced by a stereo can be modulated by the bass, treble, and volume controls. Depending on the cellular environment, a particular eNOS phosphorylation might enhance or attenuate eNOS activity or have no effect at all, like the volume of a stereo can be cranked up, or reduced to a whisper, or left unchanged. Of course, if the power switch of the stereo is shut off, the music will fade out, no matter how the other knobs are adjusted, and this is true of eNOS activity as well. The “power switch” that sustains NO production and maintains vasodilation will be discussed next.

3.4 Pregnancy-adapted programming requires capacitative calcium entry (CCE)

As stated earlier, it was known more than 25 years ago that eNOS activity and NO production were dependent on agonist-induced mobilization of [Ca2+]i in the vascular endothelium (Lopez-Jaramillo *et al.* 1990, Buckley *et al.* 1995). However, calcium signaling in response to physiologic agonists has two distinct components: an immediate [Ca2+]i peak associated with direct intracellular release of Ca2+ from the endoplasmic reticulum (ER) and a sustained phase elevation of [Ca2+]i in the form of periodic bursts dependent on the influx of extracellular Ca2+. So which component is responsible for maintaining eNOS activity—ER release or capacitative calcium entry (CCE)? This question was answered in a 2000 paper published in the Journal of Biological Chemistry. Since eNOS is localized to caveolae in the plasma membrane, Lin *et al.* (2000) hypothesized that the proximity to CCE channels on the plasma membrane might be indicative of a CCE-based activation mechanism. To test this hypothesis, two chimeras were created—**EHA** (eNOS linked to the calcium-activated photoprotein aequorin) and **MHA** (myristoylation-deficient EHA)—and each were expressed in COS-7 and bovine pulmonary artery endothelial cells. The EHA fusion protein retained the ability to traffic to the plasma membrane

and bind to caveolae, whereas the MHA fusion protein was localized to the cytosol. Measurements of eNOS activation revealed that the activity of EHA was more responsive to CCE than intracellular release, whereas MHA eNOS activity was more responsive to intracellular Ca2+ release. Furthermore, NO production via CCE was 10-fold greater than that generated by an equal rise in [Ca2+]i due to the Ca2+ ionophore ionomycin. These results demonstrated that CCE specifically, and not general [Ca2+]i level, is the principle stimulus for sustained activation of eNOS under normal physiological conditions.

Subsequent experiments performed in the Bird Laboratory revealed that the CCE phase of the Ca2+ burst response is significantly elevated in P-UAEC, and takes almost twice as long to return to basal level of [Ca2+]i, as compared to CCE in NP-UAEC. Additionally, this sustained Ca2+ influx is blocked by pharmacological inhibition of phospholipase C (PLC) or inositol 1,4,5-triphosphate receptor (IP3R), resulting in a 40-60% reduction in eNOS activity (Sullivan *et al.* 2006), but is unaffected by the L-channel inhibitor nifedipine (Gifford *et al.* 2006a), suggesting the involvement of transient receptor potentiated channels (TRPC). Indeed, TRPC3 and TRPC6 are present in UAEC (Gifford et al. 2006b), as well as IP3R1, IP3R2, and IP3R3 (Gifford et al. 2003), but no differences between expression levels of these proteins in P-UAEC vs. NP-UAEC were detected (Gifford et al 2006b). However, co-immunoprecipitation revealed an ATP-sensitive association between IP3R2 and TRPC3 in P-UAEC but not in NP-UAEC, hinting that ATP activation of TRPC3 may be the mediator of pregnancy-adapted CCE.

Further evidence of pregnancy-adapted programming occurring at the level of the CCE mechanism was obtained using Ca2+-free experimental buffer. When P-UAEC and NP-UAEC were stimulated with ATP in Ca2+-free buffer, no difference was observed between P and NP cells. ER release of Ca2+ returned to near basal levels of [Ca2+]i in both P and NP cells in 5-6 minutes (Gifford *et al.* 2006b). However, when thapsigargan was added to the Ca2+-free

experimental buffer to deplete ER stores, subsequent addition of Ca2+ to the buffer produced a much greater CCE response in P-UAEC than in NP-UAEC (Gifford *et al.* 2006a).

Together, these results suggest the difference between P and NP cells lies not in expression of IP3R or TRPC, nor in the release of ER Ca2+ stores, but specifically in the function of the IP3R-TRPC complex that facilitates CCE. A corollary of this conclusion is that we would expect any cellular process that utilizes this mechanism to be enhanced during pregnancy.

3.5 CCE requires functional connexin 43 (Cx43) gap junctions

Pregnancy-adapted programming in P-UEAC is dependent on intercellular communication. Cell density studies performed in the Bird Laboratory found that pregnancy-specific enhancement of CCE (i.e. more cells exhibiting Ca2+ bursting, more bursts per cell, and greater burst synchronization) only becomes fully apparent at higher cell culture densities. At low confluence, in which few cells establish contact with other cells, the Ca2+ response to agonists is similar to that of NP-UAEC. Lucifer yellow dye transfer analysis revealed that P-UAEC maintain a higher degree of cell-to-cell connectivity than NP-UAEC at the same cell density, and this connectivity is achieved via gap junctions (Yi *et al.* 2010a).

A gap junction is a pore that connects two cells and allows small molecules and ions to travel from one cell to another. It is formed when a connexon (made of six connexin (Cx) molecules) embedded in the plasma membrane of one cell links to a connexon embedded in the plasma membrane of an adjacent cell. To determine which type of Cx protein is assembled into connexons in UAEC, peptide mimetics of the extracellular loops of specific Cx molecules were administered to competitively block Cx interactions between cells. In UAEC, only the CX43,37-specific mimic, GAP27, completely cancelled the pregnancy-adapted programming of CCE in P-

UAEC, reducing it to the level of NP-UAEC. GAP26, specific to CX37 and 40, was completely ineffective, thus demonstrating that Cx43 is the key isoform that mediates cell synchronization (Yi *et al.* 2010a). Finally, (43,37)GAP27 inhibition of CX43 function eliminated the pregnancy-specific increase in eNOS activation in P-UAEC (Yi *et al.* 2010a), suggesting CCE bursts to be causally linked to eNOS activation, as our model would predict.

The importance of Cx43 is further supported by Western blot data, which show strong expression of Cx43 in UAEC, whereas Cx37 and Cx40 are virtually undetectable. Like other proteins involved in the CCE mechanism, no difference in the expression of CX43 was observed between P-UAEC and NP-UAEC (Yi *et al.* 2010a). Therefore, the enhanced function of gap junctions in P-UAEC must be due to post-translational modifications of Cx43 that result in more open junctions at the plasma membrane, such as differences in protein trafficking or altered Cx43 phosphorylation status.

3.6 Cx43 gap junctions are regulated by several major signaling pathways

The connexin (Cx) proteins that assemble to form gap junctions have significantly faster turnover rates than other transmembrane proteins. Cx43, the most commonly expressed Cx protein, has a half-life of only 1 to 5 hours (Reviewed by Solan and Lampe 2016). This means gap junctions are in a constant state of flux, continuously altering their function in response to the rapidly changing needs of the cells and tissues that utilize them. In addition to regulation of vasodilation, gap junctions are involved in numerous vital cellular processes, including proliferation, differentiation, and wound healing. Their essential contribution to vertebrate life is evidenced by the fact that Cx43 knockout mice die shortly after birth (Reaume *et al.* 1995). The critical

importance of Cx43 gap junctions and their dynamic nature, therefore, requires that all aspects of their function—the transport of Cx43 protein, assembly of Cx43 proteins into functional gap junctions, facilitation or inhibition of intercellular communication, and junction disassembly—must be tightly controlled. As of this writing, 19 of the 26 serines and 2 of the 6 tyrosines in the C-terminal region of Cx43 are known to be phosphorylation sites. The regulatory functions of several of these sites have been determined and the kinases that phosphorylate them have been identified, but many sites have yet to be characterized (Reviewed in Solan and Lampe 2016).

A series of phosphorylations found to be associated with gap junction assembly have been identified. First, cAMP-dependent protein kinase (PKA) promotes trafficking of Cx43 vesicles to the plasma membrane by phosphorylating S364/365 (TenBroek *et al.* 2001). At the plasma membrane, casein kinase 1 (CK1) phosphorylates some combination of S325/S328/S330 on Cx43 embedded in disordered connexons, which stimulates the organization of very small Cx43 gap junctions (Cooper and Lampe 2002). These small gap junctions then become significantly larger following phosphorylation of S373 by Akt, which enables connexon aggregation by dissociating Cx43 from ZO-1 scaffolding (Dunn *et al.* 2014).

Conversely, closure and disassembly of gap junctions can be caused by such diverse events as treatment with EGF or TPA, immune responses, or wounding. Each of these stimuli results in phosphorylation of S368 via PKC and S255 and S279/S282 via ERK1/2, which have been shown to restrict transport across the gap junction (Reviewed in Solan and Lampe 2014; 2016).

The ability of v-Src, the constitutively active avian viral form of Src, to shut down gap junctional communication (GJC) was first documented over 35 years ago, before the structure and function of connexin proteins was understood (Atkinson et al. 1981). It was soon determined that overexpressed or activated c-Src had the same down-regulating effects on GJC, and that these effects were prevented by a mutation (Y416F) of the active site of c-Src (Azarnia et al. 1988).

Later research revealed that inhibition of GJC by v-Src was dependent on tyrosine phosphorylation of Cx43 (Filson *et al.* 1990; Crow *et al.* 1990), specifically Y265 (Swenson *et al.* 1990). More recently, Src regulation of GJC has revealed itself to be far more complex. In addition to phosphorylating Cx43 on Y247 and Y265 directly, Src also induces phosphorylation of S262 and S368 via PKC and S279/S282 via the MAPK pathway, while also inhibiting phosphorylation of S364/365, perhaps inhibiting the assembly of new gap junctions by reducing the trafficking of Cx43 to the plasma membrane (Solan and Lampe 2009).

Researchers Joell Solan and Paul Lampe have created a model of gap junction regulation and turnover based on observations of a sequential recruitment of at least four kinases with several check points that they refer to as a "kinase program." In response to wounding, for example, specific serines (and tyrosines) of Cx43 are phosphorylated by Akt at 5–30 min, PKC and MAPK at 15–60 min, and Src at 30 min–24 h (Reviewed in Solan and Lampe 2014; 2016). Note that one of the key kinases associated with gap junction assembly—Akt—is also a potential trigger for gap junction closure and disassembly. This makes sense in the context of a wound site. Initially, the increase in gap junctional size following Akt phosphorylation of S373 enhances intercellular communication, allowing for greater recruitment of factors needed for a robust healing and immune response. These same growth factors and inflammatory cytokines then serve as "off switches," shutting down and dismantling the gap junctions so the damaged cells can be isolated and removed from the undamaged tissue.

One such growth factor elevated at wound sites and of particular relevance to our research is the vascular endothelial growth factor (VEGF), which is also elevated in PE (Reviewed in Hayman *et al.* 1999) and can cause PE-like symptoms in pregnant mice (Murakami *et al.* 2005). Research from the Bird Laboratory detailing the ability of VEGF to induce inhibitory phosphorylations of Cx43 and suppress pregnancy-adapted endothelial function will be discussed next.

3.7 VEGF negatively regulates CCE via ERK- and Src-mediated phosphorylations of Cx43

The vascular endothelial growth factor (VEGF) is a *family* of growth factors with at least *seven* distinct isoforms and further splice variants:

VEGF-A, VEGF-B, VEGF-C, VEGF-D, VEGF-E, VEGF-F, PlGF
|
Splice variants of VEGF-A
VEGF-A_{121}, VEGF-A_{165}, VEGF-A_{189}, VEGF-A_{206}

VEGF acts through binding to VEGF receptors, At least two of which are present in UAEC—**VEGFR-1** and **VEGFR-2**. VEGFR-1 also has a splice variant—soluble VEGF receptor type 1, or **sFlt-1**—which will be discussed in a subsequent section of this chapter. A single ligand stimulates VEGFR tyrosine kinase activity by selectively inducing the dimerization of two VEGFR monomers. Placental growth factor (PlGF), possessing a low binding affinity for VEGFR-2 (K_d > 100 nM; Park *et al.* 1994)), produces only VEGFR-1 homodimers. In contrast, VEGF-E, which possesses a nearly identical affinity for VEGFR-2 as VEGF-A_{165} (Ogawa *et al.* 1998), does not bind to VEGFR-1 and thus produces only VEGFR-2 homodimers. VEGF-A, induces the formation of both homodimers and the R1/R2 heterodimer in ratios dependent on the expression levels of VEGFR-1 and -2, and the relative binding affinity of VEGF-A to each receptor. Unless otherwise noted, all experiments presented that involved the use of VEGF were done specifically with **VEGF-A_{165}**, therefore the terms 'VEGF' and 'VEGF-A_{165}' will be used interchangeably throughout most of this dissertation.

When fresh ovine uterine arteries (UA Endo, a term that also applies to intact sheets of endothelial cells) are pretreated for 30 minutes with VEGF-A_{165} (10 ng/ml), the initial peak amplitude of the ATP-induced [Ca2+]i burst response remains the same, but the sustained CCE phase in P-UA Endo is reduced to the level observed in NP-UA Endo. Likewise, the production of NO quantified

by DAF-2 fluorescence in P-UA Endo is reduced to the level measured vessels from NP ewes (Yi *et al.* 2011). To determine which receptor—VEGFR1 or VEGFR2—mediates VEGF inhibition of the ATP-induced Ca2+ burst response, P-UAEC were pretreated with the VEGFR1-selective agonist PlGF (100 ng/mL) or the VEGFR2-selective agonist VEGF-E (100 ng/mL). Only VEGF-E reproduced the effect of VEGF-A_{165} pretreatment (~20% inhibition), albeit at 10X the VEGF-A_{165} dose, suggesting that inhibition of the CCE phase of the Ca2+ response to agonists is mediated by VEGFR2 homodimers. (The topic of VEGFR heterodimers will be discussed more thoroughly in Chapter 7.) PlGF pretreatment had the same effect as no pretreatment at all (~10% inhibition), and VEGF-E and PlGF together produced no greater effect than VEGF-A_{165} or VEGF-E alone (Boeldt *et al.* 2015). Together, these results would seem to confirm that VEGF inhibition of the pregnancy-adapted Ca2+ response cannot be mediated by VEGFR-1 homodimers. Yet, surprisingly, when VEGF-A_{165} was used in the presence of the VEGFR-2 kinase inhibitor VEGFRi (4-[(4'-chloro-2'-fluoro)phenylamino]-6,7-dimethoxyquinazo-line), it still inhibited subsequent ATP-stimulated Ca2+ bursts in P-UAEC (Boeldt *et al.* 2015). This suggests either that VEGFRi cannot completely block signaling from VEGFR-2 or that VEGF-A_{165} could also be signaling through another known target protein such as neuropilin-1 (NRP1), which may act as a coreceptor for VEGFR2; however, the latter suggestion is unlikely due to the fact that NRP1 is undetectable in UAEC by Western blot (Grummer et al. 2009) despite the use of anti-NRP1 antibodies proven to be effective in other ovine placental endothelial cell studies conducted in the UW Perinatal Research Laboratory (Tsoi et al. 2002). Alternatively, the effect of VEGF-A_{165} treatment in P-UAEC could also be mediated by VEGFR-1/VEGFR-2 heterodimers that do not require the kinase activity of VEGFR-2 for signal propagation. The observation that VEGF-E is only able to reproduce inhibitory effects at 10X the dose of VEGF-A_{165} may indicate a difference in the relative binding affinities of the two ligands for VEGFR-2 in P-UAEC, but this is not likely (Ogawa et al. 1998). However, since VEGF-E cannot bind to VEGFR-1, the higher required dose for VEGF-E also raises the possibility that the effects of VEGF-A_{165} on GJC are partially transmitted by

VEGFR-1/VEGFR-2 heterodimers. The fraction of the VEGF-A_{165} signal that is propagated by VEGFR-1/VEGFR-2 heterodimers in P-UAEC is unknown, but it is likely to be substantial. Although the expression of VEGFR-2 is several-fold higher than VEGFR-1 in endothelial cells, signaling by heterodimers must be considered because the binding affinity of VEGF-A_{165} for VEGFR-1 is significantly greater than its affinity for VEGFR-2 (K_d of 9-26 pM vs. 100-770 pM, respectively; reviewed in Mac Gabhann and Popel 2004). The poorly understood role of R1-R2 heterodimers in VEGF signaling will be discussed more thoroughly in Chapter 7.

Numerous phosphorylation sites on Cx43 have been identified, and the effect of phosphorylation of particular sites is known in many cases. The sites most clearly established to be inhibitory to Cx43 function are the Src-mediated Y265, the ERK1/2-mediated S279/282, and the PKC-mediated S368 and S262 (Lampe and Lau, 2000). In P-UAEC, phosphorylations of Y265 and S279/282 were observed after 30-minute treatment with 10 ng/mL VEGF-A_{165} or VEGF-E. Interestingly, pretreatment of P-UAEC with VEGFRi partially inhibited Y265 phosphorylation, but had no effect on S279/282 phosphorylation. In NP-UAEC, only treatment with VEGF-A_{165} stimulated phosphorylation of Y265, whereas both VEGF-A_{165} and VEGF-E stimulated phosphorylation of S279/282. VEGFRi pretreatment fully prevented phosphorylation of both Y265 and S279/282 in NP-UAEC. PlGF treatment had no effect on either Cx43 phosphorylation in P-UAEC or NP-UAEC (Boeldt *et al.* 2015).

Because prior published research indicated that phosphorylation of Cx43 at S279/282 is mediated by the MAPK pathway (Warn-Cramer *et al.* 1996), UAEC were pretreated with either the MEK-selective inhibitor U0126 (10 µM) or the Src family kinase (SFK)-selective inhibitor PP2 (10 µM) prior to VEGF administration. U0126 eliminated VEGF-A_{165}-induced phosphorylation of S279/282 in both P-UAEC and NP-UAEC. However, as expected, PP2 had no effect on S279/282 phosphorylation in either P-UAEC or NP-UAEC (Boeldt *et al.* 2015).

Similarly, prior published research indicated that Cx43 Y265 is phosphorylated by Src (Kanemitsu *et al.* 1997). In this case, the SFK inhibitor PP2 would be expected to prevent agonist-stimulated Y265 phosphorylation, and U0126 would serve as the negative control. As expected, PP2 (10 µM) inhibited VEGF-A_{165}-induced Y265 phosphorylation in P-UAEC and NP-UAEC, and the MEK inhibitor U0126 (10 µM) had no effect on Y265 phosphorylation in either cell type. However, surprisingly, PP2 also reduced *basal* Y265 phosphorylation in both P-UAEC and NP-UAEC (Boeldt *et al.* 2015).

Unpublished research from the Bird Laboratory and published data from researchers at the Fred Hutchinson Cancer Research Center (Solan and Lampe 2008) suggested that Src, in addition to acting directly on Cx43, also acts indirectly on Cx43 through the MAPK/ERK pathway. This is entirely plausible since Src is known to activate ERK1/2 via Raf-1 (Chao *et al.* 1997). To confirm prior findings, ERK1/2 phosphorylation in UAEC was quantified via Western blot after 30-minute treatment with VEGF-A_{165} in the presence or absence of the SFK inhibitor PP2. In P-UAEC, VEGF-A_{165} induced a significant ERK1/2 phosphorylation; however, following pretreatment with PP2, VEGF-A_{165} stimulation of ERK1/2 phosphorylation was significantly reduced, though it still rose above the basal level. In NP-UAEC, 30-minute treatment VEGF-A_{165} also stimulated significant ERK1/2 phosphorylation. PP2 pretreatment in NP-UAEC prior to VEGF-A_{165} treatment resulted in ERK1/2 phosphorylation not significantly different from control (Boeldt *et al.* 2015).

Finally, given the ability of U0126 and PP2 to inhibit Cx43 phosphorylations at S279/282 and Y265, respectively, and association of these phosphorylations with closing of gap junctions and concomitant loss of pregnancy-adapted CCE, pretreatment with these inhibitors would be expected to protect P-UAEC from the negative effect of VEGF-A_{165} treatment on [Ca2+]i bursting. To test this, Fura-2-loaded P-UAEC were treated with 100 µM ATP for 30 min, then washed and pretreated with either 10 µM U0126 or PP2 for 20 minutes prior to 10 ng/mL VEGF-A_{165} administration. The MEK-selective inhibitor U0126 preserved the pregnancy-adapted [Ca2+]i

burst response, eliminating the inhibitory effect of VEGF-A_{165}, producing only a 10% reduction in bursts as if no VEGF were added before the second ATP stimulation. The SFK-selective inhibitor PP2 was even more efficient at preserving ATP-induced Ca2+ bursts, keeping repeat burst numbers at initial ATP pre-stimulation levels (0% reduction) (Boeldt *et al.* 2015).

Before concluding the topic of VEGF induction of Src-mediated phosphorylations, we must ask how we can be confident the phosphorylations really are mediated by Src and not another Src family kinase (SFK) such as Fyn or Yes, which are also present in the cytoplasm of P-UAEC. Aside from direct evidence of the ability of c-Src to inhibit GJC (Azarnia et al. 1988), supporting evidence is provided by immunoprecipitation experiments and Src-kinase assays in in human umbilical vein endothelial cells (HUVEC) performed by Chou et al. (2002), which demonstrated that Src preferentially associated with VEGFR-2, whereas Fyn and Yes associated preferentially with VEGFR-1. Since VEGF inhibition of GJC is mediated by VEGFR-2, it is likely that the SFK responsible for phosphorylating Cx43 Y247 and Y265 is indeed Src. However, we cannot rule out the possibility that Fyn or Yes might also be able to phosphorylate these sites, or that multiple SFKs are involved in the regulation of GJC.

3.8 VEGF dysregulation of endothelial cell function is only one factor in the complex pathology of PE

I have focused on data associated with VEGF because these data will become particularly relevant to the hypotheses of this dissertation, but there is nothing unique about VEGF regarding its ability to inhibit GJC. For instance, the non-physiologic agonist TPA produces significantly greater inhibition of GJC than VEGF (Lampe 1994; van der Zandt *et al.* 1990, Sirnes *et al.* 2008, Boeldt *et al.* 2015) and does so through the same signaling pathways (Bird *et al.* 2013, Boeldt *et al.* 2015). TPA treatment of P-UAEC induces significant phosphorylations of S279/282 and Y265 (Boeldt *et al.* 2015) and dramatically reduces sustained phase [Ca2+]i burst responses to ATP

treatment (Cale and Bird 2006, Bird *et al.* 2013, Boeldt *et al.* 2015). More importantly, many physiologic growth factors (e.g. bFGF) and cytokines (e.g. TNFα) inhibit pregnancy-adapted programming. Studies in other cell types have shown that TNFα signals to Src kinases (Page 2009), and TNFα was found to induce Fyn inhibition of Cx43 function in human lung endothelial cells (Angelini *et al.* 2006). In HUVEC, TNFα induced Cx43 relocalization from the plasma membrane to the perinuclear region, implying loss of cell surface function (van Rijen *et al.* 1998), which the Bird Laboratory has confirmed. While IL-6 does not inhibit the ATP-stimulated Ca2+ response in P-UAEC or HUVEC, it does couple directly to ERK and Src signaling pathways in lymphatic endothelial cells (Huang *et al.* 2013). Other cytokines are likely to inhibit Cx43 function via transactivation of growth factors. For example, IL-8 induces Src signaling in natural killer cells by transactivation of EGFR (Kyriakakis *et al.* 2011). IL-8 can also transactivate EGFR in microvascular endothelium, suggesting elevation of EGFR ligands may not be necessary for the receptor to mediate Cx43 phosphorylation *in vivo* (Schraufstatter 2003).

Angiogenic biomarkers for PE have been proposed (e.g. VEGF, PlGF, sFlt-1, sEng), but their predictive power is weak. There is simply too much variation among PE cases for a given marker to be predictive for a given individual. Correlation of PE with elevation of inflammatory cytokines, for example, is moderate to high, particularly in the second trimester, but not complete. If given two sets of blood samples—one from 100 healthy pregnant women and the other from 100 preeclamptic women, measurement of serum cytokine levels will enable identification of the PE group. However, a blood sample randomly taken from any one of the 200 pregnant women will not enable a confident determination of PE status. Likewise, if the serum levels of these same cytokines were measured in a blood sample taken from a pregnant woman with high blood pressure, it would be impossible to determine whether she was diabetic, preeclamptic, or just hypertensive. So how can this problem be studied? A molecular biologist can determine if any given molecule is mediating a specific process by genetic manipulation—e.g. knocking out their

respective receptors in a rodent and observing the effects. Since our experiments cannot involve genetic manipulation of human patients, we instead start with healthy cell models (e.g. UAEC, HUVEC) and introduce specific hormones, growth factors, or cytokines at physiological levels, in isolation or combination, in an attempt to recreate the disease state.

In Chapter 4, I will address the theoretical and practical considerations of my project, the purpose of which is to further understand the molecular mechanisms of PE by creating a PE-like state in our cell model. What we observe in PE appears to be a classic positive feedforward loop, in which elevated growth factors and cytokines lead to activation of signaling pathways that close/disassemble gap junctions…which inhibits the CCE required for sustained vasodilation…which results in both placental hypoxia and general hypertension...which leads to an inflammation response…which activates growth factors and cytokines…and so on…in a dysregulated, out-of-control loop that produces increasingly severe symptoms as the pregnancy progresses and the fetal demands are not met. My project is an attempt to induce chronic endothelial dysfunction by introducing a single aberrant signaling molecule into this loop, thereby "engineering preeclampsia."

Having reviewed the necessary background information, we can now proceed to Chapter 4.

Chapter 4:

"Engineering Preeclampsia" with Adenoviral Transduction of EGFR in Pregnancy-Adapted Uterine Artery Endothelial Cells

4.1 Can preeclamptic-like dysfunction be induced in P-UAEC by overexpression of EGFR?

4.1.1 EGFR and Hypertension

The clear majority of published research conducted today on the epidermal growth factor receptor (EGFR) is primarily focused on its role in cancer due to the receptor's key involvement in a number of canonical oncogenic signaling pathways. EGFR dysregulation is a contributing factor in aggressive cancers—including lung, brain, colon, and breast (Reviewed in Normanno *et al.* 2006). Tumorigenic signaling arises when overexpression or activating mutations of EGFR confer constitutive autophosphorylation to the receptor ( ), which is normally autoinhibited until stimulated with EGF (or one of its other known ligands) or transactivated by a number of distinct mechanisms (Liebmann 2011). However, the effects of dysregulation of a central signaling molecule like EGFR would be expected to extend well beyond cancer. Indeed, dysregulation of canonical EGFR cancer signaling pathways is a feature of PE (Moslehi *et al.* 2013).

Accumulating data in rodent models suggest EGFR may also play a role in the development and/or maintenance of hypertensive diseases. For instance, elevation of EGFR mRNA transcripts and EGFR kinase activity in aortic tissue of angiotensin II-treated rats strongly correlated with blood pressure at time of sacrifice (Sambhi *et al.* 1992) and renal cortical expression of EGFR was found to be elevated in both prehypertensive and hypertensive salt-sensitive rats (Ying and

Sanders 2005). EGFR activation of the MAPK/ERK pathway was determined to be necessary for angiotensin II-induced left ventricular hypertrophy (LVH) in hypertensive rats, and the development of LVH in rats correlated with high levels of EGFR and phosphorylated ERK (Kagiyama *et al.* 2002). Conversely, antisense message to EGFR significantly reduced ERK phosphorylation, left ventricular mass, and blood pressure in these rats (Kagiyama *et al.* 2003). Furthermore, while EGF has been shown to induce contraction of aortic smooth muscle in hypertensive rats by phosphorylation of ERK1/2, there was no corresponding contraction in aortic tissue from normotensive rats (Kim *et al.* 2006; Florian and Watts 1999), suggesting that EGFR may be involved in the maintenance of hypertensive disease rather than its etiology. Evidence of EGFR-mediated vasoconstriction was also observed in a wild-type mouse model of hypertension, in which treatment with the EGFR-inhibiting drug AG1478 induced endothelium-dependent relaxation of aortic rings (Jung *et al.* 2004). More recently, the *EGFR* gene ranked highest in a mouse genome-wide association study to identify genes associated with susceptibility to high fat diet-induced pulmonary hypertension (Kelly *et al.* 2017).

The role of EGFR in the development and/or maintenance of hypertensive disorders in human pregnancy remains as yet unidentified.

4.1.2 EGF treatment disrupts gap junctional communication in many cell types

As in the case of VEGF, the ability of EGF to disrupt the function of gap junctions has been established in a variety of cell models. Almost 30 years ago, EGF was shown to inhibit gap junction-mediated intercellular communication (GJC) in normal human keratinocytes (Madhukar *et al.* 1989). A few years later, EGF treatment was shown to induce serine phosphorylations of Cx43 and inhibit GJC in T51B rat liver epithelial cells (Lau *et al.* 1992) and rat liver epithelial stem-like WB-F344 cells (Oh *et al.* 1993), and these effects occurred via MAPK pathway signaling (Kanemitsu and Lau 1993). In mouse embryonic stem cells, EGF treatment activated ERK1/2 and

PKC, resulting in Cx43 phosphorylations on S262, S279/282, and S368 and a 64% inhibition of intercellular communication (Fong *et al.* 2014). In endothelial cells and tissues, however, the results are different. Contrary to the cell types mentioned previously, treatment with EGF has a negligible effect on Ca2+ bursting in UAEC, presumably because the level of endogenous expression of EGFR in UAEC is virtually undetectable by Western blot, just as it is in HUVEC (Russell *et al.* 1999). This raises an obvious question. If the lack of an EGF-induced effect in endothelial cells were simply due to insufficient EGFR expression, would we then observe an effect if the expression of the receptor were artificially elevated? This forms the basis of our proposal to "engineer preeclampsia," which will be outlined presently. (Data on EGFR expression in P-UAEC will be presented later in this chapter. Ca2+ bursting data will be presented in Chapter 5.)

Recently, transcriptome meta-analysis has revealed that dysregulation of canonical EGFR cancer signaling pathways occurs with high frequency in the PE placenta (Moslehi *et al.* 2013). This does not necessarily mean that EGFR itself is responsible for the dysregulation of these pathways. Indeed, a recent comparison of 29 PE placentas and 19 healthy placentas found no significant differences in EGF or EGFR expression levels (Kosovic *et al.* 2017). Additionally, there are no documented cases of PE involving activating mutations of EGFR, nor do any known EGFR mutant-expressing pregnant endothelial cell lines exist. However, the fact that EGFR-associated pathways are dysregulated in the PE placenta led us to ask if the aberrant signaling resulting from overexpression of EGFR in pregnancy-adapted vascular endothelial cells might be sufficient to drive PE-associated endothelial dysfunction. Firstly, we hypothesized that overexpression of EGFR in P-UAEC would enable EGF treatment to inhibit GJC in P-UAEC and disrupt the [Ca2+]i bursting needed for enhanced vasodilation just as VEGF treatment does. Secondly, we hypothesized that overexpression of EGFR in P-UAEC at a level sufficient to induce constitutive activity (or expression a constitutively active EGFR mutant) could result in a permanent basal

inhibition of [Ca2+]i bursting, thus “engineering preeclampsia”—i.e. simulating the functionally-impaired state of the vascular endothelium in PE.

To test our hypotheses, we will need to manipulate EGFR expression level in normal P-UAECs.

4.1.3 Overexpression of EGFR in P-UAEC via Adenoviral Transduction

To overexpress EGFR in P-UAEC, we chose to employ the method of adenoviral transduction. Among the advantages of adenovirus are its ability to infect any cell type that expresses CAR (**c**oxsackie virus and **a**denovirus **r**eceptor) (Bergelson *et al.* 1997), which includes most cell types, and the simplicity of the transfection protocol. To maximize safety and to minimize the laborious process of generating the desired adenovirus at a high level of purity, we obtained replication incompetent adenovirus commercially from Vector Biolabs, a biotechnology company specializing in preconfigured or customized gene delivery systems. For our experiments, we ordered three customized adenoviruses: **Ad-EGFR(ErbB1)**, which contains the gene transcript for wild-type EGFR; **Ad-EGFR(L834R)**, which contains the gene transcript for the constitutively-active L834R-EGFR mutation; and **Ad-GJA1-eGFP**, which contains the gene transcript for an enhanced green fluorescent protein-tagged Cx43 fusion protein. Ad-GJA1-eGFP was used in microscopy experiments that will be summarized in Chapter 10.

Before conducting experiments using adenovirally-transfected cells, several questions must be answered: *Does adenoviral transduction of P-UAEC have a negative effect on cell viability? Will EGFR be expressed on the plasma membrane of P-UAEC? Can EGFR be overexpressed at a concentration that induces constitutive autophosphorylation of the receptor? Is the exogenous EGFR functionally linked to major signaling pathways—PI3K/Akt, MAPK, etc.—to enable activation of relevant effector molecules such as Akt, ERK1/2, and Src?*

The results summarized in this chapter provide the answers to these questions.

4.2 Methods

Detailed experimental protocols are presented in Chapter 9.

4.2.1 Adenoviral transduction of EGFR in P-UAEC

The Adenoviral transduction Protocol was used to generate P-UAEC-adEGFR and P-UAEC-adL834R cells.

4.2.2 Flow cytometric confirmation of plasma membrane expression of EGFR

The Flow Cytometry Protocol was used to generate the data for Figures 4.2, 4.4, and 4.5.

4.2.3 Western blot quantification of EGFR activity

Western Blot Protocol 1.0 was used to generate the data for Figures 4.1, 4.3. 4.7, 4.8 and 4.10. Western Blot Protocol 1.2 was used to generate the data for Figures 4.9.

4.3 Results

The following data were collected via Western blot and flow cytometry, as described in the previous section. Together, these results provide strong evidence that wild-type and L834 EGFR can be overexpressed in P-UAEC at a level proportional to adenoviral MOI. Furthermore, the exogenous EGFR is responsive to treatment with EGF ligand, and the wild-type receptor will exhibit constitutive autophosphorylation (like the L834R mutant) once a critical level of expression is achieved.

4.3.1 EGF treatment does not inhibit the pregnancy-adapted Ca2+ burst function in P-UAEC

While VEGF treatment significantly reduced the mean number of ATP-induced [Ca2+]i bursts, EGF treatment results were no different than the control group (Figure 4.1). As reviewed in Chapter 3, 30-minute VEGF treatment of P-UAEC reduces Ca2+ burst numbers to the level observed in NP-UAEC, an effect mediated by VEGFR-2. Furthermore, VEGF inhibition of GJC was shown to be associated with ERK- and Src-mediated phosphorylations of Cx43 that promoted the closing and disassembly of gap junctions (see 3.1.7).

4.3.2 P-UAEC adenovirally transduced with wild-type EGFR maintain viability

In the plasma membrane EGFR immunolabeling protocol, all samples of P-UAEC—whether containing cells adenovirally transduced to express wild-type EGFR, L834R-EGFR, or parental cells (i.e. cells not transduced with adenovirus)—were subjected to the same treatments and incubations. When samples of parental P-UAEC were subjected to the immunolabeling protocol and subsequent FACS analysis, including pretreatment with propidium iodide to stain dead cells, approximately 20% of the 10,000 cells that pass through the FACS machine were found to be dead. Therefore, if the viability of a sample of cells adenovirally transduced with *EGFR* were significantly lower than 80%, the higher death rate must be an effect of the adenoviral transduction, overexpression of EGFR, and/or increased binding of primary and secondary antibodies in EGFR-expressing cells.

At the completion of the immunolabeling and FACS protocol, when P-UAEC—parental or adenovirally transduced (from MOI 10 to 3200)—were labeled with IgG (nonselective binding) or mAb 528 (EGFR-selective binding) and a phycoerythrin-tagged secondary antibody, cell viability remained at approximately 80%. This result suggests that neither exposure to adenovirus containing the *EGFR* gene transcript nor increased expression of wild-type EGFR had any

deleterious effect on cell viability; however, a minor loss of live cells seems to be associated with the binding of mAb 528 to EGFR on the plasma membrane (Figure 4.2A).

In the case of P-UAEC expressing the constitutively active L834R EGFR, flow cytometric analysis did show reductions in cell viability compared to parental P-UAEC, but only at the higher multiplicities of viral infection. Cell loss seemed largely correlated with the level of binding of mAb 528 and phycoerythrin to L834R EGFR, particularly at an MOI of 3200, and due to a lesser degree to the mere overexpression of the L834R mutant receptor (Figure 4.2B).

4.3.3 Mean level of EGFR expression in P-UAEC is proportional to MOI

Consistent with data from HUVEC ( ), endogenous expression of EGFR in P-UAEC is so low that it is virtually undetectable by Western blot. Detection of overexpressed wild-type and L834R EGFR first occurs at an MOI of 100, and is robust at an MOI of 1000 (Figure 4.3A & B).

Flow cytometric quantification of immunolabeled EGFR on the plasma membrane of P-UAEC is a more sensitive technique. At an adenoviral MOI of 1000, EGFR was found to be expressed at about 6 times the level of endogenous expression in P-UAEC (Figure 4.4A & B). This means that 1/6 of the EGFR expressed in both P-UAEC-adEGFR and P-UAEC-adL834R is wild-type *ovine* EGFR. The only sequence of the ovine EGFR reported is a short fragment of 18 amino acids that shows a high homology—16 identical residues—with the EGFR sequence of human and bovine (Luna et al. 2012). The overall homology of human and ovine EGFR is presumed to be very high, but empirical data is lacking.

4.3.4 The percentage of P-UAEC expressing detectable EGFR increases with MOI

Even though my flow cytometry protocol only labels EGFR on the plasma membrane (whereas Western blotting quantifies cytosolic *and* surface EGFR), the BD FACSCalibur™ machine is able to detect wild-type EGFR in up to 22% of parental P-UAEC (Figure 4.5A). The flow cytometry data

further show that as the MOI increases (10 → 32 → 100 → 320 → 1000 → 3200) the percentage of P-UAEC that expresses wild-type EGFR on the cell surface increases in a gentle sigmoidal curve when plotted with a logarithmic x-axis (Figure 4.5B). At an MOI of 3200, 100% of P-UAEC express detectable EGFR, though the level of expression varies widely from cell to cell.

The percentage of P-UAEC that express L834R-EGFR on the plasma membrane also rises with the MOI of adenovirus containing the *L834R-EGFR* gene transcript, but there is a much smaller percentage of P-UAEC expressing surface L834R in the lower MOI samples as compared to similar cell populations transduced with wild-type *EGFR* at the same MOI (19% vs. 27% at MOI 10, and 24% vs. 48% at MOI 100) (Figure 4.6A & B). My first reaction was to suspect that these data were an aberration, and this is indeed a possibility. However, each of these percentages was the mean of two entirely independent trials with surprisingly low variance, so it seems highly unlikely that two independent sets of measurements would converge at almost precisely the same aberrant values.

An alternative interpretation of the reduced percentage of P-UAEC expressing detectable L834R-EGFR on the plasma membrane at lower adenoviral MOI is based on the receptor's unique properties. EGFR mutants observed in non-small cell lung cancer such as L834R typically cluster together on the cell surface. They also constitutively dimerize and internalize in the absence of ligand (Choi, *et al.* 2007). Together, these facts suggest that when L834R-EGFR is expressed in a cell at low concentration, almost all the receptors would be found in the cytosol, not at the cell surface. However, in cells expressing a high concentration of L834R (e.g. tumor cells), the receptor is to ligand, indicating that significant populations of the L834R remain embedded in the plasma membrane, probably due to the endocytosis machinery becoming overwhelmed by the sheer number of receptors to be trafficked, though this explanation is merely speculative at present.

4.3.5 EGFR exhibits constitutive auto-phosphorylation in P-UAEC when adenovirally transduced with the *EGFR* gene transcript at an MOI of 1000

Once I had confirmed that adenoviral transduction of the *EGFR* gene transcript into the cytosol of P-UAEC was possible at a high MOI, the next step was to determine the MOI necessary to "engineer" the type of endothelial cell dysfunction observed in PE. In the field of cancer research, it is well-established that EGFR becomes constitutively activated when overexpressed in a cell at a sufficient level. This continuous signaling of EGFR aggressively drives the cell into a dysregulated state. A key task in the engineering of P-UAEC dysfunction, therefore, was to determine the minimum level of EGFR overexpression that resulted in constitutive receptor autophosphorylation. To this end, I performed Western blots to observe EGFR autophosphorylation using the same series of samples I used for flow cytometric analysis—a parental P-UAEC control and P-UAEC transduced with wild-type *EGFR* or *L834R-EGFR* at MOIs of 10, 100, 320, 1000, and 3200. Following treatment of the cells with 10 ng/mL EGF or vehicle for 15 minutes, the cells were lysed, proteins were resolved by PAGE and electroblotted on PVDF membranes, and then probed with an antibody selective for EGFR pY1173, one of the receptor's major phosphotyrosine sites. The treatment with EGF, while not necessary for observing basal autophosphorylation, was done to provide a comparison of the magnitude of ligand-dependent and independent activity of EGFR and to serve as a rough measure of surface expression of the receptor.

The pattern of disproportionately weak surface expression of L834R-EGFR described in the previous subsection paralleled Western blot detection of L834R autophosphorylation relative to that of wild type EGFR. L834R-EGFR exhibited relatively poor responsiveness to EGF at lower MOIs (10, 100) and robust EGF responsiveness at higher MOIs (320, 1000, 3200) (Figure 4.7), possibly due to limitations of endocytosis as discussed earlier. For the purposes of my project, our "limited endocytosis capacity" hypothesis will not be explored further, but it does provide a

plausible explanation of the apparent biphasic relationship between the MOI of *L834R*-carrying adenovirus and the percentage of cells that express detectable L834R surface expression and tyrosine phosphorylation.

In P-UAEC adenovirally transduced with the wild-type *EGFR* transcript, the lowest MOI to produce a significant level of constitutive autophosphorylation was 1000 (Figure 4.8). For this reason, I used MOI 1000 cells to conduct experiments on inhibition of the Ca2+ burst response. It might seem that the higher level of constitutive EGFR autophosphorylation displayed in P-UAEC transduced at an MOI of 3200 might also be suitable since naturally-occurring A431 tumor cells express considerably more EGFR—the equivalent of perhaps 10,000 MOI in UAEC. However, because endogenous expression of EGFR in UAEC is very low and the surface area of any cell is finite, there is little doubt that a huge concentration of exogenous EGFR (or any other single protein) embedded in the plasma membrane and perhaps scattered throughout the cell would displace many other important proteins and interfere with normal cell function. I wanted to be as confident as possible that any observed disruption of the Ca2+ burst response was due specifically to inhibition of CCE mechanisms and not simply cell-wide dysfunction due to excessive overexpression of a single protein. Additionally, several Western blot images of total EGFR obtained from lysates of P-UAEC adenovirally transduced at an MOI of 3200 displayed extra bands and dark streaking along the lane (data not shown), suggesting accumulation of EGFR breakdown fragments and other debris due to an inability of the degradation machinery to accommodate excessive protein turnover. This further supported my decision to use MOI 1000 cells for conducting experiments on inhibition of the Ca2+ burst response.

NOTE: From this point forward, to avoid frequent repetition of long descriptive phrases, I will hereby use the terms ***P-UAEC-adEGFR*** *and* ***P-UAEC-adL834R*** *to refer to P-UAEC expressing exogenous wild-type EGFR and L834R-EGFR, respectively. These terms will refer specifically to P-UAEC that have been adenovirally transduced at an MOI of 1000 unless otherwise specified.*

4.3.6 Basal levels of pERK1 and pERK2 are not elevated in P-UAEC-adEGFR

As outlined earlier in the chapter, the propagation of sustained phase CCE in UAEC is dependent on the monolayer of endothelial cells being well connected by open Cx43 gap junctions. Conversely, the phosphorylation of S279/282 in Cx43 mediated by activated ERK1/2 is associated with the closing of gap junctions and inhibition of [Ca2+]i signaling. Therefore, if our intention is to induce a state of impaired intercellular communication in P-UAEC, it is important to establish the ability of exogenous EGFR to signal through the MAPK pathway. To confirm this, I performed a series of nine Western blots to quantify basal ERK1/2 phosphorylation in both parental P-UAEC and P-UAEC transduced with the *EGFR* transcript at multiplicities of infection of 10, 100, and 1000. While ANOVA revealed no significant differences in ERK phosphorylation between any cells irrespective of MOI, a distinct trend of increased MOI inducing greater pERK1/2 was observed. Cells transduced at an MOI of 1000 exhibited the greatest increases of mean basal ERK1 and ERK2 phosphorylations at 2.1- and 1.9-fold, respectively, above the levels observed in parental P-UAEC (Figure 4.9), but these elevations were not found to be significant due to the variance between trials.

4.3.7 Phosphorylation of ERK1, but not ERK2, is elevated in parental P-UAEC following 30-minute EGF treatment

Both EGF and VEGF are capable of phosphorylating ERK1/2 in P-UAEC, which peaks at 10 minutes (Bird et al. 2000). Due to the large number of proteins to be quantified (total Akt, Akt pS473, total Cx43, Cx43 pS279/282, Cx43 pY265, total EGFR, EGFR pY1173, total ERK1, ERK1 pT202/pY204, total ERK2, ERK2 pT185/pY187, and Hsp90), the 30-minute treatment time used in my experiments was selected because it correlated with optimal phosphorylation of Cx43, not ERK1/2. Following 30-minute treatment, EGF (10 ng/mL) resulted in a significant rise in phosphorylation of ERK1 above the basal level (Figure 4.10A, left). Early studies of UAEC

conducted by the Bird Laboratory found that 10-minute EGF treatment also induced a significant rise in ERK2 (Bird et al. 2000), but my data suggest it is largely gone by 30 minutes. While a few of my Western blot experimental trials did seem to show elevation of ERK2 phosphorylation remaining at 30 minutes, the increase was not statistically significant due to high variance (right).

Published research from the Bird Laboratory established that VEGF (10 ng/mL) induces maximal phosphorylation of both ERK1 (~2.4 fold above basal) and ERK2 (~1.7 fold above basal) in P-UAEC at 10 minutes (Grummer *et al.* 2009). A time course determined that ERK1 and ERK2 phosphorylations were not as robust (~1.2 fold and ~1.5 fold above basal, respectively) following 30-minute treatment with VEGF, but both values were still found to be significantly elevated above basal levels due to extremely low variance between experimental trials. My Western blot experiments showed that administration of VEGF in parental P-UAEC for 30 minutes at the same dose resulted in no significant changes in phosphorylation of either ERK1 (Figure 4.10A, left) or ERK2 (right) due to the high variance between trials. However, the mean increases of pERK1 (2.1-fold) and pERK2 (1.4-fold) at 30 minutes were similar or greater than those observed by Grummer *et al.*

4.3.8 30-minute EGF treatment induces phosphorylations of ERK1 and ERK2 in P-UAEC-adEGFR

In P-UAEC-adEGFR, treatment with EGF (10 ng/mL) for 30 minutes induced robust phosphorylations of ERK1 and ERK2 (Figure 4.10B) at several times the levels observed in control cells. However, administration of VEGF at the same dosage and treatment duration had no effect on ERK1 or ERK2 phosphorylation.

4.4 Summary of adenoviral transduction data

Before conducting experiments to determine the effect of EGFR overexpression on pregnancy-adapted Ca2+ bursting, several questions needed to be answered about our adenovirally-transfected cells.

Does adenoviral transduction of EGFR *in P-UAEC have a negative effect on cell viability?* **No.** Some loss of cell viability was observed in the transduction of L834R-EGFR at high MOI, but this was largely due not to EGFR expression, but to the flow cytometry protocol itself—i.e. widespread antibody binding to the surface of P-UAEC-adL834R at high MOI.

Will EGFR be expressed on the plasma membrane of P-UAEC? **Yes.** Surface expression of EGFR that increased with higher MOI was confirmed by flow cytometry.

Can EGFR be overexpressed at a concentration that induces constitutive autophosphorylation of the receptor? **Yes.** Western blotting confirmed that constitutive autophosphorylation is exhibited by wild-type EGFR at an adenoviral MOI of 1000.

Is the exogenous EGFR functionally linked to major signaling pathways—PI3K/Akt, MAPK, etc.—to enable activation of relevant effector molecules such as Akt, ERK1/2, and Src? **Yes.** While the poor quality of available Src-selective antibodies for Western blotting does not enable us to measure Src phosphorylation, EGF treatment of P-UAEC-adEGFR resulted in significantly greater phosphorylation of ERK1 and ERK2 than observed in EGF-treated parental P-UAEC. EGF treatment also induced a dramatic elevation of Akt phosphorylation, which will be discussed in Chapter 6.

Having passed all the preliminary benchmarks, we are now ready to proceed to Chapter 5.

Figure 4.1

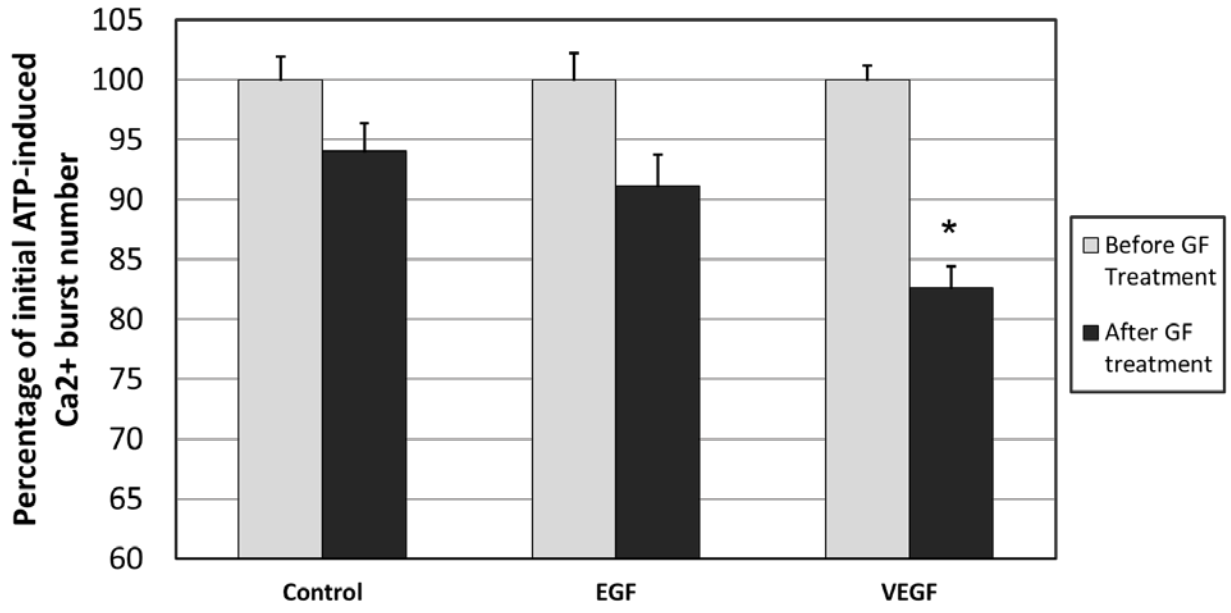

Figure 4.1 EGF treatment does not inhibit the pregnancy-adapted Ca2+ burst function in P-UAEC. P-UAEC were pre-loaded with the [Ca2+]i-sensitive dye Fura-2, stimulated with ATP (100 µM) for 30 min, and then washed with fresh buffer and allowed to sit for 30 min. Cells were treated with VEGF (10 ng/mL), EGF (10 ng/mL), or vehicle control for 30 min, then re-stimulated with ATP for 30 min. Data was collected from cells showing 3 or more ATP stimulated Ca2+ bursts prior to growth factor treatment. Black bars represent percent of initial mean burst number +/- SE. Treatment with VEGF inhibited the number of Ca2+ bursts significantly below the control level, but EGF did not. However, in P-UAEC-adEGFR and adL834R, the results are reversed; treatment with EGF induced significant inhibition, whereas VEGF treatment had no effect on Ca2+ bursting. Statistics were performed on raw data from individual P-UAEC observed in 5-22 dishes: control (n = 342), EGF (n = 226), or VEGF-165 (n = 778). Comparisons of post-treatment groups vs. control group were analyzed by rank-sum test (***** $P < 0.0001$).

Figure 4.2

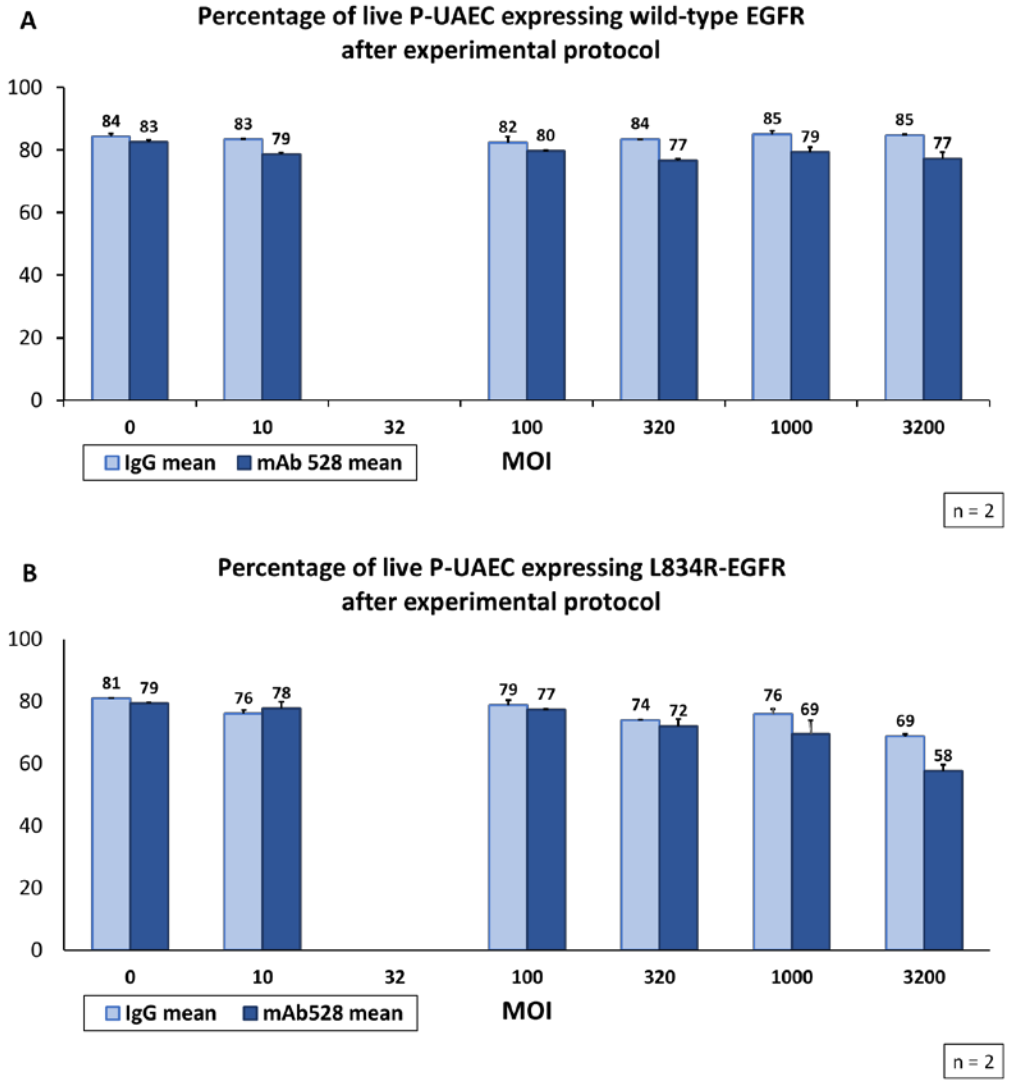

Figure 4.2 Percentage of live P-UAEC expressing wild-type EGFR or L834R-EGFR after experimental protocol. At the completion of the immunolabeling and FACS protocol, when P-UAEC—parental or adenovirally transduced (from MOI 10 to 3200)—were labeled with IgG (nonselective binding) or mAb 528 (EGFR-selective binding) and a phycoerythrin-tagged secondary antibody, cell viability remained at approximately 80%. This result suggests that neither exposure to adenovirus containing the *EGFR* gene transcript nor increased expression of wild-type EGFR had any deleterious effect on cell viability; however, a minor loss of live cells seems to be associated with the binding of mAb 528 to EGFR on the plasma membrane (A). In the case of P-UAEC expressing L834R EGFR, flow cytometric analysis did show reductions in cell viability compared to parental P-UAEC, but only at the higher multiplicities of viral infection. Cell loss seemed largely correlated with the level of binding of mAb 528 and phycoerythrin to L834R EGFR, particularly at an MOI of 3200, and due to a lesser degree to the mere overexpression of the L834R mutant receptor (B).

Figure 4.3

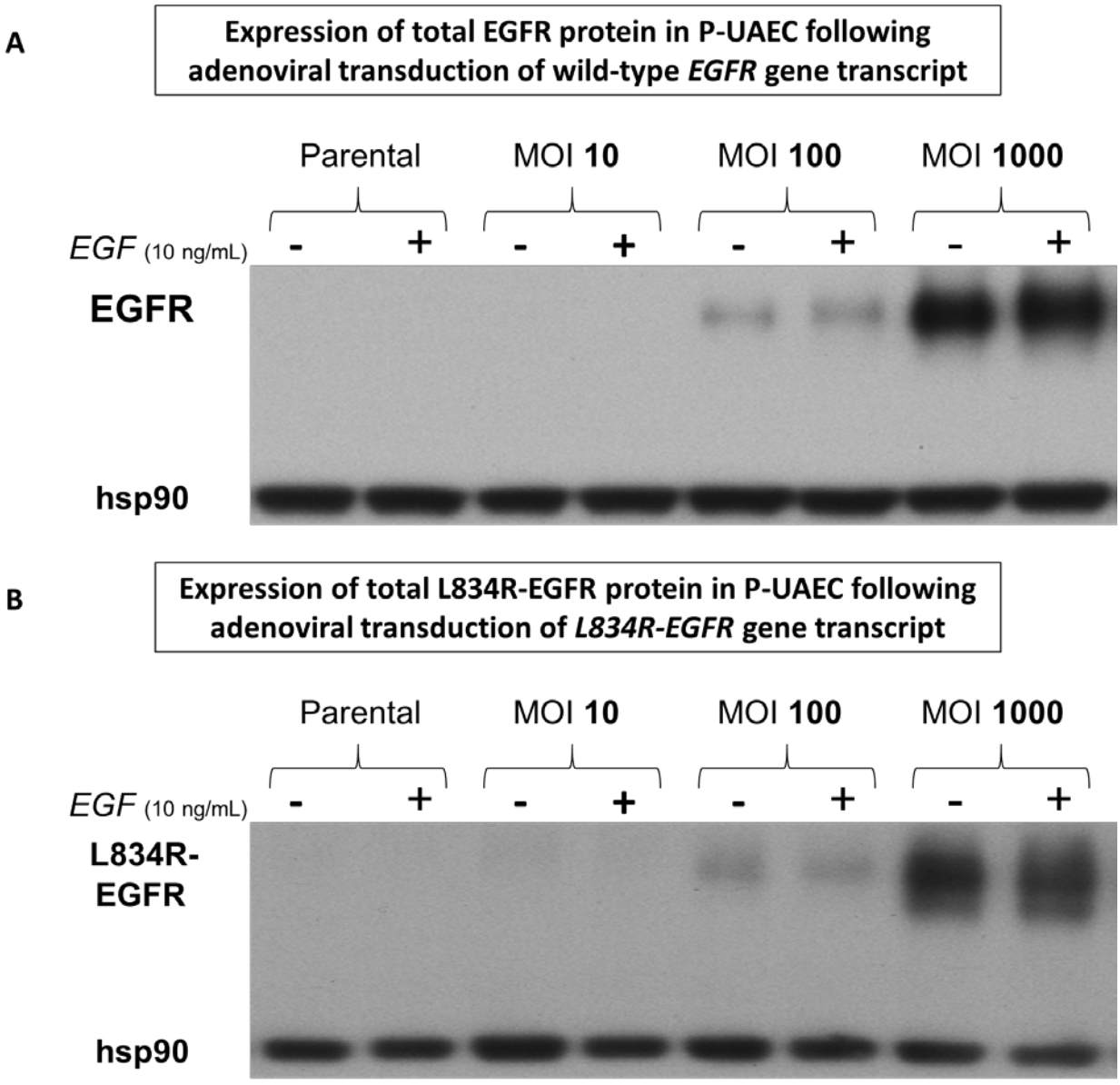

Figure 4.3 Expression of total wild-type EGFR and L834R-EGFR protein in P-UAEC following adenoviral transduction of *L834R EGFR* gene transcript. Lysates of P-UAEC adenovirally transduced with the wild-type *EGFR* or *L834R-EGFR* gene transcript at varying multiplicities of infection (MOI) were immunoblotted with EGFR(1005) antibody (Santa Cruz), which is selective for the C-terminal tail of EGFR. Expression of EGFR in P-UAEC is so low that it is undetectable in parental cells. Detectable expression (without extreme overexposure of the image) first occurs at an MOI of 100 and is robust at an MOI of 1000.

Figure 4.4

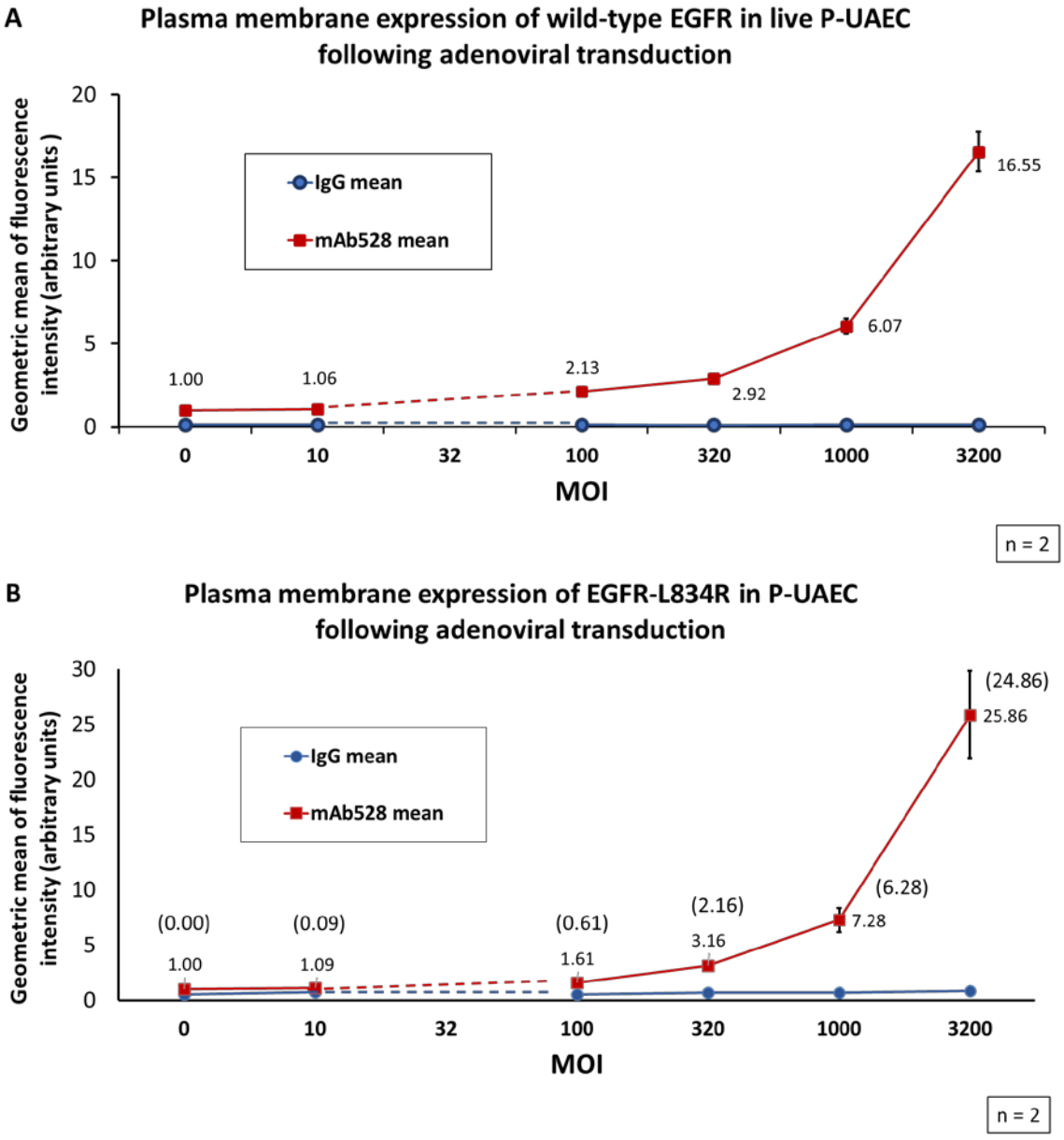

Figure 4.4 Flow cytometric quantification of plasma membrane expression of wild-type EGFR and EGFR-L834R in P-UAEC following adenoviral transduction Detection of overexpressed wild-type (A) and L834R EGFR (B) first occurs at an MOI of 100, and is robust at an MOI of 1000. At an adenoviral MOI of 1000, EGFR was found to be expressed at about 6 times the level of endogenous expression in P-UAEC. This means that 1/6 of the EGFR expressed in both P-UAEC-adEGFR and P-UAEC-adL834R is wild-type *ovine* EGFR.

Figure 4.5

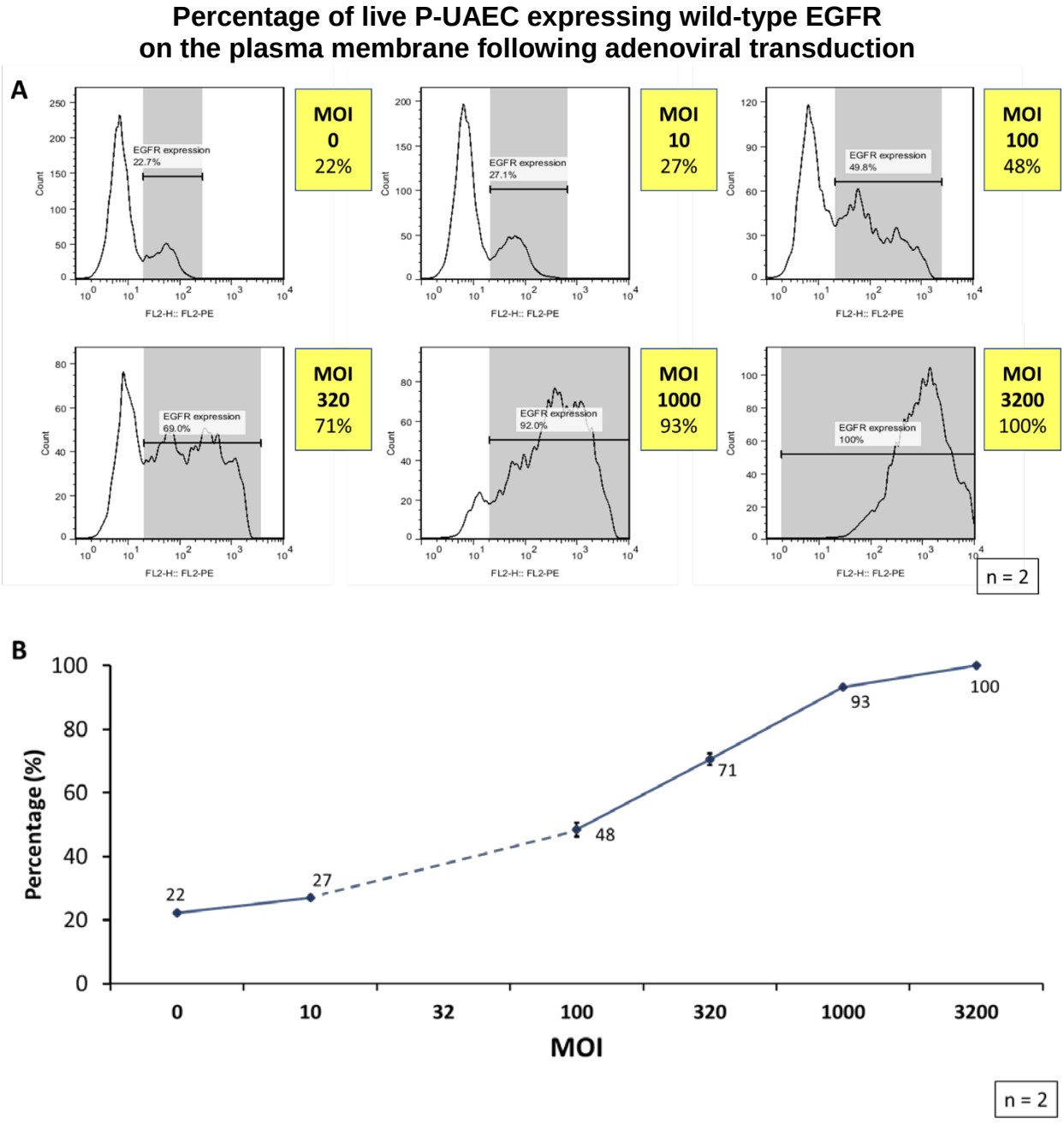

Figure 4.5 Percentage of live P-UAECs expressing WT-EGFR on plasma membrane following adenoviral transduction the BD FACSCalibur™ machine is able to detect wild-type EGFR in up to 22% of parental P-UAEC (A). The flow cytometry data further show that as the MOI increases (10 → 32 → 100 → 320 → 1000 → 3200) the percentage of P-UAEC that expresses wild-type EGFR on the cell surface increases in a gentle sigmoidal curve when plotted with a logarithmic x-axis (B). At an MOI of 3200, 100% of P-UAEC express detectable EGFR, though the level of expression varies widely from cell to cell.

Figure 4.6

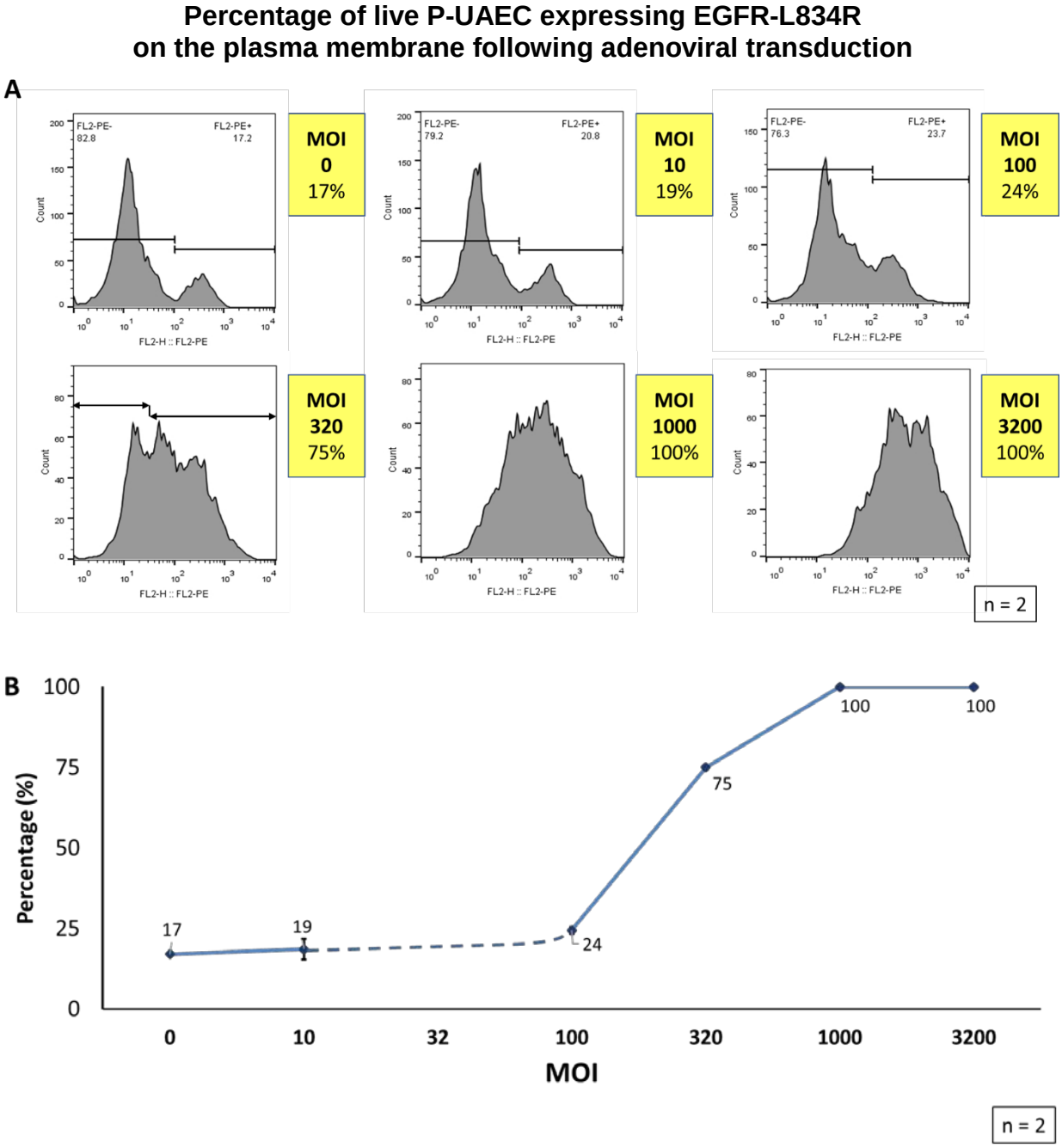

Figure 4.6 Percentage of live P-UAECs expressing EGFR-L834R on plasma membrane following adenoviral transduction The percentage of P-UAEC that express L834R-EGFR on the plasma membrane rises with the MOI of adenovirus containing the *L834R-EGFR* gene transcript, but there is a much smaller percentage of P-UAEC expressing surface L834R in the lower MOI samples as compared to similar cell populations transduced with wild-type *EGFR* at the same MOI (19% vs. 27% at MOI 10, and 24% vs. 48% at MOI 100).

Figure 4.7

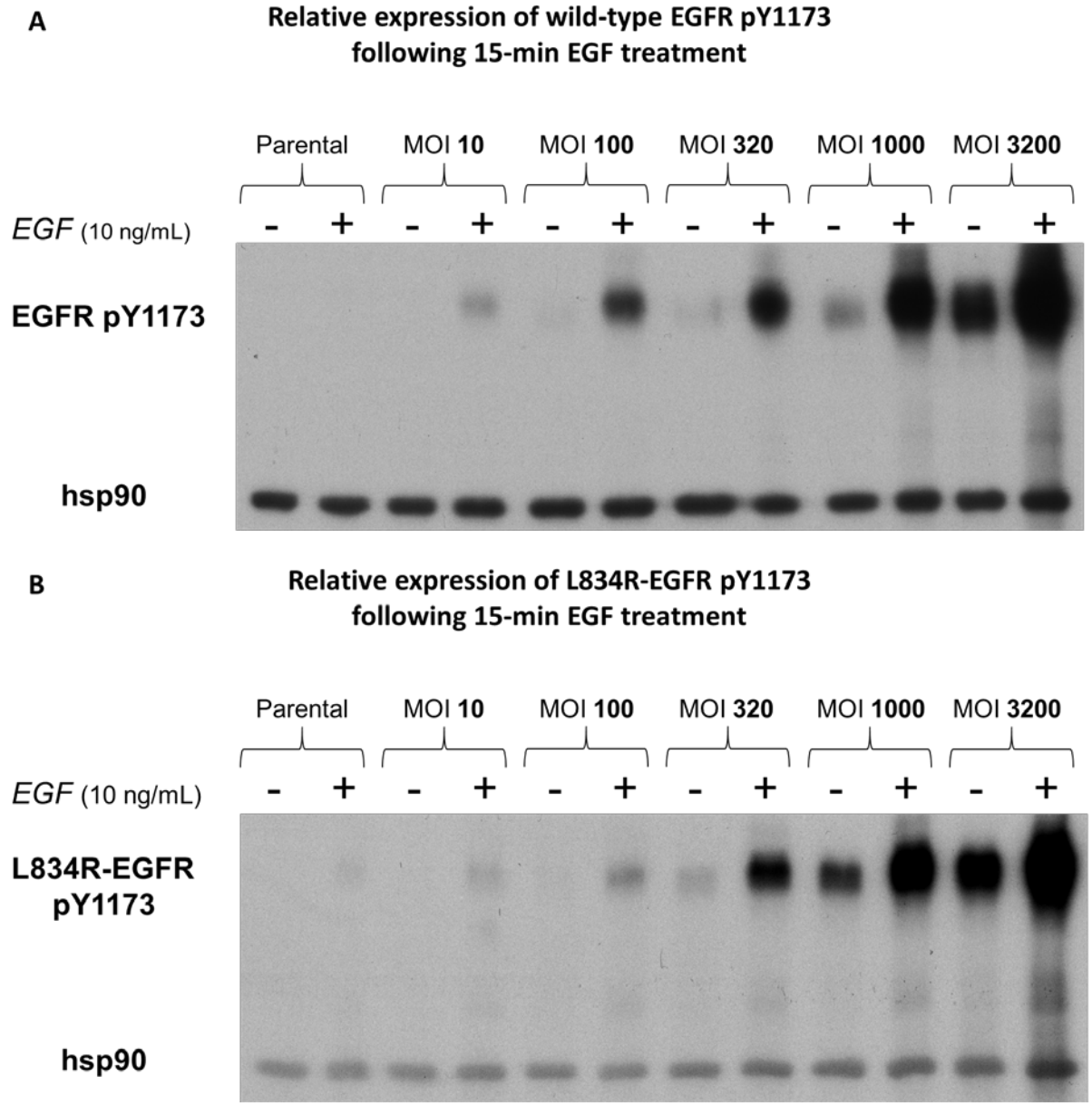

Figure 4.7 Comparison of Autophosphorylation of Wild-Type EGFR and L834R-EGFR in P-UAEC at Varying MOIs. (A) Adenoviral transduction of the *EGFR* gene in P-UAEC at an MOI of 100 resulted in significant autophosphorylation in response to 15-min EGF treatment, but did not display constitutive autophosphorylation. (B) Adenoviral transduction of the *L834R-EGFR* gene in P-UAEC at an MOI of 320 also resulted in significant autophosphorylation in response to EGF treatment but was not particularly robust. P-UAEC transduced with *L834R-EGFR* at lower MOIs (10 and 100) responded weakly to EGF, possibly due to constitutive dimerization and internalization of L834R-EGFR leaving little receptor on the plasma membrane.

Figure 4.8

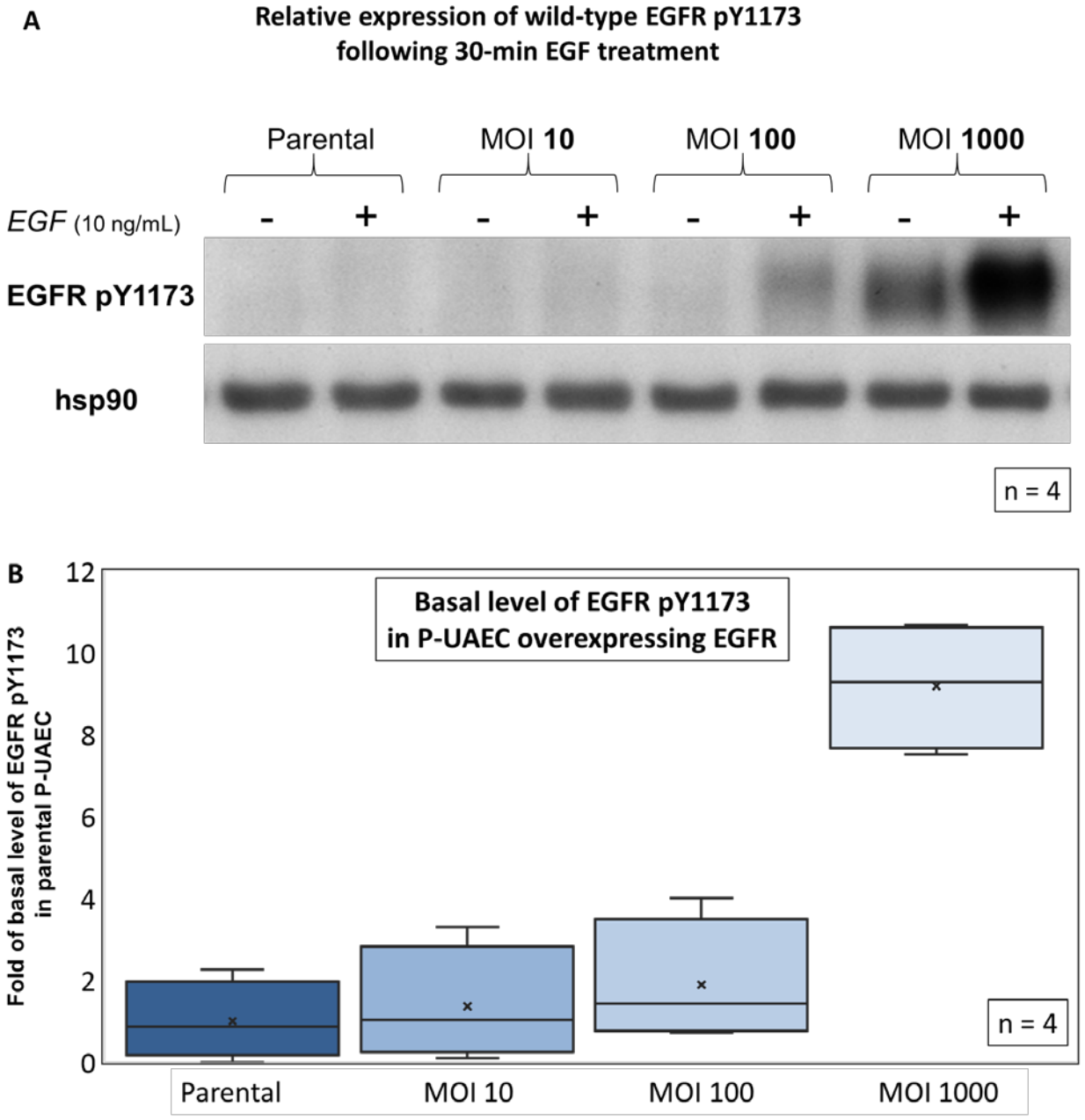

Figure 4.8 Overexpressed EGFR in P-UAEC is constitutively autophosphorylated at an adenoviral MOI of 1000. (A) Adenoviral transduction of the *EGFR* gene in P-UAEC at an MOI of 100 also resulted in significant autophosphorylation in response to 30-minute EGF treatment but did not display constitutive autophosphorylation. No significant basal or ligand-responsive autophosphorylation of EGFR was detected in parental P-UAEC or the MOI 10 cells. (B) Clear and consistent autophosphorylation of Y1173 is readily apparent when displayed as a box-and-whisker plot.

Figure 4.9

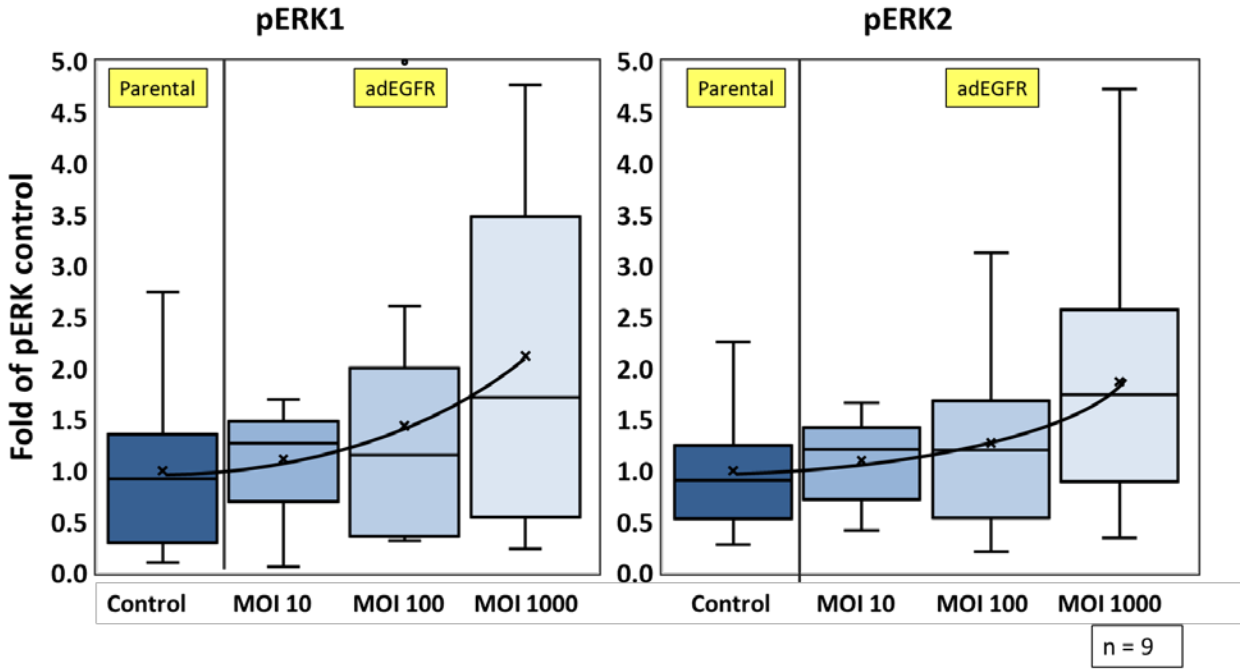

Figure 4.9 Basal levels of pERK1 and pERK2 in P-UAEC adenovirally transduced with EGFR at MOIs of 10, 100, and 1000. ANOVA revealed no significant differences in basal ERK phosphorylation between any cells irrespective of MOI; however, a trend of increased MOI inducing greater pERK1/2 was observed. Cells transduced at an MOI of 1000 exhibited the greatest increases of mean basal ERK1 and ERK2 phosphorylations at 2.1- and 1.9-fold, respectively, above the levels observed in parental P-UAEC, but these elevations were not found to be significant due to the variance between trials. Data obtained from phospho-ERK1/2-selective Western blot analysis. Results were normalized to hsp90 protein level. Mean values of 9 independent experiments are represented by an 'X' in the center of each box and whisker entry. Scale on vertical axis represents fold of basal pERK1 in parental P-UAEC.

Figure 4.10

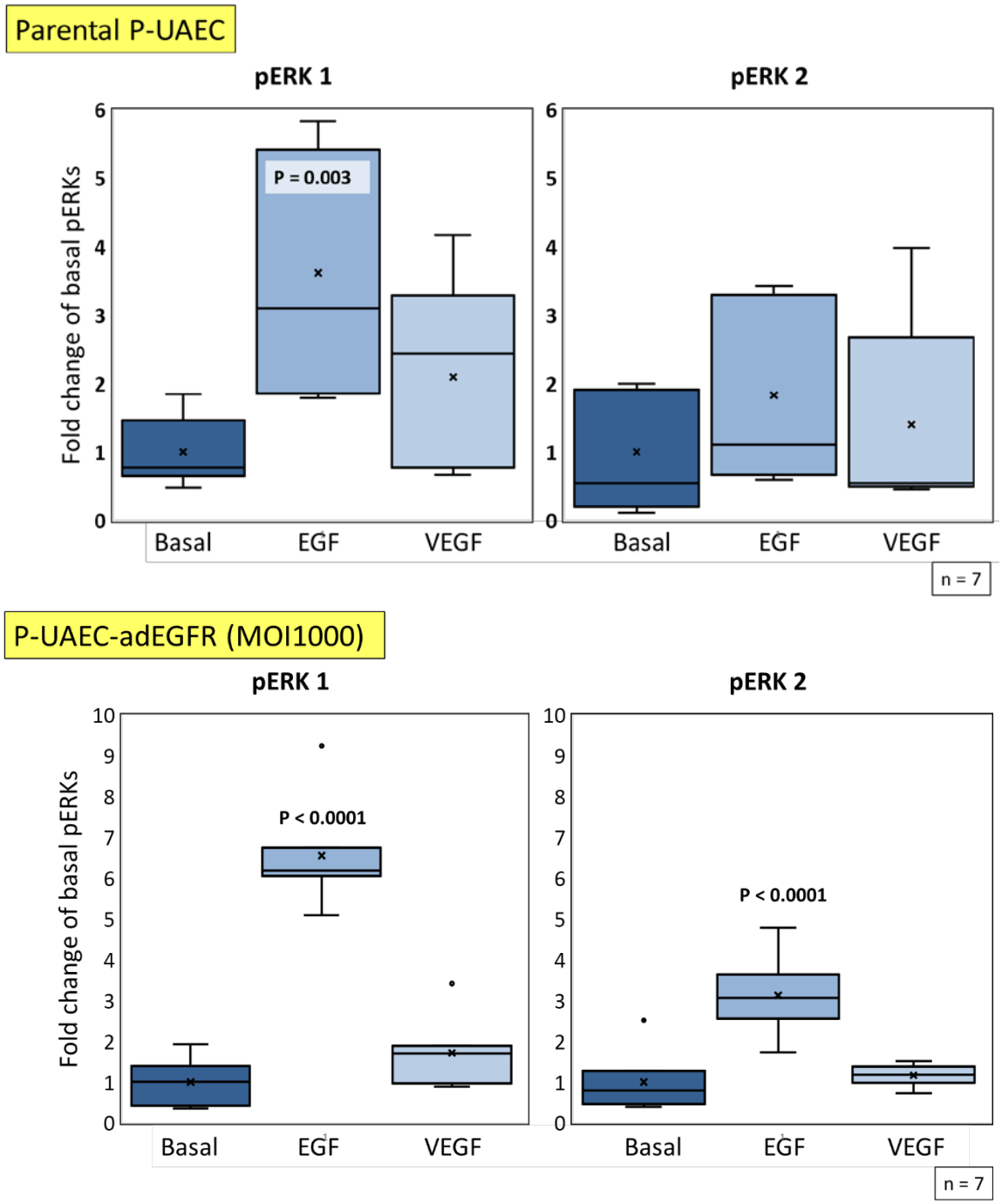

Figure 4.10 Phosphorylation of ERK1/2 in Parental P-UAEC and P-UAEC-adEGFR Following 30-minute Growth Factor Treatment Treatment with EGF (10 ng/mL) for 30-minutes induced a significant phosphorylation of ERK1 in parental P-UAEC and robust phosphorylations of ERK1 and ERK2 in P-UAEC-adEGFR. VEGF has been shown previously to induce significant phosphorylations of ERK1/2 that peak at 10 minutes (Grummer *et al.* 2009) However, administration of VEGF at 30 minutes showed no apparent increase. In parental P-UAEC, this is due to the transient nature of the phosphorylation. In P-UAEC-adEGFR, the reason is unclear. Data were obtained by Western blot and analyzed by ANOVA and Dunnett's test. (n = 7)

Figure 4.11

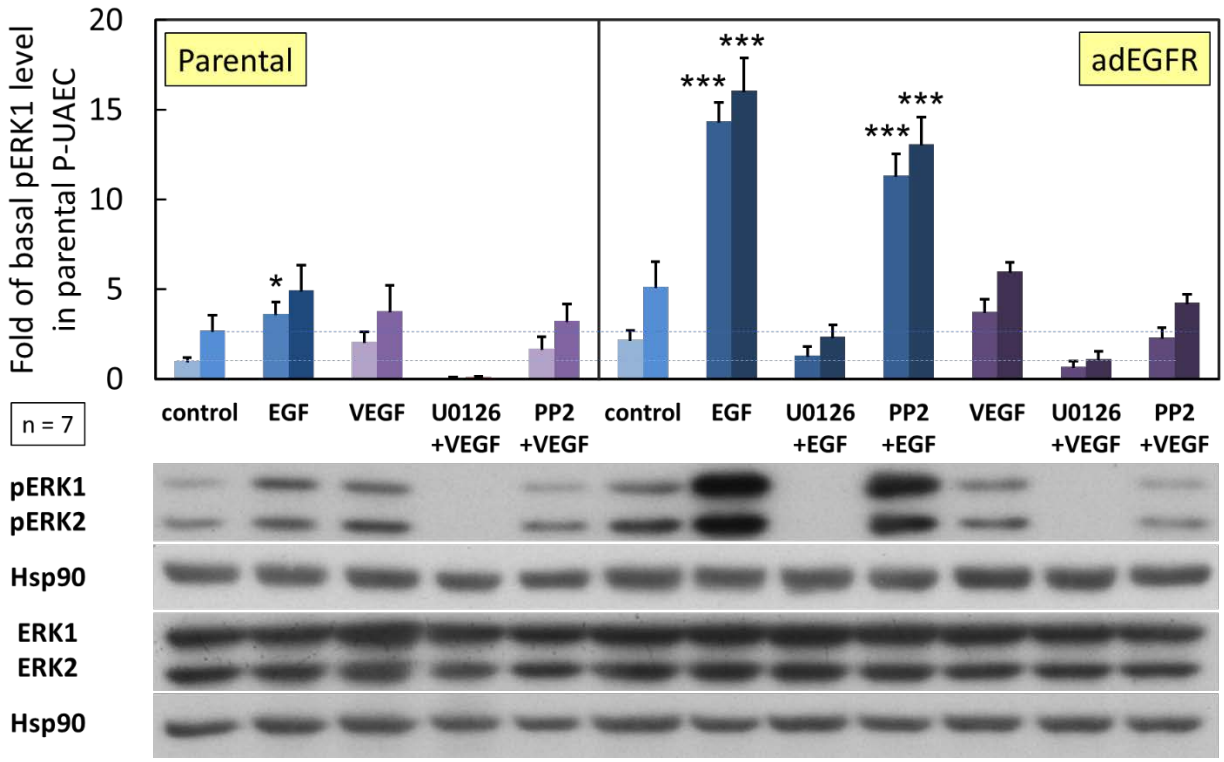

Figure 4.11 Phosphorylation of ERK1 & ERK2 following 30-min growth factor treatment These are the results for all 12 lanes of 7 independent experiments shown together. The first noticeable feature of these data is the strong effect of EGF on ERK1/2 phosphorylation in P-UAEC-adEGFR. Another important point is that the MEK-selective inhibitor U0126 was highly effective at 10 μM in blocking ERK1/2 phosphorylation. Statistical analysis by ANOVA and Tukey's range test. (*) $P < 0.05$. (***) $P < 0.0001$

Chapter 5:

Effects of overexpression of EGFR in P-UAEC on pregnancy adapted programming

Abstract

Healthy pregnancy is dependent on enhanced vasodilation, achieved by an increase in connexin 43 (Cx43) gap junctional communication (GJC) that improves sustained capacitative calcium entry (CCE). Preeclampsia, a hypertensive disorder of pregnancy associated with endothelial dysfunction, is characterized by increased levels of vascular endothelial growth factor (VEGF), which downregulates Ca2+-driven nitric oxide production through VEGFR-2-mediated ERK1/2 signaling. In a uterine artery endothelial cell model derived from pregnant sheep (P-UAEC), treatment with epidermal growth factor (EGF) or VEGF induces ERK1/2 phosphorylations, but only VEGF induces ERK-mediated inhibitory phosphorylations of Cx43. We hypothesized that Cx43-associated pools of ERK are limited in P-UAEC, and the low level endogenous EGF receptor expression in P-UAEC restricts EGFR access to these ERK pools. We further predicted that overexpression of exogenous EGFR in P-UAEC at a level that conferred constitutive autophosphorylation would not only facilitate access to Cx43-associated ERK pools, but also induce a permanent downregulation of pregnancy-adapted Ca2+ signaling. Contrary to our hypothesis, P-UAEC that express constitutively active EGFR (P-UAEC-adEGFR) did not permanently downregulate GJC. However, EGF treatment of P-UAEC-adEGFR reproduced the inhibitory effects previously demonstrated by VEGF, confirming that the higher expression level of EGFR facilitated access to the relevant ERK pools. Interestingly, in P-UAEC-adEGFR, VEGF was no longer able to downregulate CCE. This result suggests 1) that EGFR at elevated levels may have a greater affinity for effector molecules of the ERK1/2 pathway than VEGFR-2, and 2) that maintaining low endogenous EGFR expression in P-UAEC may be necessary to allow VEGFR-2 control of ERK-mediated regulation of GJC, a necessary step to initiating angiogenesis.

5.0 Perspective

Chapter 3 reviewed the necessary background information to provide context for my project. It introduced the concept of pregnancy-adapted programming—the coordination of cell signaling events in early pregnancy that enable enhanced function of the maternal vascular endothelium sufficient to accommodate the demands of pregnancy. This programming is evidenced by enhanced gap junctional communication (GJC) that facilitates greater capacitative calcium entry (CCE), which in turn amplifies the activity of endothelial nitric oxide synthase (eNOS) and results in sustained vasodilation. Chapter 3 also described how preeclampsia (PE) and other hypertensive disorders of pregnancy result from the failure of pregnancy-adapted programming, and how the growth factors and cytokines elevated during preeclampsia can suppress GJC and CCE. Though many growth factors and cytokines (and non-physiological agonists such as TPA) can suppress healthy maternal vascular function, I focused on the effects of VEGF in particular because of the nature of my project, one goal of which was to show that the inhibitory effects of VEGF-dependent VEGFR-2 signaling in P-UAEC could be duplicated with EGF via the addition of exogenous EGFR.

Chapter 4 focused on the rationale and the technical considerations for the development of my project. Decades of cancer research have resulted in a wide selection of molecular tools for exploring the mechanisms of EGFR signaling, whereas the availability of tools for VEGFR-2 study are limited. If we could establish that EGFR utilized precisely the same pathways to induce inhibition of GJC and CCE as employed by VEGFR-2, we could potentially use the many tools of EGFR research to explore the molecular mechanisms of pregnancy-adapted programming of the maternal vasculature. Additionally, while nearly all EGFR research is conducted in the context of cancer biology, we speculated that the harmful effects of dysregulation of a central signaling molecule like EGFR could be expected to extend well beyond cancer. While the role of EGFR itself in the etiology and progression of PE is unknown, our speculation is supported by the fact

that PE is characterized by dysregulation of canonical EGFR cancer *signaling* pathways. Although these EGFR-associated pathways are in fact shared by other growth factors and cytokines in PE and don't necessarily require activation by EGFR specifically, I discussed the evidence for the possible role of EGFR signaling in the development and/or maintenance of hypertensive diseases, and gave examples of the ability of EGF to inhibit GJC in a variety of cell models. Together, these data formed the basis of our proposal to "engineer preeclampsia" by overexpressing EGFR in uterine artery endothelial cells obtained from pregnant ewes (P-UAEC), which otherwise express EGFR at a negligible level. Upon activation by GPCRs or RTKs, uniquely localized pools of ERK1/2 in the cytosol are mobilized to specific cellular regions, from the nucleus to the plasma membrane (Reviewed in Luttrell 2003). Presumably due to the low level of receptor expression, EGF treatment of P-UAEC, despite inducing significant ERK1/2 phosphorylation, does not significantly activate Cx43-associated ERK pools, and thus [Ca2+]i bursting is not inhibited. However, we proposed that expression of exogenous EGFR in P-UAEC would enable EGF access these pools and thereby duplicate the inhibitory effects of VEGF. Additionally, we predicted that substantial overexpression or activating mutations of EGFR in P-UAEC might result in permanent constitutive inhibition of pregnancy-adapted GJC and CCE. To test our predictions, we manipulated EGFR expression level in normal P-UAEC by transducing the cells with adenovirus containing the wild-type *EGFR* or *L834R-EGFR* gene transcript.

The remainder of Chapter 4 provided experimental evidence that answered the key technical questions associated with overexpression of EGFR in P-UAEC. I demonstrated that adenoviral transduction of the *EGFR* gene transcript in P-UAEC at an MOI of 1000 results in expression of the receptor on the plasma membrane at a concentration that confers constitutive autophosphorylation without loss of cell viability. The exogenous EGFR was further shown to be coupled to the MEK/ERK pathway, a key signaling pathway in the regulation of Cx43 gap junctional communication (GJC).

Finally, having demonstrated that our adenovirally transduced P-UAEC passed all the relevant benchmarks of viability and functionality, I proceeded to conduct the experiments described in this chapter.

5.1 Introduction

5.1.1 The "Big" Question

The first question we will answer in this chapter is the "big" question of this dissertation: *Does overexpression of wild-type EGFR or L834R-EGFR in P-UAEC result in constitutive downregulation of GJC?* If our hypothesis is correct and the answer is yes, we should observe a significant reduction in the mean number of [Ca2+]i bursts in the 30-minute period of initial treatment with ATP. Once the ability of overexpressed EGFR to induce constitutive inhibition of GJC has been established, the adenoviral MOI will be reduced to determine the expression level of EGFR that no longer induces ligand-independent inhibition of GJC, but duplicates the effects of VEGF treatment when EGF is administered. If constitutively autophosphorylated EGFR in P-UAEC does not result in permanent inhibition of GJC, it will still be important to characterize any inhibitory effects of EGF treatment.

Remember that wild-type EGFR became constitutively autophosphorylated in P-UAEC only when the *EGFR* gene transcript was adenovirally transduced at an MOI of 1000 or more, but L834R-EGFR is constitutively autophosphorylated even at low expression levels. If basal downregulation of [Ca2+]i bursting occurs in P-UAEC expressing the mutant L834R-EGFR, I plan to reduce the adenoviral MOI of *L834R-EGFR* to determine the minimum expression level of L834R that is able to inhibit GJC.

If overexpression of EGFR in P-UAEC does induce a preeclamptic-like state of poor GJC, an important new question arises: *Is this phenomenon simply a laboratory curiosity or does overexpression of EGFR actually occur in the vascular endothelium of some pregnant women?* Might there be a subset of PE patients, or indeed anyone with hypertension, whose disease symptoms are the direct result of EGFR overexpression? Though placental expression of EGFR appears to be similar in both healthy and PE pregnancies (Kosovic *et al.* 2017), no data are available for EGFR expression in the vascular endothelium of PE patients.

5.1.2 Other Important Questions

Many additional questions will be answered in this chapter.

Does the overexpression of EGFR in P-UAEC result in elevated basal phosphorylations of Cx43 Y265 and/or S279/282? In parental P-UAEC (P-UAEC that have *not* been exposed to adenovirus), VEGFR-2-mediated inhibition of the ATP-stimulated [Ca2+]i bursting response is dependent on these phosphorylations of Cx43 (see 3.1.4). If overexpression of EGFR in P-UAEC does result in a constitutive inhibition of GJC, we would expect to observe elevated basal phosphorylation of these Cx43 sites.

In P-UAEC-adEGFR, does treatment with EGF following 30-minute ATP stimulation reduce—or further reduce beyond basal inhibition—the mean number of [Ca2+]i bursts during subsequent ATP administration? While basal phosphorylations of ERK1/2 were found not to be significantly elevated in P-UAEC-adEGFR but only trended toward an increase, EGF treatment resulted in robust elevations of ERK1/2 phosphorylation. This may correlate with more dramatic inhibition of GJC. Alternatively, overexpression of EGFR in P-UAEC may not result in constitutive inhibition of GJC, yet subsequent treatment with EGF may inhibit [Ca2+]i bursting in a manner similar to VEGF in parental P-UAEC.

Does the EGF/EGFR system utilize the same signaling pathways as the VEGF/VEGFR-2 system to effect changes in GJC? In parental P-UAEC, VEGFR-2 acts via Src and ERK1/2 to inhibit GJC. It may be possible that EGFR inhibits GJC via ERK but not Src, or vice versa, or through another kinase altogether such as PKC.

Will pharmacological inhibitions of Src and ERK pathways protect against the negative effects of EGFR signaling as they protect against the negative effects of VEGFR-2 signaling? This question follows naturally from the previous question. VEGFR-2 mediated inhibition of GJC was prevented by pretreatment with either PP2 (SFK-selective inhibitor) or U0126 (MEK-selective inhibitor) (see 5.1.7). EGFR-mediated inhibition of GJC is also likely to be prevented by these drugs.

5.2 Methods

Detailed experimental protocols are presented in Chapter 9.

5.2.1 Calcium imaging

Calcium Imaging Protocol 1.0 was used to generate the data for Figure 5.3. Calcium Imaging Protocol 1.0 and 1.1 were used to generate the data for Figure 5.6.

5.2.2 Western blotting

Western Blot Protocol 1.0 was used to generate the data for Figures 5.2 and 5.4. Western Blot Protocol 1.1 was used to generate the data for Figures 5.5 and 5.7.

5.3 Results

5.3.1 Overexpression of EGFR—wild-type or L834R—in P-UAEC does not constitutively inhibit pregnancy-adapted programming

If our hypothesis is correct that overexpression of EGFR in P-UAEC would have a permanent constitutive inhibitory effect on gap junctional communication (GJC), we would expect treatment with ATP to result in a significantly weaker [Ca2+]i bursting response in P-UAEC-adEGFR and adL834R than in parental P-UAEC. By aggregating the data from every calcium imaging trial that did not involve an overnight pretreatment (such as the insulin pretreatment trials discussed in Chapter 6), I was able to compare the mean number of ATP-stimulated [Ca2+]i bursts exhibited by parental P-UAEC (1346 cells) vs. P-UAEC-adEGFR (1147 cells) prior to any administration of kinase inhibiting drugs or growth factors. Contrary to our prediction, the mean number of bursts per cell was 4% greater ($P = 0.0051$) in P-UAEC-adEGFR than the mean number of bursts in parental P-UAEC (Figure 5.1). This alone refutes our hypothesis that the constitutive kinase activity of overexpressed EGFR would induce a permanent basal inhibition of GJC. A possible mechanism for the small but significant EGFR enhancement of capacitative calcium entry (CCE) will be discussed in Chapter 6.

The fact that neither variant of EGFR inhibited GJC in P-UAEC limited the usefulness of the L834R mutant in subsequent experiments, primarily because constitutive autophosphorylation of the receptor was shown to be much less relevant than we had anticipated. As section 5.3.4 will show, the calcium imaging experiments that were performed using P-UAEC-adL834R produced results that were largely indistinguishable from the results of experiments involving P-UAEC-adEGFR.

5.3.2 Basal phosphorylations of Cx43 inhibitory sites (Y265 and S279/282) are not elevated in P-UAEC-adEGFR

As stated in Chapter 4, we hypothesized that overexpression of EGFR in P-UAEC would result in a state of permanent inhibition of GJC, presumably by significantly increasing the basal phosphorylation of Cx43 inhibitory sites—the c-Src-mediated Y265 and/or the ERK1/2-mediated S279/282. In the previous section, this hypothesis was shown to be false by calcium imaging data, which provided surprising evidence of a small but statistically significant enhancement of CCE in P-UAEC-adEGFR. The Western blot data presented in Figure 5.2 provided further evidence to refute our initial hypothesis. Adenoviral transduction of EGFR in P-UAEC at MOIs of 10, 100, and 1000 each resulted in no change in the basal phosphorylation level of Cx43 Y265 or S279/282.

In Chapter 4, I presented Western blot evidence showing a weak trend toward adenoviral MOI of *EGFR* being proportional to basal ERK1/2 phosphorylation. This finding confirms that the basal levels of pERK1/2 observed at each respective MOI (Figure 4.8) were insufficient to raise basal elevation of Cx43 pS279/282.

5.3.3 EGF treatment inhibits the pregnancy-adapted Ca2+ burst function in P-UAEC-adEGFR and P-UAEC-adL834R to a level consistent with VEGF-induced inhibition in parental P-UAEC

In P-UAEC-adEGFR and adL834R, the results were reversed from those seen in parental P-UAEC. Treatment with EGF now induced significant inhibition of ATP-induced [Ca2+]i bursting, whereas, surprisingly, VEGF treatment no longer had an effect (Figure 5.3, right), precisely the opposite of the respective effects of EGF and VEGF observed in cells that don't express exogenous EGFR. Although the increased expression of wild-type or mutant EGFR in P-UAEC was shown to be insufficient to result in constitutive inhibition of GJC, the presence of exogenous EGFR clearly makes dramatic differences in the effects of transient growth factor treatment on

gap junction function. These results further suggest that VEGFR-2 is sufficient to mediate the inhibitory action of VEGF on GJC since we have previously shown that VEGFR-2, but not VEGFR-1, mediates VEGF-induced phosphorylation of ERK1/2 in P-UAEC (Grummer *et al.* 2009). However, these data do not rule out the possibility of VEGFR-1/VEGFR-2 heterodimer involvement, a topic that will be explored in Chapter 7.

Plausible explanations for the distinct actions of EGF and VEGF will be discussed later in this chapter as further evidence of their unique signaling mechanisms is presented.

5.3.4 EGF treatment induces phosphorylations of Cx43 at Y265 (c-Src-mediated site) and S279/282 (ERK-mediated site) in P-UAEC-adEGFR

In parental P-UAEC, Western blot analysis showed that phosphorylation of the Cx43 inhibitory site Y265 was significantly increased (1.5-fold) by 30-minute treatment with VEGF, but not by EGF treatment (Figure 5.4A, left). This is consistent with the results of my calcium imaging experiments using parental P-UAEC, in which VEGF treatment significantly reduced mean number of ATP-induced Ca2+ bursts, but the EGF treatment group results were no different than the control group (see 5.3.3). In P-UAEC-adEGFR, 30-minute treatment with VEGF again resulted in a significant 1.5-fold increase ($P = 0.048$) in Cx43 Y265 phosphorylation, while EGF treatment resulted in a 1.7-fold increase ($P = 0.008$) (Figure 5.4A, right). Since calcium imaging experiments with P-UAEC-adEGFR showed that EGF treatment induced significant inhibition of ATP-stimulated [Ca2+]i bursting and VEGF treatment had no effect (see 5.3.4), the relevance of Cx43 Y265 phosphorylation in P-UAEC-adEGFR is uncertain without further study.

In parental P-UAEC, phosphorylation of the Cx43 inhibitory site S279/282 was unaffected by 30-minute treatment with VEGF or EGF (Figure 5.4B, left). This is contrary to prior research published by the Bird Laboratory, which found that 30-minute VEGF treatment significantly elevated pS279/282 1.4-fold (Boeldt *et al.* 2015). Possible reasons for this discrepancy will be discussed

at the end of this chapter. In P-UAEC-adEGFR, 30-minute treatment with VEGF again had no effect on Cx43 S279/282 phosphorylation, but EGF treatment resulted in a highly significant ($P < 0.0001$) 2.8-fold increase (Figure 5.4B, right).

Thus far, these data suggest that the inhibition of Ca2+ bursting induced by VEGF in parental P-UAEC is likely to be mediated primarily via c-Src, whereas the inhibition of Ca2+ bursting induced by EGF in P-UAEC-adEGFR is likely to be mediated primarily via the MAPK pathway.

5.3.5 ATP-stimulated Ca2+ bursting in P-UAEC-adEGFR is fully "rescued" from EGF inhibition by blocking the MAPK signaling pathway, but not by blocking c-Src

Since Cx43 Y265 phosphorylation is mediated by Src (and perhaps Fyn or Yes), we would expect 30-minute pretreatment with the MEK inhibitor U0126 (10 μM) to have no effect on EGF-induced pY265, while the Src family kinase inhibitor PP2 (10 μM) would be expected to keep pY265 near the basal level. In Figure 5.5A, the effects of both pretreatments on Y265 phosphorylation were shown to be just as expected. U0126 pretreatment prior to 10 ng/mL EGF administration was not significantly different from EGF alone, and PP2 pretreatment kept Cx43 Y265 phosphorylation at a level not significantly different from basal pY265.

Inversely, since Cx43 S279/282 phosphorylation is mediated by ERK1/2, we would expect 30-minute pretreatment with PP2 to have no effect on EGF-induced pS279/282, while U0126 would be expected to keep pS279/282 at the basal level. Again, in Figure 5.5B, the effects of both pretreatments were shown to be just as expected. U0126 pretreatment prior to EGF administration indeed kept Cx43 S279/282 phosphorylation at the basal level, and PP2 pretreatment was not significantly different from EGF alone.

Having confirmed that both pharmacological kinase inhibitors effectively prevented their respective EGF-induced phosphorylations of Cx43 in the expected manner, we then needed to determine how their administration would affect the ATP-stimulated Ca2+ bursting response. To

answer this question, Fura-2-loaded P-UAEC-adEGFR were treated with 100 µM ATP for 30 min, then washed and pretreated with either 10 µM U0126 or PP2 for 30 minutes prior to 10 ng/mL EGF treatment and repeat stimulation with ATP. As expected, when the cells were pretreated with U0126 prior to EGF treatment, the mean number of ATP-stimulated [Ca2+]i bursts remained at the level of untreated control cells; however, when the cells were pretreated with PP2 prior to EGF treatment, the mean number of ATP-stimulated [Ca2+]i bursts dropped to the level observed when EGF alone was added (Figure 5.6). Remember that both U0126 and PP2 were able to protect the Ca2+ burst response from inhibition by VEGF (see 3.1.7), suggesting a single pathway involving both ERK1/2 and Src. However, we now see that PP2 provided no protection from inhibition by EGF. Together these data suggest that VEGF-induced inhibition of the ATP-stimulated Ca2+ response is mediated by ERK1/2 in a Src-dependent manner, whereas EGF-induced inhibition is mediated by ERK1/2 in a Src-*independent* manner.

5.4 Discussion

EGF has been shown to inhibit gap junctional communication (GJC) in a wide variety of cell types (Madhukar et al. 1989; Lau *et al.* 1992; Oh *et al.* 1993; Fong *et al.* 2014) via PKC- and ERK1/2-dependent phosphorylations of Cx43 (Kanemitsu and Lau 1993; Leykauf *et al.* 2003; Fong *et al.* 2014). Given the role of EGF in promoting wound healing, cellular migration, and growth, this is not surprising. It makes sense that EGF would act to reduce the connections between cells to allow the removal of damaged tissue and the proliferation and migration of new cells. A review of the literature on EGF and Cx43 over the past 30 years turned up only a single case of EGF-induced *enhancement* of GJC. The unique mechanism of this enhancement, observed in the K7 human kidney epithelial cell line, involved translational control of Cx43 expression, not phosphorylation of Cx43 (Rivedal *et al.* 1996). Yet in our unmodified uterine artery endothelial cell

model (UAEC), treatment with EGF neither inhibits nor enhances GJC (see 5.3.3). The lack of observable effect can be explained by the fact that EGF has only one known molecular target—EGFR—and expression of EGFR protein in UAEC is so low that it is undetectable by Western blot analysis. This led us to ask why a receptor so vital to a healthy pregnancy would be virtually absent from the uterine vascular endothelium where VEGFR2 clearly serves a vital function signaling through similar pathways.

From an evolutionary perspective, there are only two reasons why an otherwise widely expressed protein would be minimally expressed in a cell: (1) expression of the protein in the cell has no effect on the reproductive fitness of the organism—i.e. the protein is extraneous or redundant with regard to cell function, or (2) robust expression of the protein in the cell would have a deleterious effect on the reproductive fitness of the organism. The two explanations could be summarized as *absence of selection pressure for expression* and *direct selection pressure against expression*. Had overexpression of EGFR in P-UAEC at high enough level for auto activation induced a constitutive loss of GJC, the result would have supported the latter explanation. However, the absence of such an effect in our isolated cell culture doesn't necessarily mean the former explanation is correct because we cannot be certain of the extent to which exogenous EGFR could also be transactivated by circulating cytokines in the maternal vasculature over the duration of pregnancy. TNFα, IL-8, IL-1α, IL-1β, and IFNγ have all been reported to transactivate EGFR (Argast *et al.* 2004; Chen *et al.* 2004; Itoh *et al.* 2005; Tanida *et al.* 2004). IL-8, for example, has been shown to induce phosphorylations of a wide variety of signaling molecules via EGFR transactivation, including not only Src and ERK1/2, but also FAK, Jnk, p38-MAPK, STAT1 and STAT3. Transactivation was confirmed by pharmacological inhibition of IL-8 or EGFR, which abolished these phosphorylations (Kyriakakis *et al.* 2011).

Despite the magnitude of the inhibition being the same for EGF treatment in P-UAEC-adEGFR as for VEGF treatment in parental P-UAEC, the use of MEK- and SFK-selective kinase inhibitors

in calcium imaging trials and the phosphorylation data obtained by Western blotting suggest that EGFR and VEGFR-2 achieve their apparently similar effects through different mechanisms.

In P-UAEC-adEGFR, 30-minute treatment with EGF resulted in a significant 1.7-fold elevation of Cx43 Y265 phosphorylation ($P = 0.008$) compared against vehicle-treated controls, an event mediated by Src. EGF also induced a strongly significant 2.8-fold increase in the phosphorylation of Cx43 S279/282 ($P < 0.0001$), an event mediated by ERK1/2. These data support the assertion that EGFR is able to activate signaling cascades via both relevant pathways. As discussed in Chapter 3, cumulative evidence suggests that pS279/282 is associated with gap junction closure, whereas pY265 is associated with disassembly and internalization (Reviewed in Solan and Lampe 2014; 2016). In addition to directly phosphorylating Y265, activated Src has also been shown to induce phosphorylations of ERK-mediated sites on Cx43 (Solan and Lampe 2008). Similarly, published research from the Bird Laboratory has confirmed that ERK1/2 phosphorylations resulting from VEGF treatment of P-UAEC occur via both Src-dependent and Src-independent pathways (Boeldt et al. 2015). The ability of PP2 to fully protect against VEGF inhibition of [Ca2+]i bursting (Boeldt et al. 2015) suggests that Src-independent ERK1/2 activation by VEGF plays only a marginal role in its effect on GJC.

EGF inhibition of GJC appears to be mediated quite differently. When P-UAEC-adEGFR were pretreated with the SFK-selective inhibitor PP2 prior to EGF administration, Y265 phosphorylation was reduced to a level not significantly different than basal, but there was no protection from EGF inhibition of [Ca2+]i bursting. The Ca2+ burst response was inhibited by EGF just the same as if PP2 had not been added. However, the Ca2+ burst response was completely protected against the inhibitory effect of EGF when the cells were pretreated with the MEK-selective inhibitor U0126, thus cementing the case that EGF inhibition of GJC is strongly dependent on elevated pERK1/2 and only minimally or not at all dependent on the activity of c-Src (Figure 5.4A & B, right).

We attempted to duplicate the effects of VEGF with EGF and were successful, but unlike VEGF, the data suggest that EGF inhibits GJC in a Src-*independent* manner. If further research reveals Src to be a master regulator of gap junction function and Cx43 protein turnover in endothelial cells as accumulating evidence suggests (Reviewed in Solan and Lampe 2008; 2014; 2016), this may be the reason why EGFR is minimally expressed in UAEC. Its presence in the maternal vasculature would make it a "rogue agent," acting outside the regulatory control of Src.

The remainder of this section will address questions that arose from the results of my experiments.

5.4.1 Why did EGFR overexpression in P-UAEC fail to induce basal elevation of pERK1/2?

At normal physiological levels of expression of EGFR and its ligands, phosphorylation of ERK1/2 is a negative regulator of EGFR kinase activity (Reviewed in Lake et al. 2016). In many aggressive cancers, activating mutation of EGFR or overexpression of the receptor (or its ligands) overcomes this natural feedback inhibition, resulting in dysregulation of the MAPK pathway. In Chapter 4, I presented evidence that the differences in basal ERK1/2 phosphorylation in P-UAEC expressing varied levels of exogenous EGFR were not statistically significant, even though the mean phosphorylation levels of ERK1/2 appeared to rise with increasing adenoviral MOI (Figure 4.X). In any case, the level of basal Cx43 S279/282 phosphorylation in adenovirally transduced P-UAEC was the same as that observed in parental P-UAEC, irrespective of the level of EGFR protein expression. This result confirms that the weak trend toward elevated basal phosphorylations of ERK1 and ERK2 was not sufficient to induce phosphorylations of Cx43 S279/282, or perhaps involved distinct pools of ERK1 and ERK2 that had no access to Cx43.

It should be noted that even if exogenous EGFR had induced a greater and significant elevation of ERK1/2, it still might not have resulted in constitutive inhibition of GJC. A study published by Sirnes et al. (2009) found that 30-minute EGF treatment at the supraphysiological dose of 100 ng/mL (16 nM) completely blocked GJC in the rat liver epithelial cell line IAR20, as determined by

quantitative image analysis of Lucifer Yellow dye spreading. Pretreatment with the EGFR-selective kinase inhibitor AG1478 or the MEK-selective inhibitor U0126 protected GJC completely, thus confirming the EGF-induced loss of GJC to be entirely dependent on EGFR signaling via the MAPK pathway. However, after 5 hours of continuous exposure to 100 ng/mL EGF, GJC had returned to about 70% of its normal level. Admittedly, without further data, it cannot be determined where in the chain from receptor to Cx43 phosphorylations the negative feedback was initiated. However, the result does support the claim that GJC is resistant to constitutive inhibition induced by excessive EGFR-mediated MAPK signaling.

Since I was not able to obtain direct Western blot phosphorylation data for Src, I have no direct evidence to suggest that P-UAEC-adEGFR exhibit basal elevation of Src Y416 phosphorylation (activated c-Src) relative to the basal level in parental P-UAEC. Irrespective of Src phosphorylation status, however, the basal phosphorylation of Cx43 Y265 in P-UAEC-adEGFR was not significantly different from that observed in parental P-UAEC (Figure 5.2A). This result suggests that c-Src pY416 is not basally elevated in P-UAEC-adEGFR because there is plenty of evidence that expression of v-Src (the constitutively active viral form of Src) does indeed result in a permanent inhibition of GJC in multiple cell models (Atkinson *et al.* 1981; Filson *et al.* 1990; Zhou *et al.* 1999; Cottrell *et al.* 2002) accompanied by basal elevations of Cx43 pY247, pS262, pY265, pS279/282, and pS368 (Crow *et al.* 1990; Kanemitsu *et al.* 1997; Solan and Lampe 2008). Furthermore, v-Src-mediated inhibition of GJC can occur through MAPK-dependent (Zhou et al. 1999) and independent (Lin et al. 2001; 2006) mechanisms.

Clearly, despite the absence of elevated pS279/282 in P-UAEC-adEGFR, constitutive phosphorylation of S279/282 without negative feedback does indeed occur in other cell types, resulting in permanent basal inhibition of GJC, but such inhibition appears to be dependent on Src activity (see 3.1.6). Therefore, it is likely that overexpression of EGFR in P-UAEC does not

induce basal inhibition of GJC precisely because it does not induce basal elevation of activated Src.

5.4.2 Why doesn't VEGF inhibit ATP-stimulated [Ca2+]i bursting in P-UAEC-adEGFR or adL834R?

In Chapter 3, I presented evidence that VEGF inhibits ATP-stimulated [Ca2+]i bursting in P-UAEC via Src- and ERK-mediated phosphorylations of Cx43. If VEGF is unable to inhibit GJC in P-UAEC-adEGFR, it must be because the overexpression of EGFR disrupts the Src and ERK signal transduction pathways. VEGF has been shown to induce activation of Src or ERK1/2 through at least five distinct pathways:

1) VEGF → VEGFR-2 pY1175 → PLCγ → PIP2 → DAG → PKC → Raf-1 → MEK1/2 → **ERK1/2** (HUVEC, Wu *et al.* 2000**;** multiple primary endothelial cells and cell lines, Takahashi *et al.* 2001**;** oFPAE cells, Liao *et al.* 2009)
2) VEGF → VEGFR-2 pY1214 → Shc-Grb2-SOS → Ras → Raf-1 → MEK1/2 → **ERK1/2** (HUVEC, Meadows *et al.* 2001)
3) VEGF → VEGFR-2 pY???→ …???... → **Src**-CNK1-Raf-1 → MEK1/2 → **ERK1/2** (HUVEC, Alavi *et al.* 2003**;** HEp2 cells, Ziogas *et al.* 2005)
4) VEGF → VEGFR-2 pY951 → TSAd-**Src** (HUVEC, Matsumoto *et al.* 2005)
5) VEGF → VEGFR-2 pY???→ …???... → **Src** (UAEC, Boeldt et al. 2015)

Recall that in my experiments I could not detect VEGF-induced phosphorylation of Cx43 S279/282 in P-UAEC, irrespective of EGFR expression (Figure 5.4B). There is reason to doubt this result in parental P-UAEC since in Boeldt et al. (2015) VEGF was shown to induce phosphorylation of Cx43 S279/282 and inhibit ATP-stimulated [Ca2+]i bursting. The results of the new experiments I conducted also showed VEGF inhibition of Ca2+ bursting in parental P-UAEC

(Figure 5.3), so perhaps the lack of detection can be attributed to an inferior batch of α-phospho-S279/282 antibody. In P-UAEC-adEGFR, however, the apparent inability of VEGF to induce S279/282 phosphorylation makes sense for two reasons. Firstly, each of the first three pathways leads to ERK1/2 activation, and all converge on Raf-1, a key signaling molecule in the MAPK pathway. Due to EGFR overexpression, it is plausible that the molecular machinery of the MAPK pathway is largely commandeered by the EGFR signal transduction cascade, leaving little available effector molecules such as Raf-1 for VEGFR-2-mediated signaling. Secondly, VEGF was unable to inhibit [Ca2+]i bursting in P-UAEC-adEGFR, which is exactly what Boeldt et al. (2015) observed in parental P-UAEC when the MAPK pathway was pharmacologically blocked, suggesting that VEGF inhibition of GJC in P-UAEC is ERK-dependent and that VEGF cannot sufficiently activate the relevant ERK pools in P-UAEC-adEGFR to affect GJC. Pathways 4 and 5 recruit Src, the tyrosine kinase activity of which is responsible for directly phosphorylating Cx43 Y265 and suppressing GJC. Unfortunately, there is very little data on what happens in between administration of VEGF to the cells and Src phosphorylation of Y265. Furthermore, there is no evidence that the association of Src with TSAd at VEGFR-2 pY951 in pathway 4 (Matsumoto *et al.* 2005) has any connection to Src phosphorylation of Cx43. Although the 1.5-fold elevation of Cx43 pY265 in P-UAEC-adEGFR following VEGF treatment was found to be statistically significant (Figure 5.4A, right; P = 0.048), it was not sufficient to inhibit the [Ca2+]i burst response to ATP. When taken together, the Src- and ERK-mediated phosphorylation data suggest that pathway #3 may be the relevant pathway for VEGF inhibition of GJC. Pathway #3 suggests that VEGF inhibition of GJC is ERK- *and* Src-dependent since CCE is preserved when the activity of either kinase is blocked.

Additionally, the VEGF- and Src-dependent activation of the Raf-MEK-ERK pathway #3 is associated with the formation of a trimeric complex comprising Src, Raf-1, and the scaffolding protein CNK1. Administration of CNK1-specific siRNA in human epithelial HEp2 cells significantly

reduced ERK activation by VEGF, suggesting that VEGF-induced ERK activation is dependent on the CNK1-Src-Raf-1 complex (Ziogas et al. 2005). However, CNK1 (and hence the CNK1-Src-Raf-1 complex) was found to be unnecessary for EGF-dependent (or TPA-dependent) activation of ERK in HeLa cells (Bumeister *et al.* 2004). These data lend further support to the proposition that VEGF inhibition of GJC is, at least in some cell types, a Src-dependent process.

5.4.3 Why did prior research from the Bird Laboratory show that phosphorylation of pS279/282 was induced by VEGF treatment of P-UAEC, but my data did not?

Before concluding the chapter, I must discuss the results of previous experiments published by the Bird Laboratory that contradict my findings regarding phosphorylation of Cx43 S279/282 in parental P-UAEC following 30-minute VEGF treatment. In contrast to my results compiled from 6 independent experiments, which showed a 1.5-fold rise in pY265 and no increase in pS279/282, Western blot data from Boeldt et al. (2015) also compiled from 6 independent experiments showed a ~1.2-fold rise in pY265 and pS279/282. Furthermore, pretreatment with the SFK-selective inhibitor PP2 or MEK-selective inhibitor U0126 prior to VEGF administration eliminated the negative effects of VEGF on ATP-stimulated [Ca2+]i bursting, suggesting that both Src and ERK are involved in VEGF inhibition of GJC. So why did my Western blot results show no significant change in pERK1/2 or Cx43 pS279/282 following VEGF treatment of P-UAEC?

As mentioned in Chapter 4, in each Western blot experiment conducted, 12 protein targets needed to be quantified: Akt pS473, total Akt, Cx43 pY265, Cx43 pS279/282, total Cx43, EGFR pY1173, total EGFR, ERK1 pT202/pY204, ERK2 pT185/pY187, total ERK1, total ERK2, and Hsp90. Of these 12 targets, phosphorylated Cx43 (pY265 and pS279/282) were arguably the most difficult to quantify because the available antibodies for labeling the phospho-serine and phospho-tyrosine sites of Cx43 are notoriously weak. Their poor affinity for their binding targets is evident in the many rows of nonselective bands they produce no matter how meticulously even

the most stringent protocol is followed. The α-pS279/282 antibody I used in my western blot experiments was only able to detect the particularly robust phosphorylations induced by EGF in P-UAEC-adEGFR. Raising the concentration of the antibody only increased binding to nonspecific targets.

Treatment duration is another important factor. While the phosphorylations of EGFR, Akt, and ERK1/2 reach peak levels at 5-10 minutes (Kholodenko et al. 1999; Motley et al. 2002), the c-Src-mediated phosphorylation of Cx43 Y265 is not apparent until 30 minutes after growth factor stimulation (Reviewed in Solan and Lampe 2014), thus necessitating a growth factor treatment duration of at least 30 minutes. I initially considered doubling the number of experiments to generate a second data set for pEGFR, pAkt, and pERK1/2 based on 10-minute treatment, but I concluded it would be too costly (each WB requires 50+ µL of adenovirus) and ultimately unnecessary. The peak magnitudes of the EGFR, Akt, and ERK1/2 phosphorylations were not as important as simply showing an increase had occurred. This reasoning worked fine for pEGFR and pAkt, so why didn't it work for pERK1/2?

A time course of VEGF stimulation of P-UAEC published by the Bird Laboratory had found that both ERK1 and ERK2 phosphorylations peaked at 10 minutes, at 2.4- and 1.7-fold of basal levels, respectively. By 30 minutes, pERK1 and pERK2 had dropped to 1.2- and 1.5-fold of basal levels, respectively, but the elevations were still statistically significant (Grummer et al. 2009). By comparison, my Western blot analysis of 7 independent experiments found that 30-minute VEGF treatment resulted in a mean 2.1-fold rise in pERK1 and a 1.4-fold rise in pERK2. In 4 of the 7 trials, pERK1/2 levels were still elevated at 30 minutes, just as Grummer et al. had reported; however, in the other 3 trials, pERK1/2 dropped back to basal levels within 30 minutes. Therefore, neither of the mean values for pERK were found to be significant due to the high variance between samples. Nonetheless, the most convincing evidence that VEGF does induce phosphorylation of S279/282 in P-UAEC is the protective effect of the MEK-selective inhibitor U0126 on GJC. If

VEGF did not induce inhibitory phosphorylation of Cx43 via the MAPK pathway, then U0126 would not have protected [Ca2+]i bursting from the inhibitory effects of VEGF; however, Boeldt et al. (2015) found that U0126 pretreatment did provide such protection. This is strong evidence that VEGF inhibition of GJC does involve the MAPK pathway, albeit as a secondary response to Src activity.

An additional consideration is the cellular distribution of Cx43. At any given time, Cx43 protein will be localized at the plasma membrane (in functional gap junctional plaques and in disordered connexons), in the cytosol, the mitochondria, and in the nucleus (Mauro *et al.* 2013). It is highly likely that Western blot detection of Cx43 S279/282 or Y265 in gap junctional plaques is significantly attenuated by the unphosphorylated Cx43 elsewhere in the cell. If this speculation is correct, it would mean that the Western Blot quantification of, say, a 1.5-fold increase in total pY265 is actually a several-fold increase at the gap junctional plaques. Smaller but still significant changes in Cx43 phosphorylation in gap junctional plaques might be virtually undetectable by Western blot analysis.

Finally, it is important to note that my results did agree with Boeldt et al. with respect to the magnitude of VEGF inhibition of Ca2+ bursting; we both found that VEGF reduced the mean number of bursts in P-UAEC by ~10% below the number observed in untreated cells.

Figure 5.1

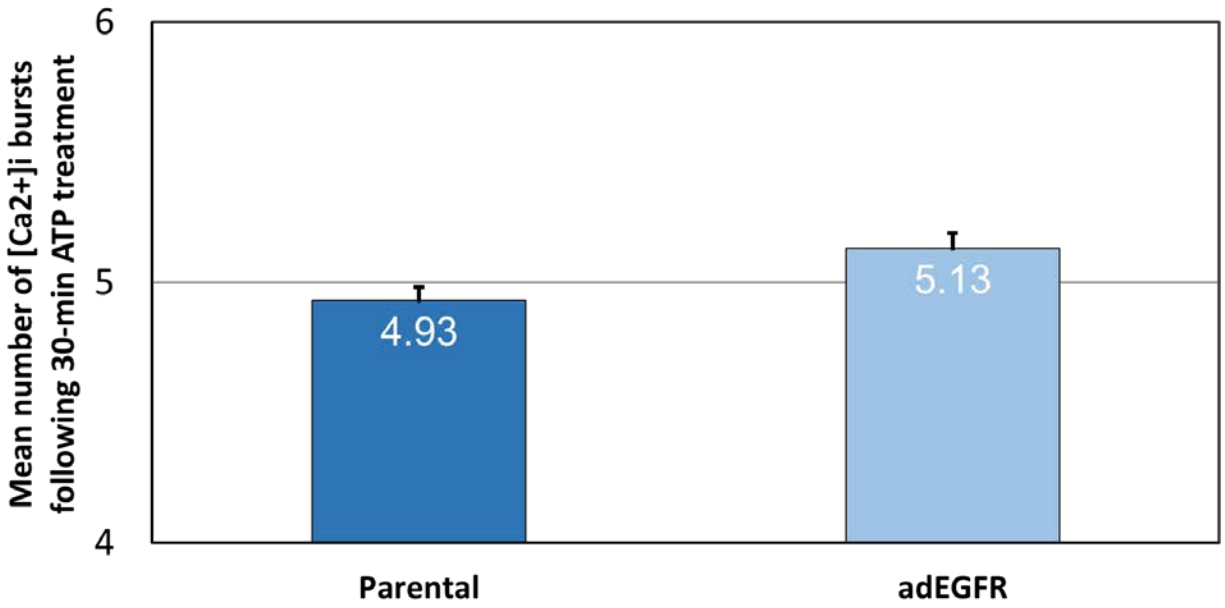

Figure 5.1 Comparison of the mean number of Ca2+ bursts in parental P-UAEC and P-UAEC-adEGFR following 30-minute ATP treatment By aggregating the data from every calcium imaging trial that did not involve an overnight pretreatment (such as the insulin pretreatment trials discussed in Chapter 6), I was able to compare the mean number of ATP-stimulated [Ca2+]i bursts exhibited by parental P-UAEC (1346 cells) vs. P-UAEC-adEGFR (1147 cells) prior to any administration of kinase inhibiting drugs or growth factors. Contrary to our prediction, the mean number of bursts per cell was 4% greater (P = 0.0051) in P-UAEC-adEGFR than the mean number of bursts in parental P-UAEC.

Figure 5.2

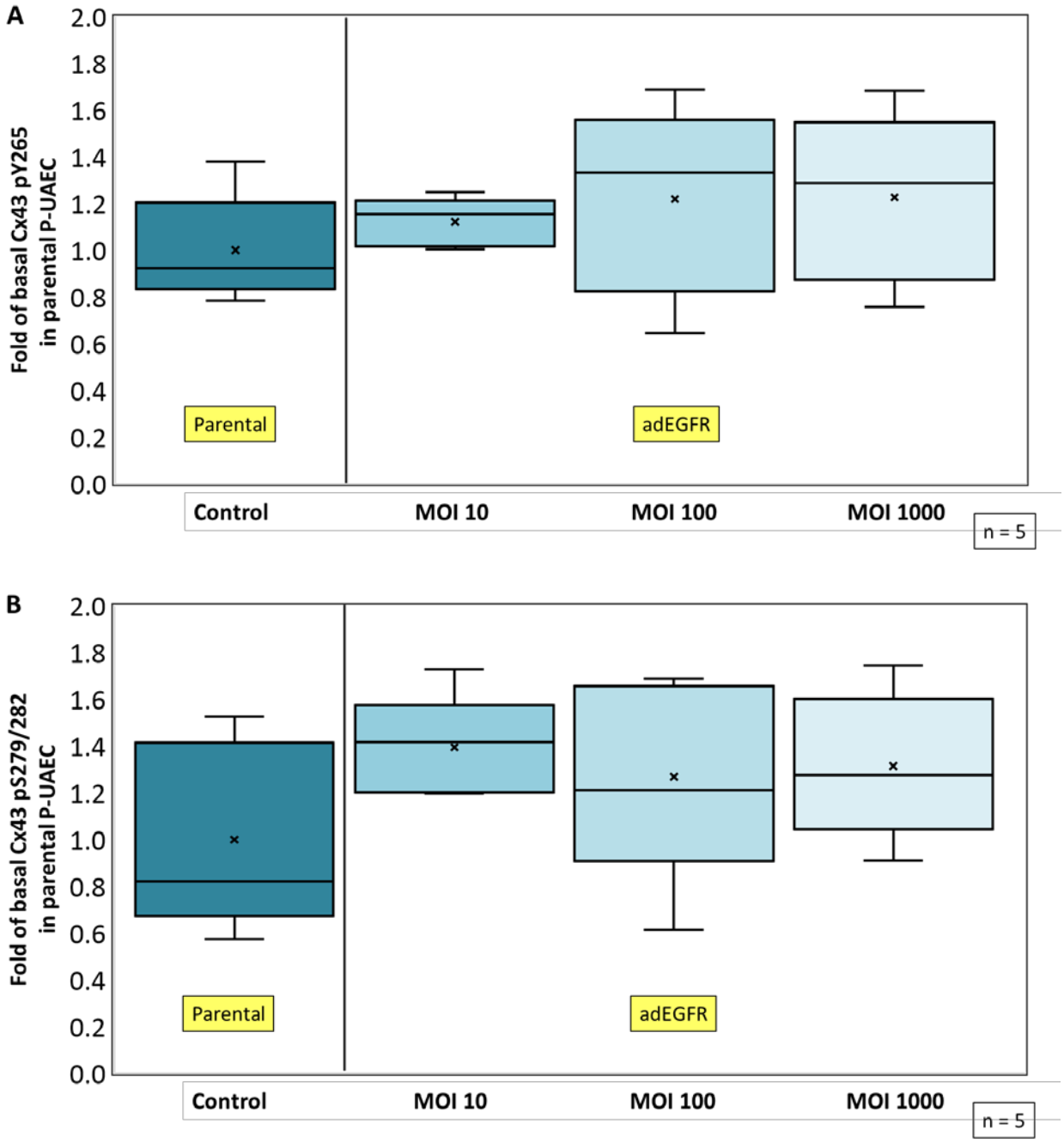

Figure 5.2 Basal phosphorylations of Cx43 inhibitory sites are not elevated in P-UAEC-adEGFR. Parental P-UAEC and P-UAEC-adEGFR at 3 MOIs were grown to near confluency. Immunoblot analysis was performed using (A) Cx43 pY265 or (B) pS279/282 antibody (Santa Cruz). Results of 5 independent experiments were normalized to hsp90 protein and expressed as fold difference from control. Adenoviral transduction with EGFR at MOIs of 10, 100, or 1000 resulted in no change in the basal phosphorylation level of Cx43 Y265 (c-Src-mediated site) or S279/282 (ERK1/2-mediated site).

Figure 5.3

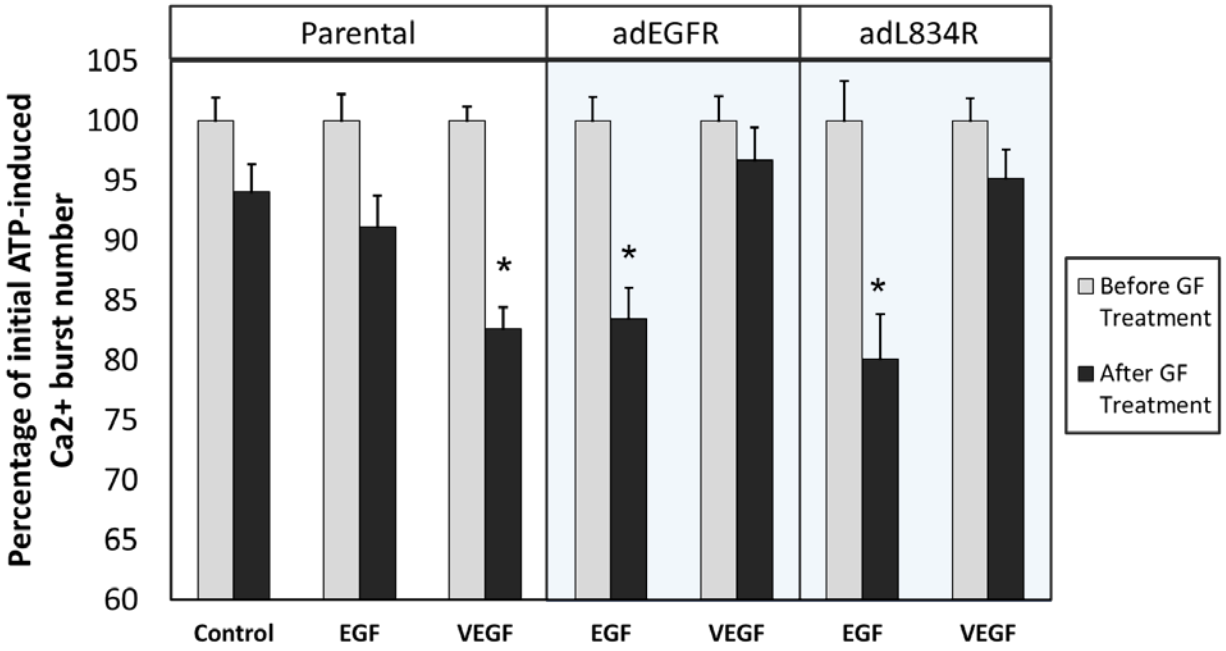

Figure 5.3 EGF inhibits the pregnancy adapted Ca2+ burst function in P-UAEC-adEGFR to a level consistent with VEGF-induced inhibition in parental P-UAEC. Parental P-UAEC, adEGFR, and adL834R, pre-loaded with the [Ca2+]i-sensitive dye Fura-2, were stimulated with ATP (100 µM) for 30 min, then washed with fresh buffer and allowed to sit for 30 min. Cells were treated with VEGF (10 ng/mL), EGF (10 ng/mL), or vehicle control for 30 min, then re-stimulated with ATP for 30 min. Data was collected from cells showing 3 or more ATP stimulated Ca2+ bursts prior to growth factor treatment. Black bars represent percent of initial mean burst number +/- SE. In parental P-UAEC, treatment with VEGF inhibited the number of Ca2+ bursts significantly below the control level, but EGF did not. However, in P-UAEC-adEGFR and adL834R, the results are reversed; treatment with EGF induced significant inhibition, whereas VEGF treatment had no effect on Ca2+ bursting. Statistics were performed on raw data from individual P-UAEC observed in 5-22 dishes: control (n = 342), EGF (n = 226), or VEGF-165 (n = 778) in parental P-UAEC; EGF (n = 362) or VEGF-165 (n = 313) in P-UAEC-adEGFR; EGF (n = 135), or VEGF-165 (n = 360) in P-UAEC-adL834R. Comparisons of post-treatment groups vs. control group were analyzed by rank-sum test (* $P < 0.0001$).

Figure 5.4

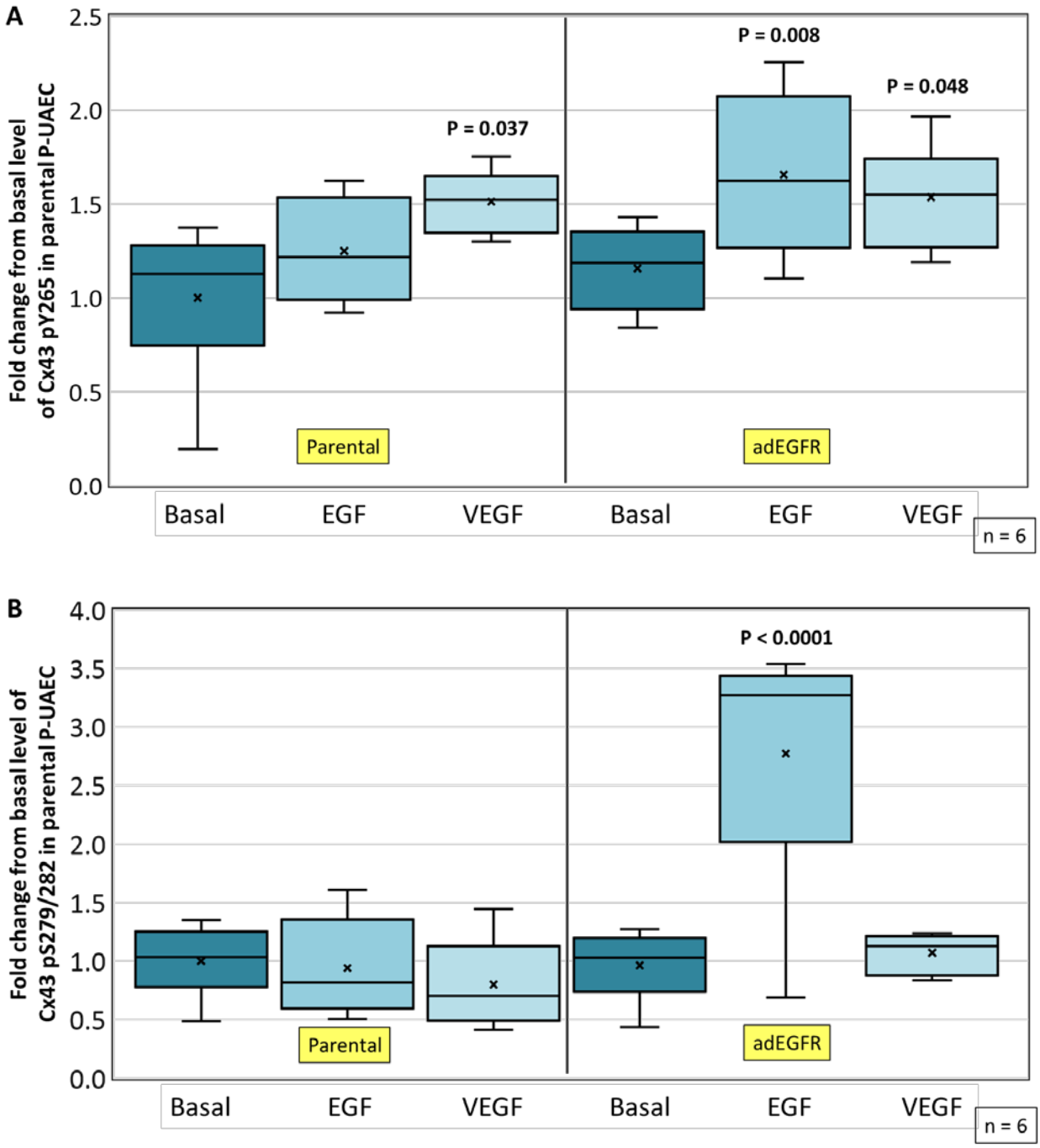
A
Fold change from basal level of Cx43 pY265 in parental P-UAEC
2.5
2.0
1.5
1.0
0.5
0.0
P = 0.037
P = 0.008
P = 0.048
Parental
adEGFR
Basal
EGF
VEGF
Basal
EGF
VEGF
n = 6
B
Fold change from basal level of Cx43 pS279/282 in parental P-UAEC
4.0
3.5
3.0
2.5
2.0
1.5
1.0
0.5
0.0
P < 0.0001
Parental
adEGFR
Basal
EGF
VEGF
Basal
EGF
VEGF
n = 6

Figure 5.4 Phosphorylation of Cx43 Y265 and S279/282 in parental P-UAEC and P-UAEC-adEGFR following 30-minute growth factor treatment In parental P-UAEC, Western blot analysis showed that phosphorylation of the Cx43 inhibitory site Y265 was significantly increased (1.5-fold) by 30-minute treatment with VEGF, but not by EGF treatment (A). In P-UAEC-adEGFR, 30-minute treatment with VEGF again resulted in a significant 1.5-fold increase ($P = 0.048$) in Cx43 Y265 phosphorylation, while EGF treatment resulted in a 1.7-fold increase ($P = 0.008$). Since calcium imaging experiments with P-UAEC-adEGFR showed that EGF treatment induced significant inhibition of ATP-induced [Ca2+]i bursting and VEGF treatment had no effect (Figure 5.3), the relevance of Cx43 Y265 phosphorylation in P-UAEC-adEGFR is uncertain without further study. In parental P-UAEC, phosphorylation of the Cx43 inhibitory site S279/282 was unaffected by 30-minute treatment with VEGF or EGF (B). This is contrary to prior research published by the Bird laboratory, which found that 30-minute VEGF treatment significantly elevated pS279/282 1.4-fold (Boeldt *et al.* 2015). In P-UAEC-adEGFR, 30-minute treatment with VEGF again had no effect on Cx43 S279/282 phosphorylation, but EGF treatment resulted in a highly significant ($P < 0.0001$) 2.8-fold increase. Statistical analysis by ANOVA and Dunnett's two-sided test. $n = 6$.

Figure 5.5

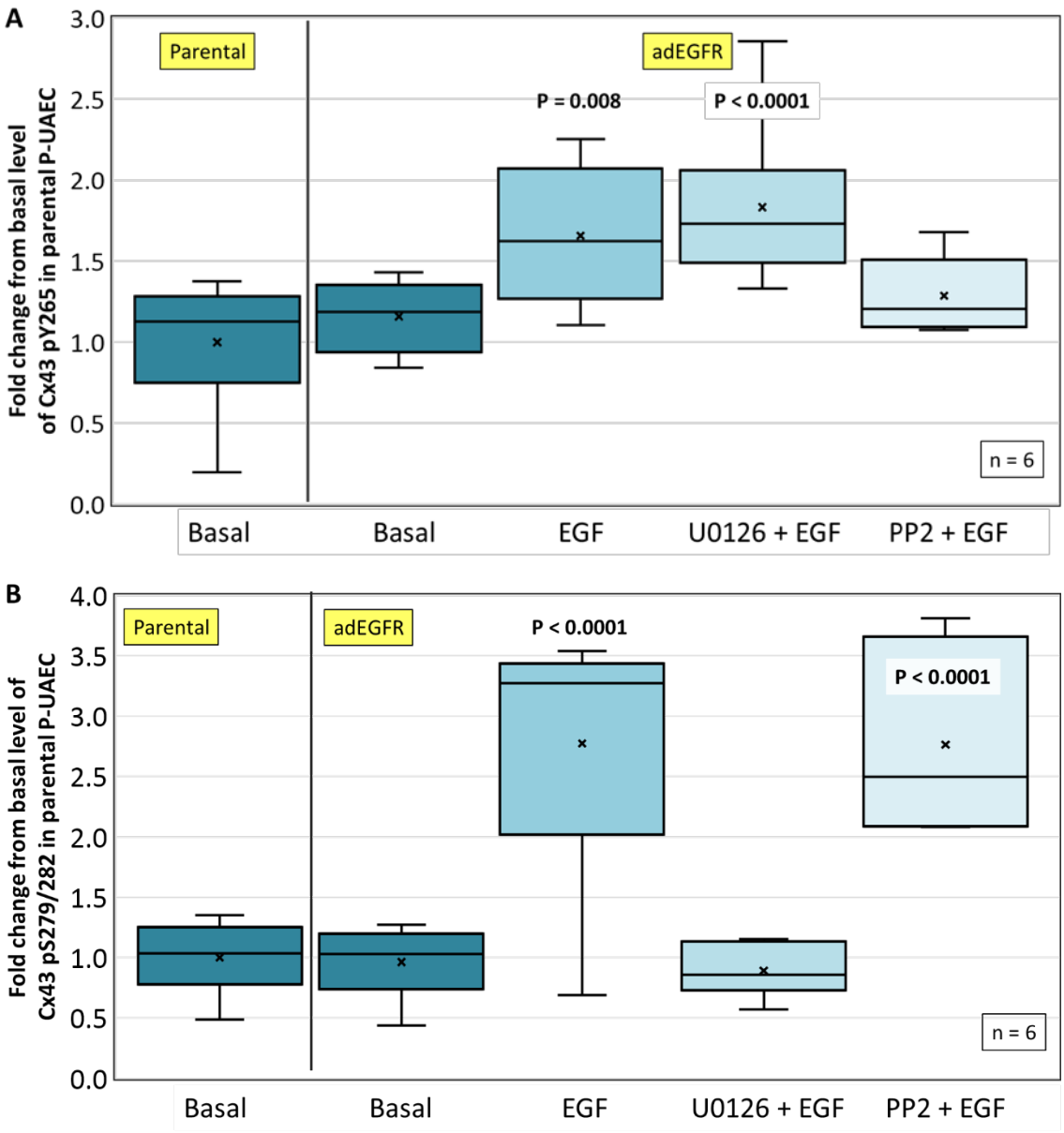

Figure 5.5 Phosphorylation of Cx43 Y265 and S279/282 in P-UAEC-adEGFR following 30-minute EGF treatment As expected, Pretreatment with the MEK-selective inhibitor U0126 prior to 10 ng/mL EGF administration had no effect on Y265 phosphorylation, which is known to be mediated by Src, but the SFK-selective inhibitor PP2 kept Cx43 Y265 phosphorylation at a level not significantly different from basal pY265 (A). Inversely, since Cx43 S279/282 phosphorylation is mediated by ERK1/2, we would expect 30-minute pretreatment with PP2 to have no effect on EGF-induced pS279/282, while U0126 would be expected to keep pS279/282 at the basal level. Again, the effects of both pretreatments were shown to be just as expected. U0126 pretreatment prior to EGF administration indeed kept Cx43 S279/282 phosphorylation at the basal level, and PP2 pretreatment was not significantly different from EGF alone (B).

Figure 5.6

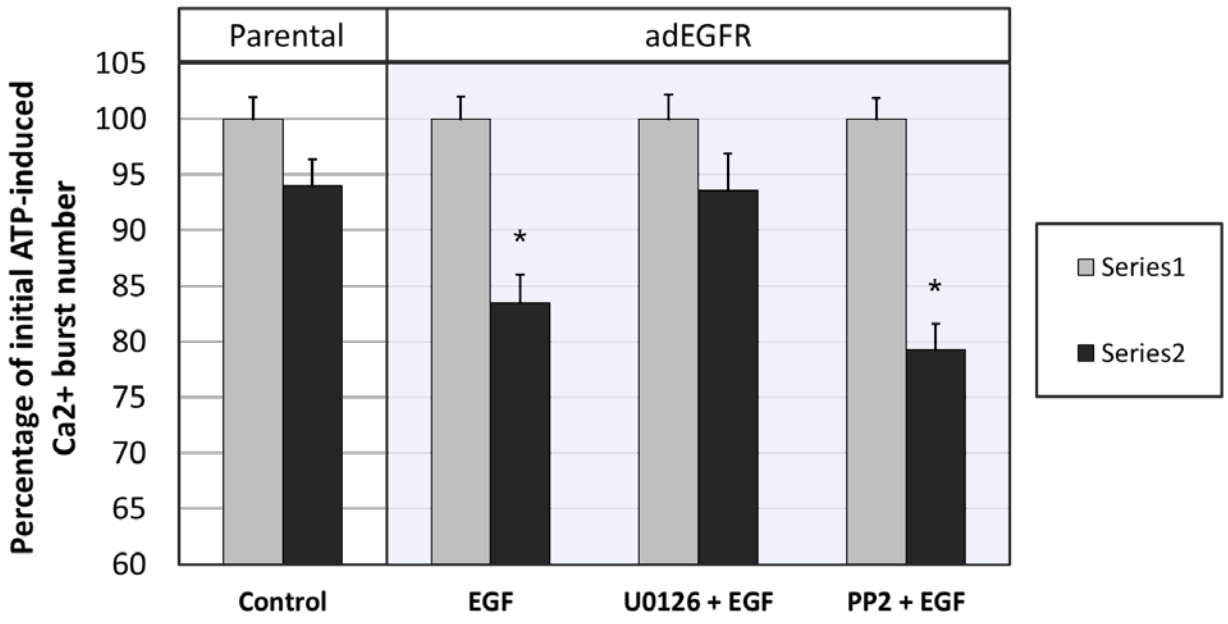

Figure 5.6 ATP-stimulated Ca2+ bursting is fully "rescued" from EGF inhibition by blocking the MEK/ERK signaling pathway, but not by blocking c-Src When P-UAEC-adEGFR are treated with EGF (10 ng/mL) for 30 min, ATP-stimulated Ca2+ bursting is inhibited relative to control cells. Pretreatment for 30 min with the MEK-selective inhibitor U0126 (10 µM) prior to EGF treatment completely protected P-UAEC-adEGFR from EGF inhibition of Ca2+ bursting. However, pretreatment for 30 min with the Src family kinase-selective inhibitor PP2 (10 µM) prior to EGF treatment did not protect against loss of Ca2+ bursts. These data suggest that EGF inhibition of CCE is mediated via the MAPK pathway, but not the Src pathway. Differences between treatments were compared by Wilcoxon rank-sum test (*) $P < 0.0005$. (Control, n = 342; EGF, n = 362; U0126 + EGF, n = 199; PP2 + EGF, n = 225)

Figure 5.7 Phosphorylation of Cx43 Y265 and S279/282 following 30-min growth factor treatment. These are the Western blot results for all 12 lanes of 6 independent experiments shown together. (A) Notice the magnitude of VEGF-induced Y265 phosphorylation is the same in parental P-UAEC and P-UAEC-adEGFR, but in adEGFR this is not correlated with downregulation of ATP-stimulated Ca2+ bursting. (B) The failure of VEGF to induce phosphorylation of S279/282 in parental P-UAEC contradicts the results of Grummer et al. (2009), which reported phosphorylation of S279/282 following 30-min treatment with VEGF. Statistical analysis by ANOVA and Dunnett's two-sided test (*) $P < 0.05$, (**) $P < 0.005$ (***) $P < 0.0001$

Figure 5.7

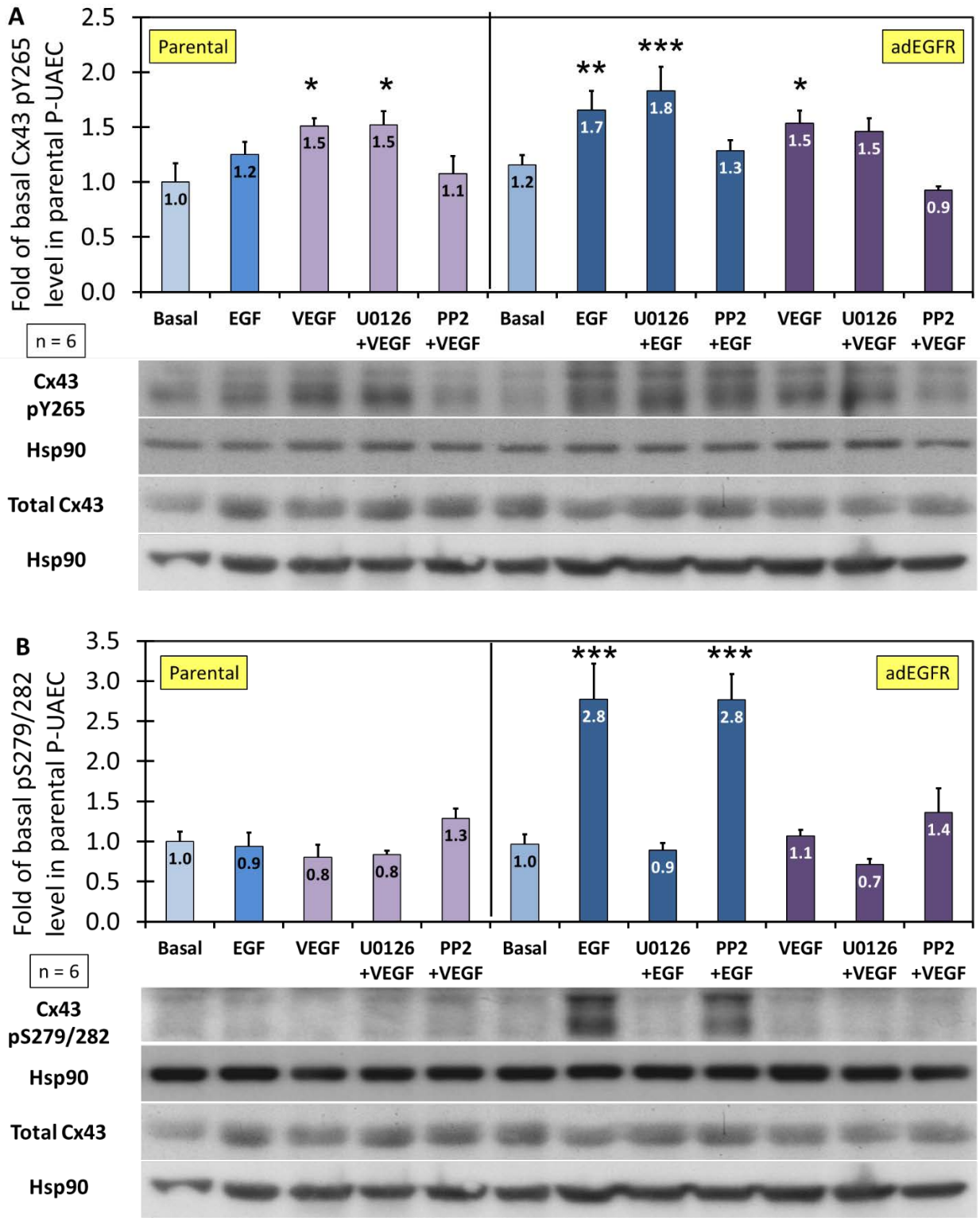
A
Fold of basal Cx43 pY265 level in parental P-UAEC
2.5
2.0
1.5
1.0
0.5
0.0
Parental
adEGFR
*
*
**
***
*
1.0
1.2
1.5
1.5
1.1
1.2
1.7
1.8
1.3
1.5
1.5
0.9
Basal
EGF
VEGF
U0126 +VEGF
PP2 +VEGF
Basal
EGF
U0126 +EGF
PP2 +EGF
VEGF
U0126 +VEGF
PP2 +VEGF
n = 6
Cx43 pY265
Hsp90
Total Cx43
Hsp90
B
Fold of basal pS279/282 level in parental P-UAEC
3.5
3.0
2.5
2.0
1.5
1.0
0.5
0.0
Parental
adEGFR
***
***
1.0
0.9
0.8
0.8
1.3
1.0
2.8
0.9
2.8
1.1
0.7
1.4
Basal
EGF
VEGF
U0126 +VEGF
PP2 +VEGF
Basal
EGF
U0126 +EGF
PP2 +EGF
VEGF
U0126 +VEGF
PP2 +VEGF
n = 6
Cx43 pS279/282
Hsp90
Total Cx43
Hsp90

Chapter 6:

The Effects of PI3K/Akt Pathway Signaling on Pregnancy-Adapted Gap Junctional Communication and Monolayer Permeability in P-UAEC

Abstract

We have previously shown that Src and MAPK/ERK pathways are negative regulators of gap junctional communication (GJC) and monolayer integrity in uterine artery endothelial cells obtained from pregnant ewes (P-UAEC). The actions of the phosphatidylinositide 3-kinase (PI3K) pathway on the regulation of junctional proteins are less well understood, with some reports showing evidence of protective effects for PI3K signaling and others suggesting downregulating effects. It is noteworthy that while VEGF does not activate the PI3K/Akt pathway in P-UAEC, EGF does activate this pathway in P-UAEC that overexpress EGFR, but the implications of this difference are unclear. To determine the effects of PI3K signaling on GJC, P-UAEC were pretreated overnight with insulin, which we have previously shown to promote an immediate increase and sustained elevation of PI3K/Akt activity in UAEC but with no parallel effect on MAPK/ERK signaling. Quantification of the Ca2+ bursting response to subsequent ATP stimulation of cells loaded with the Ca2+-sensitive dye Fura-2 was used as an indicator of GJC. The effect of insulin-enhanced PI3K/Akt activity on longer term endothelial monolayer permeability was measured by the Electric Cell-substrate Impedance Sensing (ECIS) apparatus. Conversely, the effects of PI3K inhibition were studied by pretreating P-UAEC with the PI3K-selective inhibitor LY294002. Insulin-induced prestimulation of the PI3K/Akt pathway had no effect on subsequent ATP-induced Ca2+ bursting and provided no significant enhancement of the endothelial monolayer relative to control. However, pharmacological inhibition of PI3K with LY294002 long term abrogated subsequent ATP stimulated Ca2+ bursting and induced a significant drop in electrical impedance of the endothelial monolayer, beginning at ~4 hours after treatment and reaching the minimum value at ~14 hours. Together, these results provide strong evidence of the vital importance of *basal* PI3K pathway signaling in the regulation of endothelial

monolayer permeability, and further suggest the basal level of PI3K activity in P-UAEC is both *necessary* and *sufficient* for optimal GJC required for Ca2+ bursting and the maintenance of endothelial barrier function.

6.0 Introduction

This chapter will detail the results of experiments designed to determine the role of the PI3K/Akt pathway in the regulation of GJC in P-UAEC. As Western blot evidence presented in the Results section of this chapter will affirm, one of the novel features of UAEC is that administration of VEGF does not activate the PI3K/Akt pathway. This suggests that Akt may be regulated in an unusual manner unique to UAEC and raises the question of why VEGFR is uncoupled from PI3K in these cells when the receptor is an important mediator of PI3K/Akt signaling in numerous cell types, including human umbilical vein endothelial cells (HUVEC) (Gerber *et al.* 1998; Abid *et al.* 2004) and mouse CGR8 embryonic stem cells (Bekhite *et al.* 2011). The PI3K/Akt pathway is similarly nonresponsive to EGF in P-UAEC. However, when EGF is administered to P-UAEC that have been adenovirally transduced to overexpress EGFR (P-UAEC-adEGFR), we observe an extremely robust increase in Akt phosphorylation. In Chapter 5, we presented data showing that ATP-stimulated [Ca2+]i bursting was downregulated by EGF in P-UAEC-adEGFR to a similar degree as it is by VEGF in parental P-UAEC, but the contribution of Akt signaling to the overall effect of EGF remained unknown. To determine the effect of Akt signaling on VEGF inhibition of the Ca2+ burst response, we incubated P-UAEC overnight in medium containing a high concentration of insulin, which chronically elevates basal Akt phosphorylation in P-UAEC without inducing ERK1/2 phosphorylation, prior to treatment with VEGF. We also tested the effects of complete shutdown of the PI3K/Akt pathway on GJC in P-UAEC and P-UAEC-adEGFR by incubating the cells in medium containing the PI3K-selective inhibitor LY294002.

To illustrate the vital importance of the PI3K/Akt pathway in diverse cellular processes, this chapter will include general information on Akt signaling in a variety of cell types and cellular contexts. I will bring the discussion back to the role of Akt in P-UAEC after I have presented my experimental results.

6.1 Background

6.1.1 Activation of the PI3K/Akt Pathway

Phosphatidylinositol-4,5-bisphosphate 3-kinase (also called phosphatidylinositide 3-kinase and abbreviated as PI3K) activity is stimulated by several receptor tyrosine kinases and G-protein coupled receptors, which means a great many growth factors and cytokines utilize the PI3K pathway for signal transduction. PI3K phosphorylation of the plasma membrane-bound phospholipid PI(4,5)P2 produces PI(3,4,5)P3, which serves as a binding site for proteins that contain pleckstrin homology domains such as 3-phosphoinositide-dependent protein kinase 1 (PDPK1) and the three isoforms of the serine/threonine kinase Akt. The binding of Akt to PI(3,4,5)P3 alters the conformation of Akt in a manner that allows PDPK1 to phosphorylate Akt at T308 (Calleja *et al.* 2007), one of its two activation sites. The other activation site, S473, is phosphorylated by mammalian target of rapamycin complex 2 (mTORC2) (Hresko and Mueckler 2005). Genetic ablation of any of the components of mTORC2—rictor, mSIN1 or mLST8—inhibits S473 phosphorylation, which is commonly believed to be required for full activation of Akt. However, pS473 appears to be necessary for phosphorylation of only a subset of Akt substrates (e.g. FOXO1/2a, FOXO3), while other substrates are phosphorylated independently of the presence of pS473 (e.g. TSC2, GSK3), suggesting that S473 phosphorylation status may be a determinant of target specificity rather than activity (Jacinto *et al.* 2006).

Although the presence of PI(3,4,5)P3 at the plasma membrane is necessary for recruitment and phosphorylation of Akt, it is not sufficient. In IGF1-stimulated mouse embryonic fibroblasts and HEK 293T cells, the K63-linked ubiquitination of Akt by the E3 ubiquitin ligase TRAF6 was found to be essential for trafficking of Akt to the membrane and its subsequent phosphorylation, both of which were dramatically reduced in cells expressing the E3 ligase-impaired TRAF6 C70A mutant (Yang *et al.* 2009). However, in contrast to IGF1-mediated ubiquitination of Akt, which specifically required TRAF6, EGF-mediated ubiquitination of Akt required the E3 ligase activity of the Skp2 SCF complex, but not TRAF6 (Chan *et al.* 2012). These results support the necessity of E3 ubiquitin ligase activity, but suggest that distinct E3 ligases may be recruited by different growth factor receptors.

After phosphorylation, Akt translocates to the cytosol and nucleus, where it mediates the serine and/or threonine phosphorylation of numerous downstream effector molecules for a wide variety of cellular functions. Termination of Akt signal transduction is achieved by phosphatases—protein phosphatase 2A (PP2A) and PH domain leucine-rich repeat phosphatases 1 and 2 (PHLPP1, PHLPP2) mediate the dephosphorylations of T308 (Andjelkovic *et al.* 1996) and S473 (Brognard et al. 2007), respectively.

6.1.2 A Sampling of the Many Physiological Functions of Akt

Akt substrates include transcription factors, kinases, and phosphatases. Phosphorylation by Akt stimulates the activity of some substrates and inhibits the activity of others. Akt is a key regulator of diverse cellular processes, including metabolism, protein synthesis, and proliferation. Precisely because Akt is involved in so many vital cellular events, aberrant Akt signaling is associated with major causes of death such as cancer, diabetes, and cardiovascular disease (Reviewed in Hers *et al.* 2011). Like the background sections in previous chapters, this section is not intended to be

an exhaustive overview of the PI3K/Akt pathway. However, I would like to mention a few of its cellular functions that may have relevance to this dissertation.

In 1997, a series of independent studies determined that Akt mediated cell survival signaling in Rat1 fibroblasts. Expression of v-Src was found to be protective against apoptosis. EGF was also found to be anti-apoptotic for cells overexpressing EGFR. However, protection by v-Src and EGFR tyrosine kinases against apoptosis was blocked by overexpression of kinase-impaired PI3K or wortmannin inhibition of the PI3K/Akt pathway, indicating that activated Src, like EGFR, acted upstream of PI3K. Conversely, overexpression of constitutively active PI3K was sufficient to provide protection against apoptosis (Kulik *et al.* 1997). In similar studies, the Ras-PI3k-Akt pathway suppressed c-Myc-induced apoptosis (Kauffmann *et al.* 1997) and wortmannin inhibition of PI3K increased the rate of apoptosis, whereas constitutively active Akt variants (Akt-myr and v-Akt) inhibited the activity of Ced3/ICE-like pro-apoptotic proteases in a kinase-dependent manner (Kennedy *et al.* 1997). All three teams of researchers concluded that activation of PI3K and Akt was sufficient for anti-apoptotic signaling. Since activated Src was shown to signal upstream of the PI3K/Akt-mediated anti-apoptotic pathway in fibroblasts, the possibility is raised that Src may signal upstream of PI3K in P-UAEC and other endothelial cells, and indeed may be further involved in the process of Cx43 protein turnover via the regulation of PI3K activity.

The PI3K/Akt pathway is also tightly coupled to the action of insulin. The key importance of Akt in the regulation of glucose uptake into insulin responsive tissues was confirmed in a series of experiments performed on rat adipose cells, which were co-transfected with an epitope-tagged variant of the insulin-responsive glucose transporter GLUT4 and one of three distinct forms of Akt—wild type, kinase-impaired (Akt-K179A), or constitutively active (Akt-myr). As expected, overexpression of wild-type Akt resulted in robust translocation of GLUT4 to the plasma membrane following insulin treatment, but GLUT4 translocation was significant even without insulin. Overexpression of the dominant negative Akt-K179A inhibited insulin-induced

translocation of GLUT4, while overexpression of Akt-myr resulted in the greatest membrane localization of GLUT4, an effect entirely independent of insulin. These data suggest that endogenous Akt is a critical mediator of insulin-stimulated glucose uptake in adipose tissue (Cong *et al.* 1997). Akt further potentiates the actions of insulin by phosphorylating S50 on PTP1B, a protein tyrosine phosphatase that reduces insulin sensitivity by dephosphorylating the insulin receptor. Phosphorylation of S50 inhibits the phosphatase activity of PTP1B, thus improving insulin sensitivity by preventing the attenuation of insulin receptor-mediated signaling (Ravichandran *et al.* 2001). Together, these experiments provide clear evidence of the vitally important synergistic relationship between insulin and Akt, whereby insulin-induced Akt phosphorylation not only mediates the primary function of insulin, but simultaneously protects the insulin receptor itself from deactivation, thus maintaining a robust level of phosphorylated Akt for further signaling.

The PI3K/Akt pathway is also commonly involved in angiogenesis. Overexpression of constitutively active forms of PI3K can induce angiogenesis in the chorioallantoic membrane of the chicken embryo. This has been demonstrated with the viral oncogene v-P3k and PI3K-myr, the constitutively active myristylated form of cellular PI3K. Alternatively, angiogenesis in the yolk sac of chicken embryos is inhibited by overexpression of the tumor suppressor PTEN or a dominant-negative form of the p85 regulatory subunit of PI3K, suggesting that PI3K/Akt signaling is necessary for embryonic angiogenesis. Furthermore, *VEGF* mRNA levels were reduced when cells were treated with the PI3K inhibitor LY294002 and protected from LY294002-induced reduction by overexpression of v-P3k or Akt-myr, suggesting that cellular PI3K and Akt may regulate *VEGF* transcription (Jiang *et al.* 2000). As the Results section of this chapter will show, treatment with VEGF has no effect on Akt S473 phosphorylation in P-UAEC, but it is possible that local VEGF expression is regulated by the PI3K pathway. The relationship between VEGF and

Akt in P-UAEC may be more complex than the expected but nonexistent linear path from growth factor to kinase.

6.1.3 The Role of Akt in Gap Junctional Communication (GJC)

The first published data on the effects of Akt on Cx43 GJC demonstrated that activated Akt phosphorylated Cx43 S373, and that pS373 was necessary for Cx43 interaction with 14-3-3 regulatory proteins (Park *et al.* 2006). Sequencing data confirmed that Akt phosphorylation of S373 creates a "mode 1" consensus sequence (R[SFYW]X**pS**XP) necessary for certain isoforms of 14-3-3 proteins to bind to Cx43. Confocal microscopy using antibodies that targeted Akt-phosphorylated sites or "mode 1" 14-3-3 binding sites revealed that Akt stimulation of Cx43 interaction with 14-3-3 proteins occurred at the edge of existing gap junctional plaques, suggesting that Akt could promote the incorporation of additional Cx43 multimers into existing gap junctions (Park *et al.* 2007). The PI3K-selective inhibitor LY294002 prevented S373 phosphorylation and association of Cx43 with 14-3-3 proteins, but was found to have no effect on growth factor-induced inhibition of GJC, which is typically mediated by ERK1/2, PKC, and/or Src; however, the pretreatment time for LY294002 administration was only 15 minutes, which means that no conclusions could be drawn about the effect of longer term inhibition of the PI3K/Akt pathway on GJC (Park *et al.* 2006).

Further evidence suggests Akt activity—not Cx43 ubiquitination—controls gap junction size and stability. Possessing a half-life of 1-3 hours (Laird *et al.* 1991), Cx43 proteins are in a state of continuous flux as gap junctions are assembled and disassembled at a variable rate according to the needs of the cells they connect. To determine the role of ubiquitination in regulating Cx43 protein turnover, Madin-Darby canine kidney cells (MDCK) that do not express endogenous Cx43 were transfected with either wild-type Cx43 or Cx43 K/R—a mutant version in which all 27 lysines were converted to arginines, thus eliminating all potential ubiquitin binding sites. Treatment with

proteasomal or lysosomal inhibitors revealed no differences between MDCK expressing wild-type Cx43 and Cx43 K/R in protein localization or ability to transfer dye across gap junctions, indicating that ubiquitination of Cx43 is not required for Cx43 protein turnover or gap junction stability. However, the use of Akt inhibitors and dominant negative Akt constructs showed that Akt activity was necessary to form larger stable gap junctions (Dunn *et al.* 2012). The specific mechanism of control of gap junction size was subsequently shown to involve the interaction of Cx43 with the scaffolding protein ZO-1, which limits the size of gap junctions (Hunter *et al.* 2005). In MDCK cells, Akt phosphorylation of Cx43 S373 was found to inhibit the interaction of Cx43 and ZO-1, which correlated with increased gap junctional size; however, in MDCK cells expressing the Cx43 S373A mutant, interaction of Cx43 and ZO-1 was maintained and gap junctional size remained small (Dunn and Lampe 2014).

In Chapter 3, I discussed a model of gap junction regulation and turnover proposed by Joell Solan and Paul Lampe that involves sequential recruitment of kinases with several check points. Following growth factor treatment or wounding (which increases local concentrations of growth factors and cytokines), Cx43 becomes phosphorylated first by Akt (on S373 at 5–30 min), then PKC and MAPK (on S368 and S279/S282, respectively, at 15–60 min), and finally Src (on Y247 and Y265 at 30 min–24 hrs). These phosphorylations of Cx43 were found to be coincident with increased gap junction size, inhibition of GJC, and gap junction internalization, respectively (Reviewed in Solan and Lampe 2014; 2016). Initially, enhanced GJC facilitates the wound response, allowing the cell to recruit the factors needed for a robust healing and immune response. Then inhibition of GJC allows damaged cells to be isolated and removed from the undamaged tissue (Richards et al. 2004; Becker *et al.* 2012). Although the growth factors and cytokines recruited to a wound site involve the sequential activation of multiple signaling pathways that ultimately downregulate GJC, the identification of unique roles for each pathway raises an

interesting question. *If the PI3K/Akt pathway could be activated exclusively without activating the other pathways, might we observe a constitutive enhancement of GJC?*

6.1.4 Could elevated insulin during pregnancy enhance GJC?

Treatment of endothelial cells with growth factors or cytokines (or wounding of the cells, which increases the local concentration of growth factors and cytokines) typically results in the activation of multiple signaling pathways, thereby initiating the sequential "kinase program" (Akt → PKC/MAPK → Src) that regulates Cx43 turnover as described by Solan and Lampe. However, there would seem to be no intrinsic reason why the activation of one pathway should necessitate the activation of the others. Might there be cellular contexts in which it would be advantageous to activate the PI3K/Akt pathway without facilitating Cx43 turnover? Specifically, what if there were a signaling molecule that induced the phosphorylation of Akt but not of ERK, thus promoting the enlargement of gap junctional plaques and enhancement of GJC, but not the subsequent closure and disassembly of Cx43 gap junctions? Insulin is such a signaling molecule, and it is elevated during pregnancy.

Prior unpublished research conducted by Jeremy Sullivan in the Bird Laboratory has characterized the time- and dose-dependent effects of insulin on the PI3K/Akt and MAPK pathways. Administration of IGF-1 at 10 ng/mL (1.3 nM), which strongly activates IGF receptors but only weakly activates insulin receptors (K_d = 160 pM vs.11 nM; Schumacher *et al.* 1991), had no significant effect on Akt or ERK1/2 responses in P-UAEC (Figure 6.1A), suggesting IGF receptors are either not present or not coupled to the PI3K or MAPK pathways in P-UAEC. Insulin treatment at a dose of 100 nM or greater increased the phosphorylation of Akt S473 significantly above the basal level but had no comparable effect on the phosphorylation of ERK2 at doses ranging from 1 nM to 10 µM (Figure 6.1B). A 100 nM dose of insulin stimulated a 2-fold pAkt response by 5 min that was the same at 30 min (Figure 6.1C). A maximal dose of 10µM insulin

increased phosphorylation of eNOS on the known Akt-mediated site S1179. Both responses showed the expected inhibitory effect of LY294002, which returned pAkt to the basal level or lower and eliminates the Akt component of enhanced eNOS phosphorylation (Figure 6.1D).Collectively, these data confirmed a functional coupling of insulin to PI3K/Akt signaling in P-UAEC and led us to hypothesize that, in addition to promoting increased glucose transport to the fetus during pregnancy, insulin might promote vasodilation indirectly by inducing the formation of larger gap junctional plaques, which in turn could improve GJC and promote the enhanced capacitative calcium entry (CCE) in the endothelium of the maternal uterine vasculature such that other agonist responses are amplified. The results of insulin pretreatment of P-UAEC on the basal phosphorylation of Akt and the Ca2+ burst function will be reported in this chapter.

6.1.5 The Role of PI3K in Maintaining Endothelial Monolayer Integrity

The structural integrity of the vascular endothelium is essential for keeping ions, molecules, and cells from entering or exiting the circulation without proper regulatory control. The barrier function of the endothelium is dependent on many factors, particularly the abundance of adherens junctions at the plasma membrane. Growth factors and cytokines elevated in PE have a destabilizing effect on the endothelial barrier by activating kinases that negatively regulate junctional proteins such as ZO-1 and VE-cadherin. Phosphorylation of VE-cadherin by Src family kinases, for example, results in its internalization, thus dismantling adherens junctions and increasing vascular permeability (Reviewed in Vandenbroucke *et al.* 2008). Maintenance of the endothelial barrier is also known to be dependent on maintaining a basal level of nitric oxide (NO) (Predescu *et al*. 2005). Insulin has been shown to stabilize the endothelial barrier via Akt- and NO-dependent mechanisms, which deactivate the endothelial contractile machinery and enhance cell-to-cell adhesion (Gunduz *et al.* 2010). Endothelial monolayer permeability is commonly measured by fairly crude techniques, such as dye-labeled protein transfer across confluent endothelial cells grown on polycarbonate filters (Gunduz et al. 2010). In the Bird Laboratory, we

are fortunate to have access to the Electric Cell-substrate Impedance Sensing (ECIS) system, a relatively recent technology patented in 2008 that enables measurement of endothelial cell permeability in real time. ECIS utilizes the insulating properties of cell membranes to measure electrical impedance below and in between cells in culture. Higher impedance (resistance) results from tighter cell-to-cell connectivity and is indicative of a monolayer with low permeability. Amanda Ampey, a former student of Ian Bird who successfully defended her PhD dissertation recently, has used the ECIS system extensively for precise quantitative study of endothelial barrier function, growth morphology, and motility in P-UAEC and in HUVEC obtained from pregnant women. In this chapter, I will present the results of new ECIS experiments that measured the effects of PI3K/Akt pathway stimulation and inhibition on endothelial cell monolayer permeability.

6.2 Methods

Detailed experimental protocols are presented in Chapter 9.

6.2.1 Calcium imaging

Calcium Imaging Protocol 1.2 was used to generate the data for Figure 6.6.

6.2.2 Western blotting

Western Blot Protocol 1.0 was used to generate the data for Figures 6.2, 6.3 and 6.4. Western Blot Protocol 1.1 was used to generate the data for Figures 6.5 and 6.7.

6.2.3 Electric cell-substrate impedance sensing (ECIS^{TM})

The ECIS Protocol was used to generate the data for Figure 6.8.

6.3 Results

6.3.1 Neither EGF nor VEGF induces phosphorylation of Akt S473 in parental P-UAEC

As shown in Chapter 4, expression of EGFR in parental P-UAEC is virtually undetectable by Western blot, yet treatment with EGF (10 ng/mL) for 30 minutes resulted in a measurable increase in ERK1 phosphorylation. In contrast, the results of seven independent Western blot experiments found that EGF treatment had no significant effect on phosphorylation of Akt S473 (Figure 6.2). Similarly, VEGF treatment also had no measurable effect on Akt phosphorylation in P-UAEC, and this did not change when the cells were pretreated (for other purposes) with the MEK-selective inhibitor U0126 or the SFK-selective inhibitor PP2. This result suggests that neither VEGFR-1 nor VEGFR-2 is functionally linked to the PI3K/Akt pathway in P-UAEC.

6.3.2 EGF-induced Akt phosphorylation is dramatically increased in P-UAEC-adEGFR

In P-UAEC-adEGFR, the mean level of basal Akt pS473 was elevated 11-fold above the basal level in parental P-UAEC, but surprisingly this was not found to be significant by ANOVA and Tukey's HSD multiple comparison test ($P = 0.085$). However, 30-minute EGF treatment (10 ng/mL) of P-UAEC-adEGFR induced a dramatic and highly significant increase in Akt phosphorylation (29-fold basal level in parental P-UAEC), and pretreatment with the MEK-selective inhibitor U0126 (10 μM) for 30 min prior to EGF administration resulted in still greater Akt phosphorylation (47-fold). However, pretreatment with the SFK-selective inhibitor PP2 (10 μM) for 30 min prior to EGF was no different than EGF treatment alone, suggesting that EGF stimulation of Akt phosphorylation is a Src-independent process. Akt protein is expressed at the same level in parental P-UAEC and P-UAEC-adEGFR (Figure 6.3). Therefore, all differences in pS473 were due entirely to phosphorylation and not to changes in Akt protein expression.

Firstly, these data suggest that the capacity for Akt phosphorylation in P-UAEC is much greater than typically observed. EGF treatment of P-UAEC-adEGFR radically elevates Akt pS473 above the basal level. Secondly, pharmacological inhibition of the MAPK pathway with U0126 prior to EGF treatment raises Akt pS473 levels even higher than EGF alone, hinting that the basal level of pERK1/2 in P-UAEC-adEGFR may inhibit the full potential of PI3K/Akt signaling. The implications of these observations will be discussed later in this chapter.

6.3.3 VEGF treatment of P-UAEC-adEGFR has no effect on Akt S473 phosphorylation

Just as in parental P-UAEC, 30-minute treatment with VEGF (10 ng/mL) had no effect on Akt S473 phosphorylation. This result further supports our findings that neither VEGFR-1 nor VEGFR-2 are functionally linked to the PI3K/Akt pathway in P-UAEC. Pretreatment with the SFK-selective inhibitor PP2 (10 μM) or the MEK-selective inhibitor U0126 (10 μM) for 30 min prior to VEGF treatment made no difference (Figure 6.4).

6.3.4 Overnight pretreatment with insulin doubles basal phosphorylation of Akt S473

The combined experiments performed by Jeremy Sullivan found that 20-minute insulin treatment at a dose of 100 nM raised Akt S473 phosphorylation ~2-fold (Figure 6.1). To test if the rise in Akt pS473 was merely transient or if it could be maintained by prolonged insulin treatment, we pretreated P-UAEC with 100 nM insulin overnight. The following day, after the cells were harvested and the lysates were subjected to Western blot analysis, we found that basal phosphorylation of Akt S473 was also at twice the normal level at ~20 hrs post-treatment (Figure 6.5, lane 2). Acute treatment (30-min) with 10 nM TPA—a potent suppressor of pregnancy-adapted Ca2+ bursting in P-UAEC (Boeldt et al. 2015)—downregulated Akt phosphorylation (lane 3) but this effect was cancelled out by the presence of insulin (lane 4). However, the PI3K-selective inhibitor LY294002 (20 μM) eliminated even the residual basal Akt S473 phosphorylation that remains following TPA treatment irrespective of the presence of insulin (lanes 5 & 6).

6.3.5 Insulin pretreatment does not improve GJC or protect against growth factor inhibition of the ATP-induced Ca2+ burst response

In Chapter 5, I presented data that showed that the ATP-induced Ca2+ burst response was inhibited by VEGF in parental P-UAEC (see 5.3.3) and by EGF in P-UAEC-adEGFR (see 5.3.4). After establishing that overnight (~20 hrs) treatment with insulin (100 nM) doubled the basal level of Akt S473 phosphorylation, we wondered if larger gap junctional plaques would form and if GJC would improve as a result. In physiologic terms, we were asking if elevated insulin during pregnancy might provide resistance against endothelial damage by locally elevated growth factors. Anticipating that this improvement in GJC might appear as an increase in the mean number of [Ca2+]i bursts in 30 minutes following initial ATP treatment, I compared the mean number of bursts observed in untreated parental P-UAEC (4.93; N = 1346) with the number observed in insulin-pretreated P-UAEC (4.69; N = 225). I also compared the mean number of bursts observed in untreated P-UAEC-adEGFR (5.13; N = 1147) with the number observed in insulin-pretreated P-UAEC-adEGFR (5.20; N = 181). In both cases, there were no significant increases in mean burst numbers due to the chronic presence of insulin. Additionally, elevated Akt pS473 provided no protection from growth factor inhibition of the ATP-induced Ca2+ burst response. Insulin pretreatment had no significant effect on loss of Ca2+ bursts in response to VEGF treatment of parental P-UAEC or EGF treatment of P-UAEC-adEGFR (Figure 6.6).

It is worth mentioning that, in the absence of any added insulin, overexpression of EGFR in P-UAEC did result in a small but significant improvement in GJC. As discussed in Chapter 5 (Figure 5.1), the mean number of [Ca2+]i bursts in 30 minutes following initial ATP treatment was 4% greater ($P = 0.0051$) in P-UAEC-adEGFR (5.13; N = 1147) than in parental P-UAEC (4.93; N = 1346).

6.3.6 Overnight treatment with PI3 kinase inhibitor LY294002 significantly increases basal phosphorylation of ERK1/2 in P-UAEC-adEGFR

In Chapter 4, I presented data showing no significant differences in basal ERK1/2 phosphorylation in P-UAEC irrespective of the level of exogenous EGFR expression (see 4.3.6). In Figure 6.7, I have expanded the data set to show that P-UAEC-adEGFR exhibited significantly elevated basal phosphorylations of ERK1 (3.7-fold; $P = 0.005$) and ERK2 (2.4-fold; $P = 0.016$) following overnight treatment with the PI3K-selective inhibitor LY294002 (20μM). In the previous section, pharmacological inhibition of the MAPK pathway was shown to be associated with elevated Akt phosphorylation. Here we have evidence that pharmacological inhibition of the PI3K pathway is associated with elevated phosphorylation of ERK1/2. These data suggest an inverse relationship may exist between PI3K/Akt and MAPK pathway signaling in P-UAEC.

6.3.7 Overnight pretreatment with PI3 kinase inhibitor LY294002 severely impairs Ca2+ bursting

As outlined earlier, the studies of Lampe and others suggest the PI3K/Akt pathway plays a vital role in the assembly and disassembly of Cx43 gap junctions. When P-UAEC—parental or adEGFR—were pretreated overnight (~20 hrs) with 20 μM LY294002, subsequent ATP challenge still stimulated an initial robust peak of [Ca2+]i released from the endoplasmic reticulum (ER), but the sustained CCE phase of the [Ca2+]i bursting response *was almost entirely lost*. This suggests that Akt plays the proposed role in regulating gap junction plaque size but does so at *basal levels of activity.* This would certainly explain why insulin stimulation has no further effect on Ca2+ bursting. Additionally, the basal elevation of pERK1/2 that results from pharmacological inhibition of the PI3K/Akt pathway long term might be mediating gap junction closure.

6.3.8 Insulin pretreatment does not protect P-UAEC monolayer integrity, but the PI3K-selective inhibitor LY294002 severely impairs it

ECIS quantification of the electrical impedance of confluent P-UAEC monolayers suggests that the PI3K pathway is also critical for maintaining the endothelial barrier function. In both parental P-UAEC and P-UAEC-adEGFR, pharmacological inhibition of PI3K with LY294002 (20 μM) induced a significant drop in electrical impedance, beginning at ~3 hours and reaching the minimum value at ~14 hours (Figure 6.8). However, 100 nM insulin-induced stimulation of the PI3K/Akt pathway in parental P-UAEC and P-UAEC-adEGFR provided no significant enhancement of the endothelial monolayer relative to control. Analysis by ANOVA found that neither VEGF nor EGF nor any combination of treatments had any significant effect on endothelial monolayer integrity aside from LY294002 treatment. Only the elimination of PI3K/Akt pathway signaling by administration of LY294002 induced a significant decrease in electrical impedance over time, suggesting a progressive loss of junctional attachment proteins at the cells' surfaces.

6.4 Discussion

The results of our calcium imaging experiments clearly showed that pharmacological inhibition of PI3K abrogated ATP-induced Ca2+ bursting in P-UAEC, yet added stimulation of PI3K by insulin failed to increase the mean number of bursts in 30 minutes following ATP stimulation and failed to protect against growth factor inhibition of Ca2+ bursting in parental P-UAEC and P-UAEC-adEGFR. The results of our ECIS experiments suggested basal PI3K is also a major regulator of junctional attachment proteins like those found in adherens junctions and tight junctions, although we have not yet identified which specific proteins (VE-cadherin, ZO-1, etc.) are downregulated. In both parental P-UAEC and P-UAEC-adEGFR, pharmacological inhibition of PI3K with

LY294002 induced a significant drop in electrical impedance, which is indicative of a dramatic decrease in cell-to-cell connectivity. Furthermore, insulin-induced stimulation of the PI3K/Akt pathway provided no significant enhancement of the endothelial monolayer relative to control, suggesting that PI3K at *basal* levels already achieves the maximal effect. Together, these results confirm the vital importance of PI3K pathway signaling for pregnancy-adapted GJC and suggest that the basal level of PI3K activity in P-UAEC is both *necessary* and *sufficient* for optimal maintenance of the endothelial barrier function.

Before concluding this chapter, I would like to expand on a few observations made in the Results section.

6.4.1 How does pharmacological inhibition of PI3K suppress ATP-induced Ca2+ bursting?

Evidence suggests that, once at the plasma membrane, Cx43 is embedded in disordered connexons until phosphorylated by CK1, which stimulates the organization of very small Cx43 gap junctions (Cooper and Lampe 2002). These small gap junctions then become significantly larger following phosphorylation of S373 by Akt, which enables connexon aggregation by dissociating Cx43 from ZO-1 scaffolding (Dunn *et al.* 2014). If Cx43 cannot be dissociated from ZO-1, connexons cannot aggregate into larger gap junctions. I suspect the small gap junction plaques that remain do not possess sufficient functionality to maintain tight connectivity and integrity of the endothelial cell monolayer or to propagate the periodic [Ca2+]i bursts necessary for optimal eNOS activity observed in pregnancy. When Cx43 S373 was mutated to alanine and transfected into an MDCK cell line lacking Cx43 expression, the S373A-containing cells had the smallest gap junctions and had the least functionality compared with MDCK cells expressing wild-type Cx43 (Dunn *et al.* 2014). Alternatively, the elevation in basal ERK1/2 activity that results from suppression of the PI3K/Akt pathway may facilitate gap junctional closure via the phosphorylation

of Cx43 S279/282 but attempts to confirm or refute this speculation by Western blot analysis were unsuccessful (data not shown). Of course, these two mechanisms—suppression of gap junctional plaque growth and inhibitory phosphorylation of Cx43—are not mutually exclusive, and indeed are both likely to contribute to a reduced capacity for Ca2+ bursting.

6.4.2 The Relationship Between the PI3K/Akt and MAPK Pathways

The apparent inverse relationship between pAkt and pERK1/2 may be a relevant physiological phenomenon, but it could also be irrelevant in P-UAEC outside the context of excessive EGFR signaling. On the one hand, a similar antagonism has been observed in NIH-3T3 fibroblasts, in which constitutive activation of the Raf–MEK–MAPK pathway appears to switch on a negative feedback loop that inhibits the Ras–PI3K–AKT pathway through the upregulation of the ephrin receptor EphA2 (Menges and McCance 2008). In HEK293 cells, inhibition of Akt activation by LY294002 increased Raf and ERK activities. Akt was shown to antagonize Raf by direct phosphorylation of S259, a modification that creates a binding site for 14-3-3 protein, which negatively regulates Raf (Zimmermann and Moelling 1999). On the other hand, the magnitudes of the phosphorylation responses of both Akt and ERK in P-UAEC-adEGFR far exceed the natural responses observed in parental P-UAEC. Thus, the apparent inverse relationship may be simply the functional limit of EGFR signaling capacity due to the finite number of effectors available for signal transduction. For example, in many cellular contexts, Grb2 is a critical component of the MAPK pathway that binds to phosphorylated EGFR, where it forms the Grb2-SOS complex. The subsequent activation of Ras then triggers the Raf-MEK-ERK cascade. Grb2 can also recruit the PI3K regulatory subunit p85 using the Grb2-associating binding scaffolding protein (GAB). Additionally, Grb2-SOS activation of the Ras-GTPase can activate the PI3K catalytic subunit p110 (Castellano and Downward 2011). Therefore, the appearance of an inverse relationship between Akt and ERK in P-UAEC-adEGFR may be simply due to a limit in the availability of shared

upstream effector molecules like Grb2 and Ras, thereby making simultaneous maximal activation of both pathways impossible.

6.4.3 The PI3K/Akt Pathway and Vascular Permeability

Our experiments clearly indicated that loss of PI3K signaling had a particularly devastating effect on the endothelial monolayer formed by P-UAEC in culture, but this was not a foregone conclusion due to conflicting reports on the net effect of PI3K activity on vascular permeability. In line with our results, some studies of the effects of PI3K/Akt signaling on vascular endothelial permeability have revealed a protective effect against leakage. Somasiri *et al.* (2000) found that pharmacological inhibition of PI3K disrupted adherens junctions in murine mammary epithelial scp2 cells. Reductions in E-cadherin and b-catenin expression and reduced association of these proteins with the cytoskeleton were observed at sites of cell-to-cell contact in the epithelial monolayer. In rat coronary microvascular endothelial cells, insulin stimulation of the PI3K/Akt pathway induced dephosphorylation of myosin light chains and promoted translocation of actin and vascular endothelial (VE)-cadherin to cell borders, reducing contractile activation and stabilizing cell adhesion proteins. Insulin activated the Rho GTPase Rac1, increased NO production, and reduced the permeability of endothelial monolayer. Inhibition of PI3K with wortmannin or LY294002 eliminated all these effects (Gunduz *et al.* 2010).

Other studies, however, have found that PI3K signaling *decreases* the endothelial barrier function. McKenzie and Ridley (2007) showed that TNF induces a progressive disruption of endothelial cell junctions and an increase in endothelial permeability in HUVEC over 8–24 hours after stimulation, which was mediated by PI3K. The gradual increase in PI3K activity, as measured by Akt phosphorylation, correlated well with the loss of cell-to-cell junctions. Cain *et al.* (2010) found that siRNA knockdown of the p110α subunit of PI3K increased overlapping adherens junctions by over two-fold. Depletion of p110α also raised levels of the adhesion protein PECAM-1 and the tight

junction scaffolding protein ZO-1, indicating that junctions were strengthened. Further evidence of the negative effects of PI3K signaling on endothelial monolayer integrity was provided by the study of the anti-diabetic drug rosiglitazone, which improves insulin sensitivity by binding to the peroxisome proliferator-activated receptor-γ in fat cells and stimulating the PI3K/Akt pathway. However, a meta-analysis of randomized clinical trials of rosiglitazone confirmed that patients taking the drug had a significantly higher risk of edema and heart failure (Mannucci *et al.* 2010). Very recently, Ku *et al.* (2017) discovered that rosiglitazone treatment of HUVEC increased expression of VEGF and suppressed expression of the tight junction proteins JAM-A and ZO-1, thus promoting vascular leakage. Conversely, siRNA knockdown of Akt protected against these damaging effects.

6.4.4 Summary

Our experiments strongly suggest that basal PI3K/Akt signaling in P-UAEC is sufficient to both optimize the size of the Cx43 gap junctional plaques necessary for pregnancy-adapted Ca2+ bursting and maintain robust cell-to-cell connectivity of the endothelial monolayer. Our data also suggest that ability of EGFR to couple to PI3K/Akt in contrast to VEGFR-2 is not a major concern in the interpretation of our data Chapter 5.

Figure 6.1

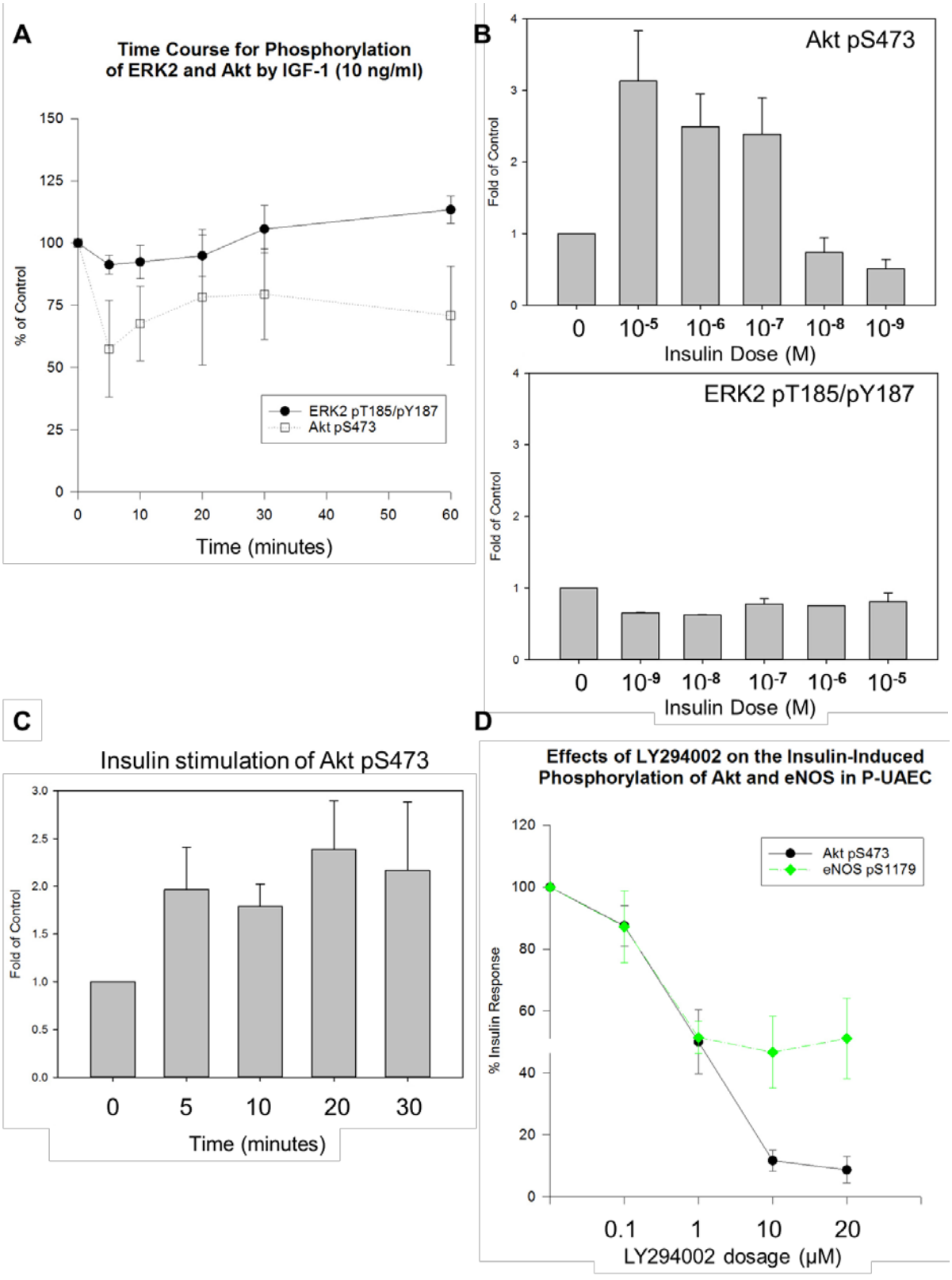
A
Time Course for Phosphorylation of ERK2 and Akt by IGF-1 (10 ng/ml)
% of Control
Time (minutes)
ERK2 pT185/pY187
Akt pS473
B
Akt pS473
Fold of Control
Insulin Dose (M)
ERK2 pT185/pY187
Fold of Control
Insulin Dose (M)
C
Insulin stimulation of Akt pS473
Fold of Control
Time (minutes)
D
Effects of LY294002 on the Insulin-Induced Phosphorylation of Akt and eNOS in P-UAEC
Akt pS473
eNOS pS1179
% Insulin Response
LY294002 dosage (μM)

Figure 6.1 Insulin induces phosphorylation of Akt in a dose-dependent manner, but is not coupled to the MEK/ERK pathway in P-UAEC. Prior unpublished research conducted by Jeremy Sullivan in the Bird Laboratory has characterized the time- and dose-dependent effects of insulin on the PI3K/Akt and MAPK pathways. Administration of IGF-1 at 10 ng/mL (1.3 nM), which strongly activates IGF receptors but only weakly activates insulin receptors (K_d = 160 pM vs.11 nM; Schumacher *et al.* 1991), had no significant effect on Akt or ERK1/2 responses in P-UAEC (A), suggesting IGF receptors are either not present or not coupled to the PI3K or MAPK pathways in P-UAEC. Insulin treatment at a dose of 100 nM or greater increased the phosphorylation of Akt S473 significantly above the basal level but had no comparable effect on the phosphorylation of ERK2 at doses ranging from 1 nM to 10 µM (B). 100 nM insulin stimulated a 2-fold pAkt response by 5 min that was the same at 30 min (C). A maximal dose of 10µM insulin increased phosphorylation of eNOS on the known Akt-mediated site S1179. Both responses showed the expected inhibitory effect of LY294002, which returned pAkt to the basal level or lower and eliminates the Akt component of enhanced eNOS phosphorylation (D).

Figure 6.2

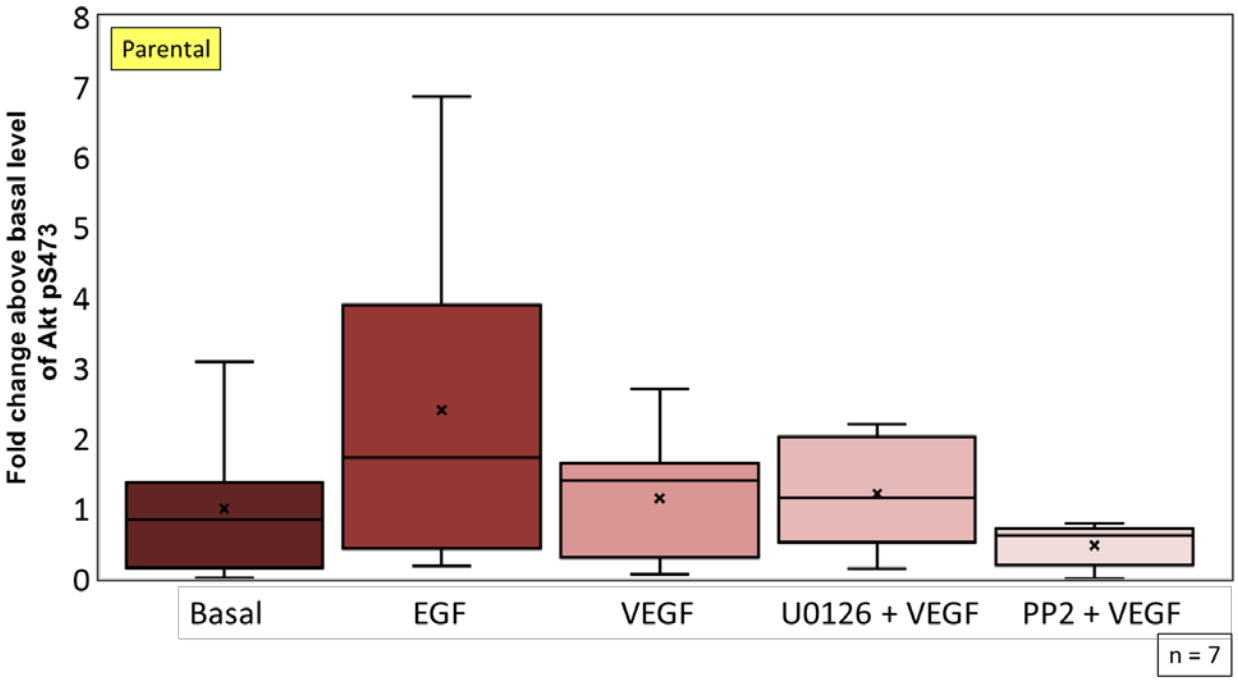

Figure 6.2 Phosphorylation of Akt S473 in parental P-UAEC following 30-minute growth factor treatment. Parental P-UAEC were grown to confluency, pretreated with 10 µM U0126, 10 µM PP2, or vehicle for 30 min prior to administration of 10 ng/mL EGF or VEGF for 30 min. Cells were then lysed and harvested. Proteins were resolved by PAGE and analyzed by Western blot using Akt pS473 antibody (Cell Signaling) and normalized by expression of hsp90 (Cell Signaling). Neither EGF nor VEGF induced phosphorylation of Akt S473 in parental P-UAEC. While PP2 pretreatment prior to VEGF administration did appear to suppress Akt phosphorylation (0.47-fold of basal level), the result was not statistically significant. Data collected from the results of 7 independent experiments. Statistical significance was determined by ANOVA and post-hoc analysis using Dunnett's two-sided test compared against basal level.

Figure 6.3

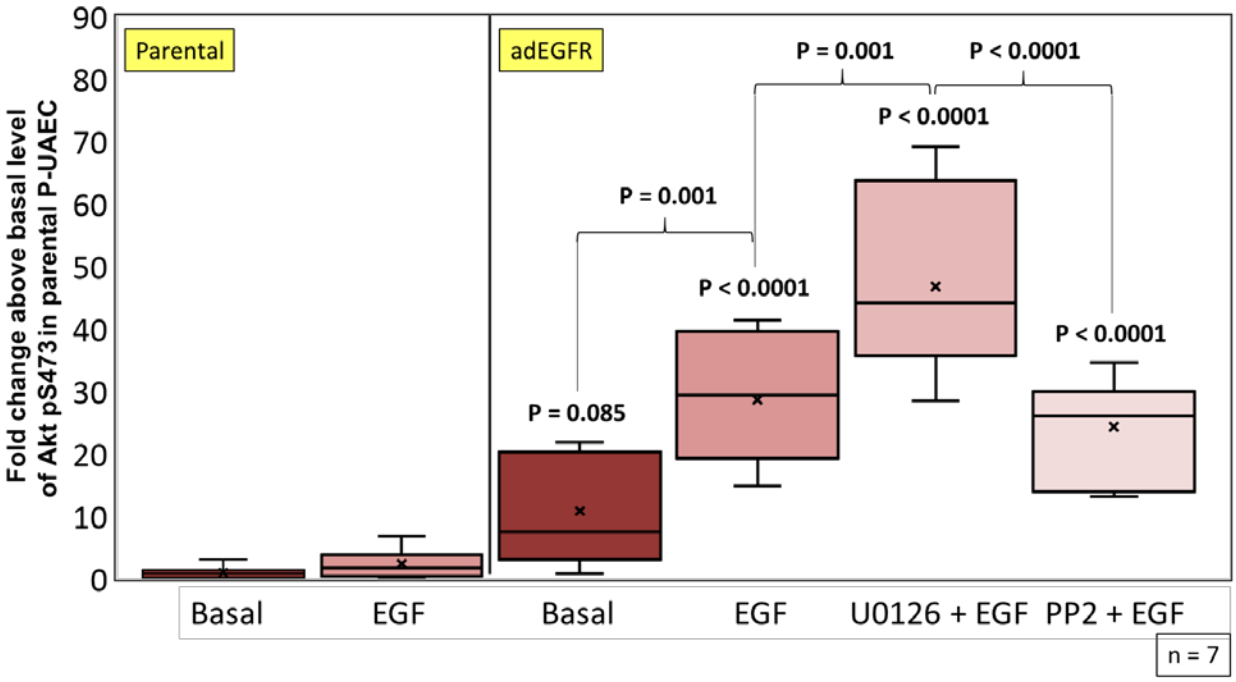

Figure 6.3 Phosphorylation of Akt S473 in P-UAEC-adEGFR following 30-minute kinase inhibitor pretreatment and 30-minute EGF treatment. Basal and EGF-stimulated Akt pS473 in parental P-UAEC from Figure 6.1 are shown on the left. EGF treatment of P-UAEC-adEGFR induced dramatic Akt phosphorylation (29-fold of basal in parental P-UAEC). Pretreatment with 10 µM U0126 for 30 min prior to EGF administration resulted in still greater Akt phosphorylation (47-fold of basal in parental P-UAEC). Pretreatment with 10 µM PP2 for 30 min prior to EGF was no different than EGF treatment alone. Quantification of Akt pS473 antibody (Cell Signaling) bands was normalized by total hsp90 protein. Data were collected from the results of 7 independent experiments. Statistical significance was determined by ANOVA and post-hoc analysis using Tukey's HSD multiple comparison test.

Figure 6.4

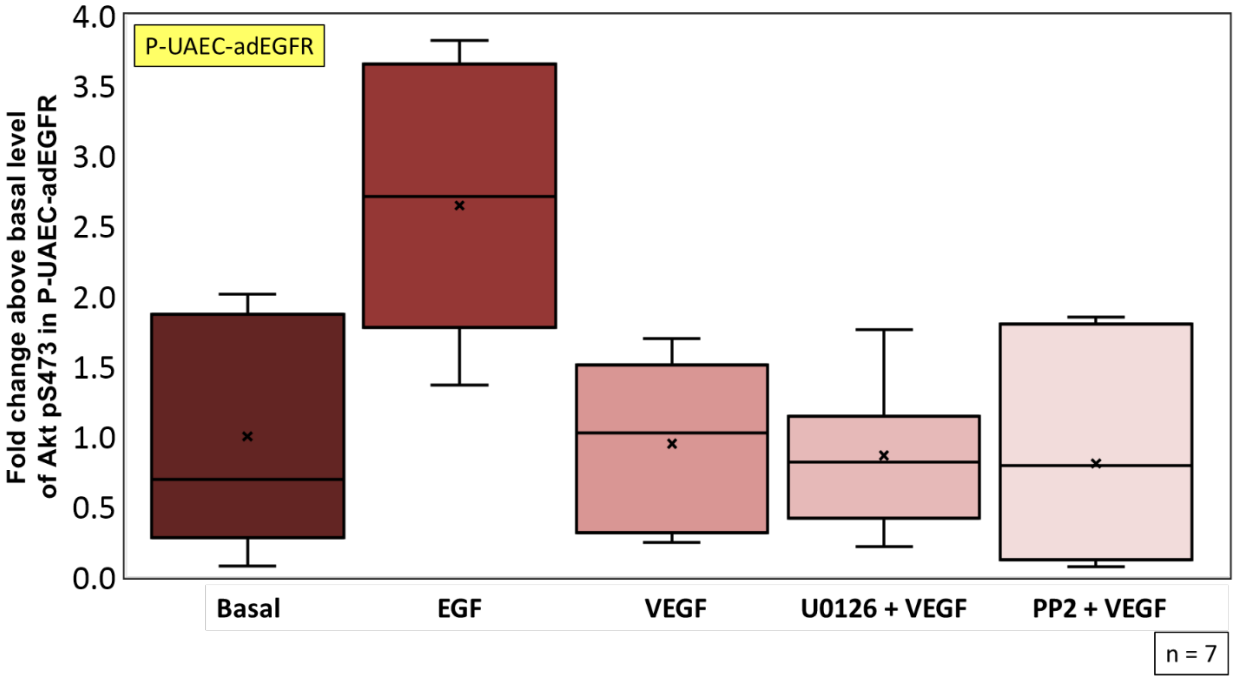

Figure 6.4 VEGF treatment has no effect on Akt S473 phosphorylation in P-UAEC-adEGFR. Whether P-UAEC-adEGFR were pretreated with 10 µM U0126, 10 µM PP2, or vehicle for 30 min, treatment with 10 ng/mL VEGF for 30 min did not alter the basal level of Akt pS7473. The EGF-induced phosphorylation of Akt is shown for comparison. (n = 7)

Figure 6.5

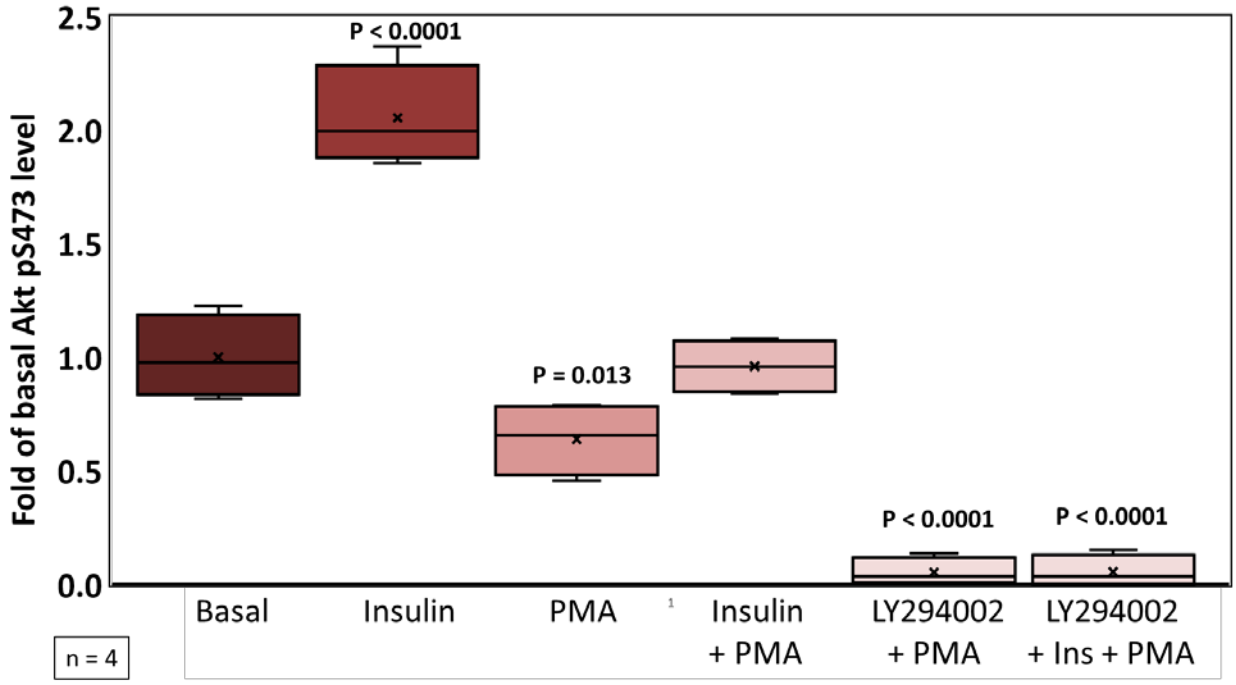

Figure 6.5 Overnight pretreatment with insulin doubles basal phosphorylation of Akt S473. To test if insulin-induced phosphorylation of Akt S473 was merely transient or if it could be maintained by prolonged insulin treatment, we pretreated P-UAEC with 100 nM insulin overnight. The next day, after the cells were harvested and the lysates were subjected to Western blot analysis, we found that basal phosphorylation of Akt S473 was also at twice the normal level at ~20 hrs post-treatment (lane 2). Acute treatment (30-min) with 10 nM TPA—a potent suppressor of pregnancy-adapted Ca2+ bursting in P-UAEC (Boeldt et al. 2015)—downregulated Akt phosphorylation (lane 3) but this effect was cancelled out by the presence of insulin (lane 4). However, the PI3K-selective inhibitor LY294002 (20 µM) eliminated even the residual basal Akt S473 phosphorylation that remains following TPA treatment irrespective of the presence of insulin (lanes 5 & 6). Statistical significance was determined by ANOVA and post-hoc analysis using Dunnett's two-sided test. (n = 4)

Figure 6.6

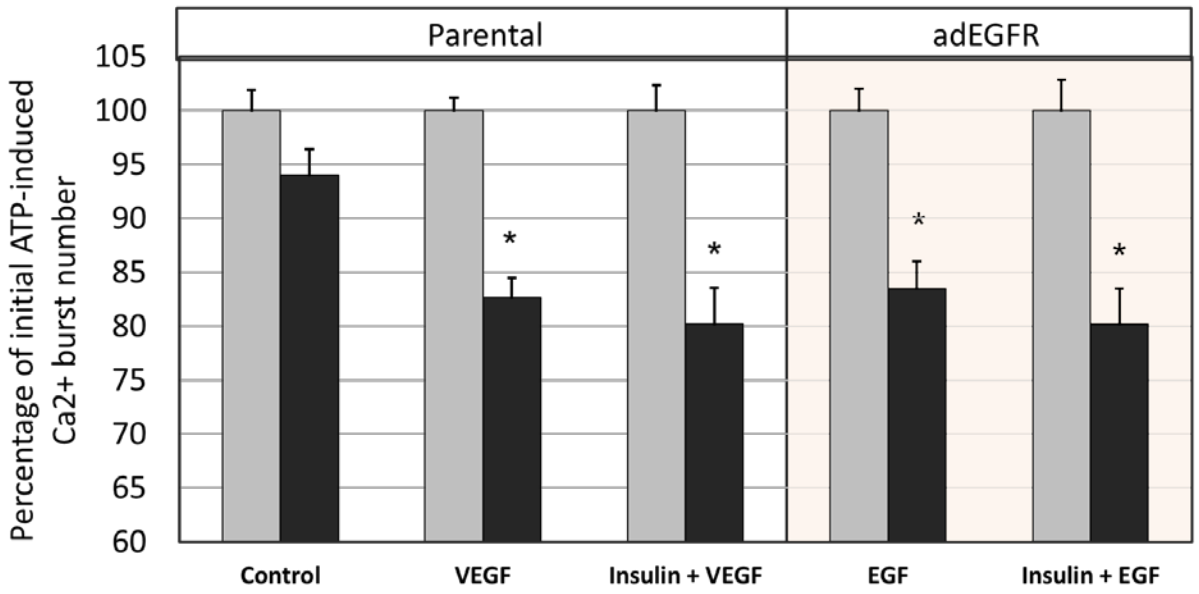

Figure 6.6 Insulin pretreatment does not protect against growth factor inhibition of the ATP-induced Ca2+ burst response. Parental P-UAEC and P-UAEC-adEGFR grown to confluency were pretreated overnight with insulin (100 nM), then pre-loaded with the [Ca2+]i-sensitive dye Fura-2. Cells were stimulated with ATP (100 µM) for 30 min, then washed with fresh buffer containing 100 nM insulin and allowed to sit for 30 min. Parental P-UAEC were treated with VEGF (10 ng/mL). P-UAEC-adEGFR were treated with EGF (10 ng/mL). Cells were then re-stimulated with ATP for 30 min. Data was collected from cells showing 3 or more ATP stimulated Ca2+ bursts prior to growth factor treatment. Data from earlier trials without insulin pretreatment (from Figure 5.2) were compared to insulin-treated cells. Black bars represent percent of initial mean burst number +/- SE. Insulin pretreatment provided no protection against growth factor inhibition of the Ca2+ bursting response. Statistics were performed on raw data from individual P-UAEC (parental or adEGFR) observed in 5-22 dishes: control (n = 342), VEGF-165 (n = 778), or insulin+VEGF (n = 225) in parental P-UAEC; EGF (n = 362) or insulin+EGF (n = 181) in P-UAEC-adEGFR. Comparisons between post-treatment groups and their respective controls were analyzed by rank-sum test (***** $P < 0.0001$).

Figure 6.7

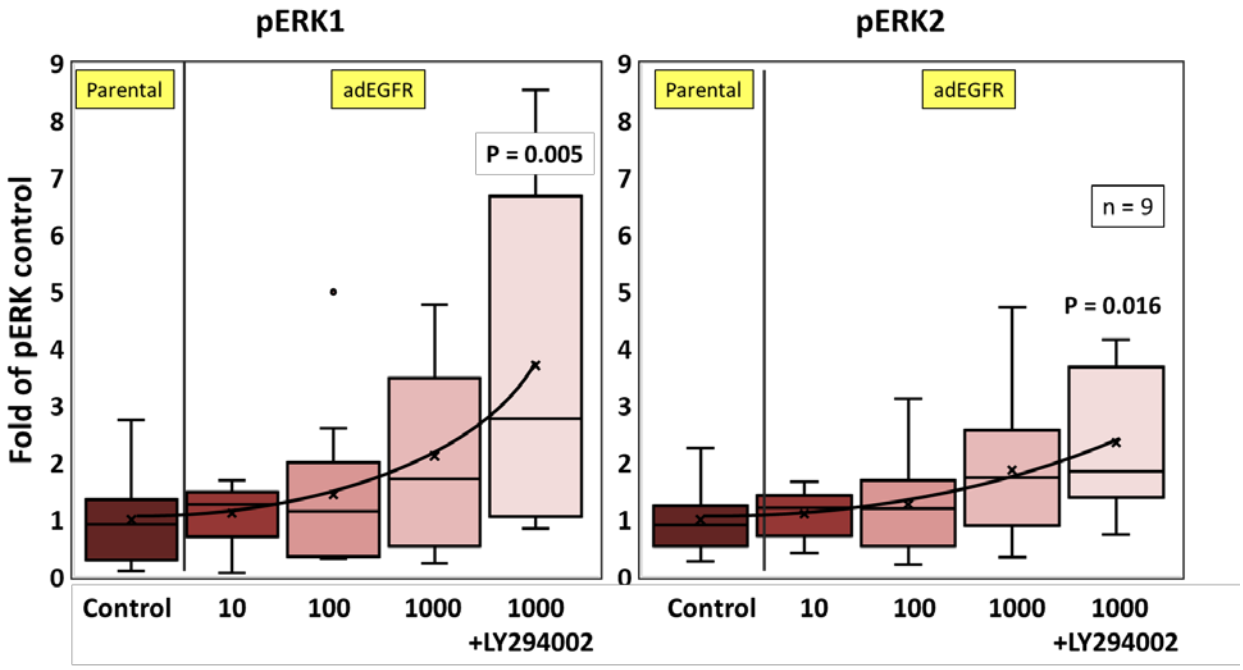

Figure 6.7 Overnight treatment with PI3 kinase inhibitor LY294002 significantly increases basal phosphorylation of ERK1/2 in P-UAEC-adEGFR. P-UAEC-adEGFR exhibited significantly elevated mean basal phosphorylations of ERK1 (3.7-fold; *P* = 0.005) and ERK2 (2.4-fold; *P* = 0.016) following overnight treatment with the PI3K-selective inhibitor LY294002 (20µM). These data suggest an inverse relationship may exist between PI3K/Akt and MAPK pathway signaling in P-UAEC. Statistical significance was determined by ANOVA and post-hoc analysis using Dunnett's two-sided test. (n = 9)

Figure 6.8

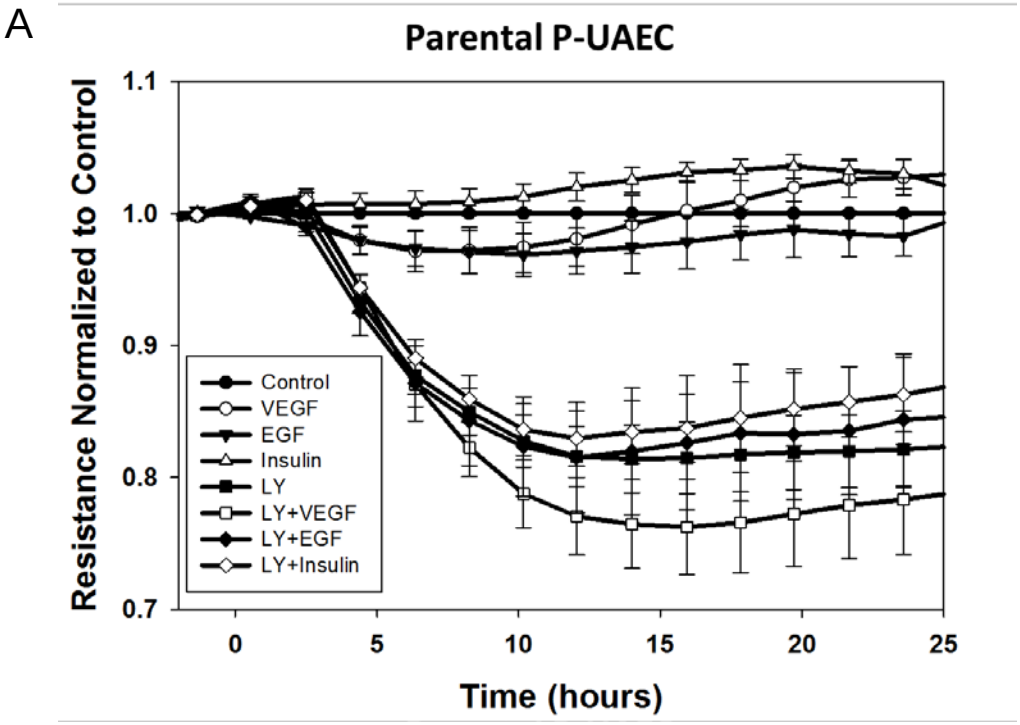
A
Parental P-UAEC
Resistance Normalized to Control
1.1
1.0
0.9
0.8
0.7
0
5
10
15
20
25
Time (hours)
Control
VEGF
EGF
Insulin
LY
LY+VEGF
LY+EGF
LY+Insulin

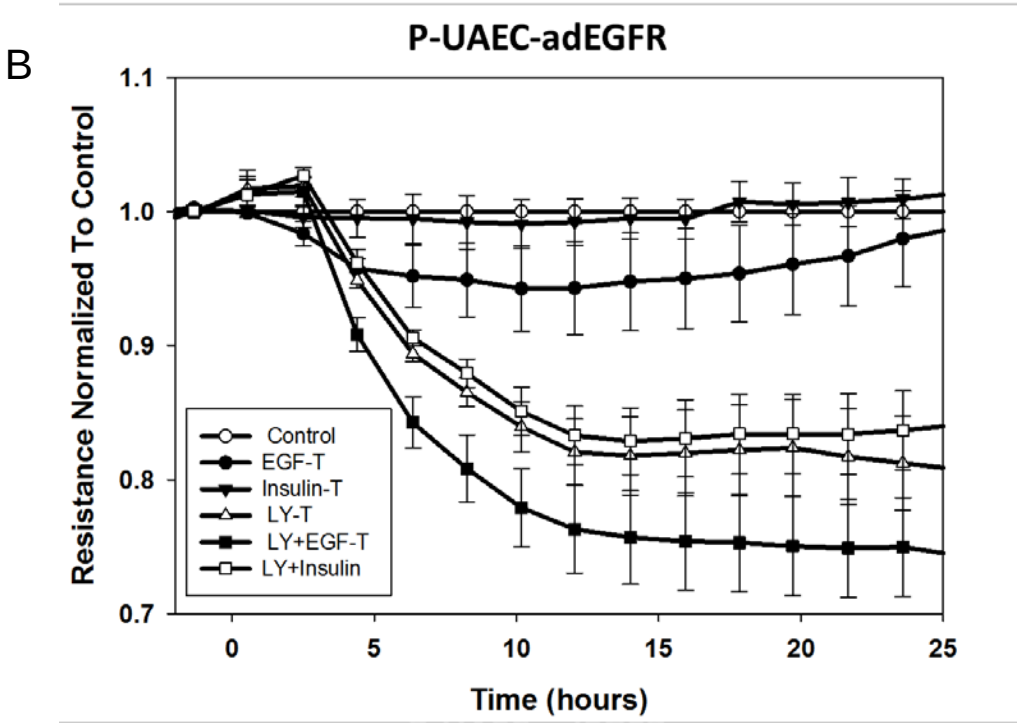
B
P-UAEC-adEGFR
Resistance Normalized To Control
1.1
1.0
0.9
0.8
0.7
0
5
10
15
20
25
Time (hours)
Control
EGF-T
Insulin-T
LY-T
LY+EGF-T
LY+Insulin

Figure 6.8 Insulin pretreatment does not protect P-UAEC monolayer integrity, but the PI3K-selective inhibitor LY294002 severely impairs it. ECIS quantification of the electrical impedance of confluent P-UAEC monolayers suggests that the PI3K pathway is critical for maintaining the endothelial barrier function. In both parental P-UAEC and P-UAEC-adEGFR, pharmacological inhibition of PI3K with LY294002 (20 μM) induced a significant drop in electrical impedance, beginning at ~3 hours and reaching the minimum value at ~14 hours. However, 100 nM insulin-induced stimulation of the PI3K/Akt pathway in parental P-UAEC and P-UAEC-adEGFR provided no significant enhancement of the endothelial monolayer relative to control. Analysis by ANOVA found that neither VEGF nor EGF nor any combination of treatments had any significant effect on endothelial monolayer integrity aside from LY294002 treatment. Only the elimination of PI3K/Akt pathway signaling by administration of LY294002 induced a significant decrease in electrical impedance over time, suggesting a progressive loss of junctional attachment proteins at the cells' surfaces.

Figure 6.9

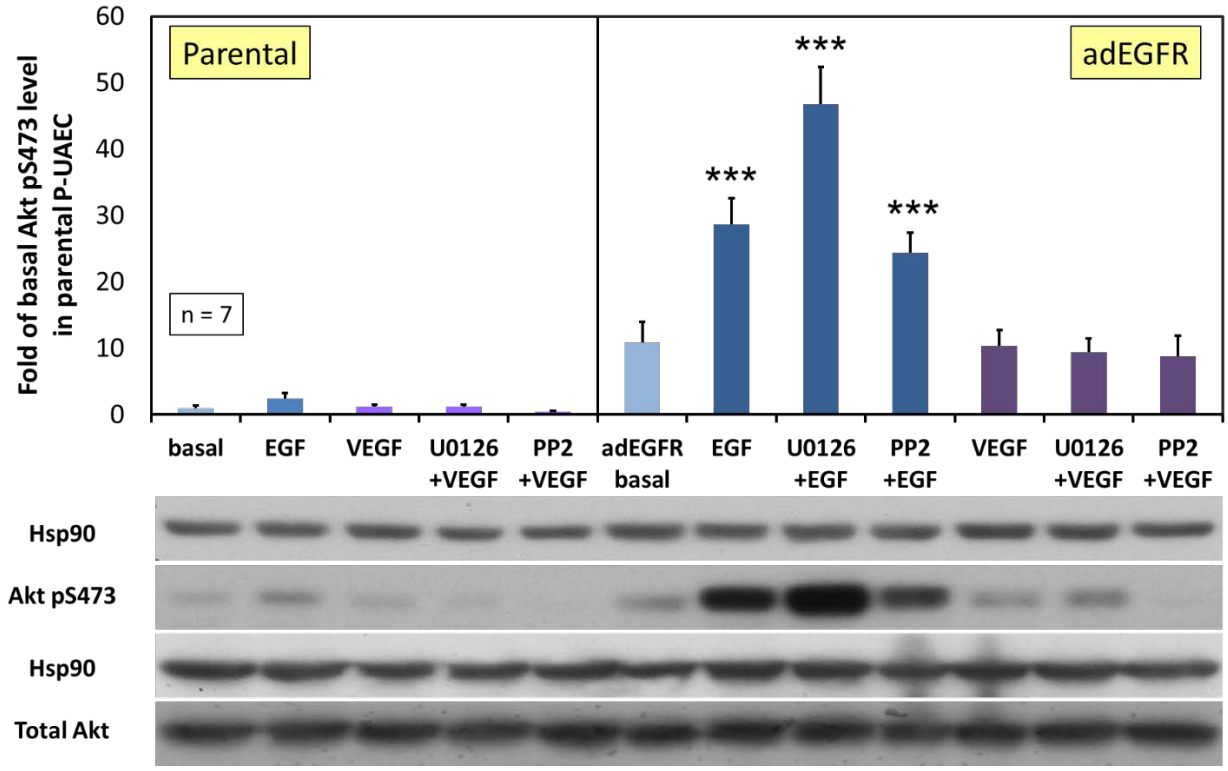

Figure 6.9 Overview of Akt S473 Phosphorylation in P-UAEC Following 30-min Growth Factor Treatment These are the results for all 12 treatment combinations in 7 independent experiments shown together. EGF treatment of P-UAEC-adEGFR induced an extremely robust phosphorylation of Akt S473, which was further amplified by the MEK-selective inhibitor U0126. While the mean basal level of pS473 in P-UAEC-adEGFR was 11 times that of parental P-UAEC, it did not achieve significance (P = 0.085). VEGF had no effect on S473 phosphorylation in either cell type. Statistical analysis by ANOVA and Dunnett's two-sided test. (***) P < 0.0001

Chapter 7:

Final Discussion

7.1 Summary of the Findings Presented in this Dissertation

To test our hypotheses that overexpression of EGFR in P-UAEC would enable EGF to reproduce the effects of VEGF, and further that EGFR overexpression would induce a permanent downregulation of gap junctional communication (GJC), we first needed to confirm that "engineering" such a feat was technically possible and, very importantly, not harmful to the cells. In **Chapter 4**, the concentration, localization, and MAPK/ERK signaling ability of adenovirally transduced EGFR in pregnancy-adapted ovine uterine artery endothelial cells (P-UAEC) were described. The purpose of which was to "engineer preeclampsia"—i.e. induce PE-like endothelial dysfunction—in these cells. Treatment with EGF has been shown to inhibit gap junctional communication (GJC) in several cell types (Madhukar *et al.* 1989, Lau *et al.* 1992, Oh *et al.* 1993), and this effect was found to be mediated through the MAPK/ERK pathway (Kanemitsu and Lau 1993). However, this is not the case in primary P-UAEC. Despite the observation that EGF treatment induced the same level of ERK phosphorylation as VEGF in P-UAEC as analyzed by Western blot, (Bird *et al.* 2000), EGF did not inhibit the ATP-stimulated Ca2+ burst response as VEGF did (Figure 4.1). We have previously speculated that this may be because EGFR expression is very low in P-UAEC, such that it is virtually undetectable by Western blot. As such, it appears that EGFR may be localized in areas of the plasma membrane distinct from VEGFR1/2 and so may for several reasons also access different subpools of ERK1/2 in P-UAEC. Studies in other cell models have shown that, upon activation by GPCRs or RTKs, uniquely localized pools

of ERK1/2 in the cytosol (Reviewed in Luttrell 2003) are mobilized to specific cellular regions, including the nucleus, mitochondria, golgi, endosomes, and the plasma membrane (Reviewed in Wainstein and Seger 2016; Zennadi *et al.* 2012). While we currently have only indirect evidence to support this hypothesis in P-UAEC, it provides a plausible tentative explanation for why VEGF-induced ERK phosphorylation in P-UAEC is correlated with loss of GJC, but EGF-induced ERK phosphorylation is not. It is also noteworthy that in P-UAEC both VEGF and EGF are equally capable of driving mitogenesis (Bird et al 2000), and in this case mitogenesis begins with translocation of ERK to the nucleus. If the low density of EGFR at the plasma membrane is in fact the reason that the receptor is unable to couple to the specific pools of ERK1/2 that mediate Cx43 phosphorylation, then it is possible that increasing the expression of EGFR will increase the probability of accessing those pools by spilling EGFR into formerly inaccessible regions of the plasma membrane. We predicted firstly that addition of exogenous EGFR at the plasma membrane of P-UAEC would enable EGF treatment to duplicate the inhibitory effect of VEGF on GJC, and secondly that sufficiently high expression of EGFR would confer constitutive activity to the receptor, inducing a state of permanent ligand-independent suppression of pregnancy-adapted GJC and capacitative calcium entry (CCE).

To attain higher levels of EGFR expression, I incubated P-UAEC overnight with adenovirus containing the *EGFR* gene transcript at several different multiplicities of infection (MOI), followed by 24 hrs of incubation in fresh antivirus-free medium. To account for the possibility that no level of wild-type EGFR expression would be sufficient to confer constitutive receptor activity, I also incubated P-UAEC overnight with adenovirus containing the gene transcript for *L834R-EGFR*, which encodes for one of the most common constitutively active EGFR mutants found in non-small cell lung cancer. Before beginning any experiments involving EGF stimulation of P-UAEC expressing exogenous wild-type EGFR or L834R-EGFR (termed “P-UAEC-adEGFR” and “P-UAEC-adL834R,” respectively), I first had to confirm that the process of adenoviral transduction

was not toxic to the cells, since it would mean little to report a significant reduction in [Ca2+]i bursting if the decrease was simply due to cell death. To determine cell viability following the adenoviral transduction protocol, multiple samples of P-UAEC—adEGFR, adL834R, and parental (i.e. not transduced with adenovirus)—were labeled with mAb 528, which is selective for the EGFR ligand binding site, and a phycoerythrin fluorophore tag. By pretreating each sample of labeled cells with propidium iodide (which permeates dead cells) before passing 10,000 cells from each sample through the BD FACSCaliber flow cytometer, the percentage of live cells could be quantified. A parental P-UAEC control sample and P-UAEC samples transduced with wild-type *EGFR* or *L834R-EGFR* at MOIs of 10, 100, 320, 1000, and 3200 were all found to exhibit the same viability, suggesting that exposure to adenovirus was not deleterious to P-UAEC (Figure 4.2A). In the case of P-UAEC adenovirally transduced with *L834R-EGFR*, flow cytometric analysis did show reductions in cell viability compared to parental P-UAEC at the highest multiplicities of viral infection. However, cell loss seemed largely correlated with the level of binding of mAb 528 and phycoerythrin to L834R EGFR protein, particularly at an MOI of 3200, and due to a lesser degree to the mere overexpression of the L834R mutant receptor (Figure 4.2B).

As mentioned earlier, endogenous expression of EGFR in P-UAEC is so low that it is virtually undetectable by Western blot. Expression levels of both wild-type EGFR and L834R-EGFR are quantifiable at an MOI of 100, and robust at an MOI of 1000 (Figure 4.3). To detect EGFR at the lowest expression levels, flow cytometric quantification of immunolabeled EGFR on the plasma membrane of P-UAEC was performed because it offers greater sensitivity of detection than Western blotting. Flow cytometry confirmed that EGFR was indeed present on the plasma membrane of parental P-UAEC—an observation which confirmed what earlier EGF-induced ERK1/2 phosphorylation data already implied—albeit only detected in up to ~22% of cells (Figure 4.5), and the mean expression level was quite low (Figure 4.4). Analysis of adenovirally transduced cells found that surface density of wild-type and mutant EGFR rose with increasing

MOI, demonstrating that the exogenous receptors could be transported successfully to the cell surface and embedded in the plasma membrane at high concentration (Figure 4.4). The percentage of EGFR-expressing cells increased with greater MOI until reaching 100% at the highest MOIs, but expression was far from uniform, differing from one cell to another by as much as two orders of magnitude (Figure 4.5). Presumably because L834R-EGFR monomers are known to cluster, dimerize, and internalize spontaneously (Choi, *et al.* 2007), relatively few L834R receptors were detected on the plasma membrane in P-UAEC adenovirally transduced at lower MOIs (Figure 4.6). We speculated that the endocytosis machinery was overwhelmed at higher levels of expression, thus stranding larger numbers of L834R receptors at the cell surface at higher MOIs, but this is merely conjecture without further data.

In the general literature on tumor cells, it is well-established that EGFR dysregulates cell homeostasis when expression at the plasma membrane achieves sufficient density to confer constitutive receptor activity. Having confirmed that adenoviral transduction of the *EGFR* gene transcript into the cytosol of P-UAEC was possible at a high MOI without loss of cell viability, the next step was to determine the MOI necessary to “engineer” the type of endothelial cell dysfunction observed in PE. To this end, I performed Western blots to observe basal and EGF-stimulated EGFR autophosphorylation using the same series of samples I used for flow cytometric analysis. Treating samples with EGF was of course not necessary for observing basal autophosphorylation, but comparison of lysates of EGF- and vehicle-treated cells revealed the difference in the magnitude of ligand-dependent and independent activity of EGFR and served as a rough measure of surface expression of the receptor. In P-UAEC-adEGFR samples, the lowest MOI to produce a significant level of constitutive autophosphorylation was 1000 (Figure 4.7A). For this reason, I used MOI 1000 cells to conduct experiments on inhibition of the Ca2+ burst response. Because endogenous expression of EGFR in UAEC is very low and the surface area of any cell is finite, I wanted to be as confident as possible that any observed disruption of the

Ca2+ burst response was due specifically to downregulation of CCE mechanisms and not simply cell-wide dysfunction due to excessive overexpression of a single exogenous protein. Both wild-type EGFR and L834R-EGFR in P-UAEC were responsive to EGF in an MOI-dependent manner; however, L834R-EGFR exhibited relatively poor responsiveness to EGF at lower MOIs (10, 100) and robust EGF responsiveness at higher MOIs (320, 1000, 3200) (Figure 4.7B), which correlated with the flow cytometric quantification of surface expression obtained earlier.

Having established that adenoviral transduction of *EGFR* in P-UAEC results in (1) EGFR expression at the plasma membrane, (2) autophosphorylation in response to EGF, and (3) constitutive receptor activity at high density, we then needed to test whether the exogenous receptor was functionally linked to the relevant signaling pathways for regulation of Cx43 gap junctions. Since previous work in the Bird Laboratory has demonstrated that Src- and ERK-mediated phosphorylations of Cx43 Y265 and S279/282, respectively, are associated with the closing of gap junctions and inhibition of [Ca2+]i signaling across endothelial cell monolayers (Boeldt *et al.* 2015), it was vital to establish the ability of exogenous EGFR to activate these kinases. Unfortunately, due to poor specificity of the antibodies available for labeling Src, we were not able to directly measure the effect of EGFR overexpression on Src phosphorylation. We were, however, able to collect reliable data for quantifying the basal and EGF-induced phosphorylation of ERK1/2 in P-UAEC-adEGFR. To determine the effect of EGFR overexpression on basal ERK1/2 phosphorylation, I performed a series of nine Western blots (from nine independent experiments) comparing the differences in pERK1/2 between parental P-UAEC and P-UAEC-adEGFR transduced at MOIs of 10, 100 or 1000. Analysis of these blots by ANOVA found no significant differences between groups. However, for both ERK1 and ERK2, there was an observable trend toward higher EGFR expression being associated with greater mean ERK phosphorylation, with cells transduced at an MOI of 1000 exhibiting the greatest increases of mean basal ERK1 and ERK2 phosphorylations at 2.1- and 1.9-fold, respectively, above the levels

observed in parental P-UAEC (Figure 4.8). Despite the lack of statistical significance due to high variance, I did not feel I could entirely rule out a cause and effect relationship due to the consistent correlation between EGFR expression and mean basal ERK1/2 phosphorylation. In any case, the real test was whether the basal level of pERK1/2 in P-UAEC-adEGFR would be enough to induce a sufficient basal elevation of Cx43 S279/282 to permanently impair the cells' capacity for GJC and pregnancy-adapted CCE. Treatment of P-UAEC-adEGFR with EGF (10 ng/mL) for 30 minutes induced strongly significant ($P < 0.0001$) phosphorylations of ERK1 and ERK2 (Figure 4.10B) at several times the levels observed in control cells. If a significant percentage of these phosphorylations are occurring in the Cx43-associated ERK1/2 pools, we should expect EGF to inhibit GJC in P-UAEC-adEGFR just as VEGF inhibits GJC in parental P-UAEC.

In **Chapter 5**, I presented the results of the experiments that tested our major hypotheses. Since optimal GJC is a critical feature of the pregnancy-enhanced CCE necessary for sustained activity of eNOS, we use growth factor inhibition of ATP-induced Ca2+ bursting as a measure of suppression of pregnancy-adapted programming. Based on the effects of EGFR overexpression or activating mutations in tumor cells, we had predicted that the constitutive autophosphorylation of EGFR would result in continuous activation of the MAPK pathway and/or Src, thereby elevating the ERK- and Src-mediated inhibitory phosphorylations of Cx43 and suppressing pregnancy-adapted CCE. If our prediction were correct, we would expect that the mean number of [Ca2+]i bursts in confluent P-UAEC-adEGFR following a single treatment of ATP to be significantly lower than the mean number of bursts exhibited by parental P-UAEC due to a reduction in the number of functionally "open" Cx43 gap junctions. Surprisingly, we found that the mean number of ATP-stimulated [Ca2+]i bursts was 4% greater ($P = 0.0051$) in P-UAEC-adEGFR (Figure 5.1). The presence of constitutively active EGFR, rather than inhibiting CCE, seems instead to facilitate a small but significant enhancement, thus showing our "permanent downregulation of GJC" hypothesis to be false. This evidence strongly suggests that overexpression of EGFR, whether

wild-type or mutant, in P-UAEC is not sufficient to inhibit the pregnancy-enhanced Ca2+ bursting response to ATP. This result correlated with our Western blot data, which found that P-UAEC-adEGFR transduced at MOIs of 10, 100, and 1000 exhibited the same unaltered basal phosphorylation levels of Cx43 Y265 and S279/282 observed in parental P-UAEC (Figure 5.2). Together, the Ca2+ bursting data and the Cx43 phosphorylation data provide enough evidence to draw the following conclusions with a high degree of confidence: Firstly, even though we cannot measure the phosphorylation of c-Src directly, basal c-Src phosphorylation is not likely to be significantly increased by the constitutive activity of EGFR in P-UAEC-adEGFR or P-UAEC-adL834R. This is because cells transfected with v-Src, the constitutively active viral form of Src, exhibit downregulated GJC and display basal elevation of Cx43 Y247 and Y265 (Swenson *et al.* 1990; Solan and Lampe 2009), and activated c-Src has the same inhibitory effects on GJC as v-Src (Azarnia *et al.* 1988). Secondly, ERK1/2 phosphorylation, or at least phosphorylation of the relevant pools of ERK1/2 for regulation of Cx43 function, is also not significantly increased by the constitutive activity of EGFR in P-UAEC-adEGFR or -adL834R. Whether or not there is a trend toward higher EGFR expression being associated with greater mean ERK phosphorylation, the basal levels of pERK1/2 in P-UAEC-adEGFR and P-UAEC-adL834R are not sufficient, or at least are not the relevant pool, to elevate Cx43 pS279/282 or inhibit pregnancy-enhanced CCE.

Having determined that ligand-independent EGFR activations of Src and ERK1/2 are insufficient to suppress pregnancy-adapted CCE in P-UAEC-adEGFR, the remaining data presented in **Chapter 5** addressed the effects of EGF-stimulated activation of EGFR. Our aim was to investigate whether overexpression of EGFR in P-UAEC would enable EGF to induce the same suppression of CCE in P-UAEC-adEGFR that VEGF induces in parental P-UAEC. Recall that 10-minute EGF and VEGF treatment at the same 10 ng/mL dose induced nearly identical elevations of ERK1/2 phosphorylation (Bird *et al.* 2000), but EGF did not inhibit the ATP-stimulated Ca2+ bursting response as VEGF otherwise did (Figure 4.1). We tentatively attributed this difference to

the minimal expression of EGFR in parental P-UAEC, which is likely to limit the receptor's access to the specific pools of ERK1/2 that are able to access/influence the regulation of Cx43; however, we anticipated that the high density of activated EGFR at the plasma membranes of P-UAEC-adEGFR and adL834R would enable the receptor, whether wild-type or mutant, to connect to these otherwise elusive ERK pools, thereby stimulating the phosphorylation of Cx43 S279/282 and downregulating pregnancy-adapted CCE. While basal pERK1/2 levels were not raised significantly in P-UAEC-adEGFR, EGF-induced phosphorylations of ERK1 and ERK2 in P-UAEC-adEGFR were further elevated ~4-fold and ~3-fold, respectively, over their corresponding EGF-induced levels in parental P-UAEC (Figure 4.11, lanes 2 and 7). This strongly suggests that adding EGFR did indeed lead to an increased probability that some of the elevated pERK1/2 might be from the pools able to access Cx43.

Our calcium imaging trials provided strong evidence that EGF activates the pools of ERK1/2 that mediate Cx43 gap junction closure, but with an unexpected side effect. In P-UAEC-adEGFR and P-UAEC-adL834R, EGF treatment was indeed able to inhibit ATP-stimulated [Ca2+]i bursting at the same magnitude of VEGF inhibition in parental P-UAEC as we hypothesized, but the inhibitory effect of VEGF treatment was now lost (Figure 5.3). The results in P-UAEC-adEGFR and P-UAEC-adL834R showed a complete reversal of the respective effects EGF and VEGF in parental P-UAEC, as if the coupling of exogenous EGFR to the key effector molecules necessitated the decoupling of VEGFR-2 to those same molecules. However, VEGFR-2 cannot be decoupled from Src, since VEGF still induces phosphorylation of Cx43 Y265 in P-UAEC-adEGFR (Figure 5.4A). I will offer an explanation for the loss of VEGF-induced inhibition of [Ca2+]i bursting in P-UAEC-adEGFR in section 7.2.5. Additionally, despite the magnitude of EGF inhibition of [Ca2+]i bursting in P-UAEC-adEGFR being the same as that of VEGF in parental P-UAEC, their respective inhibitions appear to be achieved by different mechanisms. In Boeldt *et al.* (2015), pretreatment with either the SFK-selective inhibitor PP2 or the MEK-selective inhibitor U0126 protected CCE

from the negative effect of VEGF, suggesting a single Src- and ERK-dependent pathway mediates VEGF-induced down-regulation of GJC. In P-UAEC-adEGFR, U0126 pretreatment protected against the negative effect of EGF on [Ca2+]i bursting, but PP2 provided no protection, suggesting EGF-induced down-regulation of GJC is mediated by the MAPK pathway in a Src-independent manner (Figure 5.6). Although EGF treatment of P-UAEC resulted in robust phosphorylations of Cx43 Y265 and S279/282, pretreatment with PP2 prior to EGF administration kept pY265 at a level not significantly different from the basal level and had no effect on the elevated phosphorylation of S279/282. Together these data suggest firstly that EGF-induced phosphorylation of Y265 may not be necessary for EGF-mediated inhibition of GJC and secondly that EGF-induced phosphorylation of S279/282 occurs independently of Src activity.

In **Chapter 6**, I presented evidence of another difference between the actions of EGF and VEGF that became apparent after overexpressing EGFR in P-UAEC. Neither EGF nor VEGF (10 ng/mL, 30 min) induces significant Akt phosphorylation in P-UAEC (Figure 6.2), but EGF stimulated a surprisingly dramatic rise in Akt pS473 in P-UAEC-adEGFR, 29-fold over the basal level in parental P-UAEC (Figure 6.3). Interestingly, EGF stimulation of Akt phosphorylation in P-UAEC-adEGFR was even greater (47-fold) when the cells were pretreated with the MEK inhibitor U0126. These results suggest that EGFR has the potential to activate PI3K in parental P-UAEC, but its low level of expression severely limits signal transduction via the PI3K/Akt pathway. The data further suggest that the capacity for Akt phosphorylation in P-UAEC is much greater than typically observed. In contrast with EGF, treatment with VEGF resulted in no change from the basal level of Akt pS473 in P-UAEC-adEGFR, which strongly suggests that neither VEGFR-1 nor VEGFR-2 is coupled to the PI3K/Akt pathway in P-UAEC (Figure 6.4).

Remarkably, basal Akt pS473 in P-UAEC-adEGFR exhibited a mean elevation 11-fold higher than the mean basal level in parental P-UAEC, but surprisingly this was not found to be significant by ANOVA and Dunnett's two-sided test ($P = 0.085$). However, the extreme difference between the

abilities of VEGFR and EGFR to mediate Akt signaling in P-UAEC-adEGFR suggested a putative mechanism for the small but highly significant 4% increase (P = 0.0051) in the mean number of ATP-stimulated [Ca2+]i bursts observed in 30 minutes in P-UAEC-adEGFR compared to parental P-UAEC. In the “kinase program” of Cx43 gap junction regulation described by Solan and Lampe (2016), Akt activation is associated with the aggregation of connexons into larger gap junctional plaques, which has the net effect of improving GJC. It seems likely that if overexpression of EGFR in P-UAEC resulted in even a subtle enhancement of basal Akt activity, then we might expect to see a greater capacity for CCE in P-UAEC-adEGFR as compared to parental P-UAEC. VEGF treatment of parental P-UAEC activated ERK1/2, but not Akt; the net outcome was a reduction of GJC. EGF treatment of P-UAEC-adEGFR activated ERK1/2 *and* Akt; still, the net outcome was a reduction of GJC. However, what if there were a signaling stimulus that boosted the activity of Akt, but did not affect ERK1/2 signaling? Might this molecule stimulate an increase in the mean number of [Ca2+]i bursts following ATP treatment?

Fortunately, there is such a signaling stimulus. Over a decade ago, Jeremy Sullivan, then a graduate student in the Bird Laboratory, conducted dose response experiments to characterize the time- and dose-dependent effects of insulin on the PI3K/Akt and MAPK pathways. Administration of IGF-1 at 10 ng/mL (1.3 nM), which strongly activates IGF receptors but only weakly activates insulin receptors (K_d = 160 pM vs.11 nM; Schumacher *et al.* 1991), had no significant effect on Akt or ERK1/2 responses in P-UAEC (Figure 6.1A), suggesting IGF receptors are either not present or not coupled to the PI3K or MAPK pathways in P-UAEC. However, insulin treatment at a dose of 100 nM or greater increased the phosphorylation of Akt S473 significantly above the basal level but had no comparable effect on the phosphorylation of ERK2 at doses ranging from 1 nM to 10 µM (Figure 6.1B). It is well established that pregnancy is characterized by insulin resistance. In a healthy pregnancy, serum insulin is elevated to counter increased insulin resistance and meet the need for glucose transport across the placenta. However,

circulating insulin can also affect blood vessel tone via two primary pathways. In other endothelial cell types, insulin can signal through the PI3K/Akt pathway to promote NO-mediated vasodilation (Zeng and Quon 1996) or signal through the MAPK/ERK pathway to promote endothelin-1-mediated vasoconstriction (Potenza *et al.* 2005; Reviewed in King *et al.* 2016). Since the actions of insulin are uncoupled from the MAPK pathway in P-UAEC, the PI3K/Akt-mediated effects of insulin must be favored, suggesting the possibility that insulin may promote vasodilation in the uterine vasculature. In P-UAEC, we have previously found (M Grummer, unpublished data) that insulin is not a direct activator of eNOS due to the fact that it does not mobilize [Ca2+]i, but insulin might still promote vasodilation indirectly by inducing the formation of larger gap junctional plaques, which in turn could improve GJC and promote the enhanced capacitative calcium entry (CCE) in the endothelium of the maternal uterine vasculature such that other agonist effects on Ca2+ bursts are amplified.

Jeremy Sullivan's experiments measured the acute (20-minute) Akt response to insulin. To test if the rise in Akt pS473 was merely transient or if it could be maintained by prolonged insulin treatment, we pretreated P-UAEC with 100 nM insulin overnight. At ~20 hrs post-treatment (after the cells were harvested and the lysates were subjected to Western blot analysis), we found that basal phosphorylation of Akt S473 was still at twice the normal level (Figure 6.5). This long-term elevation of phosphorylated Akt in P-UAEC is unlike the response observed following stimulation of the MAPK pathway; elevation of phosphorylated ERK1/2 following growth factor treatment returns more or less to the basal level after ~30 minutes. However, despite our speculation that the increase in basal phosphorylated Akt would promote the formation of larger gap junctional plaques, the mean number of [Ca2+]i bursts in 30 minutes following initial ATP treatment was not greater than controls in P-UAEC-adEGFR or parental P-UAEC (see 6.3.5). Furthermore, elevated Akt pS473 provided no protection from growth factor inhibition of the ATP-induced Ca2+ burst

response. Insulin pretreatment had no significant effect on VEGF treatment of parental P-UAEC or EGF treatment of P-UAEC-adEGFR (Figure 6.6).

Conversely, although basal stimulation of the PI3K/Akt pathway provided no significant protection or enhancement of GJC, pharmacological inhibition of PI3K severely impaired it. When P-UAEC were treated overnight with the PI3K-selective inhibitor LY294002 (20μM), administration of ATP induced a robust initial [Ca2+]i peak from the ER, but the subsequent sustained CCE phase of bursting was virtually eliminated. Basal ERK1 and ERK2 phosphorylation were also significantly elevated ($P = 0.005$ and $P = 0.016$, respectively; ANOVA and Dunnett's two-sided test) in P-UAEC-adEGFR following overnight incubation with LY294002 (Figure 6.7). During a visit to UW Madison in 2017, gap junction researcher Paul Lampe remarked that he had similarly observed downregulation of GJC following treatment of cells with PI3K/Akt inhibitors (PD Lampe, personal communication, May 4, 2017). It is particularly interesting that dramatic increases in Akt phosphorylation above the low basal level provided little or no improvement of GJC, but complete inhibition of the PI3K/Akt pathway had a devastating effect. We speculated that the small gap junctions that result from Akt inhibition may be insufficient for effective CCE, and/or the corresponding increase in basal ERK1/2 phosphorylation might be mediating gap junction closure. To determine the localization of Cx43 in the hours following LY294002 administration, we transduced P-UAEC with adenovirus containing the gene transcript of a Cx43-eGFP fusion protein (P-UAEC-adGJA1-eGFP), but the results of several confocal microscopy experiments were inconclusive (data not shown).

Electric Cell-substrate Impedance Sensing (ECIS) analysis of both parental P-UAEC and P-UAEC-adEGFR monolayers in culture, pharmacological inhibition of PI3K with LY294002 induced a significant drop in electrical impedance, beginning at ~3 hours and reaching the minimum value at ~14 hours (Figure 6.7), suggesting PI3K is a major regulator of junctional attachment proteins. Insulin-induced stimulation of the PI3K/Akt pathway, however, provided no significant

enhancement of the endothelial monolayer relative to control. Together, these results confirm the vital importance of PI3K pathway signaling and suggest the *basal level* of PI3K activity in P-UAEC is both *necessary* and *sufficient* for optimal maintenance of the endothelial barrier function.

7.2 Proposed Models of Growth Factor Inhibition of the ATP-Induced Ca2+ Burst Response

In this section, I will begin by discussing the model of VEGF inhibition of the ATP-induced Ca2+ response in P-UAEC proposed by Derek Boeldt (Boeldt et al. 2015). I will also present a model of EGF inhibition of the response in P-UAEC-adEGFR based on the new data presented in this dissertation. The data obtained from my calcium imaging experiments with P-UAEC-adEGFR suggest an alternative interpretation of the results reported in Boeldt *et al.*, which will be presented here as well. I will finish by offering possible explanations for the difference between the actions of VEGF-A and VEGF-E reported in Boeldt *et al.* and for the *inability* of VEGF to inhibit [Ca2+]i bursting in P-UAEC-adEGFR.

7.2.1 The Boeldt Model of VEGF-A_{165} Inhibition of [Ca2+]i Bursting in P-UAEC

Figure 7.1 depicts the model of VEGF-A_{165} inhibition of ATP-stimulated [Ca2+]i bursting in P-UAEC proposed by Derek Boeldt. In this model, based on evidence from calcium imaging and Western blotting (reviewed in Chapter 3), VEGF-A_{165} administration (10 ng/mL) triggers the formation of activated VEGFR-2 homodimers that initiate three relevant signaling cascades. The first is the direct activation of the MAPK pathway that leads to the phosphorylation of ERK1/2, which in turn mediates the inhibitory phosphorylations of Cx43 proteins at S279/282. The second is activation of the MAPK pathway via Src, possibly by direct interaction of Src with Raf-1 (Chao

et al. 1997), and subsequent ERK-mediated phosphorylation of Cx43 S279/282. The third is direct Src-mediated phosphorylation of Cx43 Y265.

Interestingly, pharmacological inhibition of Src (PP2, 10 µM) or MEK (U0126, 10 µM) protects the Ca2+ burst response from VEGF-induced downregulation. Since *either* inhibitor completely blocks the negative effects of VEGF, it follows logically from this model that either the concomitant activation of pathways #1 and #3 is necessary for VEGF to downregulate [Ca2+]i bursting or pathway 2 alone is sufficient. If the inhibitory effect of VEGF could be propagated by pathway 1 or 3 alone, then pretreatment with both PP2 and U0126 would be required to protect [Ca2+]i bursting.

7.2.2 EGF Inhibition of [Ca2+]i Bursting in P-UAEC-adEGFR

EGF inhibition of [Ca2+]i bursting in P-UAEC-adEGFR is in some ways similar to that induced by VEGF. Administration of EGF in P-UAEC-adEGFR induces phosphorylations of Y265 and S279/282 on Cx43 and downregulates the Ca2+ bursting response to ATP stimulation (Figure 7.2), just like VEGF in parental P-UAEC. However, a significance difference in the respective actions of VEGF and EGF was revealed by pharmacological inhibitors of Src and MEK. Whereas VEGF-induced downregulation of [Ca2+]i bursting in parental P-UAEC was prevented by pretreatment with PP2 *or* U0126, EGF-induced downregulation of [Ca2+]i bursting in P-UAEC-adEGFR was only prevented by pretreatment with U0126, suggesting a Src-independent mechanism for EGF-mediated suppression of [Ca2+]i bursting. Although administration of EGF did induce phosphorylation of Cx43 Y265, this phosphorylation is apparently not necessary for facilitating the acute inhibition of GJC via the closure of Cx43 gap junctions. This result invites a new interpretation of the calcium imaging data presented in Boeldt *et al.* (2015).

7.2.3 The Clemente Model of VEGF-A_{165} Inhibition of [Ca2+]i Bursting in P-UAEC

The evidence provided by EGF treatment of P-UAEC-adEGFR suggests that the ERK-mediated phosphorylation of Cx43 S279/282 is required for downregulation of the ATP-induced Ca2+ burst response, but the Src-mediated phosphorylation of Cx43 Y265 is not. If MAPK pathway activation is sufficient to propagate the inhibitory effect of VEGF on GJC, then the only interpretation of the effects of kinase inhibitors documented by Boeldt *et al.* that follows logically is that pathway #2 is dominant, pathway #1 is negligible, and pathway #3 is not important for acute gap junction closure (Figure 7.3). In this interpretation, PP2 inhibition of Src protects [Ca2+]i bursting because it prevents activation of ERK1/2. This is not to say that phosphorylation of Cx43 Y265 is unimportant, but merely that it is unnecessary for acute downregulation of GJC. As many studies examining the effects of v-Src and activated c-Src (cited in Chapter 3) have confirmed, Src-mediated phosphorylation of Cx43 Y265 does inhibit GJC, but most likely by promoting Cx43 internalization and degradation, not channel gate closure (Reviewed in Solan and Lampe 2014; 2016). The downregulation of [Ca2+]i bursting that we observe within 30 minutes of growth factor treatment appears to be a result of MAPK signaling.

The Boeldt Model was supported by Western blot data presented in Boeldt et al. (2015), which found evidence of Src-dependent *and* -independent ERK1/2 phosphorylation. The Western blot data further showed that PP2 blocked the Src-mediated phosphorylation of Cx43 Y265 but had no effect on S279/282 phosphorylation. Conversely, U0126 blocked the ERK1/2-mediated phosphorylation of Cx43 S279/282 but had no effect on Y265 phosphorylation. These data suggested that path #2—Src-dependent activation of the MAPK pathway—is of minimal significance. If this pathway played a dominant role, we would expect PP2 to inhibit the phosphorylation of Y265 *and* S279/282, but PP2 did not inhibit S279/282 phosphorylation.

The calcium imaging data presented in Boeldt *et al.* told a different story. Pretreatment of P-UAEC with either PP2 or U0126 prior to VEGF administration protected the ATP-induced Ca2+ burst

response from downregulation. In other words, if the activity of *Src or ERK1/2* was blocked, Ca2+ bursting was protected from the inhibitory action of VEGF. This result is only possible if the activities of both Src *and* ERK1/2 are necessary for VEGF inhibition of the Ca2+ burst response. Since my results in P-UAEC-adEGFR suggest that pERK alone is sufficient to downregulate Ca2+ bursting, it appears that VEGF mediates gap junctional closure through a single Src-dependent activation of the MAPK pathway—i.e. pathway #2.

Ultimately, however, the presence of seemingly contradictory data tells us that both the Boeldt Model and the Clemente Model are almost certainly incomplete. In the years ahead, future studies will identify the missing pieces in this puzzle and fit them into newer, more comprehensive models with much greater accuracy. The studies of TNFα signaling that Amanda Ampey is currently conducting may find some of those "missing pieces" in the very near future (Ampey et al., in preparation).

7.2.4 Can VEGFR heterodimers mediate VEGF-A_{165} inhibition of [Ca2+]i bursting in P-UAEC?

One of the assertions of Boeldt et al. (2015) was that only VEGFR-2 mediated the inhibition of ATP-stimulated [Ca2+]i bursting, citing evidence that only VEGF-A_{165} and VEGF-E, which both bind to VEGFR-2, downregulated the burst response, but the VEGFR-1-specific agonist PlGF had no effect, and VEGF-E in combination with PlGF had no further effect over that of VEGF-E alone. However, there was a curious detail about the actions of VEGF-E for which no explanation was provided. While VEGF-E was indeed able to induce the same magnitude of ERK1/2 phosphorylation (Grummer et al. 2009) and downregulation of [Ca2+]i bursting (Boeldt et al. 2015) as VEGF-A_{165}, it could only do so at ~11 times the dose (2.9 nM VEGF-E (100 ng/mL) vs. 0.26 nM VEGF-A_{165} (10 ng/mL)). This result is difficult to interpret since the binding affinities of VEGF-A_{165} and VEGF-E for VEGFR-2 have been reported to be nearly identical (Ogawa *et al.* 1998).

One possibility is that, despite the similar binding affinity for VEGFR-2, the tertiary structure of VEGF-E is significantly distinct from that of VEGF-A_{165} such that the VEGFR-2 homodimers formed by VEGF-E binding adopt a less active conformation than those formed by VEGF-A_{165} binding. Even subtle differences in VEGFR-2 homodimer conformation could result in a lower efficiency of the kinase domain or reduced accessibility of docking sites for effector molecules due to steric considerations or the position of charges on the receptor. Alternatively, the 11-fold greater activity induced by VEGF-A_{165} could be because VEGF-A_{165} binds to both VEGFR-1 and VEGFR-2 (Figure 7.4). While the evidence presented in Boeldt *et al.* does indeed suggest that VEGFR-2 homodimers mediate VEGF downregulation of ATP-stimulated [Ca2+]i bursting and VEGFR-1 homodimers do not, we cannot rule out the possibility that VEGFR-1/VEGFR-2 heterodimers also mediate this process, thereby conferring greater signaling power to VEGF-A_{165} over VEGF-E. As I will discuss in section 7.3, far from simply attenuating the activity of VEGFR-2 as is commonly believed, VEGFR-1 can in many cases *potentiate* VEGFR-2 activity.

I do not know whether VEGFR-1/VEGFR-2 heterodimers play any role in the regulation of GJC, nor did I perform any experiments to determine this. I am raising the subject of VEGFR heterodimers primarily because it is typically overlooked in analyses of VEGF signaling. The standard model of preeclampsia, for example, holds that VEGFR-1 is basically a dummy or decoy receptor whose function is to reduce the magnitude of VEGF activity in the endothelium, both in its standard membrane-bound form (VEGFR-1) and in its soluble, truncated form (sFlt-1). However, the role of VEGFR-1 in health and pathology may be far more complicated than generally assumed.

7.2.5 A Possible Explanation for the Failure of VEGF-A_{165} to Inhibit [Ca2+]i Bursting in P-UAEC-adEGFR

At an adenoviral MOI of 1000, EGFR is expressed at a level sufficient to confer constitutive autophosphorylation to the receptor. While this continuous ligand-independent activity failed to induce significant elevations of basal ERK1/2 or inhibitory phosphorylations of Cx43, it did have a profound effect on the local environment at the plasma membrane, as evidenced by the fact that VEGF, despite inducing a significant elevation in Cx43 Y265 phosphorylation (Figure 5.4A), was not able to inhibit ATP-stimulated Ca2+ bursting in P-UAEC-adEGFR as it did in parental P-UAEC (Figure 5.3).

The overexpression of EGFR in P-UAEC must result in the receptor being localized in membrane regions where it is normally absent and will thus possess access to effector molecules that it might otherwise be denied. The constitutive autophosphorylation of the receptor means that the C-terminal tail of EGFR is an ever-present source of active phosphotyrosine docking sites, thereby acting as a sink for effector molecules such as SOS, Grb2, the Ras-GTPase, Raf-1, Shc, Cbl and PLCγ. Even though there appears to be a negative feedback loop that resists the continuous activation of MEK and ERK, upstream effector molecules for the MAPK pathway, for example, are still likely to be “locked” in interaction with the C-terminus of EGFR for much of their time at the membrane, which will inevitably reduce the availability of these molecules for other receptors if they are rate limiting in quantity. Because it is quite likely that EGFR has a higher affinity for these effectors than VEGFR-2, the net effect is that VEGFR-2 can no longer effectively activate the MAPK pathway in P-UAEC-adEGFR (Figure 4.10B) and therefore cannot induce gap junctional closure (Figure 7.5).

7.3 The Unique Characteristics and Functions of VEGFR1/VEGFR2 Heterodimers

I have included this section because the subject of VEGFR heterodimer involvement in the regulation of Cx43 GJC remains unexplored as of this writing. There is very little published research on the role of VEGFR heterodimers in the VEGF literature, but the limited data available suggests a more complex story than is typically assumed. The common notion that VEGFR-1 is little more than a “kinase-dead” receptor whose function is to simply attenuate the activity of VEGFR-2 is most certainly wrong.

When an endothelial cell is treated with VEGF-A_{165}, a significant fraction of activated VEGFR dimers will be in the form of VEGFR-1/VEGFR-2 heterodimers. The total number of active VEGFR heterodimers formed in response to VEGF-A_{165} treatment is dependent on the relative binding affinity of VEGF-A_{165} to VEGFR-1 and VEGFR-2 monomers (K_d of 9-26 pM vs. 100-770 pM, respectively, in HUVEC; Mac Gabhann and Popel 2004) as well as the ratio of VEGFR-1 to VEGFR-2 in the cell. Plasma membrane expression of VEGFR-2 in endothelial cells is typically several-fold higher than that of VEGFR-1, but the relative surface density of the receptors is by no means a fixed ratio. Differential expression of VEGFR-1 and -2 varies significantly between endothelial cell types and is highly variable from one cell to another of the same type (Imoukhuede and Popel 2011). A computational model of VEGFR dimerization developed by Mac Gabhann and Popel (2007) predicts that significantly differing expression levels of VEGFR-1 and -2 will strongly favor the formation of heterodimers of the lesser expressed receptor. This means that VEGF-A-bound VEGFR-1 should preferentially exist in heterodimeric form and that VEGFR-1 homodimers are likely to be comparatively rare in the endothelium.

VEGFR heterodimers are naturally activated by ligands that bind both VEGFR-1 and -2—i.e. VEGF-A and the heterodimeric ligand VEGF-A:PlGF-1. The unique cellular functions of VEGFR

heterodimers have been elusive, however, because these same ligands also activate VEGFR homodimers. To investigate the actions of VEGFR heterodimers exclusively, an international team of researchers working in the United Kingdom, Saudi Arabia, China, and Germany engineered a heterodimeric ligand comprising one monomer of PlGF-1, which has a high binding affinity for VEGFR-1 but not for R2, and one monomer of VEGF-E, which has a high affinity for VEGFR-2 but not for R1 (Cudmore *et al.* 2012). Their many experiments with the new ligand, **VEGF-E:PlGF-1**, revealed that the VEGFR1/R2 heterodimer mediates functions previously believed to be regulated by VEGFR-1 homodimers. In the following paragraphs, I will detail some of their results, which suggest that VEGFR-1 does more than simply act as a negative regulator of VEGFR-2 signaling as is commonly believed.

Firstly, Western blot analysis of HUVEC lysates confirmed that VEGF-E:PlGF-1 induced phosphorylations of VEGFR-2 and ERK1/2, although the pERK1/2 bands were weak compared to those induced by VEGF-A and VEGF-E. (Cudmore et al. asserted that changes in VEGFR-1 phosphorylation were “particularly difficult” to measure in HUVEC and could not be obtained.) Knockdown of either VEGFR-1 or VEGFR-2 blocked VEGF-E:PlGF-1 induction of both VEGFR-2 and ERK1/2 phosphorylation, but knockdown of neuropilin-1 or neuropilin-2 had no effect, which suggests neuropilins are not involved in VEGFR1/R2 heterodimer autophosphorylation or heterodimer-mediated MAPK pathway signaling (Cudmore *et al.* 2012).

To compare the behavior of VEGFR homo- and heterodimers, porcine aortic endothelial cells (PAEC), which express negligible levels of endogenous VEGFR, were transfected with VEGFR-1 (PAER1) or VEGFR-2 (PAER2). A third cell-line was created that expressed both VEGFR-1 and -2 (PAER1/R2) by transfecting PAER2 with VEGFR-1. Unexpectedly, when cell lysates were probed for total VEGFR-2, significantly less VEGFR-2 was expressed in PAER2 cells than in PAER1/R2 cells. This observation suggests that VEGFR-1 stabilizes VEGFR-2 expression in the cell. This appears to be a kinase-independent effect since VEGFR-2 levels were maintained in

PAER1/R2 cells even when VEGFR-1 Y1213, vital for VEGFR-1 kinase function, was mutated. Additionally, when HUVEC were treated with a saturation dose of VEGF-E, VEGFR-2 homodimers rapidly disappeared from the plasma membrane and were completely internalized after 30 minutes, but VEGFR-1 remained at the cell surface. This is not surprising since VEGF-E only activates VEGFR-2 homodimers. However, following treatment with a saturation dose of VEGF-A or VEGF-E:PlGF-1, both of which activate VEGFR1/R2 heterodimers, VEGFR-2 remained distributed on the plasma membrane after 30 minutes along with VEGFR-1, adding further evidence that VEGFR-1 also stabilizes plasma membrane localization of VEGFR-2 by inhibiting ligand-induced internalization (Cudmore *et al.* 2012).

The role of VEGFR1/R2 heterodimers in the regulation of vascular tone was also investigated. While this dissertation dealt exclusively with the *inhibitory* effect of VEGF-A_{165} on signaling mechanisms that promote vasodilation, VEGF-A_{165} treatment also induces an immediate, albeit limited, transient elevation of nitric oxide (NO) via direct stimulation of Ca2+ release (Boeldt *et al.* 2017). Treatment of rat thoracic aortic rings with VEGF-A, PlGF-1, or VEGF-E:PlGF-1 following precontraction with phenylephrine, caused significant relaxation of the vessels. VEGF-E activation of the VEGFR-2 homodimer had a much weaker effect on vascular tone than the other VEGF ligands, thus suggesting that optimal VEGF-A-induced vasorelaxation may require VEGFR-1 involvement. The eNOS inhibitor L-NAME blocked relaxation, confirming the response is mediated by endothelial NO. To determine if VEGFR1/R2 heterodimers are directly involved in mediating NO synthesis, supernatants from VEGF-E:PlGF-1 stimulated HUVEC were analyzed for NO content using chemiluminescence. The supernatants exhibited increases in phosphorylation of eNOS S1177 and were found to release NO in proportion to the administered dose of VEGF-E:PlGF-1 (Cudmore *et al.* 2012). Of note in HUVEC, VEGFR2 is coupled to the PI3K/Akt pathway and 1177 phosphorylation of eNOS is known to be mediated by Akt in endothelial cells. Achieving eNOS activation, however, would still need a Ca2+ stimulus. While

dual phosphorylated eNOS is more sensitive to Ca2+ elevation, it still requires ~200 nM for full activity (Tran et al. 2009). In turn, PLCγ activation would require Src activation.

VEGFR-1 does not seem to be required for the release of prostacyclin, however. This is evidenced by experiments in HUVEC showing that VEGF-E, which activates only the VEGFR-2 homodimer, induced a 15-fold increase in prostacyclin release, but the VEGF-E:PlGF-1-induced prostacyclin increase was just 3-fold. Similarly, VEGF-A treatment induced a 10-fold rise in prostacyclin release in PAER2 cells, but only a 2-fold rise in PAER1/R2 cells, suggesting that prostacyclin release is optimally stimulated by the action of VEGFR-2 homodimers. Also note that prostacyclin production is initiated by cPLA2 which is Ca2+-activated, but whose affinity for Ca2+ is vastly increased by ERK phosphorylation, such that it is fully active at basal [Ca2+]i levels and activation of Src would not be necessary. This response could be explained solely as a consequence of ERK activation.

In summary, the data presented in this section casts doubt on the generally held beliefs about the function of VEGFR-1 being trivial or unnecessary. Future studies of the VEGF receptor family must account for the complex and surprising influence of this poorly understood receptor and dismiss the clearly false dogma that VEGFR-1 is merely a negative regulator of VEGFR-2.

7.4 Limitations of the Experiments Presented in this Dissertation

The first limitation is the fact that we must study pregnancy-adapted programming in primary cells. As anyone who has worked with primary cells knows, they can be particularly challenging. Primary cells generally lack the robustness of cell lines and tend to exhibit higher variance in observable behavior from one plating of cells to another. Thus, the strength of the project, that we are using early passage primary cell cultures from the uterine vasculature, is also a weakness. Pregnancy-

adapted UAEC don't lend themselves to transformation at any reasonable level of efficiency. They are not well-characterized like 3T3 cells or HEK cells or COS cells, etc. and we do not have the option of establishing a P-UAEC cell line in any case because we are limited to the study of early passage cells that retain pregnancy-adapted programming. We have learned through experience that HUVEC obtained from pregnant women lose their unique pregnancy-adapted characteristics over time and their growth rate and metabolism begin to accelerate as metabolism switches increasingly to glycolysis for ATP production and the TCA cycle provides material for protein synthesis. Therefore, we must study pregnancy-adapted programming in primary cells at early passage. Conducting experiments in immortalized cell lines with overactive pathways would have little physiologic relevance to the clinical presentation of PE.

The second important limitation is that anytime cells are transduced with an adenovirus, we cannot be completely sure the result is physiologically representative. We have essentially infected P-UAEC with an inflammatory agent. However, at the risk of seeming flippant, common sense tells us that pregnant women frequently catch colds without any measurable harmful effects to their pregnancy. Additionally, as the flow cytometry evidence presented in Chapter 3 and the calcium imaging evidence in Chapters 5 and 6 showed, the presence of the adenovirus did not negatively alter P-UAEC viability or the normal response to ATP stimulation. We have shown that ATP-induced Ca2+ bursting is maintained in P-UAEC-adEGFR, which means the higher concentration of EGFR at the plasma membrane in the basal state (i.e. in the absence of ligand) doesn't reduce the function of adherens junctions or gap junctions. Prior research in the Bird Laboratory has involved expression of a dominant-negative Akt and GFP-tagged Cx43 via adenoviral transduction with no loss of appropriate cellular responses to agonists. Furthermore, adenoviral transduction does not typically result in equal expression of the desired protein in all cells in a culture. Flow cytometric analysis revealed that expression of EGFR in P-UAEC-adEGFR varies by two (or more) orders of magnitude (Figure 4.5A), which means that every culture dish

of P-UAEC-adEGFR will contain a mix of cells expressing high, moderate and low levels of EGFR. The distribution of these cells will differ from one plate to another and this will result in generally higher variance in outcomes compared to experiments done using parental P-UAEC. In the future, we may want to utilize a transfection system that produces more uniform expression of the exogenous protein among all cells, but most methods of high efficiency incorporate the foreign gene into the genome, which we would prefer to avoid.

Another obvious weakness is that we did not look at all the kinases known to mediate Cx43 phosphorylation status. We were aware of this limitation at the start of my project and intentionally chose to avoid multiplying the number of experiments by focusing on too many target proteins. PKC, for example, appears to be involved in the gating and disassembly of Cx43 gap junction by phosphorylating Cx43 at S368 (Lampe *et al.* 2000). EGFR is a known activator of PKC and it is quite likely that it activates PKC in P-UAEC. EGFR also activates PLCγ via autophosphorylations of Y992 and Y1173, which in turn activates PKCα. Since the magnitude of downregulation of Ca2+ bursting induced by EGF in P-UAEC-adEGFR was the same as that of VEGF in parental P-UAEC, and the MEK-inhibitor U0126 completely protected Ca2+ bursting from downregulation by EGF, it is unlikely that PKC is a major mediator of EGF-induced closure of gap junctions.

Finally, one of the most important tools for drawing logical conclusions about the regulation of Cx43 also happens to be one of the greatest technical weaknesses of my experiments. The poor selectivity of the phospho-Cx43 antibodies available from Santa Cruz is a significant problem that is difficult to overcome. While batches of phospho-Cx43 antibodies produced years ago have enabled researchers in the Bird Laboratory to obtain clear results from Western blot quantification of phosphorylated Cx43 proteins, I found the batches manufactured more recently to be of generally low quality, possessing a much greater affinity for off-target proteins than for phosphorylated Cx43. In most of the Western blots I performed, the bands produced by every other antibody were crisp and well-defined, but the bands for Cx43 Y265 and S279/282 were

always muddy, and no tweaking of the protocol improved the results. It was not even possible to resolve the P0, P1, and P2 bands that characterize Cx43 in different states of phosphorylation. I sincerely hope that future students in the Bird Laboratory who must quantify Cx43 phosphorylation have access to much better antibodies (or better tools altogether) for measuring pCx43 than I did.

7.5 Unanswered Questions / Future Experiments

We know that pregnancy-adapted programming is mediated in part through the regulation of Cx43 gap junctions to optimize the capacitative bursts of [Ca2+]i required for sustained, robust production of NO, but this is only part of the story. We also know that the elevated growth factors and cytokines observed in PE can downregulate the GJC that facilitates enhanced Ca2+ signaling, but this too is only part of the story. Prior research in our laboratory suggests Ca2+-activated K+ (KCa) channels, TRPC3 channels, and Cx43 gap junctions work together in some way to maximize [Ca2+]i and NO production, but an understanding of the precise mechanism has thus far proven elusive. Roxanne Alvarez, a Bird Laboratory alumnus who obtained her PhD in 2016, investigated whether Cx43 might communicate to TRPC3 via KCa channels, but ultimately her studies were inconclusive as well. It is possible that the primary role of Cx43 gap junctions in this process is simply to facilitate the propagation of IP3 from one cell to the next to open IP3 receptor-associated TRPC3 channels to allow the free flow of [Ca2+]i. It is also possible, and indeed more likely, that the mechanism is far more complicated than this. We really have no idea at this point in our investigations.

In my experiments and in most of the research done before in the Bird Laboratory, only a small number of molecules are targeted for study in limited conditions. Determining the inter-relationships between signaling molecules is a tedious and time-consuming endeavor. In future

experiments, to get a more comprehensive view of how many kinases and other signaling molecules are behaving simultaneously in response to agonists, we are in the process of moving to high throughput screening or the multiplex cell signaling/kinase assay kits that have become commercially available in recent years. Since the publication of his dissertation in 2013, Derek Boeldt has begun to utilize a high-throughput screening [Ca2+]i assay. The first surprising finding was that most growth factors and cytokines that downregulate ATP-stimulated Ca2+ signaling at 10 ng/ml almost always have a submaximal dose—often 1 ng/ml—that produces the opposite effect. When combinations of VEGF-A_{165} and TNFα are tested at doses of 1 ng/ml VEGF-A_{165} and 0.1 ng/ml TNFα, the ATP-stimulated Ca2+ response peaks at a higher level than induced by any other dose combination. Interestingly, combinations of high doses attenuate the ATP-stimulated Ca2+ response peaks to a similar degree. Together, these results suggest to me that the "Clemente Model" of growth factor downregulation of the ATP-stimulated Ca2+ response, despite its sensible interpretation of the current data, is likely to become obsolete before anyone even learns of it. And that's a good thing.

7.5.1 Some Questions Not Answered in This Dissertation

7.5.1.1 *Is the LY294002-induced abrogation of Ca2+ bursting dependent on the phosphorylation of ERK1/2?*

Overnight pretreatment with PI3 kinase inhibitor LY294002 severely impairs Ca2+ bursting. This may be because the small gap junctions that result from the absence of Akt-mediated enlargement of gap junctional plaques are insufficient for CCE. Alternatively, the elevation of pERK1/2 that results from pharmacological inhibition of the PI3K/Akt pathway might be mediating gap junction closure. To investigate whether elevated pERK is a significant factor in LY294002-induced downregulation of Ca2+ bursting, fura-2-loaded P-UAEC could be pretreated with the MEK-selective inhibitor U0126 after overnight incubation with LY294002 but prior to ATP treatment. The mean burst number could then be quantified and compared to control.

7.5.1.2 *Do VEGFR heterodimers downregulate the ATP-stimulated Ca2+ response?*

To determine if VEGFR-1/VEGFR-2 heterodimers can inhibit the ATP-stimulated Ca2+ response, the VEGF-E:PlGF-1 hybrid ligand (which only induces the formation of R1/R2 heterodimers) could be administered to fura-2-loaded P-UAEC in the same way we treated with VEGF or EGF. The mean loss of Ca2+ bursts induced by VEGF-E:PlGF-1 could be compared to the loss induced by VEGF-A_{165} and VEGF-E at same nM dose.

7.5.1.3 *Does IL-8 or (any other cytokine) transactivate EGFR in P-UAEC-adEGFR? If so, would this enable IL-8 to downregulate ATP-stimulated Ca2+ bursting in P-UAEC-adEGFR?*

The question of cytokine-mediated transactivation of EGFR was raised in my preliminary exam but was not followed up during the course of my project. Due to the high levels of circulating cytokines observed in PE, transactivation of growth factor receptors may be relevant throughout the progression of the disease. IL-8, for example, which is elevated in PE, does not inhibit the Ca2+ burst response in normal, healthy P-UAEC. However, IL-8 is a known transactivator of EGFR, and has been shown to be elevated in PE. Would IL-8 treatment of P-UAEC-adEGFR downregulate ATP-induced Ca2+ bursting via EGFR transactivation? Could the Ca2+ burst function be protected by treatment with the EGFR kinase inhibitor AG1478?

7.5.1.4 *Are other Src family kinases (in addition to Src) involved in the regulation of vascular permeability?*

We know that c-Src is the most likely Src family kinase (SFK) to be responsible for phosphorylating Cx43 Y265, due to the work done with v-Src and activated c-Src (see 3.1.6). However, we know very little about the role of Src and other SFKs in the regulation of vascular permeability. Amanda Ampey (a recent Bird Laboratory graduate) found through the use of the ECIS system that TNFα was a strong disruptor of endothelial monolayer integrity, while the

cytokine IL-6 had no effect. However, when TNFα and IL-6 were administered together, the destructive effect on the monolayer was even worse than that of TNFα alone. The broad spectrum SFK inhibitor PP2 provided partial protection against the loss of monolayer integrity, but 10,12-conjugated linoleic acid (CLA), which is known to inhibit Src, did not. While there could be many explanations for these results, the possibility was raised that other SFKs that CLA may not inhibit, such as Fyn and Yes, could be involved in regulating vascular permeability. Indeed, IL-6 is known to activate Fyn but not Src (Hallek et al. 1997). Perhaps TNFα is necessary in some way to facilitate IL-6 recruitment of Fyn or Yes. These results also hint at a possible role for VEGFR-1 in the regulation of vascular permeability. Immunoprecipitation experiments and Src-kinase assays in HUVEC performed by Chou et al. (2002) demonstrated that Src preferentially associated with VEGFR-2, whereas Fyn and Yes associated preferentially with VEGFR-1. Further evidence of a VEGFR-1/Fyn and Yes connection was discovered by Waltenberger *et al.* (1994). VEGF-A_{165} stimulation of transfected VEGFR2-expressing porcine aortic endothelial cells (PAEC), which lack endogenous VEGF receptors, reduced phosphorylations of Fyn and Yes below the basal levels, but VEGF-A_{165} stimulation of VEGFR1-expressing PAEC resulted in 2.4-fold and 2.1-fold increases of Fyn and Yes phosphorylations, respectively. Fyn is also known to be involved in the regulation of adhesion proteins. Fyn was shown to associate with VE-cadherin in endothelial cells and was necessary for the peptide Bβ15-42 to protect the endothelial barrier function in mice. In Fyn(-/-) mice, Bβ15-42 could not prevent edema caused by the gram-negative toxin LPS (Groger *et al.* 2009). Phosphorylation of platelet EC adhesion molecule 1 (PECAM-1), which occurs when endothelial cell monolayers are stretched, has been shown to be Fyn-dependent in endothelial cells (Chiu *et al.* 2008).

Of course, the difficulty in studying Fyn is that Fyn-specific pharmacological inhibition is not possible. All known Fyn-inhibiting drugs inhibit multiple SFKs due to the strong homology they share. The most successful approach for inhibition of Src, Fyn and Yes in endothelial cell culture

in the published literature appears to be siRNA knockdown. For example, Werdich and Penn (2005) utilized RNA interference to knock down Src, Fyn or Yes in human retinal microvascular endothelial cells. Selective knockdown of each kinase revealed that all three kinases were required for VEGF-induced mitogenesis. Knockdown of Fyn significantly increased VEGF-stimulated cell migration, while knockdown of Yes significantly decreased it. In pulmonary artery endothelial cells, individual siRNA targeting of Src, Fyn, or Yes was utilized to determine the effect of each of these SFKs on the endothelial barrier function. Only siRNA knockdown of Fyn protected against TNF-α-induced pulmonary vascular permeability. Knockdown of Src or Yes had no effect. These data suggest that TNF-α promotes pulmonary vascular endothelial permeability in a Fyn-dependent manner (Angelini et al. 2006). When we begin teasing out the differences in P-UAEC between the SFKs in the regulation of Cx43 closure in the short term vs. monolayer integrity in the longer term, it is likely that siRNA interference will be necessary to identify the distinct functions of Src, Fyn and Yes.

7.6 Which Came First…? Thoughts on the Etiology of Preeclampsia

As our understanding of the etiology of PE now stands, we are confronted with a variation of the classic “chicken or egg?” problem. Do endothelial cells of preeclamptic women *fail to initiate* the adaptive programming required for enhanced vasodilation in a healthy pregnancy, thus leading to inflammation and elevated expression of growth factors and cytokines (and other yet-to-be-identified factors)? Or are these factors circulating at high levels in the blood of preeclamptic women, *suppressing* otherwise successful adaptation and thus impairing endothelial function? As of this writing, we don’t know which model is true, or if this is even a correct way to frame the question. On the one hand, we have data that support the ‘failure-to-adapt’ hypothesis, such as the increased monolayer permeability that EC from PE subjects continue to exhibit even when

cultured in healthy serum (Wang *et al.* 2002). On the other hand, we have data that support the 'suppression-of-adaptation' hypothesis. In one set of experiments, myometrial resistance vessels obtained from uterine biopsies of healthy pregnant women and incubated with plasma from nulliparous preeclamptic women showed significantly reduced endothelium-dependent vessel relaxation (Hayman *et al.* 2000). In another, treatment with 20% preeclamptic serum increased monolayer permeability (decreased monolayer integrity) in confluent endothelial cells (EC), an effect the authors tentatively attributed to elevated lipid peroxides and cytokine IL-8 in the serum (Zhang *et al.* 2003).

Derek Boeldt, formerly a student in the Bird Laboratory and now an assistant professor in the Obstetrics and Gynecology Department, speculates that the same growth factors and cytokines that are responsible for adaptive programming in early pregnancy actively drive the symptoms of PE in mid-late gestation. "Properly elevated growth factors and cytokines early in pregnancy allow for them to drop into the normal range as gestation progresses appropriately. However, if growth factors and cytokines are low early in pregnancy, adaptive programming fails and drives improper elevation of growth factors and cytokines in mid-late gestation in response to hypoxia, shear stress, etc. This would be an appropriate response in other parts of the body/physiological conditions, but the competing needs of the fetus/placenta render the response inappropriate." (DS Boeldt, personal communication, August 8, 2017)

My own (very) tentative view, perhaps due to my prior work in cancer research, is that PE may be like cancer, in that the disease could be the result of several altered cell signaling events that don't necessarily need to occur in the same order in every case of PE. What we observe in PE appears to be a classic positive feedforward loop, in which elevation of blood pressure leads to an inflammation response…which leads to elevated growth factors and cytokines…which leads to activation of signaling pathways that close/disassemble gap junctions…which inhibits the CCE required for sustained vasodilation…which results in hypertension...and so on…in a dysregulated,

out-of-control loop that produces increasingly severe symptoms as the pregnancy progresses. Regardless of anyone's view about the etiology of PE, it must be admitted that decades of research have produced multiple schools of thought rather than consensus, and no one has thus far identified the irrefutable initiating event of the disease. Perhaps any number of cell signaling events that induce the closing of gap junctions or elevate inflammatory cytokines can initiate a PE pregnancy.

Recently, researchers from the Universities of Toronto and Ottawa published a landmark paper that revealed why decades of study of PE have failed to produce consistent biomarkers or reliable treatments. By analyzing a large human placental microarray data set of 330 samples, they were able to determine that PE was very likely to have multiple causes. At least three "clusters" of PE with unique etiologies were identified (Leavey *et al.* 2016). The first cluster, which the authors called "maternal" PE, is characterized by late onset (>34 weeks), milder symptoms, and term or near-term deliveries. The placentas appear normal at the molecular and anatomical levels, but maternal endothelium may be damaged form a prior pregnancy. PE in cluster 1 likely arises due to pre-existing risk of cardiovascular disease. The second cluster, called "canonical" PE, is larger and more heterogenous than the first. This type is more severe with an earlier onset (<34 weeks) of symptoms that include elevated levels of the biomarkers *FLT1* and *ENG*, reduced placental size, elevated liver enzymes, and pre-term birth. "Canonical" PE is of placental origin. It is associated with histological abnormalities of the placenta, intrauterine growth restriction (IUGR), and other pathologies of pregnancy. The third cluster is characterized by elevated expression of immune response genes and maternal rejection of the feto-placental unit. This form, called "immunologic" PE, is also associated with severe IUGR and poor fetal outcomes, although the hypertension and proteinuria are not as severe as in canonical PE.

In summary, the identification of several categories of PE, each with a unique set of potential causes, validated the seemingly contradictory findings of researchers who had been following

distinct lines of inquiry and confirmed that a single all-encompassing explanation for the etiology of PE was an illusory goal. One advantage of our approach is that the activation of the kinase pathways regulating Cx43 closure and loss of endothelial function, and indeed the loss of monolayer integrity long term as described by Amanda Ampey (PhD Dissertation, 2017), can be achieved by the Maternal PE and Canonical PE origin models as both hypoxia and inflammation signaling exhibit crosstalk at this level.

7.7 Final Thoughts

Much of the research done on cell signaling uses immortalized cell lines and doses of agonists that far exceed any stimulus that a primary cell would ever encounter, which calls into question the physiologic relevance of such experiments. While research from the Bird Laboratory makes liberal use of the tools of molecular biology, we intentionally limit our experimental designs to employ only primary cells and isolated tissues and to administer dosages of physiologic ligands that stay within the bounds of biological reality. We stick tightly to this principle, making exceptions only in particular cases in which we wish to establish proof of principle (e.g. administration of the nonphysiologic agonist TPA or the use of 100 nM insulin in my studies of PI3K).

As is the case for all cultured cells, the conditions of growth are somewhat artificial by necessity. The smooth muscle on which endothelial cells normally grow is absent, for example. However, endothelial cells have one advantage in cell culture that most other cell types do not—namely, that they naturally proliferate *in vivo* in a two-dimensional monolayer just as they do *in vitro* in a plastic petri dish. Additionally, we have confirmed the validity of the P-UAEC cell model by duplicating our experiments in intact vessels whenever possible and obtaining similar results (Yi et al. 2010).

The aberrant EGFR signaling we introduced into our P-UAEC model admittedly may or may not have direct physiologic relevance, but it was a useful and highly controllable tool that provided a new interpretation of prior physiologically relevant data on the damaging effects of elevated VEGF in PE. It also provided new insights into the unique role of PI3K signaling in the maintenance of functional junctional protein structures. The observations that EGFR induced this or that effect in P-UAEC were of little importance in and of themselves. The value of our EGFR experiments lay in what they revealed about real cellular processes necessary for successful vascular adaptation to pregnancy.

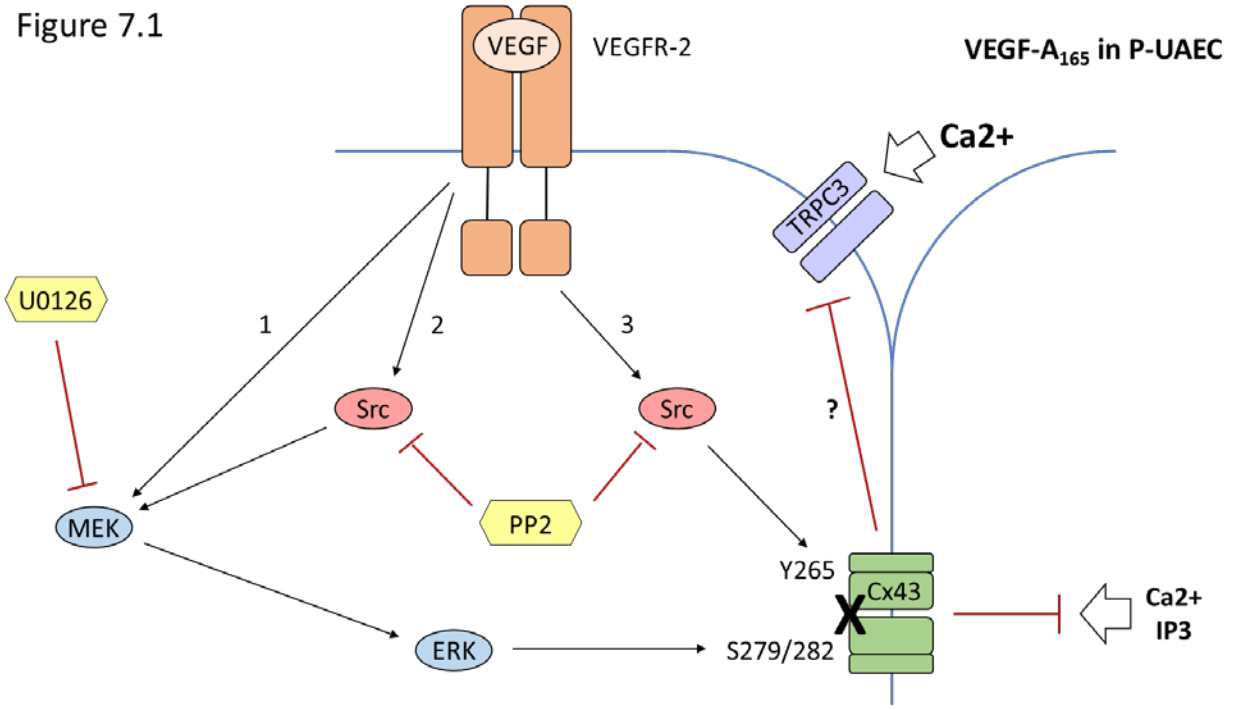

Figure 7.1 The Boeldt Model of VEGF-A_{165}-Induced Downregulation of ATP-Stimulated Ca2+ Bursting in P-UAEC In this model, based on evidence from calcium imaging and Western blotting (Boeldt *et al.* 2015), VEGF-A_{165} administration (10 ng/mL) triggers the formation of activated VEGFR-2 homodimers that initiate three relevant signaling cascades. The first is the direct activation of the MAPK pathway that leads to the phosphorylation of ERK1/2, which in turn mediates the inhibitory phosphorylations of Cx43 proteins at S279/282. The second is activation of the MAPK pathway via Src, possibly by direct interaction of Src with Raf-1 (Chao *et al.* 1997), and subsequent ERK-mediated phosphorylation of Cx43 S279/282. The third is direct Src-mediated phosphorylation of Cx43 Y265. Interestingly, pharmacological inhibition of Src (PP2, 10 µM) or MEK (U0126, 10 µM) protects the Ca2+ burst response from VEGF-induced downregulation. Since *either* inhibitor completely blocks the negative effects of VEGF, it follows logically from this model that either the concomitant activation of pathways #1 and #3 is necessary for VEGF to downregulate [Ca2+]i bursting or pathway 2 alone is sufficient. If the inhibitory effect of VEGF could be propagated by pathway 1 or 3 alone, then pretreatment with both PP2 and U0126 would be required to protect [Ca2+]i bursting.

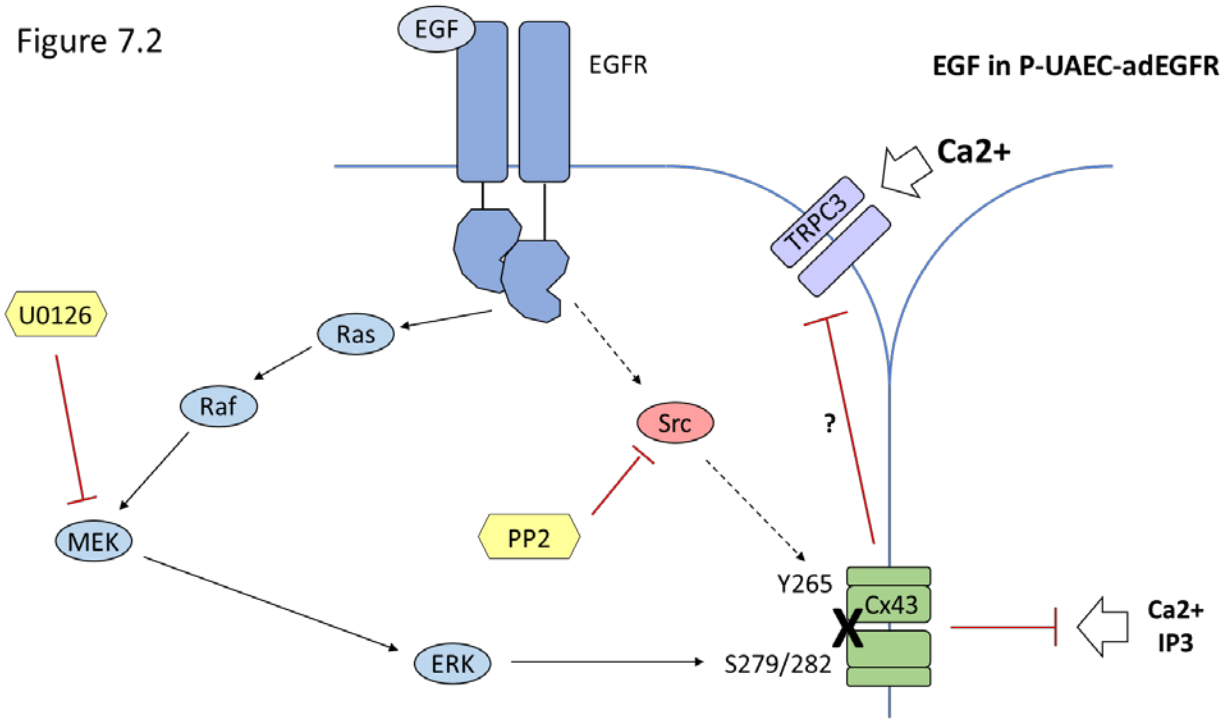

Figure 7.2 EGF-Induced Downregulation of ATP-Stimulated Ca2+ Bursting in P-UAEC-adEGFR Administration of EGF in P-UAEC-adEGFR induces phosphorylations of Y265 and S279/282 on Cx43 and downregulates the Ca2+ bursting response to ATP stimulation, just like VEGF in parental P-UAEC. However, a significance difference in the respective actions of VEGF and EGF was revealed by pharmacological inhibitors of Src and MEK. Whereas VEGF-induced downregulation of [Ca2+]i bursting in parental P-UAEC was prevented by pretreatment with PP2 *or* U0126, EGF-induced downregulation of [Ca2+]i bursting in P-UAEC-adEGFR was only prevented by pretreatment with U0126, suggesting a Src-independent mechanism for EGF-mediated suppression of [Ca2+]i bursting. Although administration of EGF did induce phosphorylation of Cx43 Y265, this phosphorylation is apparently not necessary for facilitating the acute inhibition of GJC via the closure of Cx43 gap junctions. This result invites a new interpretation of the calcium imaging data presented in Boeldt *et al.* (2015).

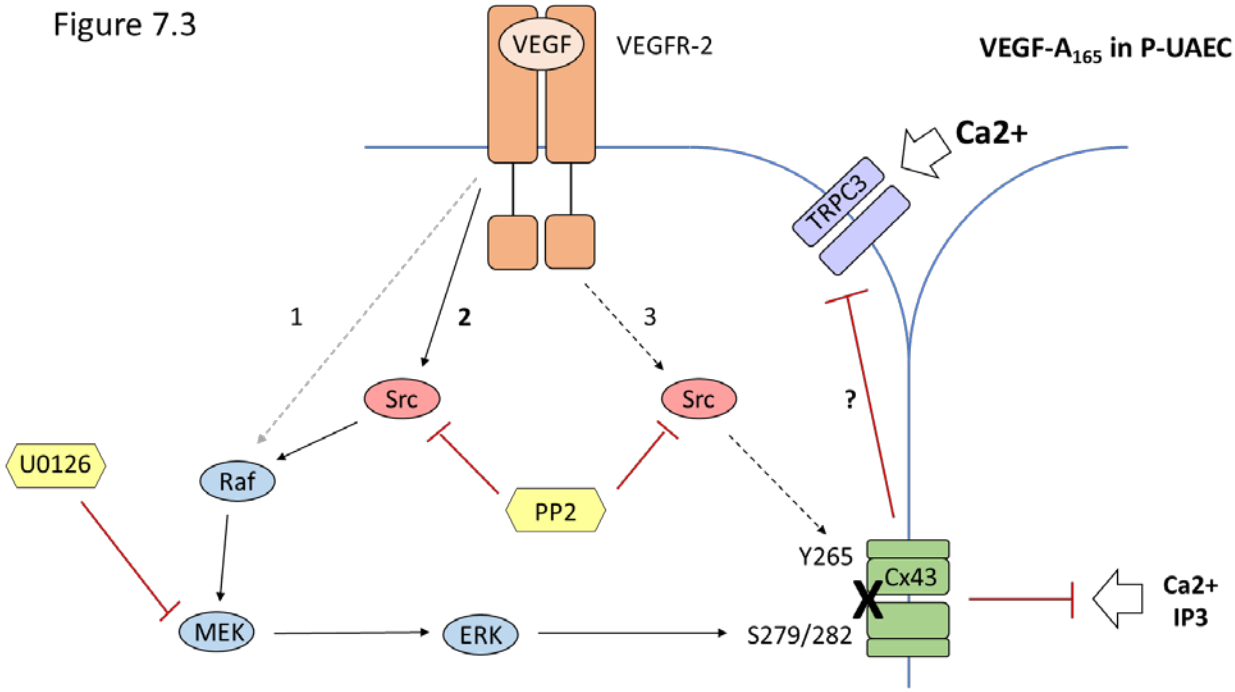

Figure 7.3 The Clemente Model of VEGF-A165-Induced Downregulation of ATP-Stimulated Ca2+ Bursting in P-UAEC The evidence provided by EGF treatment of P-UAEC-adEGFR suggests that the ERK-mediated phosphorylation of Cx43 S279/282 is required for downregulation of the ATP-induced Ca2+ burst response, but the Src-mediated phosphorylation of Cx43 Y265 is not. If MAPK pathway activation is sufficient to propagate the inhibitory effect of VEGF on GJC, then the only interpretation of the effects of kinase inhibitors documented by Boeldt *et al.* that follows logically is that pathway #2 is dominant, pathway #1 is negligible, and pathway #3 is not important for acute gap junction closure. In this interpretation, PP2 inhibition of Src protects [Ca2+]i bursting because it prevents activation of ERK1/2. This is not to say that phosphorylation of Cx43 Y265 is unimportant, but merely that it is unnecessary for acute downregulation of GJC. As many studies examining the effects of v-Src and activated c-Src (cited in Chapter 3) have confirmed, Src-mediated phosphorylation of Cx43 Y265 does inhibit GJC, but most likely by promoting Cx43 internalization and degradation, not channel gate closure (Reviewed in Solan and Lampe 2014; 2016). The downregulation of [Ca2+]i bursting that we observe within 30 minutes of growth factor treatment appears to be a result of MAPK signaling.

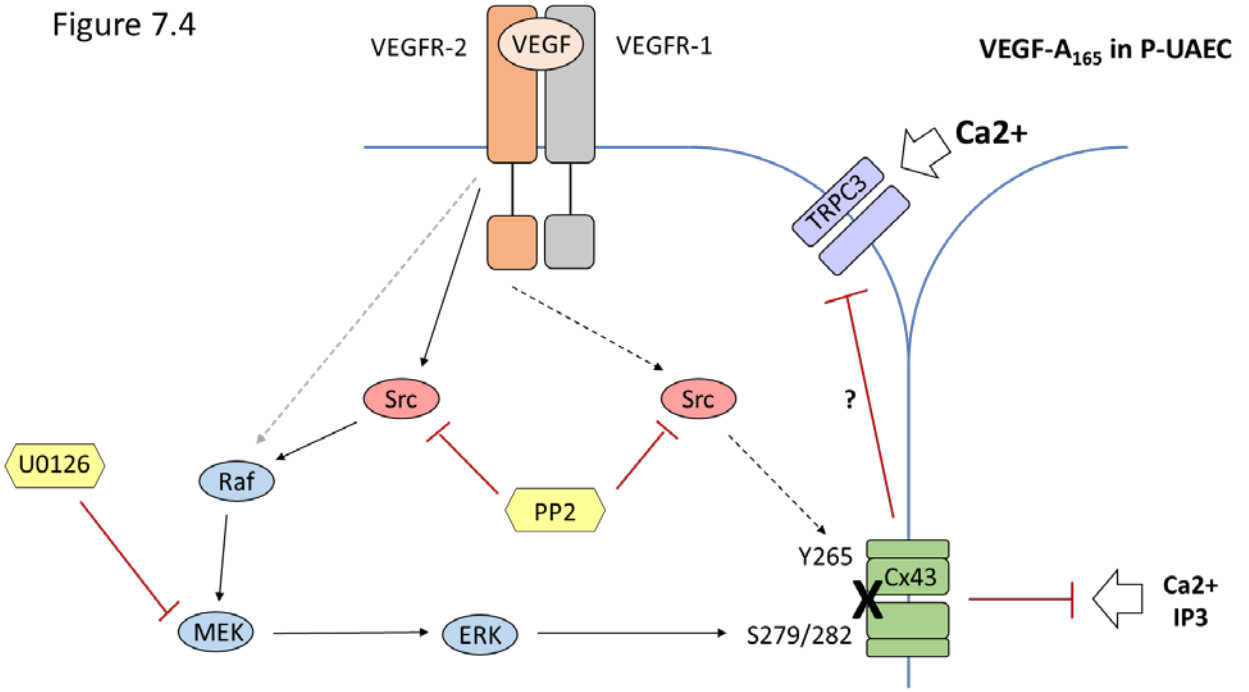

Figure 7.4 VEGFR heterodimers may mediate VEGF-A_{165} inhibition of Ca2+ Bursting in P-UAEC One of the assertions of Boeldt et al. (2015) was that only VEGFR-2 mediated the inhibition of ATP-stimulated [Ca2+]i bursting, citing evidence that only VEGF-A_{165} and VEGF-E, which both bind to VEGFR-2, downregulated the burst response, but the VEGFR-1-specific agonist PlGF had no effect, and VEGF-E in combination with PlGF had no further effect over that of VEGF-E alone. However, there was a curious detail about the actions of VEGF-E for which no explanation was provided. While VEGF-E was indeed able to induce the same magnitude of ERK1/2 phosphorylation (Grummer et al. 2009) and downregulation of [Ca2+]i bursting (Boeldt et al. 2015) as VEGF-A_{165}, it could only do so at ~11 times the dose (2.9 nM VEGF-E (100 ng/mL) vs. 0.26 nM VEGF-A_{165} (10 ng/mL)). This result is difficult to interpret since the binding affinities of VEGF-A_{165} and VEGF-E for VEGFR-2 have been reported to be nearly identical (Ogawa *et al.* 1998). One possibility is that, despite the similar binding affinity for VEGFR-2, the tertiary structure of VEGF-E is significantly distinct from that of VEGF-A_{165} such that the VEGFR-2 homodimers formed by VEGF-E binding adopt a less active conformation than those formed by VEGF-A_{165} binding. Even subtle differences in VEGFR-2 homodimer conformation could result in a lower efficiency of the kinase domain or reduced accessibility of docking sites for effector molecules due to steric considerations or the position of charges on the receptor. Alternatively, the 11-fold greater activity induced by VEGF-A_{165} could be because VEGF-A_{165} binds to both VEGFR-1 and VEGFR-2. While the evidence presented in Boeldt *et al.* does indeed suggest that VEGFR-2 homodimers mediate VEGF downregulation of ATP-stimulated [Ca2+]i bursting and VEGFR-1 homodimers do not, we cannot rule out the possibility that VEGFR-1/VEGFR-2 heterodimers also mediate this process, thereby conferring greater signaling power to VEGF-A_{165} over VEGF-E.

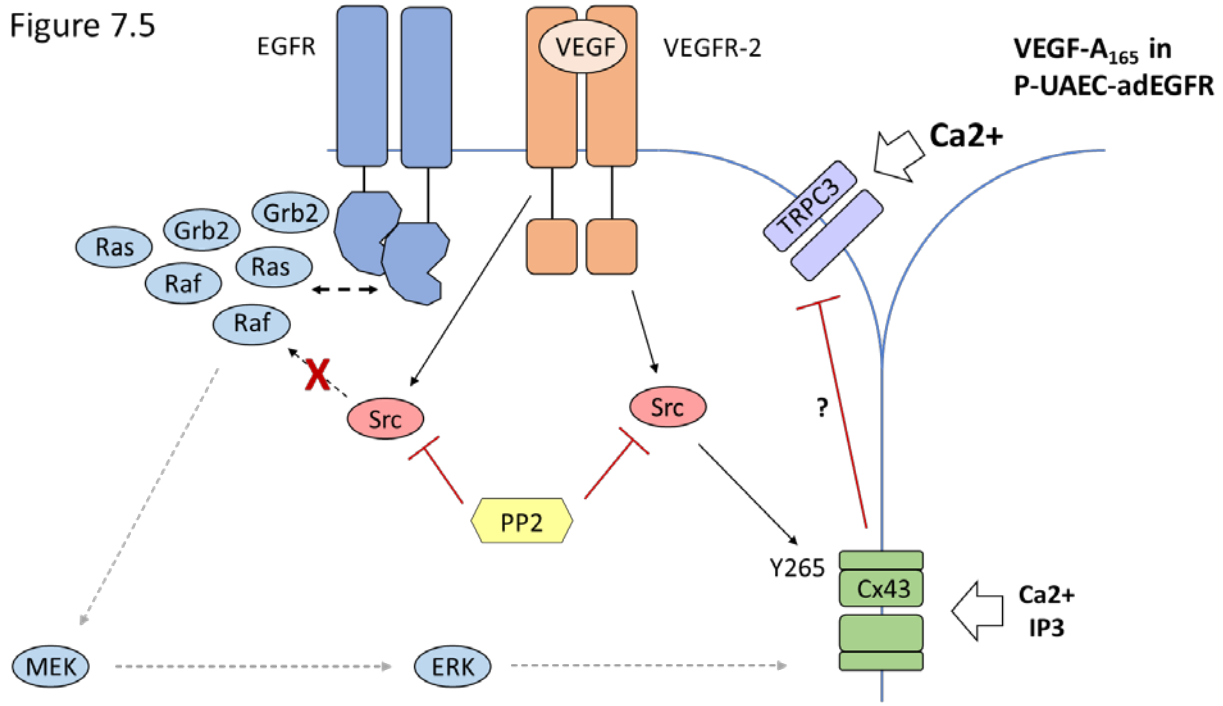

Figure 7.5 A Possible Explanation for the Failure of VEGF-A_{165} to Inhibit Ca2+ Bursting in P-UAEC-adEGFR At an adenoviral MOI of 1000, EGFR is expressed at a level sufficient to confer constitutive autophosphorylation to the receptor. While this continuous ligand-independent activity failed to induce significant elevations of basal ERK1/2 or inhibitory phosphorylations of Cx43, it did have a profound effect on the local environment at the plasma membrane, as evidenced by the fact that VEGF, despite inducing a significant elevation in Cx43 Y265 phosphorylation (Figure 5.4A), was not able to inhibit ATP-stimulated Ca2+ bursting in P-UAEC-adEGFR as it did in parental P-UAEC (Figure 5.3). The overexpression of EGFR in P-UAEC must result in the receptor being localized in membrane regions where it is normally absent and will thus possess access to effector molecules that it might otherwise be denied. The constitutive autophosphorylation of the receptor means that the C-terminal tail of EGFR is an ever-present source of active phosphotyrosine docking sites, thereby acting as a sink for effector molecules such as SOS, Grb2, the Ras-GTPase, Raf-1, Shc, Cbl and PLCγ. Even though there appears to be a negative feedback loop that resists the continuous activation of MEK and ERK, upstream effector molecules for the MAPK pathway, for example, are still likely to be “locked” in interaction with the C-terminus of EGFR for much of their time at the membrane, which will inevitably reduce the availability of these molecules for other receptors if they are rate limiting in quantity. Because it is quite likely that EGFR has a higher affinity for these effectors than VEGFR-2, the net effect is that VEGFR-2 can no longer effectively activate the MAPK pathway in P-UAEC-adEGFR (Figure 4.10B) and therefore cannot induce gap junctional closure.

Chapter 8

Bibliography

Abid MR, Guo S, Minami T, Spokes KC, Ueki K, Skurk C, Walsh K & Aird WC 2004 Vascular endothelial growth factor activates PI3K/Akt/forkhead signaling in endothelial cells. *Arterioscler Thromb Vasc Biol* **24** 294-300.

Agatisa PK, Ness RB, Roberts JM, Costantino JP, Kuller LH & McLaughlin MK 2004 Impairment of endothelial function in women with a history of preeclampsia: an indicator of cardiovascular risk. *Am J Physiol Heart Circ Physiol* **286** H1389-1393.

Aggarwal PK, Chandel N, Jain V & Jha V 2012 The relationship between circulating endothelin-1, soluble fms-like tyrosine kinase-1 and soluble endoglin in preeclampsia. *J Hum Hypertens* **26** 236-241.

Alavi A, Hood JD, Frausto R, Stupack DG & Cheresh DA 2003 Role of Raf in vascular protection from distinct apoptotic stimuli. *Science* **301** 94-96.

Andersen MR, Walker LR & Stender S 2004 Reduced endothelial nitric oxide synthase activity and concentration in fetal umbilical veins from maternal cigarette smokers. *Am J Obstet Gynecol* **191** 346-351.

Andjelković M, Jakubowicz T, Cron P, Ming XF, Han JW & Hemmings BA 1996 Activation and phosphorylation of a pleckstrin homology domain containing protein kinase (RAC-PK/PKB) promoted by serum and protein phosphatase inhibitors. *Proc Natl Acad Sci U S A* **93** 5699-5704.

Angelini DJ, Hyun SW, Grigoryev DN, Garg P, Gong P, Singh IS, Passaniti A, Hasday JD & Goldblum SE 2006 TNF-alpha increases tyrosine phosphorylation of vascular endothelial cadherin and opens the paracellular pathway through fyn activation in human lung endothelia. *Am J Physiol Lung Cell Mol Physiol* **291** L1232-1245.

Atkinson MM, Menko AS, Johnson RG, Sheppard JR & Sheridan JD 1981 Rapid and reversible reduction of junctional permeability in cells infected with a temperature-sensitive mutant of avian sarcoma virus. *J Cell Biol* **91** 573-578.

Azarnia R, Reddy S, Kmiecik TE, Shalloway D & Loewenstein WR 1988 The cellular src gene product regulates junctional cell-to-cell communication. *Science* **239** 398-401.

Baik CS, Wu D, Smith C, Martins RG & Pritchard CC 2015 Durable Response to Tyrosine Kinase Inhibitor Therapy in a Lung Cancer Patient Harboring Epidermal Growth Factor Receptor Tandem Kinase Domain Duplication. *J Thorac Oncol* **10** e97-99.

Banerjee S, Smallwood A, Moorhead J, Chambers AE, Papageorghiou A, Campbell S & Nicolaides K 2005 Placental expression of interferon-gamma (IFN-gamma) and its receptor IFN-gamma R2 fail to switch from early hypoxic to late normotensive development in preeclampsia. *J Clin Endocrinol Metab* **90** 944-952.

Bazzoni G & Dejana E 2004 Endothelial cell-to-cell junctions: molecular organization and role in vascular homeostasis. *Physiol Rev* **84** 869-901.

Beck L & D'Amore PA 1997 Vascular development: cellular and molecular regulation. *FASEB J* **11** 365-373.

Becker DL, Thrasivoulou C & Phillips AR 2012 Connexins in wound healing; perspectives in diabetic patients. *Biochim Biophys Acta* **1818** 2068-2075.

Bekhite MM, Finkensieper A, Binas S, Müller J, Wetzker R, Figulla HR, Sauer H & Wartenberg M 2011 VEGF-mediated PI3K class IA and PKC signaling in cardiomyogenesis and vasculogenesis of mouse embryonic stem cells. *J Cell Sci* **124** 1819-1830.

Benyo DF, Miles TM & Conrad KP 1997 Hypoxia stimulates cytokine production by villous explants from the human placenta. *J Clin Endocrinol Metab* **82** 1582-1588.

Bhagat K & Vallance P 1997 Inflammatory cytokines impair endothelium-dependent dilatation in human veins in vivo. *Circulation* **96** 3042-3047.

Bird IM, Boeldt DS, Krupp J, Grummer MA, Yi FX & Magness RR 2013 Pregnancy, programming and preeclampsia: gap junctions at the nexus of pregnancy-induced adaptation of endothelial function and endothelial adaptive failure in PE. *Curr Vasc Pharmacol* **11** 712-729.

Bird IM, Sullivan JA, Di T, Cale JM, Zhang L, Zheng J & Magness RR 2000 Pregnancy-dependent changes in cell signaling underlie changes in differential control of vasodilator production in uterine artery endothelial cells. *Endocrinology* **141** 1107-1117.

Bird IM, Zhang L & Magness RR 2003 Possible mechanisms underlying pregnancy-induced changes in uterine artery endothelial function. *Am J Physiol Regul Integr Comp Physiol* **284** R245-258.

Boeldt DS, Grummer MA, Yi F, Magness RR & Bird IM 2015 Phosphorylation of Ser-279/282 and Tyr-265 positions on Cx43 as possible mediators of VEGF-165 inhibition of pregnancy-adapted Ca2+ burst function in ovine uterine artery endothelial cells. *Mol Cell Endocrinol* **412** 73-84.

Boeldt DS, Krupp J, Yi FX, Khurshid N, Shah DM & Bird IM 2017 Positive versus negative effects of VEGF165 on Ca2+ signaling and NO production in human endothelial cells. *Am J Physiol Heart Circ Physiol* **312** H173-H181.

Brockelsby J, Hayman R, Ahmed A, Warren A, Johnson I & Baker P 1999 VEGF via VEGF receptor-1 (Flt-1) mimics preeclamptic plasma in inhibiting uterine blood vessel relaxation in pregnancy: implications in the pathogenesis of preeclampsia. *Lab Invest* **79** 1101-1111.

Brognard J, Sierecki E, Gao T & Newton AC 2007 PHLPP and a second isoform, PHLPP2, differentially attenuate the amplitude of Akt signaling by regulating distinct Akt isoforms. *Mol Cell* **25** 917-931.

Brooke MA, O'Toole EA & Kelsell DP 2014 Exoming into rare skin disease: EGFR deficiency. *J Invest Dermatol* **134** 2486-2488.

Buckley BJ, Mirza Z & Whorton AR 1995 Regulation of Ca(2+)-dependent nitric oxide synthase in bovine aortic endothelial cells. *Am J Physiol* **269** C757-765.

Bumeister R, Rosse C, Anselmo A, Camonis J & White MA 2004 CNK2 couples NGF signal propagation to multiple regulatory cascades driving cell differentiation. *Curr Biol* **14** 439-445.

Bussen S, Sütterlin M & Steck T 1999 Plasma endothelin and big endothelin levels in women with severe preeclampsia or HELLP-syndrome. *Arch Gynecol Obstet* **262** 113-119.

Cain RJ, Vanhaesebroeck B & Ridley AJ 2010 The PI3K p110alpha isoform regulates endothelial adherens junctions via Pyk2 and Rac1. *J Cell Biol* **188** 863-876.

Cale JM & Bird IM 2006 Dissociation of endothelial nitric oxide synthase phosphorylation and activity in uterine artery endothelial cells. *Am J Physiol Heart Circ Physiol* **290** H1433-1445.

Calleja V, Alcor D, Laguerre M, Park J, Vojnovic B, Hemmings BA, Downward J, Parker PJ & Larijani B 2007 Intramolecular and intermolecular interactions of protein kinase B define its activation in vivo. *PLoS Biol* **5** e95.

Casanello P & Sobrevia L 2002 Intrauterine growth retardation is associated with reduced activity and expression of the cationic amino acid transport systems y+/hCAT-1 and y+/hCAT-2B and lower activity of nitric oxide synthase in human umbilical vein endothelial cells. *Circ Res* **91** 127-134.

Casart YC, Tarrazzi K & Camejo MI 2007 Serum levels of interleukin-6, interleukin-1beta and human chorionic gonadotropin in pre-eclamptic and normal pregnancy. *Gynecol Endocrinol* **23** 300-303.

Castellano E & Downward J 2011 RAS Interaction with PI3K: More Than Just Another Effector Pathway. *Genes Cancer* **2** 261-274.

Chambers JC, Fusi L, Malik IS, Haskard DO, De Swiet M & Kooner JS 2001 Association of maternal endothelial dysfunction with preeclampsia. *JAMA* **285** 1607-1612.

Chan CH, Li CF, Yang WL, Gao Y, Lee SW, Feng Z, Huang HY, Tsai KK, Flores LG, Shao Y, et al. 2012 The Skp2-SCF E3 ligase regulates Akt ubiquitination, glycolysis, herceptin sensitivity, and tumorigenesis. *Cell* **149** 1098-1111.

Chao TS, Abe M, Hershenson MB, Gomes I & Rosner MR 1997 Src tyrosine kinase mediates stimulation of Raf-1 and mitogen-activated protein kinase by the tumor promoter thapsigargin. *Cancer Res* **57** 3168-3173.

Chavarría ME, Lara-González L, González-Gleason A, García-Paleta Y, Vital-Reyes VS & Reyes A 2003 Prostacyclin/thromboxane early changes in pregnancies that are complicated by preeclampsia. *Am J Obstet Gynecol* **188** 986-992.

Chesley LC 1966 Vascular reactivity in normal and toxemic pregnancy. *Clin Obstet Gynecol* **9** 871-881.

Chiu YJ, McBeath E & Fujiwara K 2008 Mechanotransduction in an extracted cell model: Fyn drives stretch- and flow-elicited PECAM-1 phosphorylation. *J Cell Biol* **182** 753-763.

Choi SH, Mendrola JM & Lemmon MA 2007 EGF-independent activation of cell-surface EGF receptors harboring mutations found in gefitinib-sensitive lung cancer. *Oncogene* **26** 1567-1576.

Chou MT, Wang J & Fujita DJ 2002 Src kinase becomes preferentially associated with the VEGFR, KDR/Flk-1, following VEGF stimulation of vascular endothelial cells. *BMC Biochem* **3** 32.

Ciesielski MJ & Fenstermaker RA 2000 Oncogenic epidermal growth factor receptor mutants with tandem duplication: gene structure and effects on receptor function. *Oncogene* **19** 810-820.

Cong LN, Chen H, Li Y, Zhou L, McGibbon MA, Taylor SI & Quon MJ 1997 Physiological role of Akt in insulin-stimulated translocation of GLUT4 in transfected rat adipose cells. *Mol Endocrinol* **11** 1881-1890.

Conrad KP, Kerchner LJ & Mosher MD 1999 Plasma and 24-h NO(x) and cGMP during normal pregnancy and preeclampsia in women on a reduced NO(x) diet. *Am J Physiol* **277** F48-57.

Conrad KP, Miles TM & Benyo DF 1998 Circulating levels of immunoreactive cytokines in women with preeclampsia. *Am J Reprod Immunol* **40** 102-111.

Cooper CD & Lampe PD 2002 Casein kinase 1 regulates connexin-43 gap junction assembly. *J Biol Chem* **277** 44962-44968.

Cottrell GT, Lin R, Warn-Cramer BJ, Lau AF & Burt JM 2003 Mechanism of v-Src- and mitogen-activated protein kinase-induced reduction of gap junction communication. *Am J Physiol Cell Physiol* **284** C511-520.

Crow DS, Beyer EC, Paul DL, Kobe SS & Lau AF 1990 Phosphorylation of connexin43 gap junction protein in uninfected and Rous sarcoma virus-transformed mammalian fibroblasts. *Mol Cell Biol* **10** 1754-1763.

Cudmore MJ, Hewett PW, Ahmad S, Wang KQ, Cai M, Al-Ani B, Fujisawa T, Ma B, Sissaoui S, Ramma W, et al. 2012 The role of heterodimerization between VEGFR-1 and VEGFR-2 in the regulation of endothelial cell homeostasis. *Nat Commun* **3** 972.

Daub H, Weiss FU, Wallasch C & Ullrich A 1996 Role of transactivation of the EGF receptor in signalling by G-protein-coupled receptors. *Nature* **379** 557-560.

Dejana E, Corada M & Lampugnani MG 1995 Endothelial cell-to-cell junctions. *FASEB J* **9** 910-918.

Dennis AT, Castro J, Carr C, Simmons S, Permezel M & Royse C 2012 Haemodynamics in women with untreated pre-eclampsia. *Anaesthesia* **67** 1105-1118.

Dimmeler S, Fleming I, Fisslthaler B, Hermann C, Busse R & Zeiher AM 1999 Activation of nitric oxide synthase in endothelial cells by Akt-dependent phosphorylation. *Nature* **399** 601-605.

Duley L 2009 The global impact of pre-eclampsia and eclampsia. *Semin Perinatol* **33** 130-137.

Dunn CA & Lampe PD 2014 Injury-triggered Akt phosphorylation of Cx43: a ZO-1-driven molecular switch that regulates gap junction size. *J Cell Sci* **127** 455-464.

Dunn CA, Su V, Lau AF & Lampe PD 2012 Activation of Akt, not connexin 43 protein ubiquitination, regulates gap junction stability. *J Biol Chem* **287** 2600-2607.

El-Salahy EM, Ahmed MI, El-Gharieb A & Tawfik H 2001 New scope in angiogenesis: role of vascular endothelial growth factor (VEGF), NO, lipid peroxidation, and vitamin E in the pathophysiology of pre-eclampsia among Egyptian females. *Clin Biochem* **34** 323-329.

English FA, McCarthy FP, McSweeney CL, Quon AL, Morton JS, Sawamura T, Davidge ST & Kenny LC 2013 Inhibition of lectin-like oxidized low-density lipoprotein-1 receptor protects against plasma-mediated vascular dysfunction associated with pre-eclampsia. *Am J Hypertens* **26** 279-286.

Feng Y, Bhatt AJ, Fratkin JD & Rhodes PG 2008 Neuroprotective effects of sodium orthovanadate after hypoxic-ischemic brain injury in neonatal rats. *Brain Res Bull* **76** 102-108.

Fenstermaker RA, Ciesielski MJ & Castiglia GJ 1998 Tandem duplication of the epidermal growth factor receptor tyrosine kinase and calcium internalization domains in A-172 glioma cells. *Oncogene* **16** 3435-3443.

Filson AJ, Azarnia R, Beyer EC, Loewenstein WR & Brugge JS 1990 Tyrosine phosphorylation of a gap junction protein correlates with inhibition of cell-to-cell communication. *Cell Growth Differ* **1** 661-668.

Fitzgerald DJ, Entman SS, Mulloy K & FitzGerald GA 1987 Decreased prostacyclin biosynthesis preceding the clinical manifestation of pregnancy-induced hypertension. *Circulation* **75** 956-963.

Fleming I, Fisslthaler B, Dimmeler S, Kemp BE & Busse R 2001 Phosphorylation of Thr(495) regulates Ca(2+)/calmodulin-dependent endothelial nitric oxide synthase activity. *Circ Res* **88** E68-75.

Florian J & Watts S 1999 Epidermal growth factor: a potent vasoconstrictor in experimental hypertension. *American Journal of Physiology-Heart and Circulatory Physiology* **276** H976-H983.

Fong JT, Nimlamool W & Falk MM 2014 EGF induces efficient Cx43 gap junction endocytosis in mouse embryonic stem cell colonies via phosphorylation of Ser262, Ser279/282, and Ser368. *FEBS Lett* **588** 836-844.

Freeman DJ, McManus F, Brown EA, Cherry L, Norrie J, Ramsay JE, Clark P, Walker ID, Sattar N & Greer IA 2004 Short- and long-term changes in plasma inflammatory markers associated with preeclampsia. *Hypertension* **44** 708-714.

Galan HL, Regnault TR, Le Cras TD, Tyson RW, Anthony RV, Wilkening RB & Abman SH 2001 Cotyledon and binucleate cell nitric oxide synthase expression in an ovine model of fetal growth restriction. *J Appl Physiol (1985)* **90** 2420-2426.

Gallant JN, Sheehan JH, Shaver TM, Bailey M, Lipson D, Chandramohan R, Red Brewer M, York SJ, Kris MG, Pietenpol JA, et al. 2015 EGFR Kinase Domain Duplication (EGFR-KDD) Is a Novel Oncogenic Driver in Lung Cancer That Is Clinically Responsive to Afatinib. *Cancer Discov* **5** 1155-1163.

Gerber HP, McMurtrey A, Kowalski J, Yan M, Keyt BA, Dixit V & Ferrara N 1998 Vascular endothelial growth factor regulates endothelial cell survival through the phosphatidylinositol 3'-kinase/Akt signal transduction pathway. Requirement for Flk-1/KDR activation. *J Biol Chem* **273** 30336-30343.

Gifford SM, Cale JM, Tsoi S, Magness RR & Bird IM 2003a Pregnancy-specific changes in uterine artery endothelial cell signaling in vivo are both programmed and retained in primary culture. *Endocrinology* **144** 3639-3650.

Gifford SM, Cale JM, Tsoi S, Magness RR & Bird IM 2003b Pregnancy-specific changes in uterine artery endothelial cell signaling in vivo are both programmed and retained in primary culture. *Endocrinology* **144** 3639-3650.

Gifford SM, Yi FX & Bird IM 2006a Pregnancy-enhanced Ca2+ responses to ATP in uterine artery endothelial cells is due to greater capacitative Ca2+ entry rather than altered receptor coupling. *J Endocrinol* **190** 373-384.

Gifford SM, Yi FX & Bird IM 2006b Pregnancy-enhanced store-operated Ca2+ channel function in uterine artery endothelial cells is associated with enhanced agonist-specific transient receptor potential channel 3-inositol 1,4,5-trisphosphate receptor 2 interaction. *J Endocrinol* **190** 385-395.

Goodwin BL, Pendleton LC, Levy MM, Solomonson LP & Eichler DC 2007 Tumor necrosis factor-alpha reduces argininosuccinate synthase expression and nitric oxide production in aortic endothelial cells. *Am J Physiol Heart Circ Physiol* **293** H1115-1121.

Grandal MV, Zandi R, Pedersen MW, Willumsen BM, van Deurs B & Poulsen HS 2007 EGFRvIII escapes down-regulation due to impaired internalization and sorting to lysosomes. *Carcinogenesis* **28** 1408-1417.

Grummer MA, Sullivan JA, Magness RR & Bird IM 2009 Vascular endothelial growth factor acts through novel, pregnancy-enhanced receptor signalling pathways to stimulate endothelial nitric oxide synthase activity in uterine artery endothelial cells. *Biochem J* **417** 501-511.

Gröger M, Pasteiner W, Ignatyev G, Matt U, Knapp S, Atrasheuskaya A, Bukin E, Friedl P, Zinkl D, Hofer-Warbinek R, et al. 2009 Peptide Bbeta(15-42) preserves endothelial barrier function in shock. *PLoS One* **4** e5391.

Gündüz D, Thom J, Hussain I, Lopez D, Härtel FV, Erdogan A, Grebe M, Sedding D, Piper HM, Tillmanns H, et al. 2010 Insulin stabilizes microvascular endothelial barrier function via phosphatidylinositol 3-kinase/Akt-mediated Rac1 activation. *Arterioscler Thromb Vasc Biol* **30** 1237-1245.

Hajjar KA, Hajjar DP, Silverstein RL & Nachman RL 1987 Tumor necrosis factor-mediated release of platelet-derived growth factor from cultured endothelial cells. *J Exp Med* **166** 235-245.

Hallek M, Neumann C, Schäffer M, Danhauser-Riedl S, von Bubnoff N, de Vos G, Druker BJ, Yasukawa K, Griffin JD & Emmerich B 1997 Signal transduction of interleukin-6 involves tyrosine phosphorylation of multiple cytosolic proteins and activation of Src-family kinases Fyn, Hck, and Lyn in multiple myeloma cell lines. *Exp Hematol* **25** 1367-1377.

Hayman R, Brockelsby J, Kenny L & Baker P 1999 Preeclampsia: the endothelium, circulating factor(s) and vascular endothelial growth factor. *J Soc Gynecol Investig* **6** 3-10.

Hayman R, Warren A, Brockelsby J, Johnson I & Baker P 2000 Plasma from women with pre-eclampsia induces an in vitro alteration in the endothelium-dependent behaviour of myometrial resistance arteries. *BJOG* **107** 108-115.

Hers I, Vincent EE & Tavaré JM 2011 Akt signalling in health and disease. *Cell Signal* **23** 1515-1527.

Hohlagschwandtner M, Knöfler M, Ploner M, Zeisler H, Joura EA & Husslein P 2002 Basic fibroblast growth factor and hypertensive disorders in pregnancy. *Hypertens Pregnancy* **21** 235-241.

Hresko RC & Mueckler M 2005 mTOR.RICTOR is the Ser473 kinase for Akt/protein kinase B in 3T3-L1 adipocytes. *J Biol Chem* **280** 40406-40416.

Huang YH, Yang HY, Hsu YF, Chiu PT, Ou G & Hsu MJ 2014 Src contributes to IL6-induced vascular endothelial growth factor-C expression in lymphatic endothelial cells. *Angiogenesis* **17** 407-418.

Hunter AW, Barker RJ, Zhu C & Gourdie RG 2005 Zonula occludens-1 alters connexin43 gap junction size and organization by influencing channel accretion. *Mol Biol Cell* **16** 5686-5698.

Imoukhuede PI & Popel AS 2011 Quantification and cell-to-cell variation of vascular endothelial growth factor receptors. *Exp Cell Res* **317** 955-965.

Jacinto E, Facchinetti V, Liu D, Soto N, Wei S, Jung SY, Huang Q, Qin J & Su B 2006 SIN1/MIP1 maintains rictor-mTOR complex integrity and regulates Akt phosphorylation and substrate specificity. *Cell* **127** 125-137.

Jeffrey PD, Russo AA, Polyak K, Gibbs E, Hurwitz J, Massagué J & Pavletich NP 1995 Mechanism of CDK activation revealed by the structure of a cyclinA-CDK2 complex. *Nature* **376** 313-320.

Jia H, Ma X, Tong W, Doyran B, Sun Z, Wang L, Zhang X, Zhou Y, Badar F, Chandra A, et al. 2016 EGFR signaling is critical for maintaining the superficial layer of articular cartilage and preventing osteoarthritis initiation. *Proc Natl Acad Sci U S A* **113** 14360-14365.

Jiang BH, Zheng JZ, Aoki M & Vogt PK 2000 Phosphatidylinositol 3-kinase signaling mediates angiogenesis and expression of vascular endothelial growth factor in endothelial cells. *Proc Natl Acad Sci U S A* **97** 1749-1753.

Jones S & Rappoport JZ 2014 Interdependent epidermal growth factor receptor signalling and trafficking. *Int J Biochem Cell Biol* **51** 23-28.

Jung O, Schreiber JG, Geiger H, Pedrazzini T, Busse R & Brandes RP 2004 gp91phox-containing NADPH oxidase mediates endothelial dysfunction in renovascular hypertension. *Circulation* **109** 1795-1801.

Jura N, Endres NF, Engel K, Deindl S, Das R, Lamers MH, Wemmer DE, Zhang X & Kuriyan J 2009a Mechanism for activation of the EGF receptor catalytic domain by the juxtamembrane segment. *Cell* **137** 1293-1307.

Jura N, Shan Y, Cao X, Shaw DE & Kuriyan J 2009b Structural analysis of the catalytically inactive kinase domain of the human EGF receptor 3. *Proc Natl Acad Sci U S A* **106** 21608-21613.

Kagiyama S, Eguchi S, Frank G, Inagami T, Zhang Y & Phillips M 2002 Angiotensin II-induced cardiac hypertrophy and hypertension are attenuated by epidermal growth factor receptor antisense. *Circulation* **106** 909-912.

Kagiyama S, Qian K, Kagiyama T & Phillips M 2003 Antisense to epidermal growth factor receptor prevents the development of left ventricular hypertrophy. *Hypertension* **41** 824-829.

Kanemitsu MY & Lau AF 1993 Epidermal growth factor stimulates the disruption of gap junctional communication and connexin43 phosphorylation independent of 12-0-tetradecanoylphorbol 13-acetate-sensitive protein kinase C: the possible involvement of mitogen-activated protein kinase. *Mol Biol Cell* **4** 837-848.

Kanemitsu MY, Loo LW, Simon S, Lau AF & Eckhart W 1997 Tyrosine phosphorylation of connexin 43 by v-Src is mediated by SH2 and SH3 domain interactions. *J Biol Chem* **272** 22824-22831.

Kauffmann-Zeh A, Rodriguez-Viciana P, Ulrich E, Gilbert C, Coffer P, Downward J & Evan G 1997 Suppression of c-Myc-induced apoptosis by Ras signalling through PI(3)K and PKB. *Nature* **385** 544-548.

Kauma S, Takacs P, Scordalakes C, Walsh S, Green K & Peng T 2002 Increased endothelial monocyte chemoattractant protein-1 and interleukin-8 in preeclampsia. *Obstet Gynecol* **100** 706-714.

Kelly NJ, Radder JE, Baust JJ, Burton CL, Lai YC, Potoka KC, Agostini BA, Wood JP, Bachman TN, Vanderpool RR, et al. 2017 Mouse Genome-Wide Association Study of Preclinical Group II Pulmonary Hypertension Identifies Epidermal Growth Factor Receptor. *Am J Respir Cell Mol Biol* **56** 488-496.

Kennedy SG, Wagner AJ, Conzen SD, Jordán J, Bellacosa A, Tsichlis PN & Hay N 1997 The PI 3-kinase/Akt signaling pathway delivers an anti-apoptotic signal. *Genes Dev* **11** 701-713.

Kenny LC, Baker PN, Kendall DA, Randall MD & Dunn WR 2002 Differential mechanisms of endothelium-dependent vasodilator responses in human myometrial small arteries in normal pregnancy and pre-eclampsia. *Clin Sci (Lond)* **103** 67-73.

Khalil RA & Granger JP 2002 Vascular mechanisms of increased arterial pressure in preeclampsia: lessons from animal models. *Am J Physiol Regul Integr Comp Physiol* **283** R29-45.

Kholodenko BN, Demin OV, Moehren G & Hoek JB 1999 Quantification of short term signaling by the epidermal growth factor receptor. *J Biol Chem* **274** 30169-30181.

Kim J, Lee C, Park H, Kim H, So H, Lee K, Lee H, Roh H, Choi W, Park T, et al. 2006 Epidermal growth factor induces vasoconstriction through the phosphatidylinositol 3-kinase-mediated mitogen-activated protein kinase pathway in hypertensive rats. *Journal of Pharmacological Sciences* **101** 135-143.

King GL, Park K & Li Q 2016 Selective Insulin Resistance and the Development of Cardiovascular Diseases in Diabetes: The 2015 Edwin Bierman Award Lecture. *Diabetes* **65** 1462-1471.

Knebel A, Rahmsdorf HJ, Ullrich A & Herrlich P 1996 Dephosphorylation of receptor tyrosine kinases as target of regulation by radiation, oxidants or alkylating agents. *EMBO J* **15** 5314-5325.

Knock GA & Poston L 1996 Bradykinin-mediated relaxation of isolated maternal resistance arteries in normal pregnancy and preeclampsia. *Am J Obstet Gynecol* **175** 1668-1674.

Kopp L, Lin T & Tucci JR 1977 Circadian rhythms in the urinary excretion of cyclic 3',5'-adenosine monophosphate (cyclic AMP) and cyclic 3',5'-guanosine monophosphate (cyclic GMP) in human subjects. *J Clin Endocrinol Metab* **44** 673-680.

Kosovic I, Prusac IK, Berkovic A, Marusic J, Mimica M & Tomas SZ 2017 Expression of EGF, EGFR, and proliferation in placentas from pregnancies complicated with preeclampsia. *Hypertens Pregnancy* **36** 16-20.

Kronborg CS, Gjedsted J, Vittinghus E, Hansen TK, Allen J & Knudsen UB 2011 Longitudinal measurement of cytokines in pre-eclamptic and normotensive pregnancies. *Acta Obstet Gynecol Scand* **90** 791-796.

Ku YH, Cho BJ, Kim MJ, Lim S, Park YJ, Jang HC & Choi SH 2017 Rosiglitazone increases endothelial cell migration and vascular permeability through Akt phosphorylation. *BMC Pharmacol Toxicol* **18** 62.

Kulik G, Klippel A & Weber MJ 1997 Antiapoptotic signalling by the insulin-like growth factor I receptor, phosphatidylinositol 3-kinase, and Akt. *Mol Cell Biol* **17** 1595-1606.

Kupferminc MJ, Peaceman AM, Wigton TR, Rehnberg KA & Socol ML 1994 Tumor necrosis factor-alpha is elevated in plasma and amniotic fluid of patients with severe preeclampsia. *Am J Obstet Gynecol* **170** 1752-1757; discussion 1757-1759.

Kurz C, Hefler L, Zeisler H, Schatten C, Husslein P & Tempfer C 2001 Maternal basic fibroblast growth factor serum levels are associated with pregnancy-induced hypertension. *J Soc Gynecol Investig* **8** 24-26.

Kyriakakis E, Cavallari M, Pfaff D, Fabbro D, Mestan J, Philippova M, De Libero G, Erne P & Resink TJ 2011 IL-8-mediated angiogenic responses of endothelial cells to lipid antigen activation of iNKT cells depend on EGFR transactivation. *J Leukoc Biol* **90** 929-939.

Laird DW, Puranam KL & Revel JP 1991 Turnover and phosphorylation dynamics of connexin43 gap junction protein in cultured cardiac myocytes. *Biochem J* **273(Pt 1)** 67-72.

Lake D, Corrêa SA & Müller J 2016 Negative feedback regulation of the ERK1/2 MAPK pathway. *Cell Mol Life Sci* **73** 4397-4413.

Lampe PD 1994 Analyzing phorbol ester effects on gap junctional communication: a dramatic inhibition of assembly. *J Cell Biol* **127** 1895-1905.

Lampe PD & Lau AF 2000 Regulation of gap junctions by phosphorylation of connexins. *Arch Biochem Biophys* **384** 205-215.

Lau AF, Kanemitsu MY, Kurata WE, Danesh S & Boynton AL 1992 Epidermal growth factor disrupts gap-junctional communication and induces phosphorylation of connexin43 on serine. *Mol Biol Cell* **3** 865-874.

Leavey K, Benton SJ, Grynspan D, Kingdom JC, Bainbridge SA & Cox BJ 2016 Unsupervised Placental Gene Expression Profiling Identifies Clinically Relevant Subclasses of Human Preeclampsia. *Hypertension* **68** 137-147.

Leykauf K, Dürst M & Alonso A 2003 Phosphorylation and subcellular distribution of connexin43 in normal and stressed cells. *Cell Tissue Res* **311** 23-30.

Liao WX, Feng L, Zhang H, Zheng J, Moore TR & Chen DB 2009 Compartmentalizing VEGF-induced ERK2/1 signaling in placental artery endothelial cell caveolae: a paradoxical role of caveolin-1 in placental angiogenesis in vitro. *Mol Endocrinol* **23** 1428-1444.

Lin R, Martyn KD, Guyette CV, Lau AF & Warn-Cramer BJ 2006 v-Src tyrosine phosphorylation of connexin43: regulation of gap junction communication and effects on cell transformation. *Cell Commun Adhes* **13** 199-216.

Lin R, Warn-Cramer BJ, Kurata WE & Lau AF 2001a v-Src phosphorylation of connexin 43 on Tyr247 and Tyr265 disrupts gap junctional communication. *J Cell Biol* **154** 815-827.

Lin R, Warn-Cramer BJ, Kurata WE & Lau AF 2001b v-Src-mediated phosphorylation of connexin43 on tyrosine disrupts gap junctional communication in mammalian cells. *Cell Commun Adhes* **8** 265-269.

Lin S, Fagan KA, Li KX, Shaul PW, Cooper DM & Rodman DM 2000 Sustained endothelial nitric-oxide synthase activation requires capacitative Ca2+ entry. *J Biol Chem* **275** 17979-17985.

Lockwood CJ, Yen CF, Basar M, Kayisli UA, Martel M, Buhimschi I, Buhimschi C, Huang SJ, Krikun G & Schatz F 2008 Preeclampsia-related inflammatory cytokines regulate interleukin-6 expression in human decidual cells. *Am J Pathol* **172** 1571-1579.

Lopez-Jaramillo P, Gonzalez MC, Palmer RM & Moncada S 1990 The crucial role of physiological Ca2+ concentrations in the production of endothelial nitric oxide and the control of vascular tone. *Br J Pharmacol* **101** 489-493.

Luksha L, Luksha N, Kublickas M, Nisell H & Kublickiene K 2010 Diverse mechanisms of endothelium-derived hyperpolarizing factor-mediated dilatation in small myometrial arteries in normal human pregnancy and preeclampsia. *Biol Reprod* **83** 728-735.

Luksha L, Nisell H, Luksha N, Kublickas M, Hultenby K & Kublickiene K 2008 Endothelium-derived hyperpolarizing factor in preeclampsia: heterogeneous contribution, mechanisms, and morphological prerequisites. *Am J Physiol Regul Integr Comp Physiol* **294** R510-519.

Luppi P, Tse H, Lain KY, Markovic N, Piganelli JD & DeLoia JA 2006 Preeclampsia activates circulating immune cells with engagement of the NF-kappaB pathway. *Am J Reprod Immunol* **56** 135-144.

Luttrell DK & Luttrell LM 2003 Signaling in time and space: G protein-coupled receptors and mitogen-activated protein kinases. *Assay Drug Dev Technol* **1** 327-338.

Mac Gabhann F & Popel AS 2004 Model of competitive binding of vascular endothelial growth factor and placental growth factor to VEGF receptors on endothelial cells. *Am J Physiol Heart Circ Physiol* **286** H153-164.

Mac Gabhann F & Popel AS 2007 Dimerization of VEGF receptors and implications for signal transduction: a computational study. *Biophys Chem* **128** 125-139.

Madhukar BV, Oh SY, Chang CC, Wade M & Trosko JE 1989 Altered regulation of intercellular communication by epidermal growth factor, transforming growth factor-beta and peptide hormones in normal human keratinocytes. *Carcinogenesis* **10** 13-20.

Mahdy Z, Otun HA, Dunlop W & Gillespie JI 1998 The responsiveness of isolated human hand vein endothelial cells in normal pregnancy and in pre-eclampsia. *J Physiol* **508 (Pt 2)** 609-617.

Mannucci E, Monami M, Di Bari M, Lamanna C, Gori F, Gensini GF & Marchionni N 2010 Cardiac safety profile of rosiglitazone: a comprehensive meta-analysis of randomized clinical trials. *Int J Cardiol* **143** 135-140.

Marsden PA & Brenner BM 1992 Transcriptional regulation of the endothelin-1 gene by TNF-alpha. *Am J Physiol* **262** C854-861.

Matsumoto T, Bohman S, Dixelius J, Berge T, Dimberg A, Magnusson P, Wang L, Wikner C, Qi JH, Wernstedt C, et al. 2005 VEGF receptor-2 Y951 signaling and a role for the adapter molecule TSAd in tumor angiogenesis. *EMBO J* **24** 2342-2353.

Mauro V, Carette D, Pontier-Bres R, Dompierre J, Czerucka D, Segretain D, Gilleron J & Pointis G 2013 The anti-mitotic drug griseofulvin induces apoptosis of human germ cell tumor cells through a connexin 43-dependent molecular mechanism. *Apoptosis* **18** 480-491.

McCarthy AL, Woolfson RG, Raju SK & Poston L 1993 Abnormal endothelial cell function of resistance arteries from women with preeclampsia. *Am J Obstet Gynecol* **168** 1323-1330.

McDonald SD, Malinowski A, Zhou Q, Yusuf S & Devereaux PJ 2008 Cardiovascular sequelae of preeclampsia/eclampsia: a systematic review and meta-analyses. *Am Heart J* **156** 918-930.

McKenzie JA & Ridley AJ 2007 Roles of Rho/ROCK and MLCK in TNF-alpha-induced changes in endothelial morphology and permeability. *J Cell Physiol* **213** 221-228.

Meadows KN, Bryant P & Pumiglia K 2001 Vascular endothelial growth factor induction of the angiogenic phenotype requires Ras activation. *J Biol Chem* **276** 49289-49298.

Mehta D & Malik AB 2006 Signaling mechanisms regulating endothelial permeability. *Physiol Rev* **86** 279-367.

Menges CW & McCance DJ 2008 Constitutive activation of the Raf-MAPK pathway causes negative feedback inhibition of Ras-PI3K-AKT and cellular arrest through the EphA2 receptor. *Oncogene* **27** 2934-2940.

Meyer RA, Laird DW, Revel JP & Johnson RG 1992 Inhibition of gap junction and adherens junction assembly by connexin and A-CAM antibodies. *J Cell Biol* **119** 179-189.

Minshall RD, Sessa WC, Stan RV, Anderson RG & Malik AB 2003 Caveolin regulation of endothelial function. *Am J Physiol Lung Cell Mol Physiol* **285** L1179-1183.

Molnár M, Sütö T, Tóth T & Hertelendy F 1994 Prolonged blockade of nitric oxide synthesis in gravid rats produces sustained hypertension, proteinuria, thrombocytopenia, and intrauterine growth retardation. *Am J Obstet Gynecol* **170** 1458-1466.

Moslehi R, Mills JL, Signore C, Kumar A, Ambroggio X & Dzutsev A 2013 Integrative transcriptome analysis reveals dysregulation of canonical cancer molecular pathways in placenta leading to preeclampsia. *Sci Rep* **3** 2407.

Motley ED, Kabir SM, Gardner CD, Eguchi K, Frank GD, Kuroki T, Ohba M, Yamakawa T & Eguchi S 2002 Lysophosphatidylcholine inhibits insulin-induced Akt activation through protein kinase C-alpha in vascular smooth muscle cells. *Hypertension* **39** 508-512.

Murakami Y, Kobayashi T, Omatsu K, Suzuki M, Ohashi R, Matsuura T, Sugimura M & Kanayama N 2005 Exogenous vascular endothelial growth factor can induce preeclampsia-like symptoms in pregnant mice. *Semin Thromb Hemost* **31** 307-313.

Murphy SP, Tayade C, Ashkar AA, Hatta K, Zhang J & Croy BA 2009 Interferon gamma in successful pregnancies. *Biol Reprod* **80** 848-859.

Myatt L & Webster RP 2009 Vascular biology of preeclampsia. *J Thromb Haemost* **7** 375-384.

Normanno N, De Luca A, Bianco C, Strizzi L, Mancino M, Maiello M, Carotenuto A, De Feo G, Caponigro F & Salomon D 2006 Epidermal growth factor receptor (EGFR) signaling in cancer. *Gene* **366** 2-16.

Ogawa S, Oku A, Sawano A, Yamaguchi S, Yazaki Y & Shibuya M 1998 A novel type of vascular endothelial growth factor, VEGF-E (NZ-7 VEGF), preferentially utilizes KDR/Flk-1 receptor and carries a potent mitotic activity without heparin-binding domain. *J Biol Chem* **273** 31273-31282.

Oh SY, Schmidt SA & Murray AW 1993 Epidermal growth factor inhibits gap junctional communication and stimulates serine-phosphorylation of connexin43 in WB cells by a protein kinase C-independent mechanism. *Cell Adhes Commun* **1** 143-149.

Orpana AK, Avela K, Ranta V, Viinikka L & Ylikorkala O 1996 The calcium-dependent nitric oxide production of human vascular endothelial cells in preeclampsia. *Am J Obstet Gynecol* **174** 1056-1060.

Ozer BH, Wiepz GJ & Bertics PJ 2010 Activity and cellular localization of an oncogenic glioblastoma multiforme-associated EGF receptor mutant possessing a duplicated kinase domain. *Oncogene* **29** 855-864.

Page EW 1972 On the pathogenesis of pre-eclampsia and eclampsia. *J Obstet Gynaecol Br Commonw* **79** 883-894.

Page TH, Smolinska M, Gillespie J, Urbaniak AM & Foxwell BM 2009 Tyrosine kinases and inflammatory signalling. *Curr Mol Med* **9** 69-85.

Park DJ, Freitas TA, Wallick CJ, Guyette CV & Warn-Cramer BJ 2006 Molecular dynamics and in vitro analysis of Connexin43: A new 14-3-3 mode-1 interacting protein. *Protein Sci* **15** 2344-2355.

Park DJ, Wallick CJ, Martyn KD, Lau AF, Jin C & Warn-Cramer BJ 2007 Akt phosphorylates Connexin43 on Ser373, a "mode-1" binding site for 14-3-3. *Cell Commun Adhes* **14** 211-226.

Pascoal IF, Lindheimer MD, Nalbantian-Brandt C & Umans JG 1998 Preeclampsia selectively impairs endothelium-dependent relaxation and leads to oscillatory activity in small omental arteries. *J Clin Invest* **101** 464-470.

Pearson JD 2000 Normal endothelial cell function. *Lupus* **9** 183-188.

Pober JS & Cotran RS 1990 Cytokines and endothelial cell biology. *Physiol Rev* **70** 427-451.

Potenza MA, Marasciulo FL, Chieppa DM, Brigiani GS, Formoso G, Quon MJ & Montagnani M 2005 Insulin resistance in spontaneously hypertensive rats is associated with endothelial dysfunction characterized by imbalance between NO and ET-1 production. *Am J Physiol Heart Circ Physiol* **289** H813-822.

Predescu D, Predescu S, Shimizu J, Miyawaki-Shimizu K & Malik AB 2005 Constitutive eNOS-derived nitric oxide is a determinant of endothelial junctional integrity. *Am J Physiol Lung Cell Mol Physiol* **289** L371-381.

Purba ER, Saita EI & Maruyama IN 2017 Activation of the EGF Receptor by Ligand Binding and Oncogenic Mutations: The "Rotation Model". *Cells* **6**.

Ravichandran LV, Chen H, Li Y & Quon MJ 2001 Phosphorylation of PTP1B at Ser(50) by Akt impairs its ability to dephosphorylate the insulin receptor. *Mol Endocrinol* **15** 1768-1780.

Reaume AG, de Sousa PA, Kulkarni S, Langille BL, Zhu D, Davies TC, Juneja SC, Kidder GM & Rossant J 1995 Cardiac malformation in neonatal mice lacking connexin43. *Science* **267** 1831-1834.

Reslan OM & Khalil RA 2010 Molecular and vascular targets in the pathogenesis and management of the hypertension associated with preeclampsia. *Cardiovasc Hematol Agents Med Chem* **8** 204-226.

Richards TS, Dunn CA, Carter WG, Usui ML, Olerud JE & Lampe PD 2004 Protein kinase C spatially and temporally regulates gap junctional communication during human wound repair via phosphorylation of connexin43 on serine368. *J Cell Biol* **167** 555-562.

Rivedal E, Mollerup S, Haugen A & Vikhamar G 1996 Modulation of gap junctional intercellular communication by EGF in human kidney epithelial cells. *Carcinogenesis* **17** 2321-2328.

Roberts JM, Taylor RN & Goldfien A 1991 Clinical and biochemical evidence of endothelial cell dysfunction in the pregnancy syndrome preeclampsia. *Am J Hypertens* **4** 700-708.

Roberts JM, Taylor RN, Musci TJ, Rodgers GM, Hubel CA & McLaughlin MK 1989 Preeclampsia: an endothelial cell disorder. *Am J Obstet Gynecol* **161** 1200-1204.

Rosenfeld CR, Cox BE, Roy T & Magness RR 1996 Nitric oxide contributes to estrogen-induced vasodilation of the ovine uterine circulation. *J Clin Invest* **98** 2158-2166.

Russell KS, Stern DF, Polverini PJ & Bender JR 1999 Neuregulin activation of ErbB receptors in vascular endothelium leads to angiogenesis. *Am J Physiol* **277** H2205-2211.

Rusterholz C, Hahn S & Holzgreve W 2007 Role of placentally produced inflammatory and regulatory cytokines in pregnancy and the etiology of preeclampsia. *Semin Immunopathol* **29** 151-162.

Rytlewski K, Huras H, Kuśmierska-Urban K, Gałaś A & Reroń A 2012 Leptin and interferon-gamma as possible predictors of cesarean section among women with hypertensive disorders of pregnancy. *Med Sci Monit* **18** CR506-511.

Sambhi M, Swaminathan N, Wang H & Rong H 1992 Increased EGF binding and EGFR messenger-RNA expression in rat aorta with chronic administration of pressor angiotensin-II. *Biochemical Medicine and Metabolic Biology* **48** 8-18.

Sanghavi M & Rutherford JD 2014 Cardiovascular physiology of pregnancy. *Circulation* **130** 1003-1008.

Schnittler HJ 1998 Structural and functional aspects of intercellular junctions in vascular endothelium. *Basic Res Cardiol* **93 Suppl 3** 30-39.

Schraufstatter IU, Trieu K, Zhao M, Rose DM, Terkeltaub RA & Burger M 2003 IL-8-mediated cell migration in endothelial cells depends on cathepsin B activity and transactivation of the epidermal growth factor receptor. *J Immunol* **171** 6714-6722.

Schumacher R, Mosthaf L, Schlessinger J, Brandenburg D & Ullrich A 1991 Insulin and insulin-like growth factor-1 binding specificity is determined by distinct regions of their cognate receptors. *J Biol Chem* **266** 19288-19295.

Shi F, Telesco SE, Liu Y, Radhakrishnan R & Lemmon MA 2010 ErbB3/HER3 intracellular domain is competent to bind ATP and catalyze autophosphorylation. *Proc Natl Acad Sci U S A* **107** 7692-7697.

Sibai BM 2003 Diagnosis and management of gestational hypertension and preeclampsia. *Obstet Gynecol* **102** 181-192.

Sibai BM & Barton JR 2007 Expectant management of severe preeclampsia remote from term: patient selection, treatment, and delivery indications. *Am J Obstet Gynecol* **196** 514.e511-519.

Sirnes S, Leithe E & Rivedal E 2008 The detergent resistance of Connexin43 is lost upon TPA or EGF treatment and is an early step in gap junction endocytosis. *Biochem Biophys Res Commun* **373** 597-601.

Solan JL & Lampe PD 2008 Connexin 43 in LA-25 cells with active v-src is phosphorylated on Y247, Y265, S262, S279/282, and S368 via multiple signaling pathways. *Cell Commun Adhes* **15** 75-84.

Solan JL & Lampe PD 2009 Connexin43 phosphorylation: structural changes and biological effects. *Biochem J* **419** 261-272.

Solan JL & Lampe PD 2014 Specific Cx43 phosphorylation events regulate gap junction turnover in vivo. *FEBS Lett* **588** 1423-1429.

Solan JL & Lampe PD 2016 Kinase programs spatiotemporally regulate gap junction assembly and disassembly: Effects on wound repair. *Semin Cell Dev Biol* **50** 40-48.

Somasiri A, Wu C, Ellchuk T, Turley S & Roskelley CD 2000 Phosphatidylinositol 3-kinase is required for adherens junction-dependent mammary epithelial cell spheroid formation. *Differentiation* **66** 116-125.

Steck PA, Lee P, Hung MC & Yung WK 1988 Expression of an altered epidermal growth factor receptor by human glioblastoma cells. *Cancer Res* **48** 5433-5439.

Steegers EA, von Dadelszen P, Duvekot JJ & Pijnenborg R 2010 Pre-eclampsia. *Lancet* **376** 631-644.

Sullivan JA, Grummer MA, Yi FX & Bird IM 2006 Pregnancy-enhanced endothelial nitric oxide synthase (eNOS) activation in uterine artery endothelial cells shows altered sensitivity to Ca2+, U0126, and wortmannin but not LY294002--evidence that pregnancy adaptation of eNOS activation occurs at multiple levels of cell signaling. *Endocrinology* **147** 2442-2457.

Svedas E, Islam KB, Nisell H & Kublickiene KR 2003 Vascular endothelial growth factor induced functional and morphologic signs of endothelial dysfunction in isolated arteries from normal pregnant women. *Am J Obstet Gynecol* **188** 168-176.

Swenson KI, Piwnica-Worms H, McNamee H & Paul DL 1990 Tyrosine phosphorylation of the gap junction protein connexin43 is required for the pp60v-src-induced inhibition of communication. *Cell Regul* **1** 989-1002.

Takahashi T, Yamaguchi S, Chida K & Shibuya M 2001 A single autophosphorylation site on KDR/Flk-1 is essential for VEGF-A-dependent activation of PLC-gamma and DNA synthesis in vascular endothelial cells. *EMBO J* **20** 2768-2778.

Takata M, Nakatsuka M & Kudo T 2002 Differential blood flow in uterine, ophthalmic, and brachial arteries of preeclamptic women. *Obstet Gynecol* **100** 931-939.

Tanbe AF & Khalil RA 2010 Circulating and Vascular Bioactive Factors during Hypertension in Pregnancy. *Curr Bioact Compd* **6** 60-75.

Taylor RN, Musci TJ, Rodgers GM & Roberts JM 1991 Preeclamptic sera stimulate increased platelet-derived growth factor mRNA and protein expression by cultured human endothelial cells. *Am J Reprod Immunol* **25** 105-108.

TenBroek EM, Lampe PD, Solan JL, Reynhout JK & Johnson RG 2001 Ser364 of connexin43 and the upregulation of gap junction assembly by cAMP. *J Cell Biol* **155** 1307-1318.

Toothill VJ, Van Mourik JA, Niewenhuis HK, Metzelaar MJ & Pearson JD 1990 Characterization of the enhanced adhesion of neutrophil leukocytes to thrombin-stimulated endothelial cells. *J Immunol* **145** 283-291.

Tosun M, Celik H, Avci B, Yavuz E, Alper T & Malatyalioğlu E 2010 Maternal and umbilical serum levels of interleukin-6, interleukin-8, and tumor necrosis factor-alpha in normal pregnancies and in pregnancies complicated by preeclampsia. *J Matern Fetal Neonatal Med* **23** 880-886.

Tran QK, Leonard J, Black DJ, Nadeau OW, Boulatnikov IG & Persechini A 2009 Effects of combined phosphorylation at Ser-617 and Ser-1179 in endothelial nitric-oxide synthase on EC50(Ca2+) values for calmodulin binding and enzyme activation. *J Biol Chem* **284** 11892-11899.

Tran QK, Leonard J, Black DJ & Persechini A 2008 Phosphorylation within an autoinhibitory domain in endothelial nitric oxide synthase reduces the Ca(2+) concentrations required for calmodulin to bind and activate the enzyme. *Biochemistry* **47** 7557-7566.

Tzahar E, Waterman H, Chen X, Levkowitz G, Karunagaran D, Lavi S, Ratzkin BJ & Yarden Y 1996 A hierarchical network of interreceptor interactions determines signal transduction by Neu differentiation factor/neuregulin and epidermal growth factor. *Mol Cell Biol* **16** 5276-5287.

van der Zandt PT, de Feijter AW, Homan EC, Spaaij C, de Haan LH, van Aelst AC & Jongen WM 1990 Effects of cigarette smoke condensate and 12-O-tetradecanoylphorbol-13-acetate on gap junction structure and function in cultured cells. *Carcinogenesis* **11** 883-888.

van Rijen HV, van Kempen MJ, Postma S & Jongsma HJ 1998 Tumour necrosis factor alpha alters the expression of connexin43, connexin40, and connexin37 in human umbilical vein endothelial cells. *Cytokine* **10** 258-264.

Vandenbroucke E, Mehta D, Minshall R & Malik AB 2008 Regulation of endothelial junctional permeability. *Ann N Y Acad Sci* **1123** 134-145.

Vanwijk MJ, Svedas E, Boer K, Nieuwland R, Vanbavel E & Kublickiene KR 2002 Isolated microparticles, but not whole plasma, from women with preeclampsia impair endothelium-dependent relaxation in isolated myometrial arteries from healthy pregnant women. *Am J Obstet Gynecol* **187** 1686-1693.

Var A, Yildirim Y, Onur E, Kuscu NK, Uyanik BS, Goktalay K & Guvenc Y 2003 Endothelial dysfunction in preeclampsia. Increased homocysteine and decreased nitric oxide levels. *Gynecol Obstet Invest* **56** 221-224.

Vince GS, Starkey PM, Austgulen R, Kwiatkowski D & Redman CW 1995 Interleukin-6, tumour necrosis factor and soluble tumour necrosis factor receptors in women with pre-eclampsia. *Br J Obstet Gynaecol* **102** 20-25.

Wainstein E & Seger R 2016 The dynamic subcellular localization of ERK: mechanisms of translocation and role in various organelles. *Curr Opin Cell Biol* **39** 15-20.

Waltenberger J, Claesson-Welsh L, Siegbahn A, Shibuya M & Heldin CH 1994 Different signal transduction properties of KDR and Flt1, two receptors for vascular endothelial growth factor. *J Biol Chem* **269** 26988-26995.

Wang Q, Villeneuve G & Wang Z 2005 Control of epidermal growth factor receptor endocytosis by receptor dimerization, rather than receptor kinase activation. *EMBO Rep* **6** 942-948.

Wang Y, Gu Y, Granger DN, Roberts JM & Alexander JS 2002 Endothelial junctional protein redistribution and increased monolayer permeability in human umbilical vein endothelial cells isolated during preeclampsia. *Am J Obstet Gynecol* **186** 214-220.

Wang YP, Walsh SW, Guo JD & Zhang JY 1991 The imbalance between thromboxane and prostacyclin in preeclampsia is associated with an imbalance between lipid peroxides and vitamin E in maternal blood. *Am J Obstet Gynecol* **165** 1695-1700.

Warn-Cramer BJ, Lampe PD, Kurata WE, Kanemitsu MY, Loo LW, Eckhart W & Lau AF 1996 Characterization of the mitogen-activated protein kinase phosphorylation sites on the connexin-43 gap junction protein. *J Biol Chem* **271** 3779-3786.

Wee P & Wang Z 2017 Epidermal Growth Factor Receptor Cell Proliferation Signaling Pathways. *Cancers (Basel)* **9**.

Werdich XQ & Penn JS 2005 Src, Fyn and Yes play differential roles in VEGF-mediated endothelial cell events. *Angiogenesis* **8** 315-326.

Wilson KJ, Gilmore JL, Foley J, Lemmon MA & Riese DJ 2009 Functional selectivity of EGF family peptide growth factors: implications for cancer. *Pharmacol Ther* **122** 1-8.

Wu LW, Mayo LD, Dunbar JD, Kessler KM, Baerwald MR, Jaffe EA, Wang D, Warren RS & Donner DB 2000 Utilization of distinct signaling pathways by receptors for vascular endothelial cell growth factor and other mitogens in the induction of endothelial cell proliferation. *J Biol Chem* **275** 5096-5103.

Yamashita H, Yano Y, Kawano K & Matsuzaki K 2015 Oligomerization-function relationship of EGFR on living cells detected by the coiled-coil labeling and FRET microscopy. *Biochim Biophys Acta* **1848** 1359-1366.

Yang WL, Wang J, Chan CH, Lee SW, Campos AD, Lamothe B, Hur L, Grabiner BC, Lin X, Darnay BG, et al. 2009 The E3 ligase TRAF6 regulates Akt ubiquitination and activation. *Science* **325** 1134-1138.

Yi FX, Boeldt DS, Gifford SM, Sullivan JA, Grummer MA, Magness RR & Bird IM 2010 Pregnancy enhances sustained Ca2+ bursts and endothelial nitric oxide synthase activation in ovine uterine artery endothelial cells through increased connexin 43 function. *Biol Reprod* **82** 66-75.

Yi FX, Boeldt DS, Magness RR & Bird IM 2011 [Ca2+]i signaling vs. eNOS expression as determinants of NO output in uterine artery endothelium: relative roles in pregnancy adaptation and reversal by VEGF165. *Am J Physiol Heart Circ Physiol* **300** H1182-1193.

Ying W & Sanders P 2005 Enhanced expression of EGF receptor in a model of salt-sensitive hypertension. *American Journal of Physiology-Renal Physiology* **289** F314-F321.

Yoshizumi M, Perrella MA, Burnett JC & Lee ME 1993 Tumor necrosis factor downregulates an endothelial nitric oxide synthase mRNA by shortening its half-life. *Circ Res* **73** 205-209.

Zeng G & Quon MJ 1996 Insulin-stimulated production of nitric oxide is inhibited by wortmannin. Direct measurement in vascular endothelial cells. *J Clin Invest* **98** 894-898.

Zennadi R, Whalen EJ, Soderblom EJ, Alexander SC, Thompson JW, Dubois LG, Moseley MA & Telen MJ 2012 Erythrocyte plasma membrane-bound ERK1/2 activation promotes ICAM-4-mediated sickle red cell adhesion to endothelium. *Blood* **119** 1217-1227.

Zhang X, Gureasko J, Shen K, Cole PA & Kuriyan J 2006 An allosteric mechanism for activation of the kinase domain of epidermal growth factor receptor. *Cell* **125** 1137-1149.

Zhang Y, Gu Y, Li H, Lucas MJ & Wang Y 2003 Increased endothelial monolayer permeability is induced by serum from women with preeclampsia but not by serum from women with normal pregnancy or that are not pregnant. *Hypertens Pregnancy* **22** 99-108.

Zhou L, Kasperek EM & Nicholson BJ 1999 Dissection of the molecular basis of pp60(v-src) induced gating of connexin 43 gap junction channels. *J Cell Biol* **144** 1033-1045.

Zimmermann S & Moelling K 1999 Phosphorylation and regulation of Raf by Akt (protein kinase B). *Science* **286** 1741-1744.

Ziogas A, Moelling K & Radziwill G 2005 CNK1 is a scaffold protein that regulates Src-mediated Raf-1 activation. *J Biol Chem* **280** 24205-24211.

Chapter 9

Materials and Methods

9.1 Materials

Fura-2 AM was obtained from Molecular Probes (Eugene, OR), CaCl2 from Calbiochem (San Diego, CA) for reasons of purity and low nitrate contamination, and ATP (disodium salt) and all other chemicals, unless noted otherwise, were from Sigma (St. Louis, MO). Also, unless noted otherwise, MEM, M199 and all other cell culture reagents were purchased from Invitrogen (Carlsbad, CA). For [Ca2+]i imaging studies, 35-mm dishes with glass coverslip windows were purchased from MatTek Corp. (Ashland, MA). Human recombinant epidermal growth factor (EGFR) was from Millipore (Temecula, CA). Vascular endothelial growth factor (VEGF-A_{165}) was from R&D Systems, Inc. (Minneapolis, MN). TPA and PP2 were from Sigma Chemicals (St. Louis, MO). U0126 was from Promega Corp (Madison, WI). R-phycoerythrin goat anti-mouse IgG (H + L) was from Molecular Probes (ThermoFisher Scientific, Waltham, MA)

9.2 Isolation of Uterine Artery Endothelial Cells

Procedures for animal handling and protocols for experimental procedures were approved by the University of Wisconsin-Madison Research Animal Care Committees of both the School of Medicine and Public Health and the College of Agriculture and Life Sciences and followed the recommended American Veterinary Medicine Association guidelines for humane treatment and euthanasia of laboratory farm animals. Uterine arteries were obtained from mixed Western breed

non-pregnant (NP) sheep and pregnant (P) ewes at 120–130 days of gestation during non-survival surgery, and UAECs were prepared by collagenase dispersion. Cells were frozen at the end of passage 3 and stored in liquid nitrogen. For protein studies a single vial of cells was grown onto a T75 and seeded to 6-well plates as required in each case. For imaging, pools of cells were created by growing 1 x T75 of cells each from 4 different NP- or P- sheep and then combining into an NP- or P- Pool before freezing down at a 1:35 split ratio. One vial was sufficient for a day of imaging studies.

9.3 Adenoviral Transduction Protocol

Day 1: Plate P-UAEC in 2 mL Minimum Essential Medium (MEM) w/20% fetal bovine serum (FBS) in 6-well plates or glass-bottom dishes in the manner required by experimental protocol (Western blotting, calcium imaging, etc.). Incubate overnight at 37^0C. ***Day 2:*** Aspirate medium from dishes/wells. Add 1 mL of control medium or adenovirus-containing medium to each well as appropriate. Adenoviral transduction medium is prepared by adding appropriate volume of adenovirus (Ad-EGFR(ErbB1) or Ad-CMV-EGFR(L834R), Vector Biolabs, Philadelphia, PA) to medium at the desired multiplicity of infection (MOI), which is determined by titer of adenovirus stock. Incubate for 24 hrs at 37^0C. ***Day 3:*** Aspirate medium from wells. Add 2 mL of fresh MEM (w/20% FBS) to each well. Incubate overnight at 37^0C. ***Day 4:*** Perform serum starvation and administer treatments as per experimental protocol.

9.4 Flow Cytometry Protocol

Begin by using the Adenoviral Transduction Protocol to generate P-UAEC that express exogenous wild-type EGFR or L834R-EGFR at multiplicities of infection (MOIs) of 10, 100, 320, 1000, and 3200. This should be done in a 6-well plate so there will be one well of control cells (parental P-UAEC) and a well for cells transduced at each of the 5 MOIs. Use two tubes of cells to create two independent sets of samples for a total of two 6-well plates. After the Adenoviral Transduction Protocol has been completed as described, aspirate medium from all wells and add 1 ml of prepared trypsin ( ) to each well for 3 – 5 min to allow cells to lift from plates. Add 3 ml of MEM w/20% FBS to each well and transfer the contents of each well (4 ml) to a separate 15 ml conical tube. There should be 12 tubes total—a tube for each of the 6 samples in the 2 duplicate sets. Centrifuge tubes at 300g for 3.5 min and pour off the supernatant. Add 1 ml MEM with 2% (not 20%) FBS to each tube and gently resuspend the cells. Pipet 100 µL of suspended cells from each tube into TWO 1.5 ml Eppendorf tubes on ice at 4^0C. There should be 12 tubes for each set of samples, each containing 100 µL of cells. The tubes should be labeled 1a, 1b, 2a, 2b,…,6a, 6b for each set. To all the "**a**" tubes, add 10 µL of murine IgG that has been diluted 1:10 in PBS. To all the "**b**" tubes, add 10 µL of the highly EGFR-selective murine mAb 528 (K_d = 1 nM) that has also been diluted 1:10 in PBS. Mix gently and allow tubes to incubate on ice for 30 min. Following incubation, add 1 ml MEM w/2% FBS to each tube and spin in a microcentrifuge for 3 min at medium speed. Carefully aspirate supernatant from each tube, add enough fresh MEM w/2% FBS to each tube to bring the volume back to 100 µL and add 10 µL of R-phycoerythrin goat anti-mouse IgG (H + L) (#P852, Molecular Probes) that has been diluted 1:10 in PBS. Mix gently and allow tubes to incubate on ice for 30 min as before. Following this second incubation, add 1 ml MEM w/2% FBS to each tube and spin in a microcentrifuge for 3 min at medium speed. Carefully aspirate supernatant from each tube. Add 300 µL PBS to each tube and gently resuspend cells. Transfer each sample to a separate 5 mL clear plastic flow cytometry tube ( ) and keep on ice.

Samples utilized for my experiments were analyzed by the BD FacsCalibur flow cytometer at the Flow Cytometry Laboratory at the Wisconsin Institutes for Medical Research (WIMR). One drop of propidium iodide solution was added to each tube before analysis to identify dead cells. For each sample, the fluorescence intensity of 10,000 cells was quantified (which served as an indicator of plasma membrane expression of EGFR) and the geometric mean was calculated. Mean fluorescence intensity of matching counterparts from the two sets were averaged to produce 12 final mean values—6 for IgG controls and 6 for EGFR-selective binding of mAb 528 at MOIs of 0, 10, 100, 320, 1000 and 3200.

9.5 Fura-2 [Ca2+]i Imaging Protocol 1.0

Pooled passage 4 P-UAEC were grown in MEM w/20% FBS in 35 mm glass-bottom microwell dishes (MatTek Corp.) until they reached near 100% confluence. Cells were then loaded with Fura-2 by adding 10 μM AM (Molecular Probes Inc., Eugene, OR, USA) in the presence of 0.05% Pluronic F127 (Molecular Probes Inc.) in 1 ml Krebs buffer (125 mM NaCl, 5 mM KCl, 1 mM MgSO4, 1 mM KH2PO4, 6 mM glucose, 25 mM HEPES, 2 mM CaCl2, pH 7.4) for 60 min at 37 °C. P-UAEC were washed with Krebs buffer, covered in 2 ml Krebs buffer, and incubated for 30 min to allow complete ester hydrolysis. The cells were then removed from the incubator and all subsequent steps were performed at room temperature. Cells were again washed and covered with 2 ml Krebs buffer, and the dish was placed in the field of view. Fura-2 loading was verified by viewing at 380 nM UV excitation on a Nikon inverted microscope (InCyt Im2, Intracellular Imaging, Inc., Cincinnati, OH, USA). The cells were (1) incubated with ATP (100 μM) for 30 min, (2) washed with Krebs buffer, given 2 ml fresh buffer, and left to sit for 30 min, (3) treated with VEFG-A_{165} (10 ng/ml), EGF (10 ng/ml), or vehicle for 30 min, and (4) stimulated a second time with ATP (100 μM) for 30 min. During steps 1,3 and 4, the data was recorded for 80-100 cells

simultaneously using alternate excitation at 340 and 380 nm at 1-s intervals and measuring emitted light using a PixelFly video camera. For all [Ca2+]i imaging experiments, data were recorded for a minimum of 5 minutes before agonist stimulation or antagonist addition to establish the basal [Ca2+]i. From the ratio of emission at 510 nm detected at the two excitation wavelengths and by comparison with a standard curve established for the same settings using buffers of known free [Ca2+] (Molecular Probes), the intracellular free [Ca2+] was calculated in real time using the InCyt Im2 software (Cincinnati, OH, USA). Ca2+ bursts were counted for the “before” and “after” ATP treatments. Those that gave 3 or more bursts during the initial ATP treatment were included in the data set and the others were discarded. Before and after comparisons data for each cell burst numbers were compared in this data set. For statistical analysis, paired t-test for each cell against itself within a single treatment group, and a rank-sum test was used to compare differences between different treatment groups.

9.5.1 Fura-2 [Ca2+]i Imaging Protocol 1.1

Identical to Protocol 1.0 except the treatment sequence is altered as follows: “The cells were (1) incubated with ATP (100 µM) for 30 min, (2) washed with Krebs buffer, given 2 ml fresh buffer containing PP2 (10 µM) or U0126 (10 µM), and left to sit for 30 min, (3) treated with VEFG-A_{165} (10 ng/ml), EGF (10 ng/ml), or vehicle for 30 min, and (4) stimulated a second time with ATP (100 µM) for 30 min.”

9.5.2 Fura-2 [Ca2+]i Imaging Protocol 1.2

Identical to Protocol 1.0 except the first sentence should be replaced with the following passage: “Pooled passage 4 uterine artery endothelial cells obtained from late pregnant ewes (P-UAEC) were grown in Minimum Essential Medium w/20% fetal bovine serum in 35 mm glass-bottom microwell dishes (MatTek Corp.) until the day before they approach 100% confluence. The medium is then replaced with fresh medium containing insulin (100 nM) or LY294002 (20 µM) and

allowed to incubate at 370C for ~20 hrs, at which point they will be ready for fura-2 incubation. From this time onward, cells will only be rinsed or incubated with Krebs buffer containing insulin (100 nM) or LY294002 (20 µM), as warranted, until the experimental trial is completed."

9.6 Western Blot Protocol

P-UAEC that had been passaged from T75 flasks (Passage 3) to 6-well plates (350,000 cells per well) were maintained overnight in MEM w/20% FBS to adhere securely to the well at approximately 50-55% confluency. At 48 hrs before agonist or growth factor treatment, Adenoviral Transduction Protocol 1.0 was performed on all wells, using either vehicle or adenovirus containing the desired gene transcript (*wtEGFR* or *L834R-EGFR*). At 4 hrs prior to treatment with either agonist or vehicle, cells were incubated in MEM with 0.01% BSA without FBS. Antagonists were added 20 min prior to 30-min agonist treatment, as appropriate. Reactions were terminated by immediate removal of media and the addition of ice-cold PBS. After removal of PBS, cells were snap-frozen liquid N2. Upon thawing, cells were solubilized in lysis buffer [4 mM Na(PO4)2, 50 mM HEPES (pH 7.5), 100 mM NaCl, 10 mM EDTA, 10 mM NaF, 2 mM Na3(VO4)2, 1 mM phenylmethylsulfonylfluoride, 1% Triton X-100, 5 µg/ml leupeptin, and 5 µg/ml aprotinin], sonicated, and centrifuged at 12,000 x g for 5 min. Solubilized protein concentration was determined using the bicinchoninic acid assay (Sigma Chemical Co., St. Louis, MO), which was followed by Western blotting (20 µg protein per lane) on 7.5% polyacrylamide gels (100 V, ~2 h; Mini- Protein II, Bio-Rad Laboratories Inc., Hercules, CA) and transfer to Immobilon P membrane (100 V, 2 hrs; Millipore Corp., Billerica, MA). Phosphorylation of proteins specified below were detected by use of phosphorylation-state specific antibodies; goat anti-rabbit HRP-conjugated secondary antibody (# 7074; Cell Signaling Technology, Inc., Danvers, MA) was used at 1:3250 for all antibodies unless otherwise noted. For blocking, Starting Block TBS blocking buffer

(ThermoFisher Scientific, Waltham, MA) was used for all antibodies. proteins were detected on 4 separate membranes using the following antibodies: pS279/282 Cx43 (#sc-12900-R; Santa Cruz Biotechnology, Santa Cruz, CA) 1:667; pY265 Cx43 (#sc-17220-R; Santa Cruz Biotechnology) 1:667; total Cx43 (#sc-9059; Santa Cruz Biotechnology) 1:2000); ERK1/2 pT202/pY204 (#4377S, Cell Signaling Technology) 1:2500; total ERK1/2 (#9102S, Cell Signaling Technology) 1:2000; pS473 Akt (9271L, Cell Signaling Technology) 1:1000; total Akt (9272, Cell Signaling Technology) 1:4000; pY1173 EGFR (#44-794G, Invitrogen, Rockford, IL) 1:1000; total EGFR (#sc-03, Santa Cruz Biotechnology) 1:1000. To ensure consistent protein loading, antibodies were normalized to levels of Hsp90 (#4874S, Cell Signaling Technology) 1:2500. For pS279/282 and pY265 Cx43, specific binding was detected by enhanced chemiluminescence (ECL) 2 reagent detection system (GE Healthcare BioSciences, Piscataway, NJ); for all other proteins ECL was used. Bands were quantified by using the HP Deskscan system in transmission scanning mode (Hewlett-Packard, Palo Alto, CA) and ImageJ software (version 1.50i, Wayne Rasband, National Institutes of Health, USA).

9.7 Electrical Cell-substrate Impedance Sensing (ECIS) Protocol

P-UAEC monolayer permeability was assessed by measuring changes in trans-endothelial electrical resistance (TER) using an ECIS (Electrical Cell-substrate Impedance Sensing) system. Decreased TER is an indication of increased monolayer permeability, thus, a decrease in monolayer integrity. P-UAEC or P-UAEC-adEGFR were grown on a gelatin-coated 96-well plate (#96W10idf PET, Applied BioPhysics). Each well contained gold electrodes spaced in a 10 inter-digitated finger configuration. A small alternating current was applied across the electrodes to measure TER. TER was monitored uninterrupted before, during, and after treatments. In this study, P-UAEC were plated at a density of 1.2x105 cells/mL in 200uL per well and grown for 4

days. At confluence (indicated by a plateau of TER), serum containing growth media was removed and serum free media added for a minimum of 3 hours. Cells were treated with the following agonists (or combinations of agonists): EGF (10 ng/ml), VEGF-A_{165} (10/ng/ml), insulin (100 nM), LY294002 (20 μM), LY294002 + EGF, LY294002 + VEGF, LY + insulin. The experiment was run for 20 hours. Resistance values for each well were normalized to untreated control and expressed as a ratio of measured resistance to baseline resistance, plotted as a function of time.

9.8 Statistical Analyses

For each Fura-2 [Ca2+]i imaging experiment, fluorescent signal was averaged from at least 20 responding cells. Imaging data were from 5 to 22 separate dishes. For other assays, 4 - 9 independent experiments and are presented as columns of means ± SE or box-and-whisker plots. Calcium imaging data were analyzed by student's t-test, paired t-test, Wilcoxon rank-sum test or ANOVA, as appropriate. Western blot data and ECIS data were analyzed by ANOVA. Post hoc analysis utilized Tukey's range test for multiple comparisons or Dunnett's two-sided test for comparison of several treatment groups to a single control group. A value of $P < 0.05$ was considered statistically significant.